COBSCOOK BAY TIDAL ENERGY PROJECT

2016 ENVIRONMENTAL MONITORING REPORT

FERC PROJECT NO. P-12711-005

April 28, 2017

ORPC Maine, LLC
254 Commercial St., Suite 119B
Portland, ME 04101
Phone (207) 772-7707
www.orpc.co

CONTENTS

LIST OF FIGURES

LIST OF TABLES

LIST OF APPENDICES

APPENDIX A: Adaptive Management Team Meeting Minutes (January 4, 2017)

APPENDIX B: Adaptive Management Team Presentation (January 4, 2017)

APPENDIX C: Hydroacoustic Analysis of the Effects of a Tidal Power Turbine on Fishes

APPENDIX D: Behavioral Responses of Fish to a Current-Based Hydrokinetic Turbine Under Multiple Operational Conditions: Final Report

APPENDIX E: PNNL Triton: Igiugig Video Analysis, FY 16 Progress Report, September 2016

1.0 INTRODUCTION

1.1   PROJECT BACKGROUND

ORPC Maine, LLC, a wholly-owned subsidiary of Ocean Renewable Power Company, LLC, (collectively, ORPC), is a Maine-based developer of hydrokinetic power systems and projects that harness the power of oceans and rivers to generate clean, predictable renewable energy. In partnership with coastal and river communities, ORPC works to create and sustain local jobs while promoting energy independence and protecting the environment.

ORPC received a pilot project license for the Cobscook Bay Tidal Energy Project (Project) from the Federal Energy Regulatory Commission (FERC) on February 27, 2012 (FERC Project No. P-12711-005). The purpose of the Project is to evaluate the potential for a new source of clean, renewable energy generation using tidal energy resources in Cobscook Bay, Maine. ORPC obtained a preliminary permit for the Project area in Cobscook Bay from FERC on July 23, 2007; FERC issued a successive preliminary permit on January 13, 2011. Feasibility studies, including environmental surveys, and pre-filing consultation were conducted, resulting in ORPC's filing of a draft pilot project license application with FERC on July 24, 2009 and subsequently, the final pilot project license application in September 2011. The FERC pilot project license boundary for the Project encompasses the proposed development area (Figure 1).

In March 2012, ORPC began construction of the Project off the coast of Eastport and Lubec, Maine (Figure 1). Following installation of the initial phase of the Project during the spring and summer of 2012, the Project began delivering electricity to the Emera Maine grid in September 2012. This is the first grid-connected installation of ORPC's TidGen® Power System.

TidGen® Power System
ORPC designed the TidGen® Power System to operate in water depths of 60 to 150 ft. The core component of the TidGen® Power System is ORPC's proprietary turbine generator unit (TGU). The TGU utilized four advanced design cross-flow (ADCF) turbines to drive a permanent magnet generator mounted between the turbines on a common driveshaft. The ADCF turbines rotated in the same direction regardless of tidal flow direction; rotational speed of the turbines was directly related to water flow speed. The TGU was 98 ft in length, 17 ft high and 17 ft wide. It was attached to a bottom support frame, which held the TGU in place approximately 15 ft above the sea floor. The bottom support frame was 98 ft long by 50 ft wide by 15 ft high. The bottom support frame was constructed of steel, and the TGU was constructed of steel and composite material. The coupled TGU and bottom support frame comprised the TidGen® device (Figure 2). The TidGen® device was connected to an underwater power consolidation module, which was then connected to an on-shore station through a single underwater power and data cable. The on-shore station was interconnected to the local power grid. The TidGen® device and the related cabling and on-shore station comprised a complete TidGen® Power System.
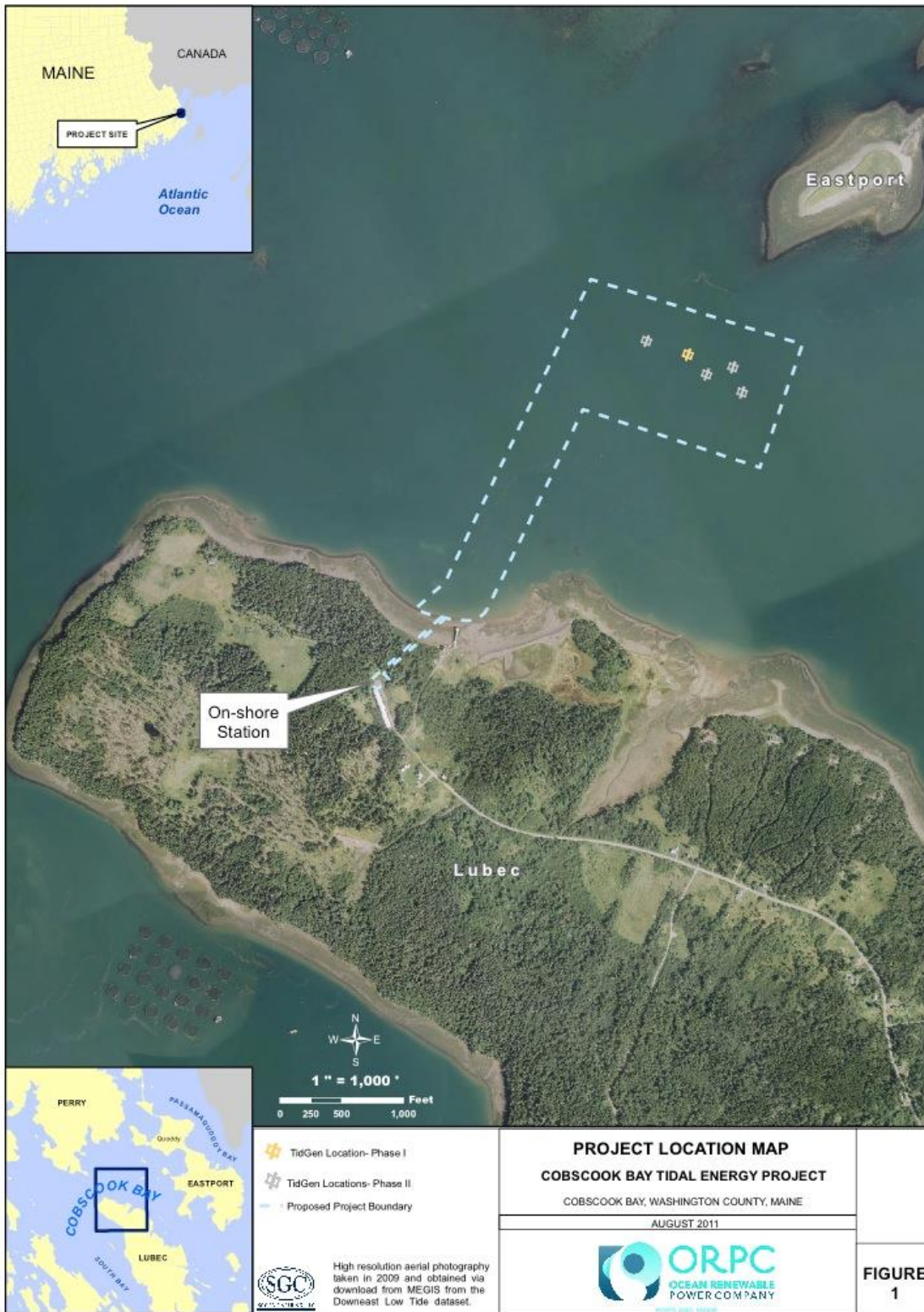
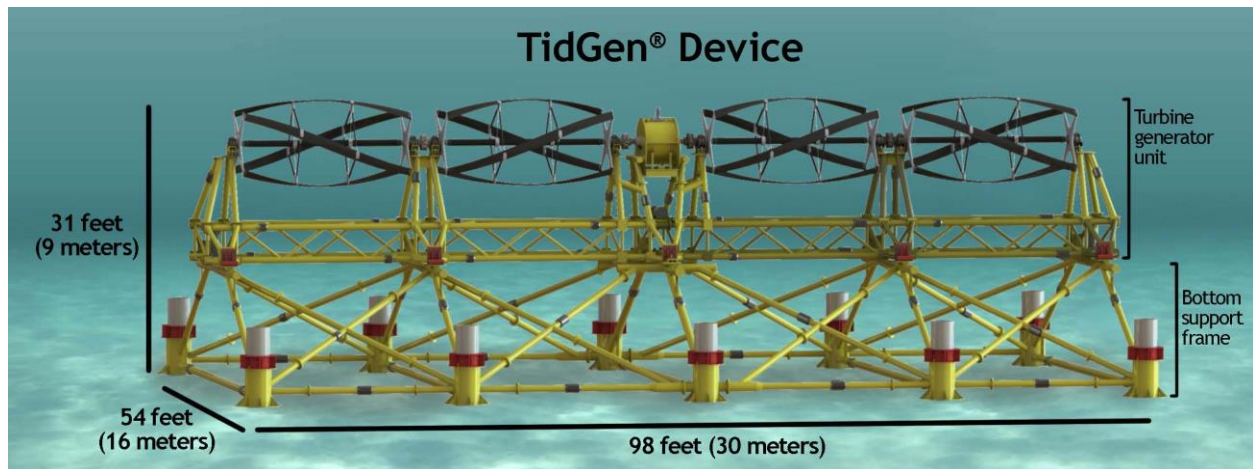*Figure 1.* Cobscook Bay Tidal Energy Project location map.

Figure 2. TidGen® device illustrating turbine generator unit (TGU) and bottom support frame

1.2 TECHNOLOGY OPTIMIZATION PHASE

The TidGen® TGU was retrieved from the Cobscook Bay Tidal Energy Project site in July 2013. Prior to retrieval, ORPC logged considerable operational time, achieved multiple milestones and gathered important lessons learned regarding deployment and retrieval procedures, and turbine operation, performance, and environmental interactions. To take immediate advantage of the lessons learned, ORPC decided to proceed with significant engineering improvements to the TidGen® Power System while the TGU was out of the water. This approach allowed ORPC to properly address issues with the generator and identify and implement longer-term design and component part improvements for future versions of the TidGen® Power System. This effort will result in a greater technology gain over time and help sustain successful operations locally.

Advanced TidGen® Power System
ORPC has focused our technical strategy on leveraging lessons learned from multiple projects towards cross-platform designs and advanced design tools. Turbine, fairing structure, and control system design improvements will improve performance of the power systems. These advances, combined with the integration of new generator and driveline technologies, will provide the basis for the optimized power system to be installed in Cobscook Bay.

U.S. Senators Susan Collins and Angus King announced on August 31, 2016 that Ocean Renewable Power Company (ORPC) would receive $5,350,000 through the Department of Energy (DOE) to enhance the performance of its tidal turbine system. ORPC was one of 10 organizations across the country to receive funding to support the development of a commercially viable marine and hydrokinetic industry. This contract was signed with DOE on January 3, 2017.
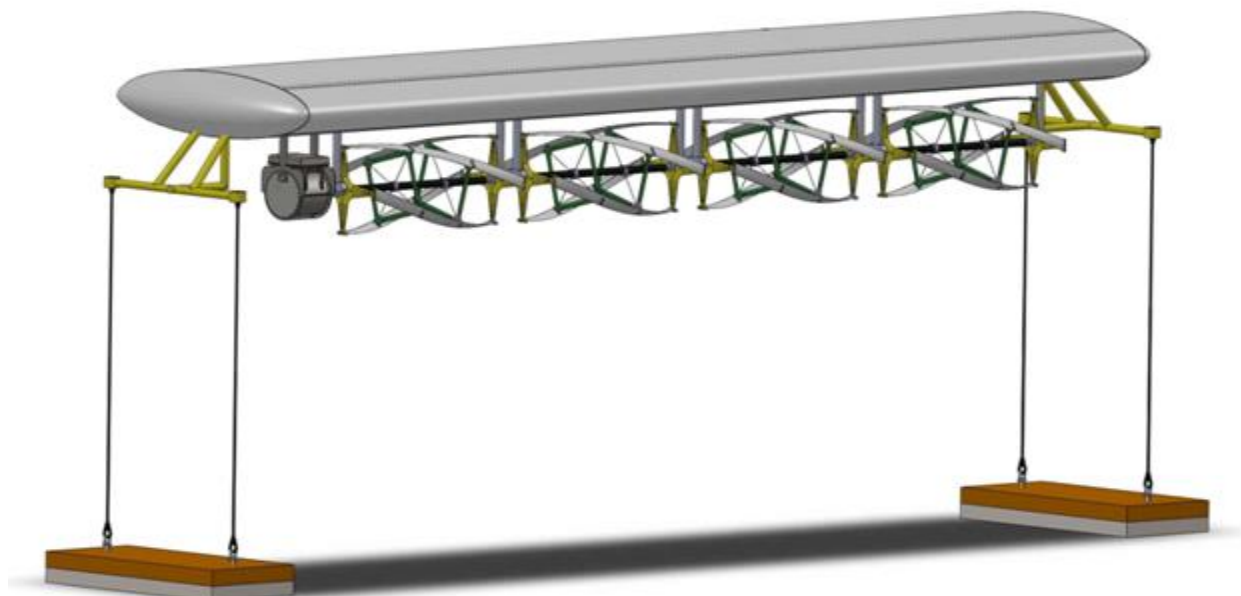
Figure 3. Advanced TidGen® Power System

ORPC's funded project, Advanced TidGen® Power System, will incorporate the many innovations and system advancements achieved by ORPC in the past through multiple DOE and privately sponsored engineering and technology projects. These efforts have resulted in demonstrated reductions to levelized cost of electricity (LCOE) and increased annual energy production (AEP). The proposed system is based on a significant design effort performed in 2016, which included validation of an advanced non-linear control system that reduced operational losses from near 20% to less than 1%, and improved system efficiencies of 35% due to structural and turbine design enhancements. A driveline test rig has been fabricated with a full driveline section, scheduled for characterization testing in Q1 2017. An advanced encapsulated generator, which will be utilized for the project, is currently in production.

The new system will be built, installed, operated, and performance benchmarked in ORPC's permitted sites in the Eastport and Lubec region, including the Cobscook Bay Tidal Energy Project, and employ local contractors and services providers. ORPC will continue its industry-leading environmental monitoring efforts in collaboration with state and federal regulators that to date have shown no adverse effects on the marine environment.

A timeline of completed design elements and ongoing efforts is shown on Figure 4.

Figure 4. Advanced TidGen® design roadmap
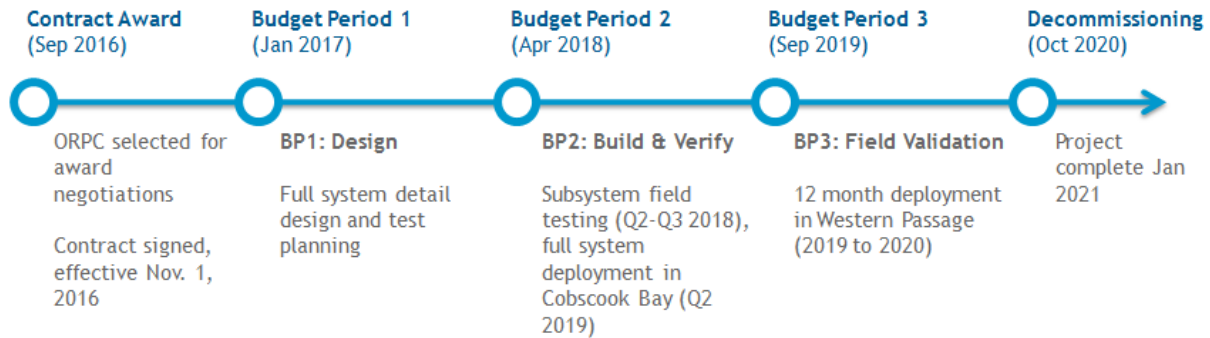
1.3   TEMPORARY VARIANCE FROM ENVIRONMENTAL MONITORING

The status of the TidGen® TGU led ORPC to consult with FERC and the Project's Adaptive Management Team to determine an appropriate level of environmental monitoring while the TGU was out of the water. This effort culminated with the issuance of a temporary variance from environmental monitoring from FERC on October 29, 2013. The essential elements of granting a variance were the following: an environmental, safety, hydrologic or third party issue that renders the license condition impracticable or counterproductive; a defined period of time and specific plan of action for the variance has been identified; no unreasonably adverse environmental impact is likely; and consent from the consulting agencies is documented.

ORPC continued some opportunistic environmental monitoring at the Project site in 2014 despite the temporary variance. These activities were associated with the deployment of ORPC's OCGen® Module Mooring Project at the site. Environmental monitoring included review of dive video for benthic growth on subsea components (Section 3.0 of this report). In addition, ORPC and the University of Maine School of Marine Sciences (UMaine) continued fisheries and marine life interaction research at the site in 2014 and 2015 through a separate UMaine funding award from DOE.

ORPC provided FERC and the Project's Adaptive Management Team updates during the temporary variance period in 2015 related to project activities and technology optimization progress. ORPC held an Adaptive Management Team meeting on November 19, 2015, which included further updates on the technology optimization phase and a request for feedback on the potential for an extension to the temporary variance to align with the engineering and design schedule. Based on feedback from the Adaptive Management Team, ORPC explored the option of requesting a two-year variance extension.

Based on these discussions, ORPC requested a two-year temporary variance extension to environmental monitoring from FERC on December 31, 2015. The request took the following factors into account:

- Comprehensive pre-deployment environmental studies have contributed to an understanding of inter-annual variability.
- Environmental monitoring results-to-date indicated negligible effects to marine life for ongoing operations.
- TGU operational status makes adherence to license condition impractical and will not advance the conditions purpose.
- No undue impacts or impedance of other license requirements are anticipated.
- ORPC plans to return to adherence of condition once TGU operation recommences.

The request for the two-year extension to the temporary variance for environmental monitoring was granted by FERC on March 2, 2016.

1.4   LICENSE SELECTION PROCESS

On February 27, 2012, the Federal Energy Regulatory Commission (Commission) issued a pilot project license to ORPC Maine (ORPC) for the Cobscook Bay Tidal Energy Project (FERC No.12711) for a period of eight years, effective the first day of the month in which the order was issued. This made the effective date of the license February 1, 2012, with a termination date of January 31, 2020. On June 5, 2015, ORPC filed a request with the Commission to extend its license term for the Cobscook Bay Tidal Energy Project from eight years to ten years. This would extend the expiration date from 2020 to 2022. The Commission issued an order on December 16, 2015 accepting ORPC's license extension request given the experimental nature of hydrokinetic devices, the licensee's dedication to expanding and improving the technology and design of its project, and the insignificant or no impact to the surrounding environment.

In a letter dated November 25, 2015 the Commission instructed that between 5 and 5.5 years before ORPC's existing license expires, we will need to notify the Commission whether or not we intend to file an application for a new license. Concurrent with the filing of this notice of intent (NOI) to relicense the project, a Pre-Application Document (PAD) would need to be filed with the Commission and the PAD distributed to appropriate federal, state, and interstate resource agencies, Indian tribes, local governments, and members of the public likely to be interested in the project's relicensing. The PAD must include: (1) a process plan and schedule; (2) a description of the project's location, facilities, and operation; (3) a description of the existing environment at the project and its resource impacts; (4) a preliminary list of issues and proposed studies; and (5) a list of contacts.

The Cobscook Bay Tidal Energy site has served a pivotal role in the advancement of ORPC's technology specifically and the domestic marine hydrokinetic industry generally. ORPC

anticipates that the project infrastructure in place, the environmental monitoring and data analysis efforts, resource information documentation, and collaborative relationships with existing marine users will continue through the duration of the existing pilot license term. With concurrence of the Project Adaptive Management Team, we will be testing new generations of system components and assembled systems at the project site and will keep FERC informed regarding these efforts.

While the project site serves as an excellent testing area, ORPC considers the tidal current velocities at the Project site inadequate to justify pursuing a commercial license. In a March 14, 2017 submittal to FERC, ORPC stated that it did not intend to file a NOI or PAD for the Project at this time.

2.0 ADAPTIVE MANAGEMENT (License Article 404)

2.1 ADAPTIVE MANAGEMENT PLAN AND TEAM

ORPC developed an Adaptive Management Plan (AMP) as required by the FERC pilot project license (P-12711-005, Article 404) for the Project. The AMP is an integral part of ORPC's implementation of the Project and provides a strategy for evaluating monitoring data and making informed, science-based decisions to modify monitoring as necessary. As required by Article 404, the AMP was drafted in consultation with the U.S. Fish and Wildlife Service, National Marine Fisheries Service, U.S. Coast Guard, Maine Department of Environmental Protection, and Maine Department of Marine Resources. ORPC also consulted with technical advisors, who were involved with the development of each of the elements of this Project. The AMP reflects the collaborative approach that has been an integral part of the Project since its beginning. Table 1 lists the members of the Adaptive Management Team (AMT) and their respective roles. Several former members of the AMT have changed positions within their organizations; therefore, ORPC is in the process of identifying appropriate replacements.

Table 1. Cobscook Bay Tidal Energy Project Adaptive Management Team

NAME	ORGANIZATION	ROLE	RESPONSIBILITY
Nathan Johnson	ORPC	Project Developer	Communication
Steve Shepard	U.S. Fish & Wildlife Service	Government Regulator	Compliance with established regulations
Sean McDermott	NOAA NMFS, Habitat Conservation Division	Government Regulator	Compliance with established regulations (Essential Fish Habitat)
David Bean	NOAA NMFS, Protected Resources Division	Government Regulator	Compliance with established regulations (Endangered Species)
Denis-Marc Nault	Maine Department of Marine Resources	Government Regulator	Compliance with established regulations

Daniel Hubbard/Michele DesAutels	U.S. Coast Guard, First District	Government Regulator	Compliance with established regulations
Lt. David Bourbeau	U.S. Coast Guard, Sector Northern New England	Government Regulator	Compliance with established regulations
Jim Beyer	Maine Department of Environmental Protection	Government Regulator	Compliance with established regulations
Jordan Carduner	NOAA NMFS, Office of Protected Resources	Government Regulator	Compliance with established regulations (Marine Mammals)
ADVISORY			
Gayle Zydlewski	University of Maine	Technical Advisor	Fisheries Monitoring
Moira Brown	New England Aquarium	Technical Advisor	Marine Mammal Monitoring
Jay Clement	U.S. Army Corps of Engineers	Government Regulator	Advisory

The collaborative approach that was adopted for the AMP was first utilized for the 2009 memorandum of understanding (MOU) between the State of Maine and FERC, that included a working structure to develop and permit Maine's first hydrokinetic power project. An important component of the MOU was to develop appropriate and cost effective environmental studies and monitoring plans. It was clear from the onset that knowledge of the eco-system and its many facets potentially affected by this new hydrokinetic power project would require new methods of inquiry to collect, monitor, and evaluate environmental data. Many of the new scientific methods that were developed for the Project have become a new basis for learning, and the scientific community has begun modifying approaches to environmental studies using these new methodologies in other programs. This learning has helped to bring the agencies and industry to a point where they have more tools to confidently address the needs of permitting of a commercial development. ORPC's AMP was designed to utilize not only the environmental studies at the Project site, but also environmental studies from other hydrokinetic projects and related studies from around the world.

ORPC's AMP recognized that many scientific uncertainties exist and that environmental conditions constantly change. The AMP, therefore, was designed to be modified within the Project time line and acknowledged that elements such as key environmental uncertainties, applied studies and institutional structure may evolve over time. The plan has worked well for the agencies, stakeholders, and ORPC as the Project evolved from a concept to the first pilot installation and operation.

The AMP summarized the minor and major license modification process required to make changes to environmental monitoring. ORPC strongly supported the involvement and concurrence of the AMT in applicable license modification requests, and the AMP process establishes a path to proceed in this manner.

2.2 2017 ADAPTIVE MANAGEMENT TEAM MEETING

ORPC met with the AMT on January 4, 2017 to provide an update on technology optimization as well as environmental monitoring.

Specific agenda items included:
- Introductions
- Brief overview of ORPC and Adaptive Management Team Experience to Date
- Cobscook Bay Tidal Energy Project update
- Western Passage Tidal Energy Project update
- Igiugig, Alaska Hydrokinetic Project update
- New DOE (DE-EE0007280) award for Advanced TidGen® System
  - Project description
  - Research to date (UMaine School of Marine Sciences update) and proposed environmental monitoring
  - Anticipated product benchmarking in both Cobscook Bay and Western Passage

Minutes from the January 4, 2017 AMT meeting are included in Appendix A. The presentation to the AMT, which includes an update from the UMaine, is included as Appendix B.

2.3 COBSCOOK BAY TIDAL ENERGY PROJECT LICENSE MODIFICATIONS

The Cobscook Bay Tidal Energy Project has successfully demonstrated the ability to modify license requirements based on knowledge gained, engagement and concurrence of the AMT, and clear communication with FERC.

Table 2 summarizes license modifications completed since 2013. It should be noted that modifications related to rated capacity and inspection and maintenance did not involve the Project's AMT.

Table 2. Summary of Cobscook Bay Tidal Energy Project license modifications

Submittal/License Article(s)	Requested Modifications	FERC Order Date
Exhibit A, Project Description and Operation	Rated capacity of the TidGen® Power System revised from 60kW to 150kW.	February 21, 2013
FERC Division of Dam Safety and Inspection - Article 306. Inspection and Maintenance	Clarification of inspection and maintenance activities and frequencies	April 8, 3013
2012 Environmental Monitoring Report - Article 405. Acoustic - Article 406. Benthic & Biofouling - Article 407. Fisheries and Marine Life Interaction - Article 409. Hydraulic - Article 410. Marine Mammal - Article 412. Bird	Modifications vary by license article but generally clarify monitoring plans or reduce frequency of monitoring surveys based on increased knowledge of species presence and environmental effects.	May 8, 2013
Temporary Variance Request - Article 405. Acoustic - Article 406. Benthic & Biofouling - Article 407. Fisheries and Marine Life Interaction - Article 409. Hydraulic - Article 410. Marine Mammal - Article 412. Bird	Hiatus in environmental monitoring during technology optimization phase	October 29, 2013
Temporary Variance Extension Request - Article 405. Acoustic - Article 406. Benthic & Biofouling - Article 407. Fisheries and Marine Life Interaction - Article 409. Hydraulic - Article 410. Marine Mammal - Article 412. Bird	Hiatus in environmental monitoring during technology optimization phase	December 22, 2014
Pilot License Extension	Two-year extension to existing 8-year pilot license	December 16, 2015
Temporary Variance Extension Request - Article 405. Acoustic - Article 406. Benthic & Biofouling - Article 407. Fisheries and Marine Life Interaction - Article 409. Hydraulic - Article 410. Marine Mammal - Article 412. Bird	Two-year hiatus in environmental monitoring during technology optimization phase	March 12, 2016

3.0 FISHERIES AND MARINE LIFE INTERACTION MONITORING (License Article 407)

The goal of the Fisheries and Marine Life Interaction Monitoring Plan was to collect pre-deployment and post-deployment information, provide an initial description of fish distribution and relative abundance within Cobscook Bay and supplement existing information for the general Passamaquoddy Bay area. Specific objectives included:

- Characterize fish presence and vertical distribution in Cobscook Bay with acoustic technologies
- Conduct stratified sampling to evaluate tidal cycle, diel, and seasonal trends
- Characterize fish distribution, species, and relative abundance and summer seasonal occurrence with multiple netting efforts in open-water pelagic and benthic areas, near-shore sub-tidal areas, and intertidal areas of outer, middle, and inner bays within Cobscook Bay
- Use data gathered to develop a preliminary assessment of the potential effects of the Project on fish populations in the Deployment Area and to the extent possible in Cobscook Bay
- Monitor indirect fish interactions with the TidGen® device(s) to evaluate potential Project effects
- Evaluate potential cumulative effects of the Project based on this comprehensive data set and the direct interaction monitoring data collected

The Project requires monitoring to assess potential effects of the TidGen® Power System on the marine environment. ORPC's monitoring plan regarding marine life has two parts: (1) Fisheries Monitoring Plan and (2) Marine Life Interaction Monitoring Plan.

Fisheries Monitoring Plan
The Fisheries Monitoring Plan is a continuation of research started by UMaine researchers in 2009. The study was designed to capture tidal, seasonal and spatial variability in the presence of fish in the area of interest (near the TidGen® device deployment site). The design involved down-looking hydroacoustic surveys during several months of the year, and examined the vertical distribution and relative abundance of fish at the project and control site (for relative comparison). Pre-deployment data were collected in 2010, 2011, and early 2012, and post-deployment data were collected from August 2012 through September 2013. Data from the Project site were compared to the control site to quantify changes in fish presence, density, and vertical distribution that may be associated with the installation of the TidGen® Power System.

Marine Life Interaction Monitoring Plan
As part of the Marine Life Interaction Monitoring Plan, ORPC uses side-looking hydroacoustics collected at the Project site to assess the interaction of marine life with the TidGen® device. This monitoring focuses on the behavior of marine life (primarily fish) as they approach or depart

from the region of the TGU and attempts to quantify changes in behavior in response to the TidGen® unit.

3.1 COBSCOOK BAY 2016

In 2016 UMaine's Fish Assessment Study Team continued processing, analyzing, and interpreting data collected at the Cobscook Bay Tidal Energy Project site in 2012-2014 as part of their DOE award (DE-EE0006384), *Interactions of aquatic animals with the ORPC OCGen® in Cobscook Bay, ME: Monitoring behavior change and assessing the probability of encounter with a deployed MHK device.* A final report was submitted to USDOE on

3.1.1 UNIVERSITY OF MAINE DATA ANALYSIS

The University of Maine's Fish Assessment Study Team conducted the following tasks in 2016:

- Completed analyses of data collected in 2014 associated with the OCGen® deployment. This included testing for differences in relative fish density and vertical fish distributions around the device. Manuscripts prepared (listed below): Staines et al. (to be submitted).

- Completed research of dB differencing methods on down-looking hydroacoustics data to separate Atlantic mackerel from swimbladdered fish. Analyses included previous stationary, down-looking hydroacoustics data from 2011-13 and data collected in 2014. Resulting methods from this research were used to remove zooplankton from all relative fish density estimates for all stationary, down-looking hydroacoustics data (2011-2014). Data analyses and interpretation can be found in the DOE report listed below: Zydlewski et al. 2016.

- Completed probability of encounter model and submitted manuscript. These analyses included stationary, down-looking hydroacoustics data from 2011-13, and 2014 data collected using stationary and mobile hydroacoustics. This work was published in *Renewable Energy* in 2016: Shen et al. 2016.

- Completed long-term, side-looking hydroacoustics data collection at TidGen® location. Analyses of fish response to a static device and long-term, temporal trends in fish densities have been accepted for publication in PLOSOne (Viehman and Zydlewski) and one more paper will be submitted to *Environmental Biology of Fishes.*. Haley Viehman's Dissertation is included as Appendix C.

- A final report was submitted to USDOE in October 2016: https://tethys.pnnl.gov/sites/default/files/publications/Zydlewiski-et-al-2016.pdf.

3.1.2 OTHER STUDIES

A Final Report was completed for a research project, titled "Behavioral Responses of Fish to a Current-based Hydrokinetic Turbine under Multiple Operational Conditions," in February 2017. The overall goal of this project was to monitor fish movements around an ORPC TGU, use the data to characterize the magnitude and ecological significance of behavioral responses, and investigate the potential variables driving the observed behavioral responses. This multi-year project spanning fiscal years (FYs) 2013–2016 was collaboration between Principal Investigator Mark Grippo (Argonne National Laboratory), Dr. Andrew Goodwin (U.S. Army Engineer Research and Development Center), Dr. Gayle Zydlewski (University of Maine), and Prof. Huijie Xue (University of Maine). The report describes activities to (1) collect hydroacoustic fish survey data, (2) produce high-resolution simulated flows for Cobscook Bay for the survey period, and (3) examine whether fish responded to visual and auditory stimuli generated by the turbine as well as natural and turbine-related changes in flows within the channel.

Key conclusions from the Report are:
- The hydroacoustic surveys indicated that there was a significant decline in fish density closer to the turbine beginning approximately 140 m from the free-spinning OCGen® prototype device.
- Noise and natural flow patterns appeared to be the most plausible explanations for the observed patterns in fish behavior.
- The Eulerian-Lagrangian-Agent Method (ELAM) analysis could not be conducted as planned, because the naturally high turbulence and flow in channel masked the hydrodynamic signal of the turbine. The ELAM is primarily used in rivers, and it appears to be less useful in large tidal applications with one turbine.
- The ELAM did suggest that natural flow patterns could reproduce the observed decline in fish density with decreasing distance to the turbine.
- The study provides additional confirmation that a single turbine is unlikely to result in more than negligible impacts to fish communities.

The full report is included as Appendix D.

3.2 IGIUGIG, ALASKA DATA ANALYSIS AND AUTOMATION
In 2016 the Pacific Northwest National Laboratory (PNNL) conducted a fish video data analysis of LGL's full fish event dataset that detailed fish interactions with ORPC's RivGen® Power System during July 19-25 and August 19-28, 2015 in Igiugig, Alaska. PNNL reviewed the quality of the data and developed a manual and automatic analysis of the Igiugig fish video data. The CBTEP Adaptive Management Team has followed the progress of the project in Igiugig and PNNL's assessment due to the relevance the work has to the overall body of knowledge of fish interactions with ORPC power systems.

ORPC participated in several Advisory Council meetings with PNNL and other technical advisors to discuss progress and results of the data analysis and algorithm development in 2016 and early 2017. These included a meeting to discuss progress reports in 2016 and presentations of preliminary results on February 10, 2017. PNNL's September 2016 Progress Report is included as Appendix E.

3.2.1   MANUAL DATA ANALYSIS

PNNL's presentation of preliminary manual data analysis was based on video data collected on July 22, 2015 (24 hrs). The following summarizes results of the analysis and is shown in Figure 5.

- PNNL defined:
  - daytime from 06:00 – 23:00
  - nighttime from 23:00 – 06:00 Processed data in 1 hr blocks
- Events were recorded as "fish" or "maybe" visualizations ("maybe" events were important for software development)
- Daytime files from 06:00 to 15:00 (missing 15:00 – 23:00)
- Nighttime files from 00:00 – 02:00 02:00 – 06:00 for first half-hour only (added interpolated next half-hour for 1 hr estimate) More fish events during nighttime than daytime More effort is required for nighttime processing
- The average number of events per hour for nighttime was ~300
- The average number of events per hour for daytime was ~30
- Based on number of recorded events there is an approximate order of magnitude effort increase for nighttime processing There are ~5.5 times more "maybe" events than "fish" events
- Processing first 10 minutes of each hour block seems to be valid, except for events that have numerous fish (smolt schools)
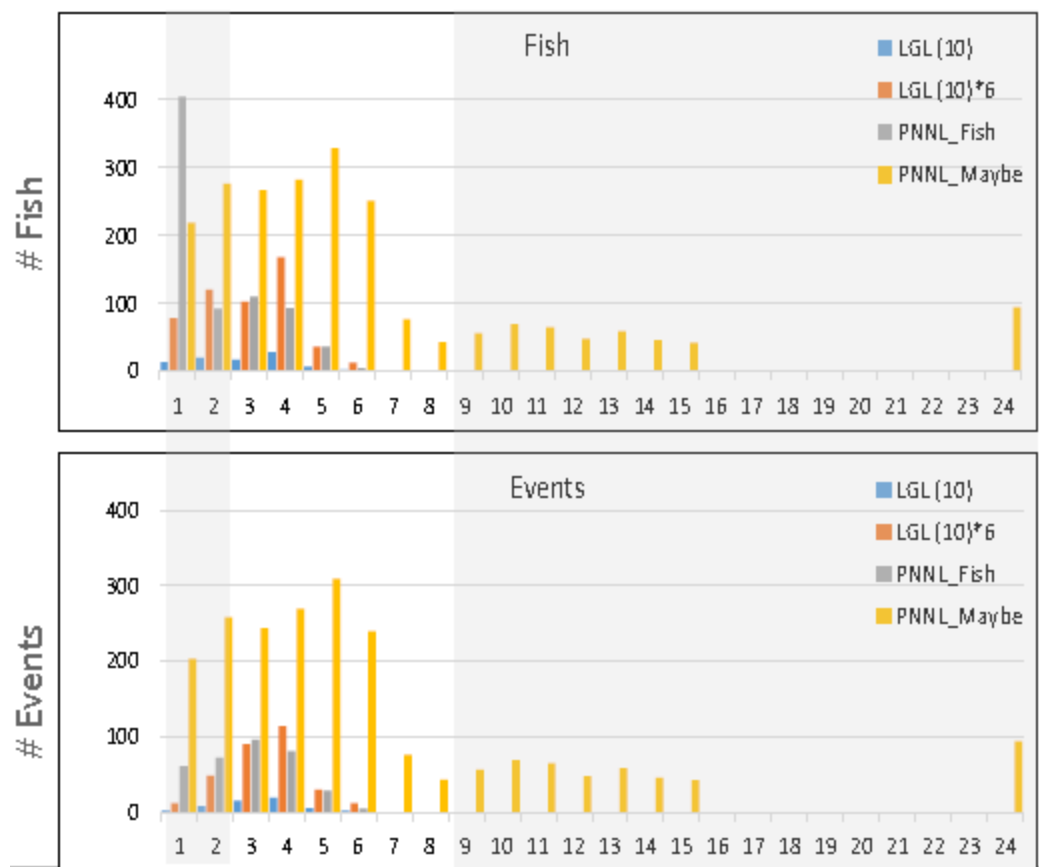
Figure 5. PNNL Manual Data Analysis for July 22, 2015

Preliminary on PNNL's manual data analysis for July 22, 2015 indicated:

- No "fish" during daytime
- Most "fish" and "maybe" events occur during nighttime
- Some single events had numerous fish
- Processing first 10 mins seems to be valid; except for events that have numerous fish (smolt schools)

3.2.2 ALGORITHM DEVELOPMENT

PNNL is developing algorithms to automate review of the 2015 Igiugig video data. The goal is to develop a process that will drastically reduce time and efforts associated with manual data analysis and contribute to future monitoring methods.

Research objectives include:

- Develop automated processing of underwater video to detect when fish are present in the scene.
- Detect 90% of all fish
- No more than 30% false positives

- Offline tool for efficient, consistent analysis
- Web-based video playback, download
- Fast-forward to fish using automation algorithms
- Annotations captured in database

Preliminary results indicate an ability to detect 94% of fish with 10% false positives for targets ("blobs") greater than 100 pixels. For targets or blobs greater than 5 pixels and less than 100 or equal to 100 pixels 81% of fish were detected with 82% false positives.

Table 3 summarizes progress to date and upcoming tasks associated with PNNL's algorithm development:

Table 3. Progress to date on PNNL tasks

Activity	Completion (2017)
Integrate statistical models	mid Feb
Complete optical flow investigation	early March
Combine background subtraction and optical flow	mid March
Process all analyzed data, evaluate performance	late March
Manuscript submitted for publication	early May
Integrate automated processing into EyeSea	TBD

3.3   DEVELOPMENT OF BEST AVAILABLE SCIENCE

Data analysis in 2016 by the ORPC team continued to grow the knowledge base of its power system interactions with the environment. This knowledge will inform the permitting and licensing process moving forward for ORPC's projects as well as the greater marine and hydrokinetic industry. This publically available information demonstrated continued progress in an industry where several years ago there was little or no information about environmental interactions of hydrokinetic devices.

The following products were completed by UMaine in 2016:

Viehman H, Zydlewski GB. Accepted. Multi-scale temporal patterns in fish passage in a high-velocity tidal channel. PLoS ONE.

Shen, H., Zydlewski, G.B., Viehman, H.A., Staines, G. 2016. Estimating the probability of fish encountering a marine hydrokinetic device. Renewable Energy 97: 746-756.

Viehman H, Zydlewski GB, Halteman W, Degan D. Complete - to be submitted. Behavior of fish near a static tidal energy device. Environmental Biology of Fishes .

Staines, G., G.B. Zydlewski, H. A. Viehman. *To be submitted*. Changes in relative fish density around a deployed marine hydrokinetic (MHK) device in Cobscook Bay, Maine. Estuaries and Coasts.

Reports

Zydlewski, G.B., Staines, G., Viehman, H., Shen, H., Altenritter, M. 2016. Interactions of aquatic animals with ORPC TidGen® in Cobscook Bay, Maine: Monitoring behavior change. DOE report 14 November 2016, budget period: 1/1/2015 – 6/30/2016.
https://tethys.pnnl.gov/sites/default/files/publications/Zydlewiski-et-al-2016.pdf

Copping, A.; Sather, N.; Hanna, L.; Whiting, J.; Zydlewski, G.; Staines, G.; Gill, A.; Hutchison, I.; O'Hagan, A.; Simas, T.; Bald, J.; Sparling, C.; Wood, J.; Masden, E.. 2016. Annex IV 2016 State of the Science Report: Environmental Effects of Marine Renewable Energy Development Around the World. pp 224. https://tethys.pnnl.gov/publications/state-of-the-science-2016

Staines, G., G.B. Zydlewski. 2015. Environmental Effects Monitoring Program for fish at the Fundy Ocean Research Center for Energy (FORCE). Prepared for SLR consultants for the Fundy Energy Research Network.

Presentations

Zydlewski, G.B., Staines, G., Viehman, H. Interactions of aquatic animals with the ORPC OCGen® in Cobscook Bay, Maine: Monitoring behavior change and assessing the probability of encounter with a deployed MHK device. Webinar 14 December 2016.

Zydlewski, G.B., Staines, G., Viehman, H., Shen, H., Altenritter, M. 2016. Interactions of aquatic animals with ORPC TidGen® in Cobscook Bay, Maine: Monitoring behavior change. DOE report 14 November 2016. Water Power Technologies Office Peer Review of Marine and Hydrokinetics Program. Presented on 14 February 2017.

ORPC made the following presentations in 2016 that included discussion of environmental monitoring of our power systems and the adaptive management process:

Johnson, N.E. 2016. Adaptive Management Webinar. *OES Annex IV, January 27.*

Ferland, J. 2016. Ocean Renewable Power Company Update. *Mandela Washington Fellowship for Young African Leaders, 20 July, Orono, ME*

Johnson, N.E. 2016. Ocean Renewable Power Company Update. *International Network on Offshore Renewable Energy (INORE), 2016 North American Symposium, 31 October, Orono, ME*

ORPC also continues to contribute project information to U.S. Department of Energy's Tethys website, which houses global data on ocean energy (http://mhk.pnl.gov/).

4.0   CONCLUSIONS AND RECOMMENDATIONS

In 2016 ORPC continued to focus on a technical optimization strategy that leverages lessons learned from multiple projects towards cross-platform designs and advanced design tools. Technological and operational experience gained through the OCGen® Module Mooring Project in Cobscook Bay, Maine, and the RivGen® Project in Igiugig, Alaska, will directly contribute to the optimized TidGen® Power System that is reinstalled in Cobscook Bay. This process has been bolstered by the award of DOE funding for the Advanced TidGen® Power System.

Despite the issuance of a temporary variance from FERC, this Environmental Monitoring Report addresses continued data analysis associated with the Cobscook Bay Tidal Energy Project and ORPC power systems in general.

4.1   THE ROLE OF ADAPTIVE MANAGEMENT

The Project continues to demonstrate the ability to modify license requirements based on the results of science based data collection, the engagement and concurrence of the AMT, and clear communication with FERC. This process has garnered international attention as a model for adaptive management.

ORPC met with the Project Adaptive Management Team on January 4, 2017 to provide an update on technology optimization as well as environmental monitoring data analysis.

4.2   ENVIRONMENTAL MONITORING RESULTS

The 2016 data analysis continued to build an increased knowledge of marine life interaction with ORPC Power Systems and indication of negligible environmental effects.

Fisheries and Marine Life Interaction
In 2016 UMaine's Fish Assessment Study Team continued research related to marine life interaction data around ORPC power systems. This work was supplemented by a research project titled "Behavioral Responses of Fish to a Current-based Hydrokinetic Turbine Under Multiple Operational Conditions." The overall goal of this project was to monitor fish movements around an ORPC TGU, use the data to characterize the magnitude and ecological

significance of behavioral responses, and investigate the potential variables driving the observed behavioral responses. In addition, ongoing data analysis by PNNL on video data collected in Igiugig, Alaska, in 2015 continues to build the knowledge of fish interactions with ORPC power systems.

Development of Best Available Science
Data analysis in 2016 by the ORPC team continued to grow the knowledge base of its power system interactions with the environment. This progress will contribute to informing the permitting and licensing process moving forward for ORPC's projects as well as the greater marine and hydrokinetic industry.

5.0   AGENCY REVIEW

5.1 AGENCY REVIEW PERIOD AND RESPONSES

The 30-day agency review period for the draft report ended on April 27, 2017. ORPC provided a reminder notice to the AMT on April 19, 2017. No comments were received from the AMT.

5.2 PUBLIC DISSEMINATION OF 2016 ENVIRONMENTAL MONITORING RESULTS

In accordance with ORPC's AMP, the 2016 Environmental Monitoring Report will be made available to the public. In addition to the Report being available on FERC's website, it will also be posted to ORPC's website. Hard copies of the full report will be available in ORPC's Eastport office and we will coordinate further dissemination with community organizations.

Appendix A

Adaptive Management Team Minutes, January 4, 2017

**Cobscook Bay Tidal Energy Project
ADAPTIVE MANAGEMENT TEAM
MEETING MINUTES
January 4, 2017**

Attendance: Dr. Gayle Zydlewski - University of Maine School of Marine Sciences; Nathan Johnson, Ocean Renewable Power Company; John Ferland, Ocean Renewable Power Company; Cian Marnagh, Ocean Renewable Power Company; Autumn Obomsawin, Ocean Renewable Power Company; Onni Irish, US Coast Guard; Jim Beyer ME DEP; Michele DesAutels, US Coast Guard; Lt. David Bourbeau, US Coast Guard; Denis-Marc Nault, Maine Department of Marine Resources

Participating by phone: Sean McDermott, NOAA; Steven Shepherd USFWS; Jeff Murphy and David Bean (NOAA NMFS)

Welcome and Introductions

The meeting began at 10:20 am. Participants introduced themselves, and then Nathan Johnson, ORPC, reviewed the agenda and the following meeting objectives:

- Provide a brief overview of ORPC and Adaptive Management Team experience to date
- Provide the Adaptive Management Team with an update on ORPC's Cobscook Bay Tidal Energy Project with specific regards to the FERC Pilot License and Maine General Permit
- Update the AMT on ORPC's Western Passage Tidal Energy Project with regards to the FERC Preliminary Permit
- Give a brief update on ORPC's Igiugig, Alaska Hydrokinetic Project update (IHP)
- Introduce the AMT to ORPC's new Department of Energy Award for Advanced TidGen® System.
- Dr. Zydlewski, University of Maine School of Marine Sciences, will provide an update on environmental monitoring research to date and propose environmental monitoring procedures based on previous experience.

ORPC and Adaptive Management Team Experience to Date

John Ferland, ORPC, gave a quick recap of the Adaptive Management Team meetings since 2012. He said that guidance and concurrence from the AMT has led to direct actions taken in the FERC permitting process. He stated that the permitting process for tidal energy in the U.S. is still evolving, and the adaptive management and advisory process is widely applicable and favorably received across the country. Additionally, technology development and deployments have informed the knowledge of environmental interactions with ORPC power systems.

Cobscook Bay Tidal Energy Project Update
10:25 AM
Mr. Johnson, ORPC, provided the following project update:

- The pilot license for the Cobscook Bay tidal site was originally an 8 year license issued in 2012. ORPC, with the concurrence of the AMT, received FERC approval to extend the license term to 10 years to accommodate the length of deployment and the license will now expire in 2022.

- ORPC filed for a Temporary Variance to its Environmental Monitoring plan in 2016 and has since continued to submit 4-month progress reports. ORPC will submit a 2016 Annual Environmental Report to FERC in the spring of 2017.
- ORPC will need to make a decision regarding the pursuit of a Commercial License for the site five years prior to the expiration of the pilot license.
- Due to current velocity levels at the Cobscook Bay site, ORPC believes that there is not a commercial development opportunity at this time.
- ORPC will formally notify FERC of our decision within the next several months.
- There is potential to use the site for other uses, including continued MHK testing. ORPC is seeking guidance from the AMT on this topic.
- Additionally, ORPC is planning for a temporary grid-connected deployment at the Cobscook Bay site as part of its Advanced TidGen® System project.

Ms. DesAutels asked if ORPC could use the Cobscook Bay site for testing up until the expiration of the Pilot License, even if not pursuing a commercial license. Mr. Johnson replied that we could.

Mr. Beyer asked if there were other types of technology that would benefit from the use of infrastructure at the Cobscook Bay site. Mr. Johnson thought that there were, especially since there is existing environmental monitoring data and cable infrastructure. Mr. Beyer remarked that he would like to see continued use of the pilings and cables. Mr. Johnson agreed and said he would characterize that infrastructure as an asset.

Ms. DesAutels asked if FERC would require us to remove the cable and other remaining infrastructure at the end of our license. Mr. Johnson said that they would, and Mr. Beyer agreed. Mr. Ferland added that we would seek additional guidance from FERC at that time, regarding the repurposing of the remaining infrastructure. He added that there are some existing regulatory options, such as the Verdant Exemption and others.

Mr. Nault thought that it would make sense for ORPC to retain its submerged land lease at the Cobscook Bay site.

Ms. DesAutels noted that Department of Energy recently awarded Oregon a wave energy test site, and wondered if the same application had been considered for Cobscook Bay. Mr. Ferland said that ORPC has advertised the site in such a way in the past, and that there are many such sites and that they coexist well with academic research. Mr. Johnson agreed, and added that the Cobscook Bay site would also be a great location for an underwater data storage center.

Dr. Zyldewski asked when the submerged land lease expired. ORPC indicated they would confirm (The submerged land lease term coincided with the original 8-year FERC liecense. Therefore it is scheduled to end in 2020).

Mr. Beyer said that the next use of the site will determine the permitting process we will go through. Mr. Bourbeau suggested the next intended purpose for the site could be to use it for MHK or other ocean energy testing. Mr. Nault added that there are few competing uses for the site, and that there is local support for ORPC's continued presence at the Cobscook Bay site.

Dr. Zyldewski wondered what regulatory regime would apply if a testing site were to be used without grid connection. Ms. DesAutels said it would then be an Army Corps site. Mr. Johnson added the Verdant exemption would apply. Mr. Beyer said the Maine Waterway Development and

Conservation Act could apply in that situation, but the National Resources Protection Act permitting process might be more suitable.

Mr. Nault added the build-out of the Downeast Institute (DEI), part of UMaine Machias will attract researchers from all over, and this type of marine research site could be very useful, of which marine energy testing could still be relevant. He said to contact Brian Beal.

Mr. Johnson thanked everyone for their feedback and said we would consult FERC on the possibility of using the Cobscook Bay site for MHK and other marine energy and marine biological testing.

Western Passage Tidal Energy Project
10:40 AM
Mr. Johnson then provided the following update regarding ORPC's WPTEP Project:

- FERC issued ORPC a preliminary permit for the Western Passage Tidal Energy Project on July 13, 2016
- The Advanced TidGen® System will be benchmarked at the Western Passage site following a temporary deployment in Cobscook Bay
- NREL will be taking resource measurements in Western Passage as a follow-on to its Marine and Hydrokinetic 'Hot Spots' Report in early 2017
- Current velocity and turbulence measurement data will become public following the completion of NREL's work. The work should last about three months.

Ms. DesAutels asked if the testing in Cobscook Bay would occur in the summer of 2017. Mr. Johnson said it would occur in late 2018, to which Cian Marnagh, ORPC, added that we will provide a detailed project timeline in the following slides. Ms. DesAutels thought it would be prudent for ORPC to notify regulators at least two years ahead of time in order to provide the proper notices to local stakeholders.

Mr. Beyer added that it is important to study turbulence at the site because it will likely affect the efficiency of ORPC's turbine. Mr. Johnson agreed, adding that the bathymetry in the Western Passage area is complex and the ebb and flood conditions are different. Additionally, Mr. Johnson said that understanding the site will benefit the whole industry.

Igiugig, Alaska Hydrokinetic Project
10:45 AM
Mr. Johnson gave a brief summary of the Igiugig Hydrokinetic project.

- ORPC filed a draft pilot license application with FERC in 2015
- ORPC deployed its RivGen® device in the Kvichak River in Igiugig in 2014 and 2015
- The Department of Energy has awarded follow-on funding to the Iguigig Village Council for work to improve the reliability and availability of the RivGen® for the next project. The work will address the impact of ice to turbine operation, and will seek to address regulatory concerns surrounding the impact of the turbine on salmon smolt.
- ORPC and partners gathered a voluminous data set from the site on fish/turbine interaction. This data is being processed by the Pacific Northwest National Laboratory. PNNL will be working with the University of Washington to develop an automated data review process using video.

Mr. Beyer asked if the data analysis project prevented us from deploying a device in 2016. Mr. Johnson said there was also a funding gap for field work. Mr. Ferland added that the RivGen® device, which was an early prototype, was also likely nearing the end of its operational life.

Advanced TidGen® Power System Project
10:50 AM

Mr. Marnagh then reviewed several slides regarding ORPC's new Department of Energy award for the Advanced TidGen® Power System. He explained ORPC's intent to integrate various subcomponent advancements into its next generation platform, and to validate overall system performance during a 12 month consecutive deployment at the Western Passage site. ORPC's technology progression includes the development of a low-RPM advanced control system for operation in turbulent conditions, several hydrodynamic improvements, and the integration of diamond bearings and an encapsulated generator from Rolls Royce Marine. Mr. Marnagh added that ORPC would be testing the new driveline and bearings at the University of Maine next month.

Mr. Beyer asked if the foils rotate (pitch) in the new design. Mr. Marnagh said that it would not be part of our Advanced TidGen® design, but would be part of a future design configuration.

Mr. Marnagh continued summarizing the technical goals of ORPC's new project. He explained that ORPC will test two different designs that can be towed to site and deployed, and that accompanying software development will allow ORPC to monitor stability during deployment. Mr. Johnson added that the original TidGen® deployment was successful but expensive, and challenging from engineering and environmental perspective. ORPC also had to file an Incidental Harassment Authorization (IHA) with NOAA for marine mammals, which is not anticipated for deployment of the new TidGen® configuration.

Ms. DesAutels asked how big the new TidGen® is compared to the footprint of the current site. Mr. Johnson said that the footprint of the new device will be slightly smaller than the previous generation due to a gravity foundation versus the previous fixed pile foundation. In addition, the Cobscook Bay site was permitted for a up to five devices. Dr. Zyldewski asked where within the Cobscook Bay site the new TidGen® will be installed. Mr. Johnson answered that it would likely be tested near to the OcGen®'s former test site. He added that the short term deployment in Cobscook Bay would be grid connected.

Mr. Marnagh then introduced the project timeline for the development of the Advanced TidGen®, including that one component of the project would be to work with DNV-GL to certify the new design. He added that the field testing and validation in Cobscook Bay would be critical to this process, as field testing yields different results than tank testing. Mr. Marnagh said his team expects to see 25 year life from the composite foils used in the design.

Mr. Marnagh then walked through the budget periods for the Advanced TidGen® project.
- Budget Period 1 focuses on System Feasibility and Design. This will include the bulk of certification work with DNV-GL. Certification will determine thresholds for reliability, performance, etc.
- Budget Period 2 includes the subcomponent and system build and short-term deployment at the Cobscook Bay site. Budget Period 2 will determine 'towability' and stability during deployment, including some subcomponent testing off a barge.

- Budget Period 3 will focus on operational monitoring of the Advanced TidGen® at the Western Passage site. This testing will prove that the 20 year life span of components is achievable. At the beginning of this Budget Period, ORPC will also outfit Western Passage with necessary electrical infrastructure. Mr. Johnson clarified that ORPC currently does not see the Western Passage deployment as being grid-connected.

Ms. DesAutels asked if the timeline was dictated by the DOE award. Mr. Johnson said yes.

Mr. Beyer said that ORPC would need to secure a pilot license by 2019. Mr. Johnson said that would be the case if the project is grid connected, however ORPC is still undecided on that aspect of the project. Mr. Beyer indicated that it might be difficult to secure a pilot license within two and a half years. Mr. Johnson said he anticipated the regulatory process to be similar to ORPC's Beta TidGen® testing, but that there are many factors to consider.

Mr. Johnson then explained environmental licensing and permitting approach to timeline. The first Budget Period will focus on reviewing permitting and environmental monitoring work to date and identify lessons learned. He introduced Dr. Zyldewski from the University of Maine School of Marine Sciences to present research findings to date.

UMaine Data Analysis
11:10 AM

Dr. Zyldewski outlined research to date, highlighting several works completed and ongoing. These included baseline environmental monitoring data collected at a control site in Cobscook Bay, as well as several studies on fish and turbine interaction. Mr. Johnson said that the advanced TidGen® will look the same from afar as the image in Dr. Zyldewski's slide 16. He added that turbulence monitoring to be undertaken during ORPC's Advanced TidGen® project has relevancy to fish monitoring as well. Dr. Zyldewski said another research goal is to determine seasonal variation in fish presence over time. She stressed that improving acoustic monitoring will help shape environmental monitoring protocols for the Western Passage Tidal Energy project as well as others.

Dr. Zyldewski introduced the research questions related to the environmental monitoring work undertaken in Cobscook Bay during ORPC's TidGen® and OcGen® deployments. The objectives of her research is to determine the effect of turbines on fish density and vertical distribution, to improve identification of fish species through new processing methods for hydro-acoustic datasets, and to develop an encounter probability model using the data collected over this time period.

Ms. DesAutels asked how marine scientists follow fish with a mobile transect. Dr. Zyldewski said that a control site was used to establish a baseline, and that model uses probability instead of tracking individual fish. Dr. Zyldewski explained that mobile transects record the fish very close to the TidGen® device, but that the monitoring equipment has a narrow beam which her team extrapolated to make the model.

Dr. Zyldewski gave a recap of the research work performed by Hayley Viehman, a former graduate student of the UM School of Marine Servives. Her research focused on determining fish behavior in front of and in the wake of the turbines at the Cobscook Bay site. Ms. DesAutels asked what tools researchers should use to predict fish to turbine interactions. Dr. Zyldewski said that this was one of their research questions. She added that additional meetings in the future would be help determine what metrics ORPC and regulators would want to use to develop monitoring regimes for

the new project. Mr. Johnson agreed, and said that as the Advanced TidGen® project moves forward ORPC will want to engage the Adaptive Management Team more frequently on such topics.

Dr. Zyldeski then reviewed several slides. She stated that the research found that the fish densities at the control site and project site are similar. During construction of ORPC's 2012 Cobscook Bay TidGen® deployment, fish may have been impacted by piling at site or other in-water activity, although the findings were not conclusive. Dr. Zyldewski explained that it was difficult to collect monitoring data when the TidGen® is operational because of acoustic interference. However, monitoring during non-operation is still valuable because it helps determine avoidance patterns of fish around TidGen®. Hayley Vehman collected data regarding fish orientation around device, and found that there is a slight divergence of fish relative to flow. Her research suggests that variation is larger directly in front of turbine.

Onni Irish, U.S. Coast Guard, asked how Dr. Zyldewski's team distinguished between a school of fish and individual fish in their data, and additionally how they distinguish between acoustic signatures of fish. Dr. Zyldewski clarified by saying that her team only looked at individual fish, not at schools of fish. She added that the target strength of fish moving through the beam is pretty low. Her team identifies species from data previously recorded from catching representative fish, and that signals were usually consistent. Her team groups fish based on similar target strengths, which she said are homogenous.

Mr. Beyer asked if the sample size identified fish bypassing the device. Dr. Zyldewski said that as you move further away from the turbine it gets harder to identify fish because of acoustic interference, which impacts useable data. Dr. Zyldewski said that mobile transects showed fish numbers declining on the approach to the turbine, and tracks showed fish going to the side. She added that she thinks the fish change direction farther away from the turbine to avoid it.

Dr. Zyldewski concluded that her team observed a slight change in behavior between 8-25 meters from device, representative of an avoidance pattern. She added that periodicity affects monitoring protocols, therefore it is important to take continuous measurements when possible. Dr. Zyldewski anticipates using this dataset to inform future surveying work in Cobscook Bay and likely in other sites as well. Her team concludes that there is a small amount of avoidance behavior in the range of 0-3 m in front of turbine, though small fish may simply pass through the turbine. Side looking sonar also showed slight movement in 7-15 m range. Diversion behavior is recorded in the 10-140 m range, with more diversion occurring on the further end. The behavioral effect footprint seems to be between 10-140 meters. Her team anticipates that more work will need to be done to determine different species' behavior.

Dr. Zyldewski posed several questions to be explored in further research: can researchers use knowledge of periodicity to inform sampling frequency? What is the change in seasonal passage rates according to the running mean of the data? Her team believes that a 24-hour survey with an informed baseline data set makes the most sense.

Mr. Beyer asked if Dr. Zyldewski's team looked at hourly fish abundance as they relate to the tidal cycle. Dr. Zyldewski said that the baseline data set was taken during same tidal cycle at the same time of day and night, therefore establishing consistent fish abundance in their sample.

Ms. DesAutels asked if fishermen would want to use this data to improve their catch for the area. Mr. Johnson said most likely, and that Dr. Zyldewski has previously held meetings with the fishing community to inform them on her team's work. Mr. Johnson added that there is not a big ground-

fishing industry at the Cobscook Bay site. Due to regional tidal dynamics, lobstering occurs outside of the high flow area. Scalloping and other dragging activities do occur in the area.

Mr. Nault agreed, adding that scallops generally avoid high flow areas. Mr. Nault asked if there were any river herring (Alosa) present in their data or mostly ocean herring. Dr. Zyldewski said marine herring. Ms. DesAutels asked if there would be an increase in marine boat activity in that area after completion of the Cobscook Bay Tidal Energy Project. Mr. Johnson said he did not anticipate that it would, and that the site is large and well-marked to aid navigation. He added that the local fishermen helped to inform the location of that site in order to minimize impacts to marine traffic. Mr. Nault added that the subsea cable in fact has a bigger commercial impact to dragging activities because geological conditions at the site sometimes prevent burying the cable.

Mr. Johnson stated that ORPC would like to do a survey of existing infrastructure as part of the Advanced TidGen® project. Observations in the area so far conclude that the additional structure from the CBTEP, as well as limitations on dragging has resulted in an increase in scallops, urchins and blue mussels, which has been favorably received by the local fishing industry.

Mr. Johnson briefly paused the presentation to ask if anyone on the phone had questions. There were no questions.

CBTEP Update Continued (ORPC slide 15)
11:50 AM

Mr. Johnson then reviewed additional slides pertaining to the environmental monitoring approach to the upcoming Advanced TidGen® project. He presented the outline of work to be completed during the budget periods of the project. The suggested approach is to continue taking moored stationary surveys of fish density at specific sites, along with seasonal mobile transects to monitor the flux of biomass, and physical sampling for pelagic species.

Mr. Beyer asked how a mobile transect is recorded across a current. Dr. Zyldewski remarked that it is difficult to do, but that a zig-zag transect might be possible. She added that it will take additional thought, but that it is crucial to obtain data when the tides are flowing. Detectability of fish will also be impacted by the current.

Mr. Johnson said that a lot of environmental monitoring data collected pertains to single device deployments. Developers and researchers are getting a better understanding of how to reduce environmental risk around single device, but eventually the protocols will have to be applied to arrays. Dr. Zyldewski suggested taking more transects during Budget Period two of the project. Mr. Beyer asked if the monitoring efforts would be undertaken in Cobscook Bay or at the Western Passage site, adding that the latter may be more important in order to establish a baseline. Mr. Nault added that depth, current, and fish presence at the site will be different than at the Cobscook Bay site.

Mr. Johnson agreed, adding that marine mammal monitoring will be a bigger part of the effort in Western Passage as opposed to the Cobscook Bay site. ORPC would like to incorporate passive acoustic monitoring during this project. It is anticipated that Dr. Moira Brown from the New England Aquarium will work with ORPC on monitoring for marine mammal presence, as well as the University of Maine. The goal is to test new fish monitoring techniques for validation in Cobscook Bay, and to gather baseline data in Western Passage at the same time. Mr. Nault asked if down-looking transects were used to collect environmental data. Dr. Zyldewski answered that the 24-

hour surveys were taken with down-looking transects. Mr. Johnson added that there were also surveys taken with bottom-looking transects. However, side-looking transects give a better sense of interaction between the turbine and the environment because you can see a profile across the turbine.

Mr. Beyer asked if the Adaptive Management Team would transition from providing guidance on the Cobscook Bay Tidal Energy Project to providing guidance on the Western Passage Tidal Project. Mr. Johnson said yes.

Lieutenant David Bourbeau, U.S. Coast Guard, asked what involvement ORPC has had with tribal entities. He suggested having them involved with and invited to Adaptive Management Team meetings in the future. He recalled there being significant commentary from the tribe during the permitting for the Downeast LNG project, as well as the Pennamaquin tidal project. Mr. Ferland said ORPC has consistently reached out to the Passamaquoddy Tribe throughout all of its activities in the Eastport area and Lt. Bourbeau's comments are timely as ORPC intends to continue to keep the tribe informed.

Mr. Johnson stated that the tribe had previously been granted a permit for a site near Western Passage, and one for a tidal barrage in Half Moon Cove. The tribe had also submitted comments to ORPC's Western Passage application with concerns about cultural impact. ORPC needs to determine the appropriate contact within the tribe as the project moves forward .

Steve Shepherd, U.S. Fish and Wildlife Service, added that waterfowl and eagle issues will be different in Western Passage than in the Cobscook Bay site. He stated that the highest density of eagles in Maine are found in the Western Passage area, and suggested that ORPC be prepared to monitor and determine use of those species as the site is developed.

Mr. Bourbeau asked what DNV-GL uses to benchmark its classification, and whether the rules were similar to the shipping industry. Mr. Marnagh said there is an overall hierarchy of rules. Mr. Ferland added that TC114 put together draft standards for MHK and Wave Energy Converter devices, and that DNV-GL and companion organizations are involved in that process as well.

ACTION ITEMS

Mr. Johnson reviewed the following action items from the meeting:

- ITEMS

Please note that ORPC has moved our office location in Portland in October 2016. Our new address is:

254 Commercial St., Suite 119 B
Portland, ME 04101

Adaptive Management Team Presentation, January 4, 2017

Ocean Renewable Power Company

Presenting to

**Cobscook Bay Tidal Energy Project
Adaptive Management Team Meeting**

January 4, 2017

ORPC
**OCEAN RENEWABLE
POWER COMPANY**

Meeting Agenda

- Introductions
- Brief overview of ORPC and Adaptive Management Team Experience to Date
- Cobscook Bay Tidal Energy Project (CBTEP) update
- Western Passage Tidal Energy Project (WPTEP) update
- Igiugig, Alaska Hydrokinetic Project (IHP) update
- New Department of Energy (DOE) award for Advanced TidGen® System
  - Project description
  - Research to date (UMaine School of Marine Sciences update) and proposed environmental monitoring
  - Anticipated product benchmarking in both Cobscook Bay and Western Passage

ORPC
OCEAN RENEWABLE
POWER COMPANY

ORPC and Adaptive Management Team Experience To Date

- Meetings annually since 2012
- Guidance and concurrence from the AMT has resulted in FERC license modifications and associated actions
- International interest garnered in CBTEP adaptive management process
- Technology development and deployments have informed the knowledge of environmental interactions with ORPC power systems

ORPC
OCEAN RENEWABLE
POWER COMPANY

CBTEP Update

- Commercial License Decision

  FERC requires a pilot license holder to apply for a commercial license five years prior to the expiration:
  - The CBTEP pilot license will expire in February 2022.
  - ORPC believes the velocity levels do not support commercial site development at this time.
  - ORPC will formally notify FERC of our decision this month
  - ORPC is exploring other site use options (e.g. continued MHK testing) and is interested in Adaptive Management Team feedback on this topic
- Temporary Variance
  - ORPC continued to submit 4-month progress reports in 2016
  - 2016 Annual Environmental Report will be submitted to FERC in spring 2017
- Planning temporary, grid connected deployment as part of Advanced TidGen® System project.

ORPC
OCEAN RENEWABLE
POWER COMPANY

Western Passage Tidal Energy Project

- New Preliminary Permit (P-14743)
  - FERC issued ORPC a preliminary permit for the Western Passage Tidal Energy Project on July 13, 2016
  - The Advanced TidGen® System will be benchmarked at the site following the temporary deployment in Cobscook Bay
- National Renewable Energy Laboratory (NREL) MHK Resource Characterization
  - NREL's Marine and Hydrokinetic (MHK) "Hot Spots" report identified Western Passage as a premier tidal energy site
  - ORPC Solutions will support NREL to conduct current velocity and turbulence measurements near Western Passage in early 2017. The data will be publically available and benefit the industry's understanding of the resource

Igiugig Hydrokinetic Project

- Draft pilot license application filed with FERC in 2015
- Successful in water deployments in 2014 and 2015
- DOE award to the Igiugig Village Council
- PNNL Data Analysis and Automation Project

ORPC
OCEAN RENEWABLE
POWER COMPANY
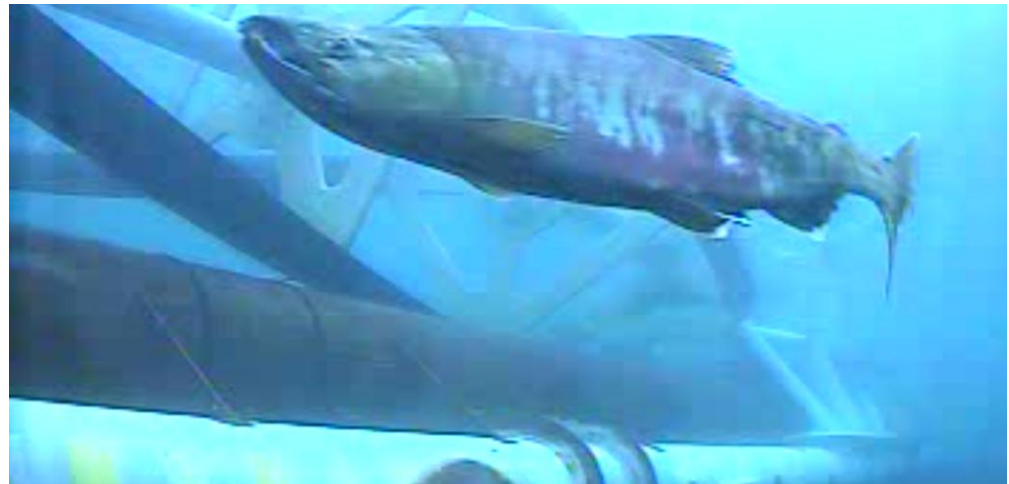
New DOE Award: Advanced TidGen® Power System

Project Team: Maine Marine Composites, Composites Engineering Research Laboratory, University of Maine School of Marine Sciences, Montana State University, DNV GL, BluSource Energy & Aerocraft

Project's key idea: Successfully develop, test, and integrate MHK subsystems and validate a full system in a commercial site over twelve months verifying the Project's LCOE target.

Goals:
- Design, construct, test and verify subsystems
- Perform system integration; verify system performance
- Validate system reliability and availability during a continuous twelve month deployment

Technology Impact:
- Demonstrate the economic viability in markets with high cost of electricity,
- Provide practical demonstration that the system is technically and economically viable, with limited environmental impact.

ORPC
OCEAN RENEWABLE
POWER COMPANY

Advanced TidGen® Power System

- ## System Integration
    - A commercial ready system that builds off the success and lessons learned from previous technology platforms
    - Both Cobscook Bay and Western Passage will be benchmark sites

ORPC
OCEAN RENEWABLE
POWER COMPANY

Advanced TidGen® Device

Buoyancy Pod/fairing

Generator supplied by Rolls Royce Marine

Low RPM Advanced Control System

Tension Mooring Lines

Gravity anchors
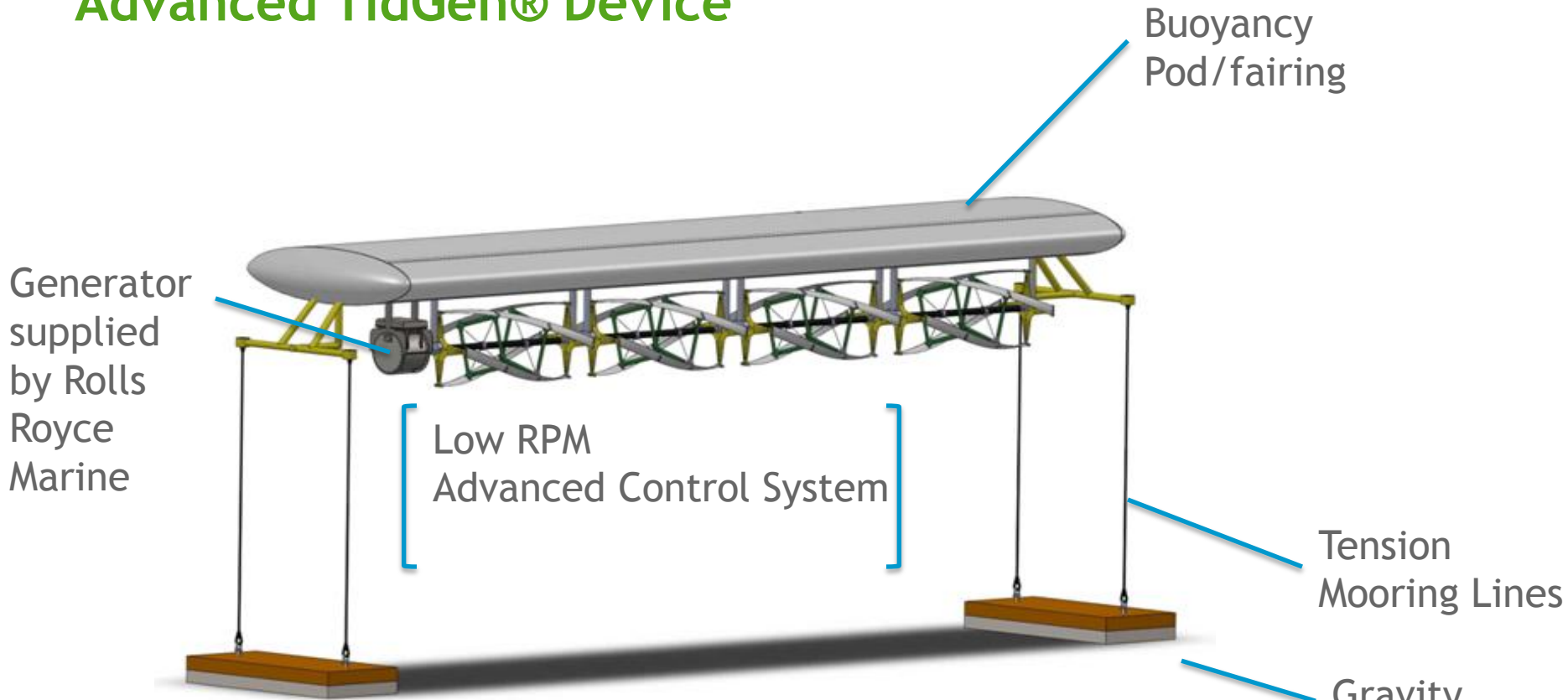
- Prototype successfully deployed and environmentally monitored in Cobscook Bay, 2014
- Easier and less expensive to install and retrieve
- Less intrusive foundation system compared to previous design

ORPC
OCEAN RENEWABLE
POWER COMPANY

Advanced TidGen® Power System Timeline

Contract Award
(Sep 2016)

Budget Period 1
(Jan 2017)

Budget Period 2
(Apr 2018)

Budget Period 3
(Sep 2019)

Decommissioning
(Oct 2020)

ORPC selected for award negotiations

Contract signed, effective Nov. 1, 2016

BP1: Design

Full system detail design and test planning

BP2: Build & Verify

Subsystem field testing (Q2-Q3 2018), full system deployment in Cobscook Bay (Q2 2019)

BP3: Field Validation

12 month deployment in Western Passage (2019 to 2020)

Project complete Jan 2021

ORPC
OCEAN RENEWABLE
POWER COMPANY

Advanced TidGen® Power System– Environmental Approach

BP1
- System Feasibility and Design
- 13 months + 3 month review period OR 16 months

BP2
- Technology Completion, Validation and Monitoring (CBTEP site)
- 14 months + 3 month review period OR 17 months

BP3
- Operational Monitoring (WPTEP site)
- 17 months

ORPC
OCEAN RENEWABLE
POWER COMPANY

Environmental Approach

Budget Period 1: System Feasibility and Design (13 months + 3 month review period)

Focus Area 1: Review what has been done and identify lessons learned

- Permitting process
- *Research* results
- How were results used in the process?

www.orpc.co

ORPC
OCEAN RENEWABLE
POWER COMPANY

Environmental Approach

Previous Research Experience

- Density estimates at control and impact sites
- Near field (acoustic camera) assessment of fish interactions with MHK foils
- Physical capture of fish (trawling)
- Continuous monitoring near device (side-looking sonar)
- Mobile seasonal transects

ORPC
OCEAN RENEWABLE
POWER COMPANY

Environmental Approach

- UMaine Data Research update (Insert Slides)

www.orpc.co

Environmental Approach

Budget Period 1: System Feasibility and Design

Focus Area 2:Determine *monitoring* methods for new deployment

- How can results be used to inform future deployment?
- Conduct cost and risk analysis

Environmental Approach

Suggested approach for this deployment and assessment of future thresholds for decision-making:

- Continued density estimates at specific sites (moored, stationary surveys)
- Seasonal mobile transects – flux of biomass (monitoring of fish approaching device)
- Physical sampling for pelagic species – species identification (best idea of species present)
  - Passive acoustics and visual observations for marine mammal presence MARU to monitor low frequency calls (baleen whales)
  - PAM for high frequency calls (porpoises)

www.orpc.co

Environmental Approach

Budget Period 1: System Feasibility and Design

Focus Area 3: Determine thresholds based on new *monitoring* methods

- What are acceptable metrics and thresholds for this single deployment and future deployment in other locations or arrays?

- Define acceptable monitoring approach

Environmental Approach

Budget Period 1: System Feasibility and Design

Planning for environmental monitoring:

- Conduct preliminary testing of new metric approach (mobile transects cross- and along-Passage)

- Finalize monitoring approach

- Finalize Test Plan

- Integrate equipment with engineering plans

ORPC
OCEAN RENEWABLE
POWER COMPANY

Environmental Approach

Budget Period 2 : Technology Completion, Validation and Monitoring (14 months + 3 month review period)

Validate new methods
•Purchase equipment as needed
•Test survey in Cobscook Bay

Conduct initial monitoring
Environmental monitoring- based on suggested approach

Adaptive Management Team
Assessment of thresholds for decision-making

ORPC
OCEAN RENEWABLE
POWER COMPANY
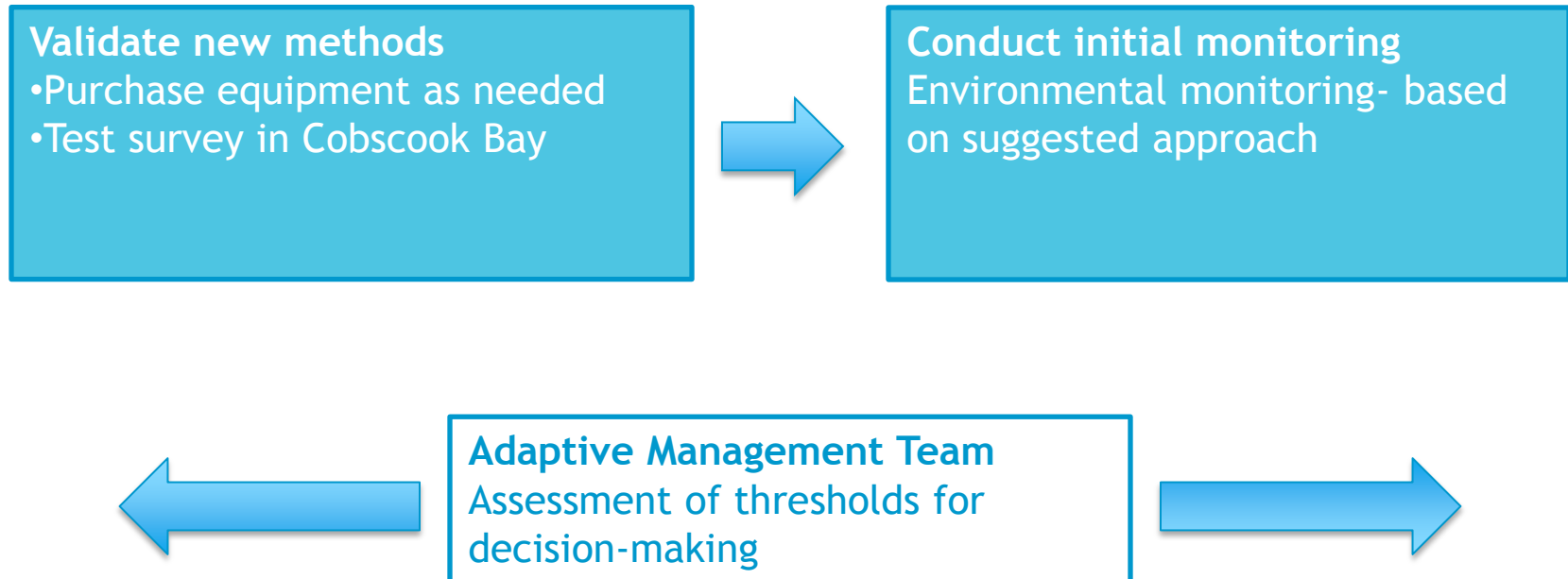
Environmental Approach

Budget Period 3 : Operational Monitoring (17 months)

Environmental monitoring - based on suggested approach
- Fish
    - Density trends
    - Flux of biomass moving past a single device
    - Separation by species
- Mammals
    - Passive acoustic monitoring
    - Visual observations
    - Video with stationary hydroacoustic surveys

Environmental analysis

Finalize decision-making process for other MHK sites and arrays

Questions and AMT Guidance

Thank you

Ocean Renewable Power Company

ORPC
OCEAN RENEWABLE
POWER COMPANY

Appendix C

Hydroacoustic Analysis of the Effects of a Tidal Power Turbine on Fishes, Haley A. Viehman, December 2016

HYDROACOUSTIC ANALYSIS OF THE EFFECTS

OF A TIDAL POWER TURBINE ON FISHES

By

Haley A. Viehman

B.S. Cornell University, 2009

M.S. University of Maine, 2012

A DISSERTATION

Submitted in Partial Fulfillment of the

Requirements for the Degree of

Doctor of Philosophy

(Interdisciplinary in Engineering and the Natural Sciences)

The Graduate School

The University of Maine

December 2016

Advisory Committee:

    Gayle B. Zydlewski, Associate Professor of Marine Science, Co-advisor

    Michael Peterson, Professor of Mechanical Engineering, Co-advisor
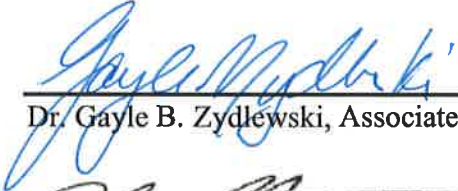
    Huijie Xue, Professor of Marine Science

    William Halteman, Professor Emeritus of Mathematics and Statistics

    Donald Degan, President of Aquacoustics, Inc.

DISSERTATION ACCEPTANCE STATEMENT

On behalf of the Graduate Committee for Haley Viehman, I affirm that this
manuscript is the final and accepted dissertation. Signatures of all committee members
are on file with the Graduate School at the University of Maine, 42 Stodder Hall, Orono,
Maine.

Dr. Gayle B. Zydlewski, Associate Professor of Marine Science   11-22-16
                                                                                Date

Dr. Michael Peterson, Professor of Mechanical Engineering   11-22-16
                                                                                Date

LIBRARY RIGHTS STATEMENT

In presenting this dissertation in partial fulfillment of the requirements for an advanced degree at the University of Maine, I agree that the Library shall make it freely available for inspection. I further agree that permission for "fair use" copying of this dissertation for scholarly purposes may be granted by the Librarian. It is understood that any copying or publication of this dissertation for financial gain shall not be allowed without my written permission.

Signature: *Haley Viehman*

Date: *11/27/2016*

HYDROACOUSTIC ANALYSIS OF THE EFFECTS

OF A TIDAL POWER TURBINE ON FISHES

By Haley Viehman

Dissertation Co-Advisor: Dr. Gayle Zydlewski
Dissertation Co-Advisor: Dr. Michael Peterson

An Abstract of the Dissertation Presented
in Partial Fulfillment of the Requirements for the
Degree of Doctor of Philosophy
(Interdisciplinary in Engineering and the Natural Sciences)
December 2016

Tidal currents help shape coastal marine environments and are essential in the life cycles of many marine and diadromous fishes. Areas with strong tidal currents are also targeted by humans for energy extraction via marine hydrokinetic (MHK) turbines. The effects of these devices on fishes are difficult to predict because the presence and behavior of fish within fast tidal currents is largely unstudied. Based at a tidal energy site in Cobscook Bay, Maine, this work sought to characterize nearfield fish responses to an MHK device, to describe the natural presence of fish at the site, and to provide guidance for monitoring MHK device effects in these highly dynamic environments. A bottom-mounted hydroacoustic echosounder monitored the behavior of fish 7-14 m away from the static MHK device for several weeks. Fish mainly moved with the current, but those approaching the device showed signs of avoidance via slight divergence from the main current direction. The same echosounder was used to collect a two-year time series of hourly fish passage rate at turbine depth after device removal. Fish passage rate, and therefore potential encounter rate with the turbine, varied greatly over multiple time scales, and reflected the dominant environmental patterns, including tidal, diel, lunar, and seasonal cycles. When simulated discrete surveys of fish presence were informed by

these cyclic components (e.g., 24-hr surveys occurring at the same lunar stage throughout the year), variation in the results was reduced. This approach to discrete survey design at tidal energy sites could increase the power of before-after-control-impact comparisons to detect device effects without requiring expensive continuous or high-frequency sampling over the long-term. Additionally, deconvolution techniques applied to narrow-angle (7°) single beam data yielded target strength distributions comparable to corresponding split beam data. Depending on study aims, the use of single beam echosounders could substantially reduce study costs while supplying sufficient information on device effects for use in management decisions. Results from Cobscook Bay are likely applicable to other study sites with similar environmental forcing, but study designs and results should be considered in the context of each site's fish assemblage.

Finally, I wish to thank my friends and family for their endless love and support.

TABLE OF CONTENTS

LIST OF TABLES

LIST OF FIGURES

CHAPTER 1

FISH BEHAVIOR NEAR A STATIC TIDAL ENERGY DEVICE

1.1 Abstract

Tidal energy is a developing form of renewable energy that uses free-standing turbines to generate electricity from tidal currents. The effects of these marine hydrokinetic (MHK) devices on fish are uncertain but of concern. Interactions of fish with MHK devices, such as avoidance, evasion, blade strike or aggregation, depend on where and how individuals detect and respond to the device. We investigated the responses of fish to a non-operational (static) MHK device in Cobscook Bay, ME, USA. Using a bottom-mounted, side-looking, split beam hydroacoustic echosounder, we observed the horizontal movements of fish in an area spanning 7-14 m from the face of the turbine. The fish detected were generally small (on the order of a few cm in length), and moved almost exclusively with the tidal current. However, when fish were approaching the device, the presence of the static turbine resulted in a greater difference between their movement and that of the current, suggesting avoidance. This divergence of fish movement from the current was present both day and night, suggesting that fish used visual as well as non-visual (e.g., hearing or lateral line) cues to avoid the obstacle. When fish were departing from the device, we detected no significant changes in their horizontal movement relative to fish behavior. Together, these data suggest that fish avoidance behavioroccurred as far as 18 m upstream of the static device and wake effects on behavior did not extend beyond 7 m downstream. Operating turbines would emit different physical cues than a static one, and responses would likely differ under those conditions as well as with fish species and life stage. More information on the visual,

acoustic, and hydrodynamic signatures of MHK devices (static and operational), and sensory response thresholds of the fish likely to encounter them, could inform future efforts to better understand behavioral responses. Further mechanistic understanding of cues and their relation to behavior change would aid in predicting effects of single devices and commercial arrays on individual fish and populations.

1.2 Introduction

Tidal energy is a form of renewable energy converts the kinetic energy of water currents generated by tidal forces to electricity, using free-standing underwater turbines. Any fast-flowing water can be used in this way, including ocean currents, tidal streams, and rivers (Charlier and Finkl 2010). Many different marine hydrokinetic (MHK) devices have been designed for this purpose, and generally consist of one or more large turbines and a static support frame or mooring system holding the turbine(s) in place. Though difficult to estimate, globally, MHK devices may be able to generate up to 180 TWh of energy per year if all sites were fully developed (Jacobson 2009; estimate excludes riverine applications).

As tidal currents are considered for renewable energy development, concerns arise regarding the effects of MHK devices on the environment. Deploying MHK structures in fast-moving ocean (or river) currents is likely to affect the surrounding ecosystem, but because very few MHK devices have been deployed worldwide, their actual effects are not yet well understood (Boehlert and Gill 2010, Copping et al. 2016). Harvesting energy from tidal currents may cause changes to the physical environment, including flow patterns (Rao et al. 2016, Shapiro 2011), water quality (Wang et al. 2015), sediment transport (Martin-Short et al. 2015), and underwater noise and electromagnetic

fields (Boehlert and Gill 2010). Such environmental alterations may in turn have implications for the biotic components of the ecosystem, including seabirds (Waggitt and Scott 2014), benthic organisms (Broadhurst and Orme 2014), and pelagic animals (e.g. marine mammals and fish; Gill 2005).

Fish are a key biological component of marine ecosystems and coastal economies, both of which could be affected by MHK devices. Many fish species target the same strong tidal currents ideal for tidal energy extraction to carry out large-scale movements to complete their life cycles (Gibson 2003). Potential effects of MHK devices are diverse and numerous, from direct effects, such as strike by rotor blades, to less direct effects, such as population-level responses to altered physical environments or disruption of migratory pathways (Copping et al. 2016, Boehlert and Gill 2010, Gill 2005). Simply adding structure to a dynamic environment could also provide new shelter and prove to be an attractant (Čada and Bevelhimer 2011, Broadhurst et al. 2014, Kramer et al. 2015, Inger et al. 2009).

Effects of MHK devices on fish can occur on multiple spatial and temporal scales, and these effects are being explored with a combination of laboratory and field studies. In the laboratory, fish responses to MHK turbines can be examined at very close-range (within 1-2 m), blade strike can be observed, and rates of survival and injury of entrained fish can be calculated, which is currently virtually impossible in a field setting. These flume laboratory studies indicate high survival rates (>90%) for the species entrained in MHK turbines, with behavior, injury, and survival being species- and size-dependent (Amaral et al. 2015, Castro-Santos and Haro 2015). Efforts in the field have so far focused on two spatial scales: the near-field (within the first few meters of MHK

3

devices), and the far-field (the general area of MHK devices, e.g. >10 m away). Near-field studies of fish interactions with MHK turbines in the field echo results of laboratory studies, finding that behavior approaching a turbine depends on fish size, species, and turbine visibility (Hammar et al. 2013, Bevelhimer et al. 2015, Viehman and Zydlewski 2015a). Farther-field studies (hundreds of meters from MHK turbines) have focused on predicting the probability for spatial and temporal overlap of MHK turbines and fish based on natural fish distributions. These studies indicate that the probability of interactions varies on a wide range of temporal scales (Seitz et al. 2011, Bradley et al. 2015, Staines et al. 2015, Shen et al. 2016, Viehman et al. 2015, Viehman and Zydlewski 2015b, Chapter 3).

A gap in knowledge exists between the near-field (within meters) and the far-field (hundreds of meters) of MHK devices. Shen et al. (2016) made progress toward linking these two spatial scales in the field by conducting hydroacoustic transects over an MHK device, analyzing fish presence in the space from 10 m to 200 m upstream of the turbine. The numbers of fish detected over this distance showed some evidence of avoidance beginning as far as 140 m upstream. Shen et al. (2016) combined data on the vertical distributions of fish in the region (Staines et al. 2015, Viehman et al. 2015) with near-field behavioral observations (Viehman and Zydlewski 2015a) to model the probability that fish would encounter the device. They concluded that the probability of fish upstream of the device encountering the turbine was 0.058 (0.043, 0.073 = 95% CI), and the probability of entrainment in the turbine was on the order of 0.028 (0.022, 0.037). This model relied on what was known of fish behavior as they approach the device at distances less than 10 m (Viehman and Zydlewski 2015a), but there remains a need to

determine at what ranges, beyond 10 m, fish begin to respond.   This distance depends on many environmental and biological factors, including (but not limited to) how the device alters the physical environment, the ability of the life stages of fish species present to sense those alterations, how individual fish perceive the device (e.g., as a threat to be avoided), and the ability of individuals to control their movement within the tidal current (Lima et al. 2015, Weihs and Webb 1984, Kim and Wardle 2003).

The presence of a static MHK device, be it the unmoving structural components or the turbine itself during slack tides, may affect fish and the surrounding ecosystem (Boehlert and Gill 2010, Copping et al. 2016, Frid et al. 2012). Very little has been published on the effects of the MHK device infrastructure. However, other static offshore platforms have been reviewed in this context (Kramer et al. 2015). The static portion of MHK devices could act as an artificial reef, providing hard surfaces for the attachment of sea life and shelter for various species, including fish (Broadhurst and Orme 2014, Wilhelmsson and Langhamer 2014). Hydraulic shelter is structure that creates areas of low-velocity water in an otherwise high-velocity flow field, and has mainly been examined in the context of river channel usage by resident and migratory fishes (Čada and Bevelhimer 2011). Some evidence of the use of MHK device structures as hydraulic shelter in tidal flows has been reported. Viehman and Zydlewski (2015a) observed fish pausing within the wake (within 3 m) of a test MHK device in the field, but because the fish were quite small it was unclear whether this was voluntary use of shelter or if the fish were caught within the turbulent flow. Broadhurst et al. (2014) found that pollack (Pollachius pollachius) aggregated around an MHK device, particularly at lower current speeds (< 2 m·s^{-1}). They speculated that predatory fish like these may be inclined to use

the sheltered area downstream of such obstacles to lie in wait for passing prey, a common predation method in many fish species. Aggregation of fish downstream of MHK device structures may have effects at higher trophic levels, where marine mammals and diving birds could also target areas adjacent to MHK turbines to forage (Waggitt and Scott 2014, Williamson et al. 2015).

This study examines the behavior of fish in the vicinity of a static MHK device at distances between those examined by near-field and far-field studies that have occurred to date, 7-14 m from the turbine face. Fish behavior was observed with a bottom-mounted split-beam echosounder, both in 2013 when a complete MHK device was present (i.e. bottom support frame and turbine, with the brake applied and therefore static) and in 2014 when the turbine was absent from the device (only the bottom support frame remained). Fish behavior was examined upstream and downstream of the MHK turbine, the former for signs of avoidance and the latter for signs of wake effects such as those seen by Viehman and Zydlewski (2015a). Upstream observations made at this static MHK device may be applied to understand fish behavior at an operational device. For example, the range at which fish detect and react to a static MHK device may represent a minimum distance of detection and avoidance for a rotating, power-generating MHK turbine.

1.3 Methods

The MHK device studied was the Ocean Renewable Power Company, LLC (ORPC) TidGen® Power System (Fig 1.1). The system consists of four helical cross-flow rotors aligned along a central axis, with a permanent magnet generator at the center. Each rotor has a diameter of 2.8 m and length of 5.6 m. A bottom support frame holds

the turbine 6.7 m above the sea floor, for a total device height of 9.5 m. When

operational, this turbine begins to rotate at current speeds of approximately 1 m·s^{-1} (from

either direction), with a maximum rotational velocity of approximately 40 rpm (ORPC

2013). A device of this design was deployed in Cobscook Bay, Maine, in August 2012.

It operated until the brake was applied to the turbine in April 2013, after which time the

turbine did not rotate (was static). The turbine was removed in July 2013, though the

bottom support frame remained on the sea floor. This study used data collected while the

turbine was present but static (April to July 2013), and data collected at the same time the

following year (April to July 2014), when only the bottom support frame was present.
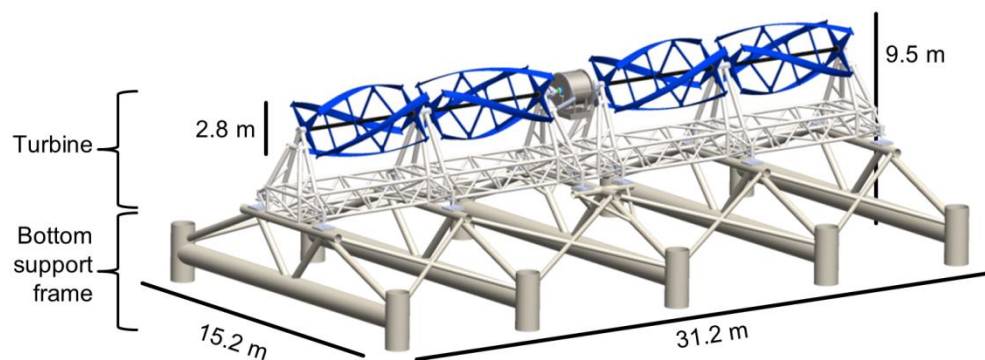
Fig 1.1 Ocean Renewable Power Company's TidGen® Power System. The TidGen® was
deployed in outer Cobscook Bay, Maine from August 2012 to July 2013.

The TidGen® was deployed in outer Cobscook Bay, Maine (Fig 1.2). At this

location, the tidal range is approximately 6 m, and current speed ranges from 0 to

approximately 2 m·s^{-1} over the course of a tidal cycle (Viehman et al. 2015, Brooks

2006). In Cobscook Bay, the fish community changes dramatically over the course of a

year, with strong seasonal cycles in both the species and life stages of fish present (Vieser

2014). The extensive intertidal areas of the inner bays are highly productive and serve as

nursery habitats for the juveniles of many fish species. Based on physical sampling in

May and June 2013 (Vieser 2014), fish present while the turbine was present and static

were likely to be mainly larval Atlantic herring (*Clupea harengus*) and juvenile winter flounder (*Pseudopleuronectes americanus*), as well as a lesser number of juveniles of several other species. Physical sampling at the site in May 2014 (while the turbine was absent) mainly captured juvenile red hake (*Urophycis chuss*) and adult Atlantic herring (Zydlewski et al. 2016).
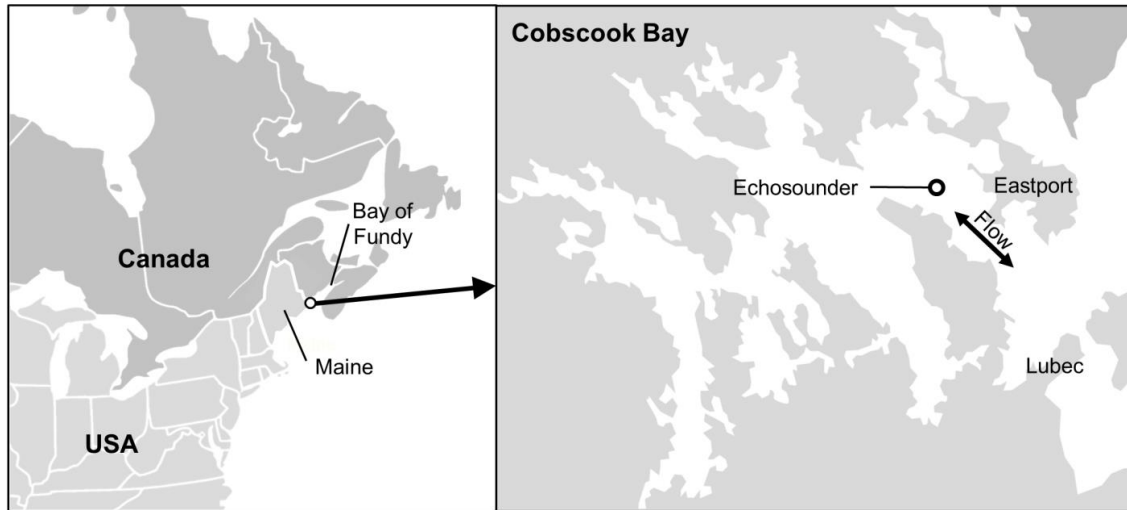
Fig 1.2 Map of study area. Location of bottom-mounted echosounder shown in right panel, at the location of Ocean Renewable Power Company's TidGen® Power System.

Acoustic data were collected using a calibrated 200 kHz, 7° split beam Simrad EK60 echosounder installed by ORPC in August 2012 on the sea floor near the TidGen® bottom support frame (Fig 1.3). The echosounder was mounted 3.3 m above the sea floor, 45.7 m from the TidGen® support frame, and angled 6.2° above horizontal. The transducer was angled away from the turbine using a pan and tilt unit until most backscatter from the turbine support structure was no longer visible in the echogram (approximately 10.2° between the acoustic beam's central axis and the face of the turbine). The echosounder sampled an approximately conical volume of water 5 times per second, using a pulse duration of 0.256 ms and transmit power of 120 W. The current flowed approximately perpendicular to the sampled volume, though this varied slightly

between ebb and flood tides (Fig 1.3b). Most fish moved with the current and were

therefore detected by several sequential pings as they passed through the acoustic beam,

even at peak tidal flows.
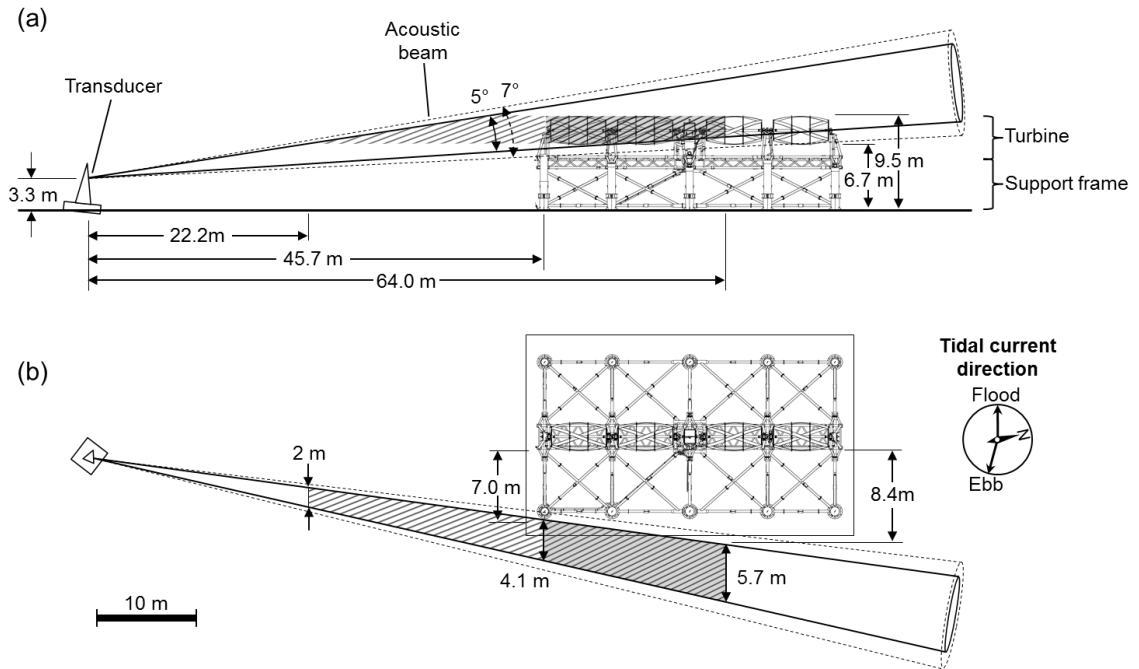
Fig 1.3 Echosounder and TidGen® setup. (a) Side view; (b) view from above. The "turbine" zone of the sampled volume is indicated by the darker hatched region, and the "beside" zone by the lighter hatched region. The median current direction for each tidal stage, estimated from fish heading data (see text), is shown at right in (b).

Only the sampled volume at the depth of the turbine was used in this study,

spanning 6.7 to 9.5 m above the sea floor (Fig 1.3a). This analysis volume was then

partitioned into two zones: the "turbine" zone, which was directly aligned with the

turbine face, and the "beside" zone, which included the area sampled to the side of the

turbine. The inner 5° of the sampled volume were used in analyses (see below).

Data were collected while the turbine was present and its brake was applied

(static, not rotating), which occurred from April 25 to July 5 2013. Data could not be

collected while the turbine was fully operating (rotating at current speeds > 1 m·s^{-1} and

generating power) because the cable carrying the generated power to the shore interfered

with the echosounder data transfer cable at these times. The echosounder continued to

collect data after the turbine was removed in July 2013, so a comparison dataset was

selected when the turbine was absent (though the bottom support frame was still present),

spanning April 24 to July 5 2014. Matching the dates of the 'absent' dataset to that of the

'braked' one helped best match the species and life stages of fish during the two

collection periods, despite seasonal changes, though interannual variability could not be

controlled.

The echosounder operated nearly continuously, but there were several gaps in

data collection due to technical issues or necessary shut-down of the echosounder during

turbine-related activities, such as diver inspection (Table 1.1). The final dataset included

38 complete days of data collected while the turbine was present and static and 63 days

collected while the turbine was absent. More gaps occurred while the turbine was present.

Table 1.1 Summary of hydroacoustic data collection. Dates of continuous data collection by
the bottom-mounted echosounder at the TidGen® site in Cobscook Bay, ME.

Turbine state	Year	Dates of continuous data collection	Total time in dataset
Turbine present, static	2013	4/25 - 5/02 5/07 - 5/14 5/24 - 6/04 6/26 - 7/05	38 days
Turbine absent (bottom support frame present)	2014	4/24 - 5/27 6/04 - 6/26 6/30 - 7/05	63 days

1.3.1 Data processing

Acoustic data were processed using Echoview® software (6.1, Myriax, Hobart,

Australia). There were several types of 'noise' in the data (signals not from individual

fish) that had to be removed before fish could be tracked. These included small, non-fish

targets (e.g., large zooplankton), interference from the surface and entrained air near the

surface, schools of fish (in which individual fish could not be tracked accurately), and a

mobile object that frequently appeared in the beam during ebb tide in the 2013 dataset

(perhaps a rope attached to the seafloor; Fig 1.4). Target strength (TS) measures the

proportion of sound energy that is reflected back to the transducer by an object. A TS

threshold of -50 dB was used to eliminate most signal from small, non-fish targets and

fish less than roughly 4 cm in length (Love 1971). Surface interference was removed by

limiting the maximum analysis range to 64 m from the transducer face, which is the range

at which entrained air from the surface began interfering with the acoustic signal.

Background noise tended to increase with range but also varied over time with water

height (which changed with the tide) and weather conditions. This type of noise, which

gradually changed over time, was removed using the method developed by De Robertis

and Higginbottom (2007), slightly modified to apply to TS data. Intermittent noise such

as schools, entrained air, and the moving 'rope' object was removed using multiple

resampling and masking steps with Echoview® virtual operators. All of these methods

were worked into an Echoview® template, which was then applied to all data using

Echoview®'s scripting module (Fig 1.4).
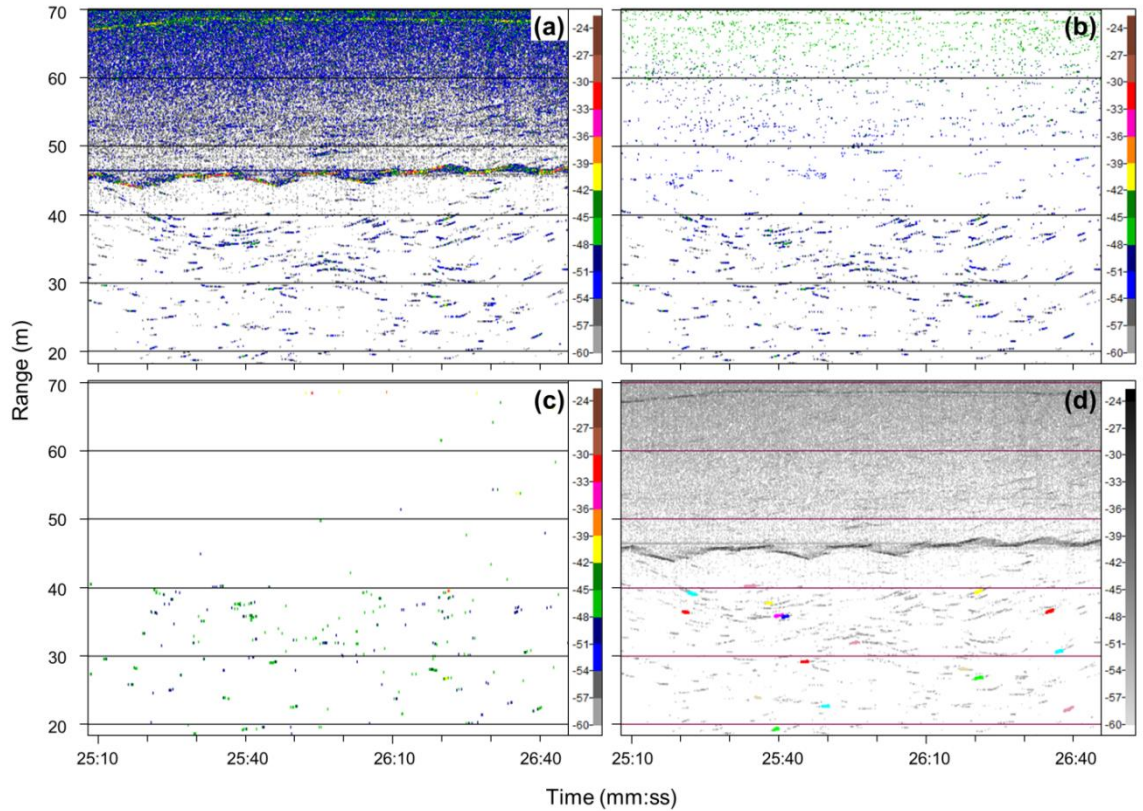
Fig 1.4 Processing steps for hydroacoustic data. Data were collected by the bottom-mounted echosounder near the static TidGen® device in Cobscook Bay, Maine in 2013 and 2014. This example is from 22:25 to 22:26 on 30 June 2013. The x-axis is time (minutes and seconds after 22:00) and the y-axis is range from transducer. (a) Raw target strength data (scale in dB, to right of each panel) showing multiple fish tracks, background noise gradient, and 'rope' object near 46 m range. (b) Target strength data with noise and 'rope' removed and -50 dB TS threshold applied. (c) Single targets detected from cleaned target strength data. (d) Fish tracks (colored lines) overlaid on raw target strength data (in grayscale).

Once noise was removed from the acoustic data, single targets were detected and

fish were tracked using Echoview®'s 4D fish tracking algorithm (Fig 1.4, Table 1.2).

Information about the tracks and the single targets within them were exported from

Echoview® to be further processed in R (3.1.1, R Core Team, Vienna, Austria).

Table 1.2 Single target and fish tracking parameters. Parameters were used in Echoview® software to detect and track individual fish.

Process	Parameter	Value
Single target detection	TS threshold	-50 dB
	Pulse length determination level	6.00 dB
	Minimum normalized pulse length	0.20
	Maximum normalized pulse length	2.00
	Beam compensation model	Simrad LOBE
	Maximum beam compensation	12.00 dB
	Maximum standard deviation of:	
	Minor-axis angles	0.500°
	Major-axis angles	0.500°
Single target filters	Angle filters:	
	Minor-axis range	-2.5° – 2.5°
	Major-axis range	-2.5° – 2.5°
	Pulse length filters:	
	Pulse length at 18 dB range (normalized)	0.40 – 1.50
Fish tracking	Data	4D
	Alpha (major, minor, range)	0.7, 0.7, 0.8
	Beta (major, minor, range)	0.5, 0.5, 0.5
	Exclusion distance (major, minor, range)	1.5, 1.5, 0.5 m
	Missed ping expansion (major, minor, range)	0, 0, 0 %
	Weights:	
	Major axis	0
	Minor axis	0
	Range	0
	TS	0
	Ping gap	0
	Minimum number of single targets in a track	5 targets
	Minimum number of pings in a track	5 pings
	Maximum gap between single targets	3 pings

Single target detection and fish tracking parameters were chosen to exclude the worst-quality data from fish tracks, but visual inspection of fish tracks after they were exported from Echoview® indicated that some error remained. This was particularly true within the ranges spanned by the turbine, where echoes from the support frame, turbine (when present), and sea surface and bottom interfered with the location data of detected fish (i.e., the angular measurements along the major and minor axes of the beam). Many tracks that were detected in the area of the turbine had accurate range measurements and minor-axis angle estimates (position in the beam's horizontal cross-section), but highly

variable major-axis angle measurements (position in the beam's vertical cross-section; Fig 1.5a). For this reason, the following analyses were carried out in 2 dimensions, focusing only on fish heading (movement trajectory in the horizontal plane, relative to north) and ignoring fish inclination (movement trajectory in the vertical plane, relative to horizontal).

Even after limiting analyses to the horizontal plane, some poor-quality tracks needed to be identified and removed from the 2D dataset. Poor-quality tracks were therefore those that were physically improbable. These were tracks with highly tortuous paths (Fig 1.5c,d), which were unlikely to be accurate. given the speed of the current and the short time each fish spent within the beam (95% of fish detected remained in the beam for 3 seconds or less. In reality, fish were most likely traveling in a roughly straight line across the sampled volume (Fig 1.5a,b), consistent with previous observations at this site (Viehman and Zydlewski 2015a). To help separate good and bad tracks, a line was fit to each track using the time and position of the track's single targets. Six parameters were then calculated (in the horizontal plane) for each track to classify it as either good or bad: the R^2 of the line fit, the ratio of the straight-line distance between the start and end points and the distance covered by the path, the polarity of the track segments, the average distance of the track's single targets from the fitted line, and the average and standard deviation of the angles between consecutive track segments. Four-hundred tracks were manually scrutinized and categorized as either 'good' or 'bad.' Half of these tracks were used to build a general additive model (GAM) to predict track quality based on the six factors, and half were used to test the model's accuracy. This method was found to reduce the prevalence of poor-quality tracks to less than 10% of the

final dataset. The prevalence of poor-quality tracks was similar (12%) when the model was fit using the other half of the manually-scrutinized tracks, indicating a consistent model regardless of the track subset used for fitting. More poor-quality tracks were present in the turbine zone due to the acoustic interference from the support frame and the turbine. The numbers of fish reported in each zone are therefore unlikely to represent the true proportion of fish that passed through each, but their direction of movement direction can still be used to assess their responses to the turbine. After poor-quality tracks were removed from the dataset, the fitted line of each remaining track was used to define fish heading, i.e., the direction of the track with respect to north.
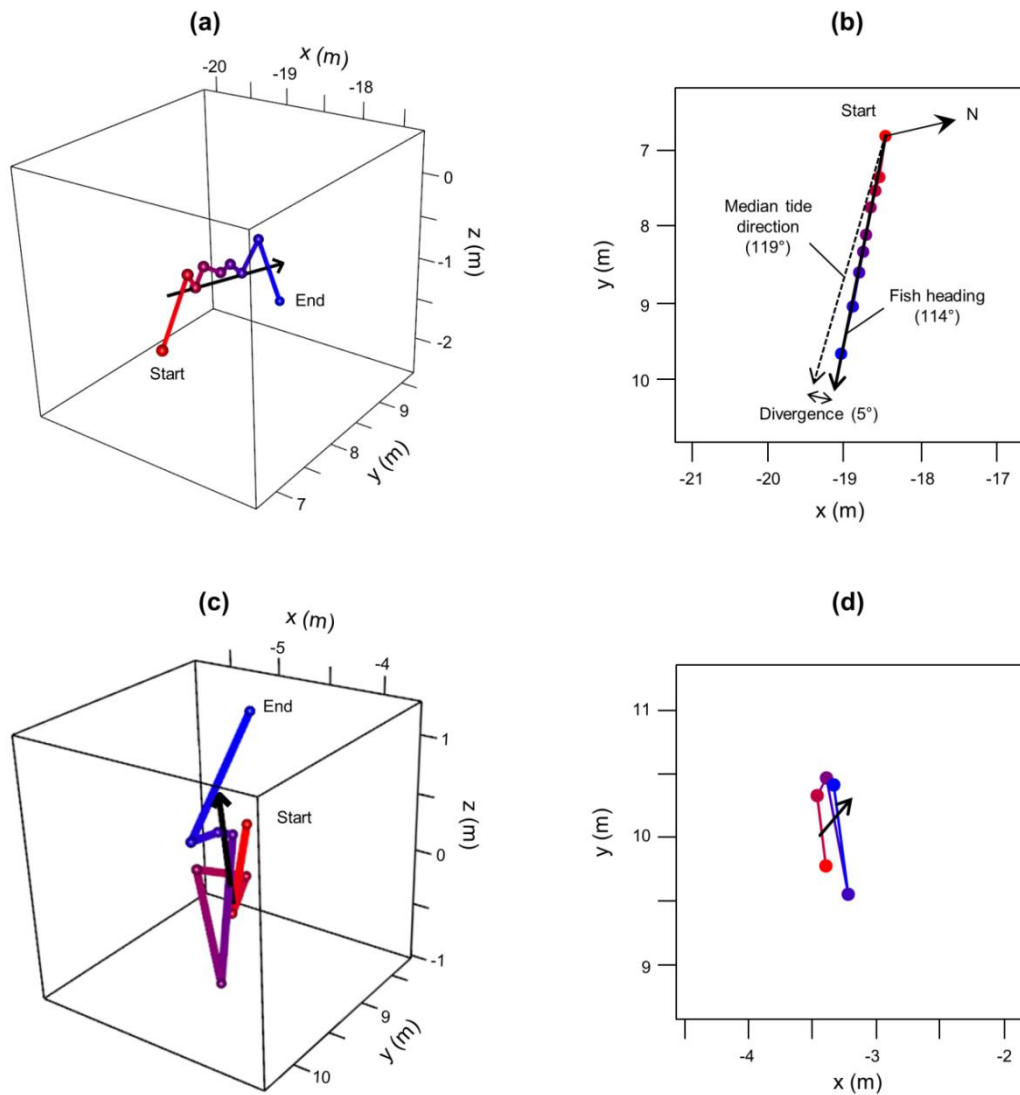
Fig 1.5 Example fish tracks. Two tracks of individual fish detected during the flooding tide, collected using a side-looking split beam echosounder in Cobscook Bay, Maine. (a) Single targets (spheres) and fitted line (black line) of a fish track classified as "good" in the horizontal plane, showing the typical high variation in the vertical dimension. (b) Same track as in A, shown in the horizontal plane with fitted line (black), true North (N), fish heading (black arrow), median direction of the tidal current (red arrow), and divergence of fish heading. (c) Poor-quality ("bad") track with fitted line (black). (d) Same track as in c, shown in horizontal plane. Single target color indicates order of detection (red = first point, blue = last point). Axes are in meters, with the origin at the center of the turbine face: the x axis is parallel to the turbine face, with the positive direction away from the transducer; the y axis is perpendicular to the turbine face, with the positive direction away from the turbine; and the z axis is vertical, with the positive direction upward.

1.3.2 Data analysis

The metric used to assess device effects on fish behavior was fish heading divergence: the difference between each fish heading and the direction of the water current. Generally speaking, at this site, fish move almost exclusively with the current during the flowing tides and exhibit random 'milling' behavior at slack tides when current speed is low (Viehman and Zydlewski 2015a). If fish normally travel with the current, departure from the direction of the current may indicate a change in their regular behavior, such as avoidance of the turbine or response to its wake.

We approximated water current direction as the median fish heading for each individual tide. This approach was validated by comparing current speed data from an ADCP briefly deployed on the sea floor at this site in March 2013 to concurrent fish heading data collected using the same hydroacoustic setup from this study (Fig 1.6). Fish heading in the March 2013 data followed a square-wave pattern (Fig 1.6a), with shifts between high and low values corresponding to periods of slack tide as indicated by the ADCP velocity data (Fig 1.6b). This pattern was very similar to current direction measured and modeled at a nearby location by Xu et al. (2006). Additionally, fish heading during the ebb and flood tides aligned very well with the average current directions at this site (approximately 120° and 285°, respectively; ORPC personal communication). Based on the March 2013 data, slack tides were defined as the 2-hour periods which encompassed each shift in fish heading between ebb and flood directions. For the current study, the times of these shifts were determined for the duration of the dataset by fitting a sinusoidal model with tidal periodicities to the fish heading data, as shown in Fig 1.6a and Chapter 3.

17
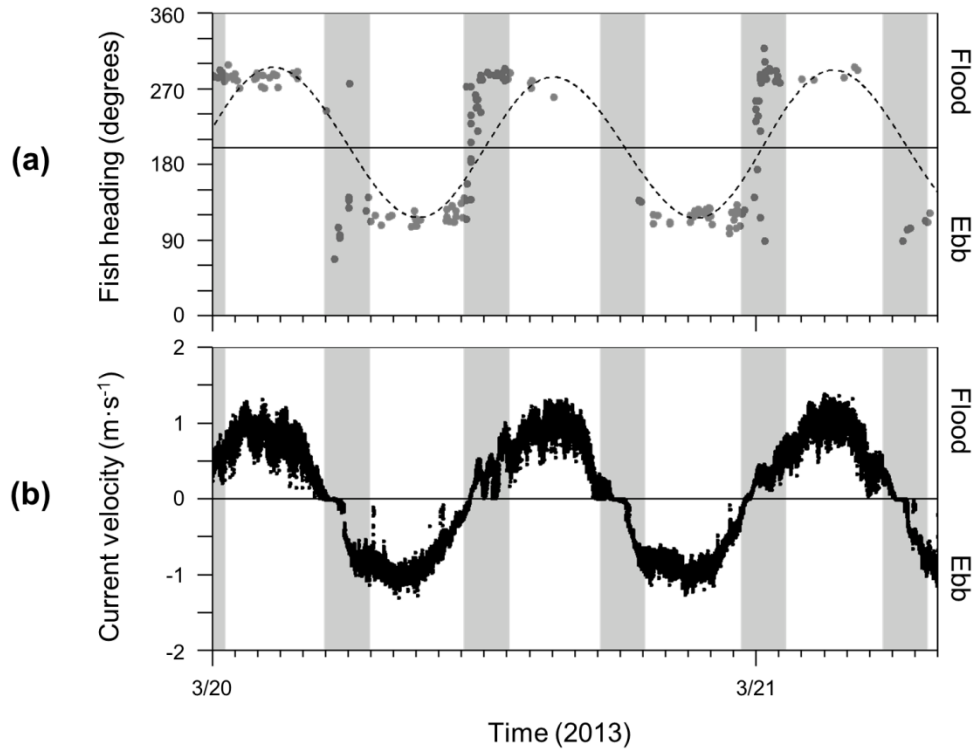
Fig 1.6 Fish heading and current velocity. Example from data collected at the TidGen® site in March 2013. (a) Individual fish heading (gray points) shown with fitted tidal model (dashed line) used to calculate times of slack tide (gray areas). (b) Current velocity collected concurrently by a bottom-mounted ADCP at the same site.

Once slack tide periods were removed from the data, the median fish heading for each individual ebb and flood tide was used as current direction during that time. If fewer than 10 fish were present in a given tide, the median was not considered reliable, and tracks from that tide were omitted from further analysis. Divergence was then calculated for each fish track as the magnitude of the difference between its heading and the corresponding estimated tidal current direction. This method helped avoid false inflation of variation in fish heading due to shifts in flow over time.

Ebb and flood tides were analyzed separately because during flood tide, fish were approaching the device, and during ebb tide, fish were departing from it. For each tidal stage, a linear model (function *lm* in package *stats* in R) was used to test for effects of four factors and their interactions on fish divergence from the current: static turbine state

18

(absent or present), sampling zone (beside or turbine), diel condition (day or night), and fish size (TS). The continuous factor, TS, was centered at its mean, and to meet assumptions of residual normality, the normal scores of divergence were used as the response variable. The initial models included main factor effects as well as interaction terms, and final models included only those terms that were found significant at the 5% level (single terms that were part of significant interaction terms were also included).

1.4 Results

While the static turbine was present (2013), 4,104 good-quality fish tracks were identified, and 4,696 while the turbine was absent (2014). More fish were tracked beside the turbine than in the turbine zone during both the flood (Fig 1.7) and ebb (Fig 1.8) tides, likely due to acoustic inference at turbine-zone ranges. More fish were detected during the ebb tide than the flood tide. During the flood tide, we detected many more fish at night than during the day (Fig 1.7), but there was not a large diel difference for the ebb tide (Fig 1.8).

Over 90% of fish had TS ranging from -48 to -38 dB (Figs 1.7 and 1.8). This TS range equates to fish lengths of approximately 4 to 11 cm using Love's general lateral-aspect equation, though this relationship varies greatly with fish species and orientation (Love 1971). TS tended to be higher in the turbine zone than beside the turbine, indicating larger fish, and this difference was more substantial when the turbine was present. This apparent difference in size between zones was likely due to acoustic interference from the MHK device (particularly the turbine), which made weaker acoustic targets more difficult to track at the further range, where the turbine was located. TS also appeared higher during the ebb tide than the flood tide, but this may have been due to

slightly different orientation of the fish with respect to the acoustic beam during different

tide phases than to actual size differences. The ebb tide current, and presumably the fish

moving with it, was more perpendicular to the acoustic beam's central axis than the flood

tide current (Fig 1.3b), increasing the TS of fish detected at ebb tide relative to those

detected during flood-tide, which would travel at a more oblique angle (Boswell et al.

2009).
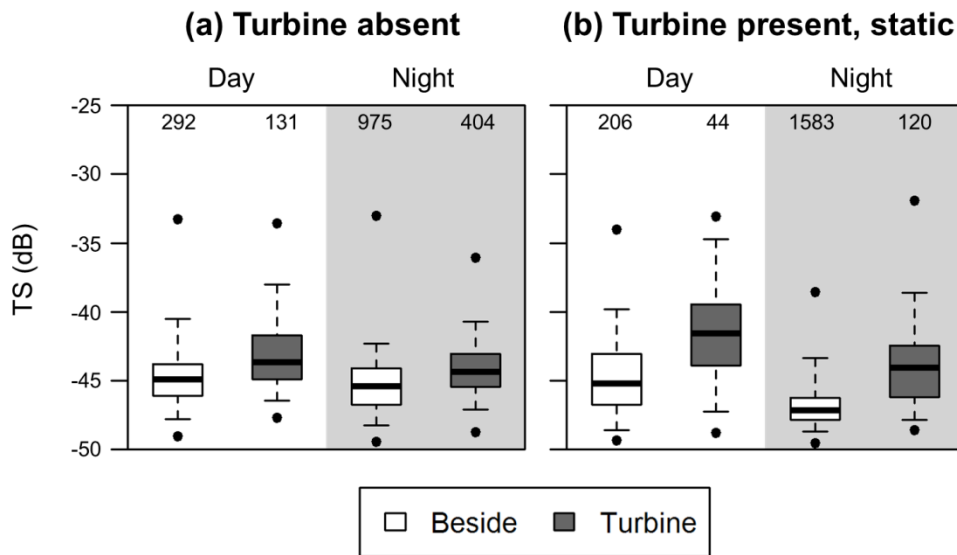
Fig 1.7 Target strength of fish detected during the flood tide. Fish moving with the current would be approaching the MHK device. Shown is the distribution of target strength (TS) of fish beside the turbine (white boxes) and in the turbine zone (grey boxes) during the day and night, (a) when the turbine was absent, 2014; (b) when the turbine was present and static, 2013. Horizontal line is the median, boxes span interquartile range, whiskers span 5th to 95th percentile, and points indicate minima and maxima. Numbers are sample size of each group.
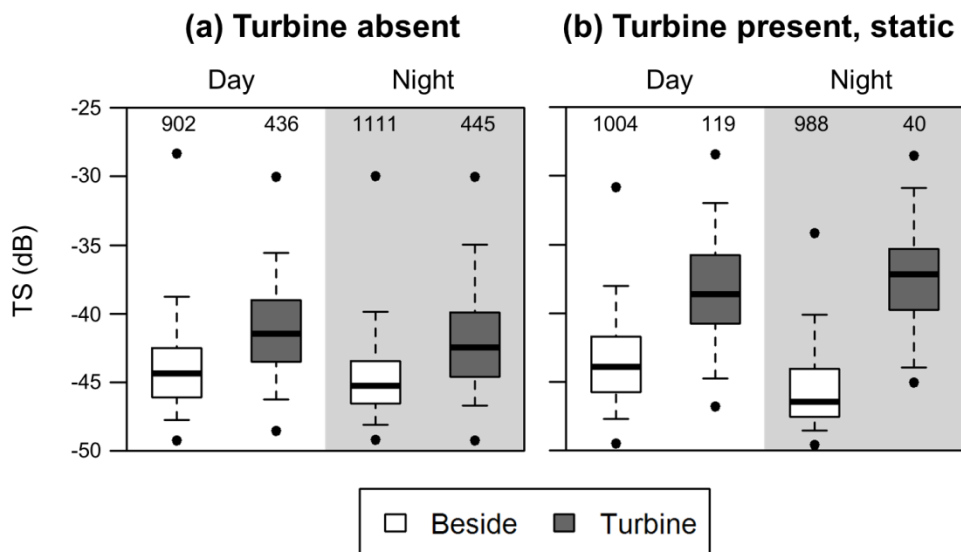
Fig 1.8 Target strength of fish detected during the ebb tide. Fish moving with the current would be departing from the MHK device. Shown is the distribution of target strength (TS) of fish beside the turbine (white boxes) and in the turbine zone (grey boxes) during the day and night, (a) when the turbine was absent, 2014; (b) when the turbine was present and static, 2013. Horizontal line is the median, boxes span interquartile range, whiskers span 5th to 95th percentile, and points indicate minima and maxima. Numbers are sample size of each group.

Fish divergence from the current direction suggested that fish swam in the direction of the current when the tide was flowing (Figs 1.9 and 1.10). Ninety-five percent of all fish trajectories diverged from the current direction by 15° or less. Median fish heading (e.g., estimated tidal current direction) ranged from 115° to 128° during ebb tide and from 279° to 290° during the flood tide. Against-current movement was only visually obvious in the turbine zone at night, when the static turbine was present (Fig 1.9b, lower right panel): approximately 4% of fish diverted more than 100° from the median direction, whereas no more than ~0.3% did so in any of the other sets of conditions. During this time, the polarity of the fish headings was 0.91, as opposed to 0.99 for all others (polarity of 0 would indicate completely random headings, and 1 would indicate completely uniform).

21
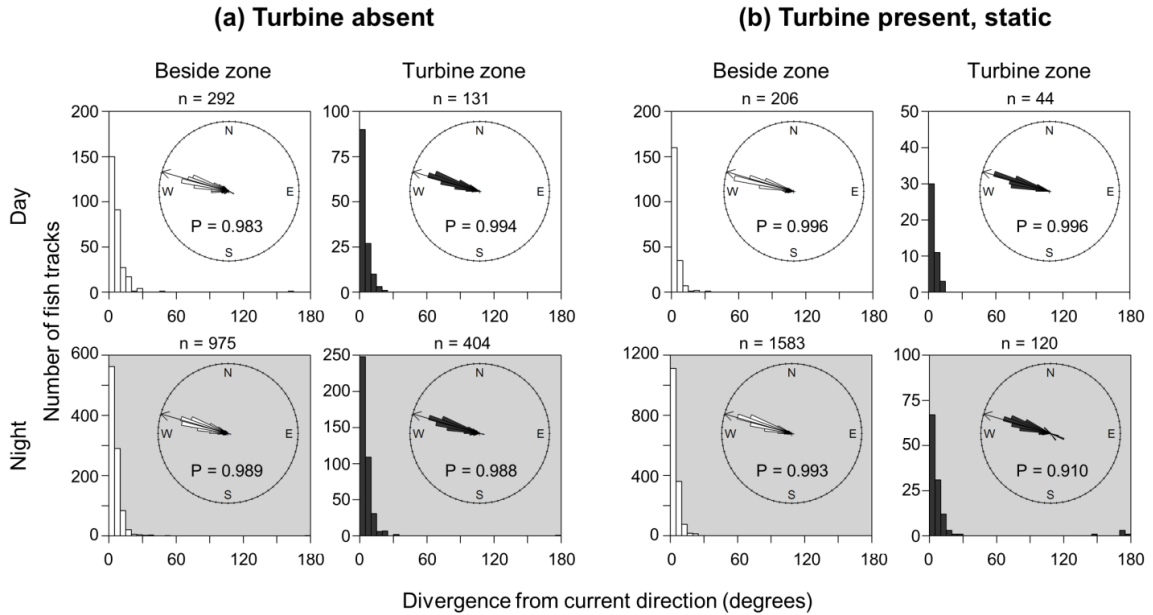
Fig 1.9 Fish heading and divergence during the flood tide. Fish moving with the current would be approaching the MHK device. Histograms are heading ivergence from current direction, and inset rose diagrams are fish heading relative to North. (a) When the turbine was absent, 2014; (b) when the turbine was present and static, 2013. White and black bars correspond to the beside-turbine zone and turbine zone, respectively. Gray background indicates night. The number of fish (n) and the polarity of their headings (P) are shown for each group.
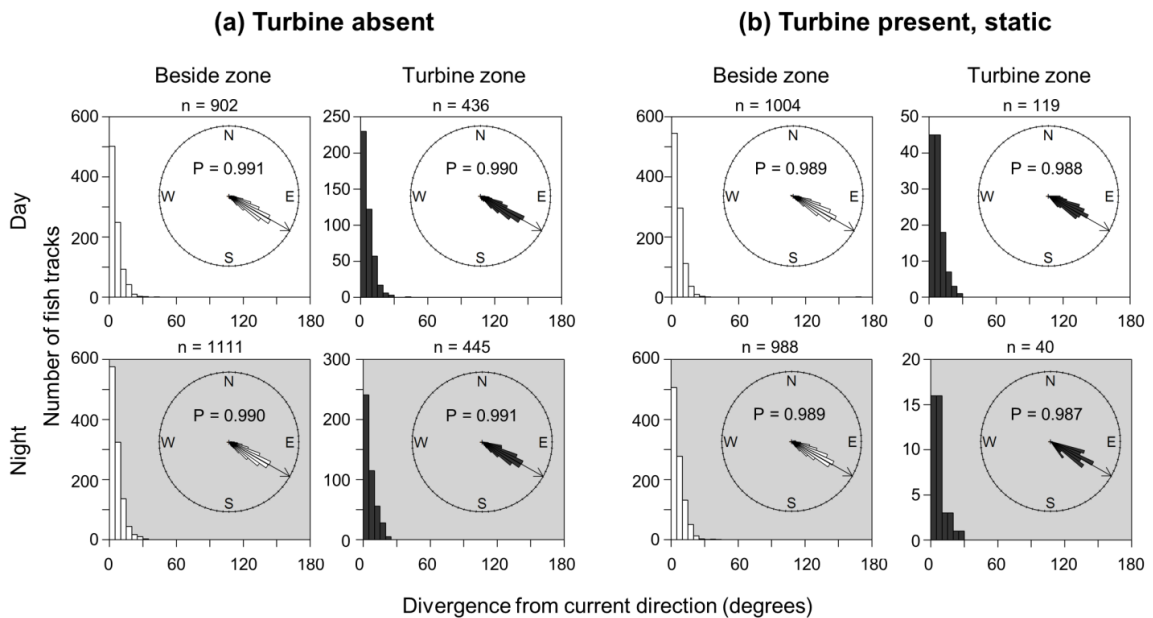
Fig 1.10 Fish heading and divergence during the ebb tide Fish moving with the current would be departing from the MHK device. Histograms are heading ivergence from current direction, and inset rose diagrams are fish heading relative to North. (a) When the turbine was absent, 2014; (b) when the turbine was present and static, 2013. White and gray bars correspond to the beside-turbine zone and turbine zone, respectively. Gray background indicates night. The number of fish (n) and the polarity of their headings (P) are shown for each group.

22

Linear models fit to flood and ebb tide data were both statistically significant (model p-values < 0.05), suggesting a relationship between the dependent variable (fish divergence) and independent variables (turbine state, zone, diel stage, and TS). The model fits were low, accounting for only 2.0% and 0.6% of the variation in fish divergence for flood and ebb tides, respectively. The model therefore had little predictive power. However, it did indicate that several factors affected fish behavior.

During the flood tide, when fish would have been approaching the MHK device, turbine state and sampling zone had statistically significant main effects on fish divergence at the 5% level (Table 1.3). There were also interaction effects involving turbine state, sampling zone, and diel stage. Given these interaction effects, the fitted values of the model for each combination of factors can best illustrate the relative differences in divergence (Fig 1.11). These modeled values indicated that when the turbine was absent, divergence was greater beside the turbine than in the turbine zone during the day, but at night, there was no zone effect (Fig 1.11a). When the static turbine was present, divergence was greater in the turbine zone than beside the turbine during both day and night (Fig 1.11b). Divergence was higher at night for both sampling zones, but the difference between zones was greater during the day.

23

Table 1.3 Linear model of fish heading divergence. Divergence is the difference between fish heading and median direction. Shown are model results from fish detected during the flood tide (when fish would have been approaching the MHK device).

Model term	Coefficient estimate	Standard error	P-value
Intercept	0.208	0.058	<0.001
Turbine state (static)	-0.554	0.090	<0.001
Zone (turbine)	-0.348	0.104	0.001
Diel stage (night)	-0.110	0.066	0.095
Turbine state (static):zone (turbine)	0.855	0.194	<0.001
Turbine state (static):diel stage (night)	0.363	0.098	<0.001
Zone (turbine):diel stage (night)	0.349	0.119	0.003
Turbine state (static):zone (turbine):diel stage (night)	-0.475	0.223	0.033
Adjusted R^2	0.019		
Model p-value	<0.001		
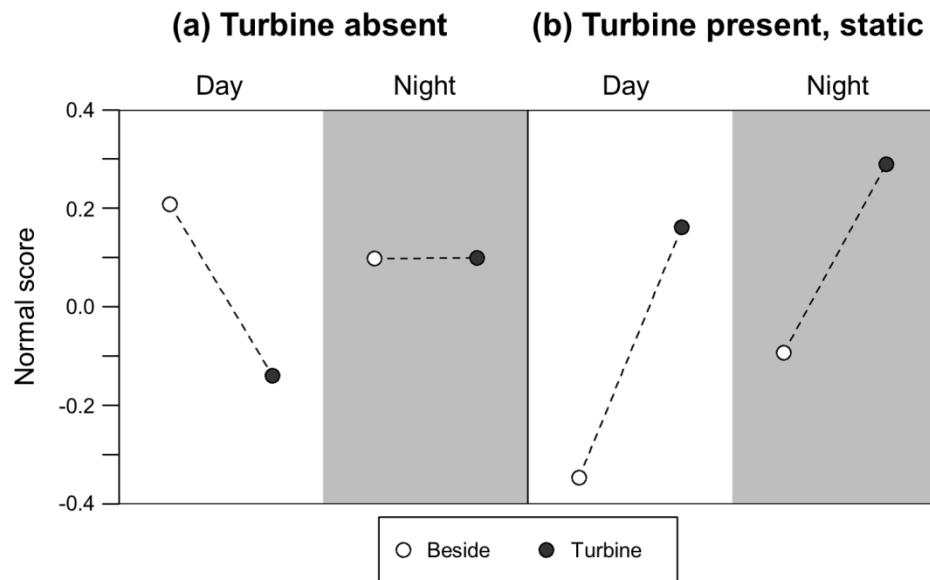
Fig 1.11 Normal scores of divergence estimated by the linear model. Graphical representation of the model summarized in Table 1.3, showing main and interaction effects of significant factors: turbine state (static turbine absent or present), diel stage (day or night), and sampling zone (beside or turbine). (a) Static turbine absent; (b) static turbine present. White and gray points correspond to the beside-turbine zone and turbine zone, respectively. Gray areas indicate night.

During the ebb tide, when fish would have been departing from the MHK device, the only significant factor affecting divergence was TS (coefficient estimate: 0.038; standard error: 0.012; p-value: 0.001). This indicated that larger fish showed greater

variation in movement with respect to the current than smaller fish, but divergence was not influenced by turbine state, diel stage, or sampling zone.

1.5 Discussion

Fish approaching the MHK device responded to the static turbine at the distances observed. The fish sampled were mainly small, likely on the order of a few cm in length, and they generally traveled in the same direction as the tidal current. However, those directly upstream of the static turbine showed more variable movement with respect to the current than those that were to the side. This difference occurred when the static turbine was present but was not apparent when the turbine was absent, and suggests turbine avoidance. Previous studies of fish evasion of operating MHK devices have sampled the first few meters from the turbine and observed evasion (Hammar et al. 2013, Viehman and Zydlewski 2015a). As we observed a volume spanning 7-14 m from the face of the static TidGen® turbine, our results suggest the range of MHK device effects on fish behavior extends at least 18 m upstream, and perhaps farther for an operating device. Shen et al. (2016) carried out transects over an MHK device similar to the TidGen® with a rotating, but not generating, turbine, and they found evidence that fish were moving out of the path of the device as far as 140 m upstream.

Reactions to the static turbine that we observed were generally confined to small-scale adjustments in trajectory, as most fish (95% of tracks) diverged 15° or less from the current direction. Evasion maneuvers have been observed to range from small-scale adjustment to complete reversal of movement (Hammar et al. 2013, Viehman and Zydlewski 2015a), but these studies occurred within a few m of the devices and involved rotating turbines. At the distances from the turbine which we sampled here, slight

25

deflection from the strong current is likely an effective and energy-efficient method of downstream obstacle avoidance. For the small fish that we sampled, it may also be the only possible maneuver, as fish swimming power is directly related to length (Beamish 1978). Fish of Cobscook Bay are generally small, and consist mainly of juveniles of multiple species (Vieser 2014, Zydlewski et al. 2016). During this study, a large portion of fish sampled were likely larval or recently-metamorphosed juvenile Atlantic herring (Vieser 2014, Zydlewski et al. 2016), which would be weak swimmers relative to the tidal current. In their transects over a similar ORPC device, in August 2014, Shen et al. (2016) observed slightly larger fish, which were likely a mix of juvenile Atlantic herring (~20 cm) and adult Atlantic mackerel (~30 cm; Vieser 2014, Zydlewski et al. 2016). Those fish would be stronger swimmers than the ones observed here in Apr-Jun 2012 and 2013, and they, too, moved almost exclusively with the current. As their numbers decreased beginning 140 m upstream, and vertical distribution did not change, they too were likely using small movements to avoid the downstream obstacle.

At multiple meters upstream of an MHK device, small movements in relation to the current may be the chosen method of avoidance for both the small (≤ 10 cm) and large (10-30 cm) fish. Within a few meters of the turbine, size may be of greater importance to evasive behavior. In the first 3 m upstream of a rotating MHK turbine, Viehman and Zydlewski (2015a) found that small fish (10 cm and under) tended to enter the turbine if it was in their path, with at most 2% actively evading by swimming up, down, or against the current. Larger fish (most of which were still less than 20 cm) had a greater likelihood of evading the turbine (up to 11%), likely due to greater maneuverability in the fast currents. Studies of fish responses to trawls have also found

close-range evasion to be stronger in larger fish (e.g., Rakowitz et al. 2012 and Sajdlová et al. 2015). Fish size, and therefore species and life stage, is therefore an important factor when considering if and how fish avoid MHK devices.

Avoidance of an MHK device also depends on whether fish can detect the device, and at what range this occurs. Fish have a variety of sensory systems to alert them to approaching objects, including visual and auditory senses and the lateral line system, which is sensitive to the local flow field and may play a role in detecting distant, low-frequency sounds (Popper and Schilt 2008, Bleckmann and Zelick 2009, Evans 1993). As we saw evidence of avoidance during both day and night, fish were likely detecting and responding to visual cues and non-visual cues (e.g. acoustic and hydrodynamic) from the device. The turbine had a larger effect on fish divergence from the current during the day than at night, indicating that sight played an important role in eliciting avoidance behavior. This agrees with the close-range studies by Viehman and Zydlewski (2015a) and Rakowitz et al. (2012), which found the probability of turbine and trawl evasion, respectively, to be higher during the day than at night. However, at night we also observed a small portion of fish (~4%) in the turbine zone that moved against the current, which was not seen during the day or beside the turbine. It is possible that in the absence of vision, the acoustic and hydrodynamic cues of the static device evoked stronger and less uniform reactions to its presence. This would be in agreement with the less-directed responses of herring to obstacles in the dark (Blaxter and Batty 1985) and of various fish species to approaching trawls at night (Rakowitz et al. 2012).

We cannot rule out that the behavioral difference which we observed at night could be related to different species or life stages of fish being sampled at that time.

27

During the flood tide, many more fish were detected at night than during the day, which could have been the result of the activity of nocturnal species within the water column (Reebs 2002, Vieser 2014), or of schools spreading out at night and the individuals from the schools becoming trackable (Pitcher 2001). The result of either would be sampling a different community of fish at night than during the day, and therefore comparing the responses of fish with different sensory and locomotory abilities. TS during day and night indicated that fish size did not change dramatically, but different species may respond to the same cues in different ways. Species-dependent responses have been observed for other MHK devices. Amaral et al. (2015) and Castro-Santos and Haro (2015) found fish responses to turbines in laboratory flumes to be species-dependent, with turbine responses related to each species' swimming behavior (e.g., active rheotaxis or passive drifting) and direction of travel (upstream- or down-stream migrating). Hammar et al. (2013) found the same in the field, where they observed certain species (mainly predatory fish) to be approach MHK turbines more than others, hypothesizing that they were 'bolder' individuals. The species of fish present at a tidal power site and how species composition changes over time must therefore be considered when predicting or interpreting their responses to MHK devices, as the type of response will largely determine the risk of entrainment, injury, and mortality.

In this study, we examined fish movement in the horizontal plane, but it is also possible that fish responses to the MHK device were taking place in the vertical plane (i.e., swimming upward or downward to avoid the upcoming turbine). Diving is commonly observed as the primary reaction of fish to disturbances such as passing vessels and approaching trawls (Ona et al. 2007, Sajdlová et al. 2015), often seen before

lateral movements and at great ranges (450 m, Handegard and Tjøstheim 2005; 75-275 m, Handegard et al. 2003). Additionally, Bevelhimer et al. (2015) found evidence of downward fish movement 0-15 m from an HK device deployed in the East River, NY. As such, we cannot rule out vertical avoidance of the TidGen® device at the ranges we observed. Two other studies carried out at the same site as the present work provided conflicting evidence of vertical movements in response to MHK devices. In their transects over the MHK device, Shen et al. (2016) did not observe vertical fish movements related to the device. On the other hand, Staines et al. (2015) found some differences in the vertical distributions of fish near the TidGen® (~50 m away) before and after its installation that may have been related to device presence. The different vertical distributions may have resulted from vertical movements by fish, but this movement could not be inferred from the distribution data used when observing these differences.

The acoustic data contamination which prevented us from assessing vertical movement is a common issue in hydroacoustics, particularly when collecting data near solid boundaries such as an MHK device, the seafloor, and the sea surface. Possible methods of addressing this issue include using a narrower beam, (which could reduce surface and bottom interference), moving the beam farther from the device (though this could reduce the likelihood of observing fish responses), or using multibeam sonars (Williamson et al. 2015, Melvin and Cochrane 2014). Additional improvements could be made to the data processing techniques used here. Automated processing is necessary for such large datasets, which are too time-consuming to process manually. The processing method used here was effective at removing many types of noise from the data, but it was also conservative and likely omitted many useable fish tracks from

analyses. Improvements to acoustic data processing techniques, such as incorporating visual signal processing, could help reduce unnecessary data omission. Changing levels of noise in different parts of the sampled volume resulted in unequal detection probabilities over time and in different parts of the acoustic beam, making it impossible to use fish numbers as indicators of turbine effects (e.g., beside vs. turbine zones, or present vs. absent). However, overall, the diel and tidal differences in fish numbers that we observed were consistent with a more detailed assessment of temporal patterns of fish passage rate at this site (Chapter 3) and likely reflected natural patterns as opposed to device effects.

Unlike the flooding tide, we saw no effects of MHK turbine presence on fish movement during the ebbing tide, when they would be departing from the device. The wake of the device can extend over 100 m before flow velocity reaches 90% of its undisturbed magnitude (Rao et al. 2016), but fish apparently were not responding to it in a way which we could detect. The only statistically observed effect on fish movement downstream of the device was of fish TS, which suggested that larger fish were diverging farther from the current direction than smaller ones, regardless of turbine presence. Viehman and Zydlewski (2015a) reported that fish were almost always milling in the wake of the test turbine they examined, though that viewing window extended only 3 m downstream of the device. Those fish may have been sheltering from the fast currents in the low-velocity area just behind the turbine structure (Čada and Bevelhimer 2011), or were potentially disoriented by turbine passage or the sudden change in flow conditions. Regardless of the cause of the turbine-wake milling behavior, if it was occurring near the

static TidGen® in the present study, it did not extend beyond 7 m downstream of the turbine.

To predict and interpret fish responses to MHK devices, we need a better understanding of the physical signature of the static and dynamic devices. To date, detailed measurements of the visibility, noise generation, and hydrodynamic signatures of MHK devices are sparse and spread over a wide range of designs and deployment configurations (Copping et al. 2014). Measuring these physical conditions around MHK devices in strong tidal currents poses its own set of challenges (e.g., Martin and Vallarta 2012) but in many cases is more easily accomplished than observing fish behavior at all the possible spatial and temporal scales of interaction. The distance at which fish detect and respond to MHK devices will depend on the fish present and site characteristics, as detection thresholds of fish sensory systems (e.g. vision, hearing, and the lateral line) vary with species and life stage and their sensitivity is modified by environmental conditions (Kim and Wardle 2003, Bleckmann and Zelick 2009, Blaxter 1986). Knowledge of the physical "footprint" of MHK devices, combined with knowledge of the sensory capabilities of the fish that may encounter them, would aid in planning studies of fish behavior by identifying where fish are most likely to detect and respond to the device, and would afterward inform interpretation of study results. Our understanding of fish sensory abilities is limited, and more information on a wider range of marine species would be necessary for this approach.

To develop a better understanding of how fish interact with MHK devices, we should aim to collect concurrent information on the physical signatures of devices and the behaviors of fish encountering them. Williamson et al. (2015) have taken a step in this

31

direction by developing a bottom-mounted monitoring platform that includes multibeam and split beam echosounders, a flow meter, and a fluorometer, with the possibility for adding other equipment. Collecting data with these instruments simultaneously may allow animal behavior to be linked to local physical conditions affected by MHK devices; for example, fish movement with respect to the turbulence generated downstream. Studies using integrated approaches such as this will help build a more complete understanding of how and why MHK devices affect fishes and other marine organisms.

The results of this study and others indicate the effects of an MHK device on fish will vary with the species and life stages that are present at the same location. At a tidal energy site, the composition of the fish community is likely to change on a variety of spatial and temporal scales (Chapter 3, Vieser 2014), and the effects of proposed MHK devices must be assessed with these changes in mind. As more individual devices are deployed and monitored, preferably with integrated biological and physical monitoring systems, we can begin to expand predictions of effects from individual animals and devices to population-level effects and device arrays. This information can inform the design and location of MHK device arrays as we seek to responsibly develop this renewable energy source.

CHAPTER 2

POTENTIAL OF SINGLE BEAM ECHOSOUNDERS FOR

ASSESSING FISH AT TIDAL ENERGY SITES

2.1 Abstract

Hydroacoustics is a valuable tool for assessing fish presence, relative abundance, and size. Scientific-grade split beam echosounders provide the most information on individual fish but can be prohibitively expensive for start-up companies exploring potential tidal energy development sites where fish interactions with their devices must be monitored. Commercial-grade, single beam echosounders are significantly less expensive than split beam echosounders but provide less information as they cannot correct the echo strengths of individual fish (TS) to account for the effect of the beam pattern, complicating size and species estimates. Statistical methods, i.e. deconvolution, exist to correct TS distributions for the beam pattern effect and could expand the utility of single beam systems for tidal energy site assessment. We applied deconvolution techniques to single beam data from a study at a tidal energy site in Cobscook Bay, Maine. Fish were detected in hydroacoustic data collected concurrently with a wide-angle (31º) single beam echosounder and a narrow-angle (7º) split beam echosounder in two 24-hr surveys in August 2012 and March 2013. For each survey, the distribution of TS data from the split beam echosounder (compensated for beam pattern) was the reference distribution. This was compared to two deconvolved "single beam" TS distributions: one from the wide-angle single beam TS data, and one from the narrow-angle split beam TS data uncompensated for beam pattern, which represented data from a narrow-angle single beam. We found that deconvolution was not effective in March,

when few fish were present (141 and 80 detected fish, for single and split beam, respectively), but was more effective in August, when more fish were sampled (501 and 377 fish). In August, the deconvolved TS distribution from the wide-angle single beam did not resemble the reference TS distribution, likely due to a large proportion of multiple-target echoes being misclassified as single targets. On the other hand, the deconvolved distribution of the uncompensated split beam TS did resemble the reference distribution, indicating narrow-angle single beam echosounders may provide good estimates of fish TS. However, the smaller volume sampled by a narrow beam could also hamper investigations of shallower, faster sites, or when fewer fish are present. If TS information is not needed, wide-angle single beam echosounders may be sufficient for tidal energy site monitoring as they can still provide a relative index of fish density. Depending on the required information, the use of either single beam system could greatly reduce costs of environmental assessment for tidal energy developers.

2.2 Introduction

Tidal energy is a new form of renewable energy that uses large, underwater turbines to convert the kinetic energy of tidally-generated currents to electricity. Few of these marine hydrokinetic (MHK) devices have been deployed worldwide, so their environmental effects remain largely unknown. In most permitting procedures, developers are required to carry out assessments of the environmental effects of their devices (Jansujwicz and Johnson 2015, Henkel et al. 2013).

Fish are a key part of the marine ecosystem that may be affected by MHK devices (Copping et al. 2016). Hydroacoustics is one of the best tools for collecting data on fish at sites targeted for tidal power development (Viehman et al. 2015). Hydroacoustics is a

34

type of sonar specialized for detecting fish in the water column, and allows large volumes of water to be sampled simultaneously with high temporal and spatial resolution (Simmonds and MacLennan 2005). Additionally, it is well-suited to collecting data in areas with fast currents and complex bottom bathymetry, where physical sampling methods, such as trawling, would not be safe or effective (Viehman et al. 2015, Vieser 2014, Williamson et al. 2015).

Echosounding systems range in complexity and accuracy. Scientific-grade split-beam echosounders allow fish to be tracked within their beam in three dimensions, which is useful in assessing their responses to stimuli (Chapter 1; McKinstry et al. 2005). The ability to pinpoint a fish's location within the acoustic beam also allows their returning echo strengths to be accurately corrected for the effect of beam pattern (Simmonds and MacLennan 2005). An acoustic beam ensonifies an approximately conical volume extending away from the transducer, and is strongest along its central axis ("on-axis") and weakens toward the edges ("off-axis"). The acoustic reflection, or target strength (TS), of a fish on-axis will be recorded at its true strength, but those at greater angles relative to the central beam axis will be recorded as weaker acoustic targets than they actually are. If the beam pattern is known, the location of each fish relative to the beam's central axis can be used to correct, or compensate, the TS of each individual. The resulting compensated TS can then be used to roughly estimate fish size and therefore, to some extent, species (Simmonds and MacLennan 2005). However, the cost of these systems, upwards of $50,000 US, is often unrealistically high for small-scale tidal developers, particularly if a site has not yet proven to be worth developing.

A less expensive alternative is the single beam echosounder, on the order of $10,000 US, which is the precursor to dual- and split-beam systems. These echosounders can be used to determine the range of an acoustic target but cannot locate it within the beam's cross-section. They therefore cannot be used to track fish in 3D or correct the returning echoes for beam pattern effects, resulting in less accurate TS and size estimates. Commercial-grade single beam echosounders are the least expensive, but require careful calibration by the user since factory calibrations are not as thorough as for scientific-grade equipment. Their lower cost makes them much more attainable for tidal power developers that are beginning to explore potential sites. However, the information that can be directly provided by these systems (e.g., TS) is limited without the application of more involved statistical techniques.

We used a commercial-grade single beam echosounder to conduct the initial assessments at targeted tidal power sites in Western Passage and Cobscook Bay, Maine (Viehman et al. 2015). Ocean Renewable Power Company (ORPC) was interested in installing its MHK device, the TidGen® power system (Fig 2.1), in one or both of these channels. Industry regulators were interested in the vertical distribution of fish in the water column, and if they were likely to encounter the fixed-depth tidal power turbine or not. Additionally, regulators wanted a baseline index of fish abundance for comparison to future data that would be collected if development continued.
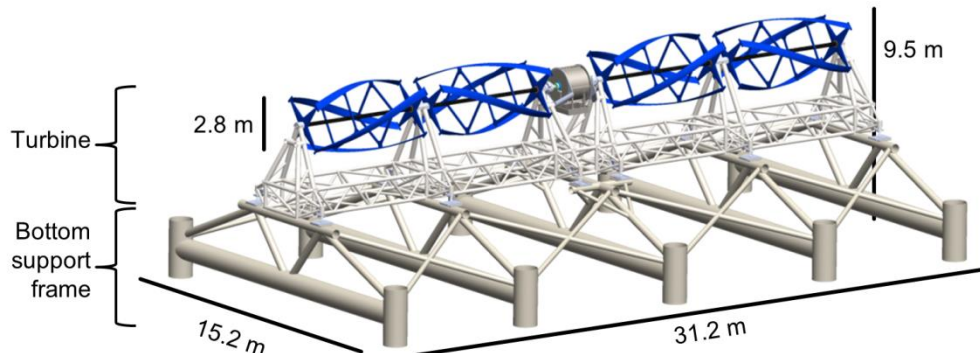
Fig 2.1 Ocean Renewable Power Company's TidGen® Power System. Turbine image provided by ORPC.

A single beam echosounder was sufficient to meet these research goals, as volume backscatter (S_V), a summation of the acoustic energy reflected within the acoustic beam, serves as a relative index of fish density that does not require correction for beam pattern effects.   We chose to use a wide-angle (31°), dual-frequency (38 and 200 kHz) commercial-grade transducer (the Simrad 38/200 Combi W), which we mounted over the side of a vessel that was moored at each site for 24 hrs. The wide beam allowed us to sample fish more effectively in the fast currents than a narrow beam, particularly in the upper part of the water column where the beam was narrowest. The dual frequencies were useful in separating fish from other sound scatterers, such as zooplankton (Staines et al., submitted), and we found that fish tended to be densest near the surface or seafloor (depending on the time of year), outside of the depth of the turbine (Viehman et al. 2015). Based on the baseline results from that study and other environmental studies carried out by ORPC and its partners, a pilot license permit was issued to further develop the Cobscook Bay site (FERC 2012) At that point, more detailed information about fish became important to regulators, including their sizes, species, and their behavior in response to the MHK device.

37

The necessity for more detailed information on individual fish justified the use of a scientific-grade split beam echosounder. This was especially needed to study the movements of individual fish near the MHK device (Chapter 1). However, it is possible that a single beam echosounder could be sufficient for obtaining information on the TS of the fish sampled. Before the more complex dual and split beam echosounders were developed, data from single beam echosounders were corrected for the effect of beam pattern using statistical techniques, including deconvolution (Clay 1983). While not as accurate as distributions obtained using individually-compensated fish TS from split beam systems, some comparisons have found that narrow-angle (7°) single beam TS distributions corrected in this manner agree well with dual- and split-beam data (Clay and Castonguay 1996, Rudstam et al. 1999).

Only data from single fish should be used in deconvolution (Clay 1983, Stanton and Clay 1986), so deconvolution in fisheries hydroacoustics has typically been confined to narrower acoustic beams. This is because the volume sampled per range increment is smaller for narrower beams, which lowers the likelihood that multiple fish would pass through the same sampled volume at once and be falsely recorded as a single fish (Simmonds and MacLennan 2005). In shallower areas, particularly with fast currents, it can be beneficial to sample with a wider beam, as fish passing by quickly may be under-sampled at closer ranges if the beam is very narrow. We wanted to determine if the acoustic returns from a wide-angle single beam echosounder could be corrected to account for the effect of its beam pattern via deconvolution techniques. If so, more information could be provided by initial site assessments using the wide-angle single beam echosounder, and we could improve the continuity between initial assessments

made with the single beam and later assessments carried out with the narrow-angle split beam. If the method works, a single beam system could be sufficient for much of the monitoring at tidal energy sites. This could greatly reduce costs for developers while still providing detailed information for industry regulators.

To assess the utility of the deconvolution method for this application, we used data collected concurrently with our narrow-angle scientific-grade split beam and wide-angle commercial-grade single beam echosounders at the tidal energy site in Cobscook Bay, Maine. The deconvolution methods of Clay (1983) were applied to the single beam backscatter data, as well as to the uncompensated split beam backscatter, which is effectively data from a narrow-angle single beam. These results were compared to compensated split beam backscatter from the split beam echosounder, which was assumed to represent reality. In this way, we assessed the utility of wide- and narrow-angle single beam echosounders in tidal power site assessment.

2.3 Methods

Data were collected simultaneously with single and split beam echosounders, using survey protocols at a tidal energy site in Cobscook Bay, Maine (Viehman et al. 2015). The split beam was a Simrad EK60 echosounder with a 7° circular-beam transducer, and the single beam was the same as that used in initial site assessments: a Simrad ES60 echosounder with a 38/200 Combi W 31° single beam transducer. The transducers were mounted over the side of a vessel, which was moored near the TidGen® (Fig 2.2) for 24 hr per survey, as in Viehman et al. (2015). Both transducers had a ping rate of 2 s^{-1} (sampled the water column twice per second). The split beam operated with a pulse duration of 0.064 ms (vertical resolution of approximately 5 cm) and power of 120

W, and the single beam used a pulse duration of 0.512 ms (vertical resolution of approximately 38 cm) and power of 225 W. The single beam system used a longer pulse duration than the split beam in order to match previously collected data (Viehman et al. 2015), in which a long pulse duration was required to reduce interference between the single beam and DIDSON acoustic camera that was operating simultaneously.
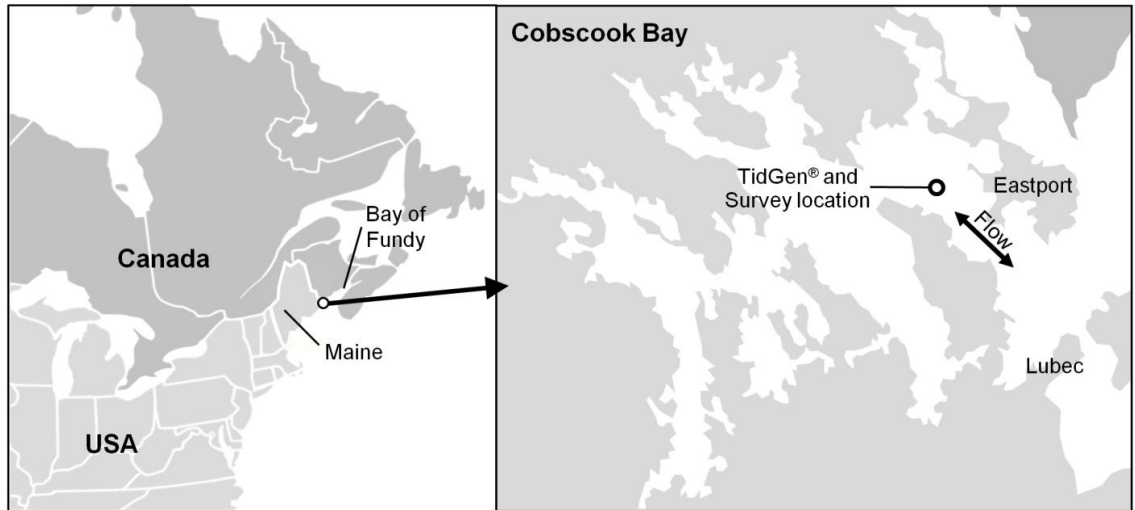
Fig 2.2 Study area. Location of TidGen® and down-looking 24-hr hydroacoustic surveys shown in right panel.

Two 24-h surveys were used for these comparisons: one from August 2012 and one from March 2013. These two surveys were chosen based on the number of fish present: fish abundance peaks in Cobscook Bay in the late summer into fall, and reaches a minimum in the winter and early spring (Viehman et al. 2015, Chapter 3). Generally, deconvolution requires many fish detections in order to work (Simmonds and MacLennan 2005), so it was necessary to determine if the method could be useful for data from a typical 24-hr survey when fish were scarcest. These two datasets are typical of the BACI surveys that we have carried out at this site, and therefore are representative of the data that would be available for this method in the future.

The single beam echosounder collected data with 38 kHz and 200 kHz frequencies. Only the 200 kHz data were used in the following analyses. Future reference to the single beam data therefore only refers to the 200 kHz frequency.

2.3.1 Echosounder calibration

Both echosounders were calibrated using a 13.7 mm copper calibration sphere, with nominal TS of -45 dB.

The EK60 split beam echosounder was calibrated using the Simrad Lobes program. This program records the position and uncompensated TS of the sphere as it is swung through the beam multiple times, until many readings have been obtained from all parts of the beam cross-section. The program then returns minor and major axis beam angles, gain, and S_a corrections (Table 2.1). These calibrations were done *in situ* during surveys.

The ES60 single beam echosounder cannot record the 3D location of targets within the beam, so calibration was carried out differently. *In situ* on-axis calibrations were performed at slack tide during surveys but were meant only to detect any significant equipment malfunction, as the water was never still and the sphere could not be accurately positioned. Full ES60 calibrations took place on a frozen-over lake in the winters of 2011, 2013, and 2014. For these calibrations, the transducer was lowered below the ice through one hole, leveled, and stabilized. The calibration sphere was then lowered to known depths through a series of holes at known distances from the transducer, including at the central beam axis. As the water was very still, we were able to position the sphere within the beam at a variety of known off-axis angles and obtain

the corresponding uncompensated sphere TS. With these measurements, we calculated the beam pattern parameters needed for deconvolution, as well as gain and S_a corrections.

2.3.2 Data processing

Hydroacoustic data were processed in Echoview® software (6.1, Myriax, Hobart, Australia). The calibration parameters obtained from the frozen lake calibrations (single beam) and *in situ* calibrations (split beam) were applied to the data collected in Cobscook Bay. A -60 dB threshold was then used for single beam TS data, which would ensure fish of -54 dB and higher were detected within the half-power beam angle and eliminate most backscatter from small non-fish targets (e.g., zooplankton; Simmonds and MacLennan 2005). A -54 dB threshold was applied to the compensated split beam TS data (TS that had already been corrected for beam pattern). Additionally, after being exported from Echoview®, split beam fish tracks with minimum uncompensated TS below -60 dB were removed from the split beam dataset. These two thresholding steps helped ensure that the fish included in the split beam data were similar to those included in the single beam data, making the datasets more directly comparable.

The only noise removal necessary was to omit any data that were contaminated by entrained air, and to remove any data where echoes from individual fish were likely to overlap. To reduce the number of multiple targets falsely identified as individuals, single target tracking parameters were chosen to accept the least distorted echoes (Table 2.1). Fish tracks were additionally visually inspected to remove any that clearly came from more than one fish (e.g., crossed tracks).

Table 2.1 Single target detection parameters. Parameters were used in Echoview® software to detect and track individual fish.

Process	Parameter	Value
Single target detection: single beam method 2	TS threshold	-60 dB
	Pulse length determination level	6.00 dB
	Min. normalized pulse length	0.20
	Max. normalized pulse length	2.00
Single target detection: split beam method 2	TS threshold	-54 dB
	Pulse length determination level	6.00 dB
	Min. normalized pulse length	0.20
	Max. normalized pulse length	2.00
	Beam compensation model	Simrad LOBE
	Max. beam compensation	10.00 dB
	Max. standard deviation of:	
	Minor-axis angles	0.6°
	Major-axis angles	0.6°
	Pulse length at 6 dB (normalized)	0.70 to 1.30
	Pulse length at 12 dB (normalized)	0.70 to 1.30
	Pulse length at 18 dB (normalized)	0.60 to 1.40

Fish were tracked using Echoview®'s 2D tracking algorithm for single beam data and the 4D tracking algorithm for split beam data (Table 2.2). Track TS was then exported for further analysis in R. TS data exported for the single beam were uncompensated for beam pattern, and TS data exported for the split beam included both compensated and uncompensated values.

Table 2.2 Single beam (2D) and split beam (4D) fish track detection parameters.
Parameters were used in Echoview® software to detect and track individual fish.

Process	Parameter	Value
Fish tracking: 2D	Data	2D
	Alpha (range)	0.7
	Beta (range)	0.5
	Exclusion distance (range)	0.4 m
	Missed ping expansion (range)	0 %
	Weights:	
	Range	40
	TS	0
	Ping gap	0
	Min. number of single targets in a track	5
	Min. number of pings in a track	5 pings
	Max. gap between single targets	3 pings
Fish tracking: 4D	Data	4D
	Alpha (major, minor, range)	0.7, 0.7, 0.7
	Beta (major, minor, range)	0.5, 0.5, 0.5
	Exclusion distance (major, minor, range)	4, 4, 0.4 m
	Missed ping expansion (major, minor, range)	0, 0, 0 %
	Weights:	
	Major axis	30
	Minor axis	30
	Range	40
	TS	0
	Ping gap	0
	Min. number of single targets in a track	3
	Min. number of pings in a track	3 pings
	Max. gap between single targets	5 pings

2.3.3 Deconvolution

Deconvolution is a signal processing technique which reverses the effects of convolution, which is when a signal is modified by another signal prior to measurement. In the case of data from a single beam echosounder, the true probability density function (PDF) of the backscatter of fish randomly distributed across the beam, $w_F(e)$, has been convolved with that of the beam pattern, $w_T(b)$, to result in the measured backscatter

PDF, $w_E(e)$ (see calculation of the PDFs, below). Using the notation of Clay (1983), the convolution is

$$w_E(e) = w_T(b) * w_F(e) \qquad [1]$$

where * indicates convolution, the character "e" represents backscattering strength (instead of the conventional σ_{bs}, for consistency with Clay 1983 and Stanton and Clay 1986), and b is beam intensity. Convolution becomes simple multiplication if the signals are represented in the frequency domain:

$$W_E(\alpha) = W_T(\alpha)W_F(\alpha) \qquad [2]$$

where $W_E(\alpha)$, $W_T(\alpha)$, and $W_F(\alpha)$ are the Fourier transforms of the PDFs. Deconvolution consists of solving equation [2] for $W_F(\alpha)$ and using the inverse Fourier transform to recover $w_F(e)$.

The numerical deconvolution approach presented in Clay (1983) was used to recover $w_F(e)$ from $w_E(e)$, using the known beam pattern PDF $w_T(b)$. This method applied z-transforms to convert the two known PDFs into polynomial expressions in the frequency domain. Polynomial long division was then used to calculate $w_F(e)$ using equation [2]. Matlab's function *deconv,* adapted to work in R, was used for this purpose. The result, $w_F(e)$, was the fish backscatter PDF that had been corrected for the effect of the beam pattern. The PDF was translated to a number of fish per backscatter bin by multiplying the PDF probabilities by the total number of fish detected, as the sum of all probabilities in a PDF is 1. For ease of visualization and interpretation of results, backscatter was converted to TS (with units of dB) using the relationship

$$TS = 10 \log_{10}(e) \qquad [3]$$

2.3.4 Beam pattern PDF

For both transducers, data from calibrations were used to calculate the dB dropoff $(dB_{drop}(\theta))$ at different off-axis angles (θ) within the beam:

$$dB_{drop}(\theta) = \frac{TS_{exp} - TS_{meas}(\theta)}{2} \qquad [4]$$

where TS_{exp} is the expected on-axis TS (in dB re 1 m^2) of the standard sphere under the given environmental conditions (salinity, temperature, and pressure; http://swfscdata.nmfs.noaa.gov/AST/SphereTS), $TS_{meas}(\theta)$ is the measured TS of the sphere at θ, and $dB_{drop}(\theta)$ is the dB dropoff at θ, in dB. The difference in TS is divided by 2 because the observed TS difference includes energy lost while sound traveled the distance between the transducer and the sphere twice: first, to the sphere from the transducer, then once reflected, to the transducer from the sphere. The beam pattern, $B(\theta)$, was modeled as a function of θ using a second order polynomial

$$B(\theta) = 0 + c_1\theta + c_2\theta^2 \qquad [5]$$

where $B(\theta)$ is in dB, and c_1 and c_2 are constants. $B(\theta)$ was then converted to its linear form

$$b(\theta) = 10^{B(\theta)/10} \qquad [6]$$

where $b(\theta)$ is the directivity of the transducer, ranging from 1 on the central axis and decreasing toward 0 as θ increases. For a given distance from the transducer, $b(\theta)$ is the ratio of the echo amplitudes of a target at off-axis angle θ and a target located on-axis. The beam PDF is the function that describes the probability of a point randomly located within the beam's cross section having intensity b. To estimate the beam PDF function, equations [5] and [6] were used to calculate b for 1000 generated points, randomly distributed across the acoustic beam with beam pattern $B(\theta)$. These points were divided

into intensity bins of equal width in the log domain, and the proportion within each bin was calculated to estimate the beam PDF. More fish were present in August 2012, which allowed the use of smaller intensity bins than March 2013 (see below), so beam intensity was divided into 20 equally spaced bins per decade (order of magnitude difference) for deconvolution of August data, and into 10 bins per decade for March data. The PDF of the beam pattern, $w_T(b)$, was then fit to the estimated probabilities, $P(b)$, in the form:

$$w_T(b) = A \cdot P(b)^{-B} \hspace{2cm} [7]$$

where A and B are constants. In this process, b was limited to the range 0.005 to 1. The minimum value of 0.005, which corresponds to a dB dropoff of -23 dB, was chosen based on recommendations in Clay (1983) and Stanton and Clay (1986) to avoid the first side-lobe level.

2.3.5 Fish echo PDF

The mean backscattering strength (units of m^2) of tracked fish was treated in the manner outlined by Stanton and Clay (1986). Fish TS was first converted to backscattering strength (e) using

$$e = 10^{\frac{TS}{10}} \hspace{2cm} [8]$$

The next steps followed the process for the beam pattern PDF: fish backscatter data were divided into backscattering bins of equal width in the logarithmic domain, with 20 steps per decade in August 2012 (in the TS scale, each bin was 0.5 dB wide) and 10 steps per decade in March 2013 (1.0 dB wide in the TS scale). The counts from these backscatter bins were divided by their sum to attain the fish echo PDF, $w_E(e)$. Deconvolution is sensitive to noise, so $w_E(e)$ was then smoothed with a method similar to that described by Stanton and Clay 1986 (Fig 2.3). A smoothing window of length n was

chosen, and a third-order polynomial was fit to the first n/2 points on either side of each

point in the PDF. The modeled values within each intensity bin were then averaged to

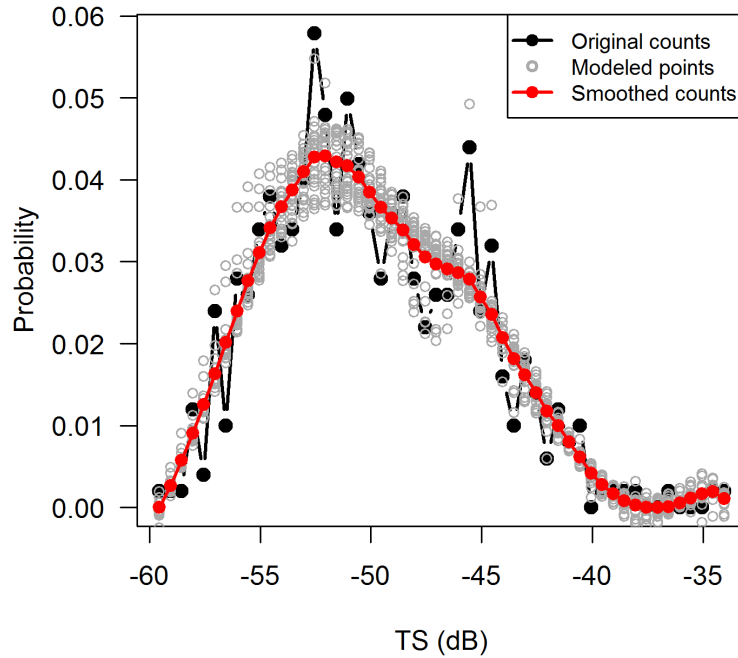achieve the values for the final smoothed PDF to be used in deconvolution.

Fig 2.3 Smoothing of the echo PDF of fish detected. Shown is the echo PDF of fish detected in August 2012 by the wide-angle single beam echosounder. The vertical axis is the probability that fish backscatter falls within each backscatter bin, with points located horizontally at the center of their respective bins. Original PDF shown in black, modeled points from smoothing process shown in gray, and final smoothed PDF (average of modeled points in each backscatter bin) shown in red. TS is the logarithmic form of fish backscatter, and has units of decibels. Smoothing window was 0.5 times the length of the PDF.

Deconvolution results were sensitive to the width of the smoothing window that

was used. Previous work has chosen smoothing parameters by visual inspection of the

results (Clay 1983), judging whether variation was real or noise. We also chose the best

smoothing window by eye, but in addition to evaluating the deconvolved fish TS

distributions, we inspected the effects of the smoothing window on deconvolved

calibration sphere TS (Fig 2.4). The longest windows (0.6 or more times the length of

the echo PDF) worked the best for the calibration sphere but appeared to over-smooth the

fish TS distributions, and the shortest windows (0.4 or less times the length of the echo

PDF) preserved variation in the fish TS distributions but introduced large noise spikes to the calibration sphere TS distribution. The final smoothing window was a compromise between the two extremes (window width of one half the length of the PDF; Fig 2.4b).
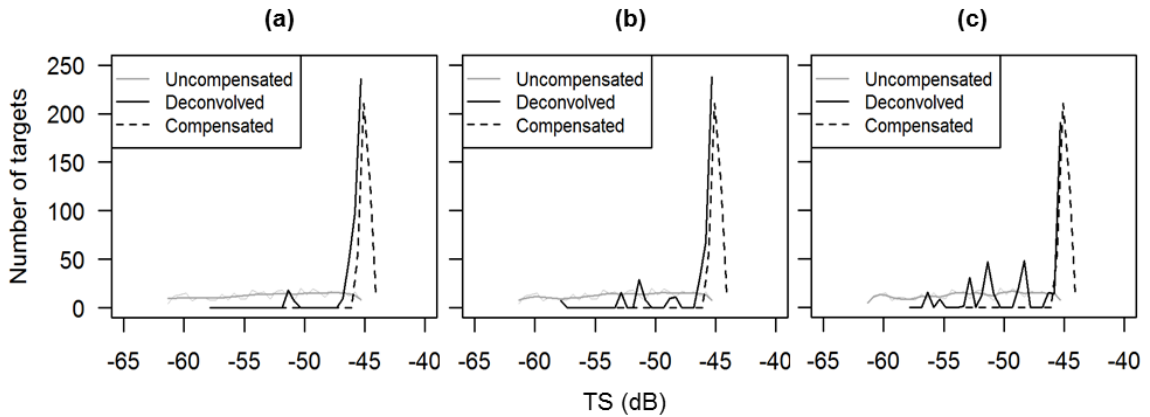
Fig 2.4 Results of deconvolution of sphere TS. Three different smoothing window lengths were used: (a) 0.7, (b) 0.5, and (c) 0.3 times the length of the PDF.

2.3.6 Assessment of deconvolution accuracy

To test the performance of the deconvolution method, the compensated backscatter from the split beam echosounder was used as a reference. Compensated backscatter is backscatter that has been corrected for beam pattern for each individual fish based on its location within the beam, and was assumed to be representative of reality. Uncompensated backscatter from the split beam is equivalent to backscatter from a single beam of equal dimensions, as it has not been corrected for beam pattern. Uncompensated split beam data were deconvolved using the split beam pattern, and the result was compared to the compensated data to assess the functionality of the method for a narrow-angle single beam echosounder. The backscatter of fish detected with the wide-angle single beam echosounder was deconvolved using the single beam pattern (generated from the ice calibration data), and those results were also compared to

49

compensated backscatter from the split beam echosounder. Kolmogorov-Smirnov tests with a significance level of 0.05 were used to verify visual comparisons.

2.4 Results

2.4.1 Transducer calibration

The scientific-grade split beam calibration matched the factory-provided calibration data (Fig 2.5, Table 2.3). The commercial-grade single beam echosounder had a slightly narrower beam than expected (Fig 2.5, Table 2.3). The greater uncertainty in sphere position with the single beam echosounder is evidenced by the greater variation in readings at each off-axis angle, compared to the split beam. Both transducers' beam patterns were well-represented by the second degree polynomial fit to the data in the TS domain.
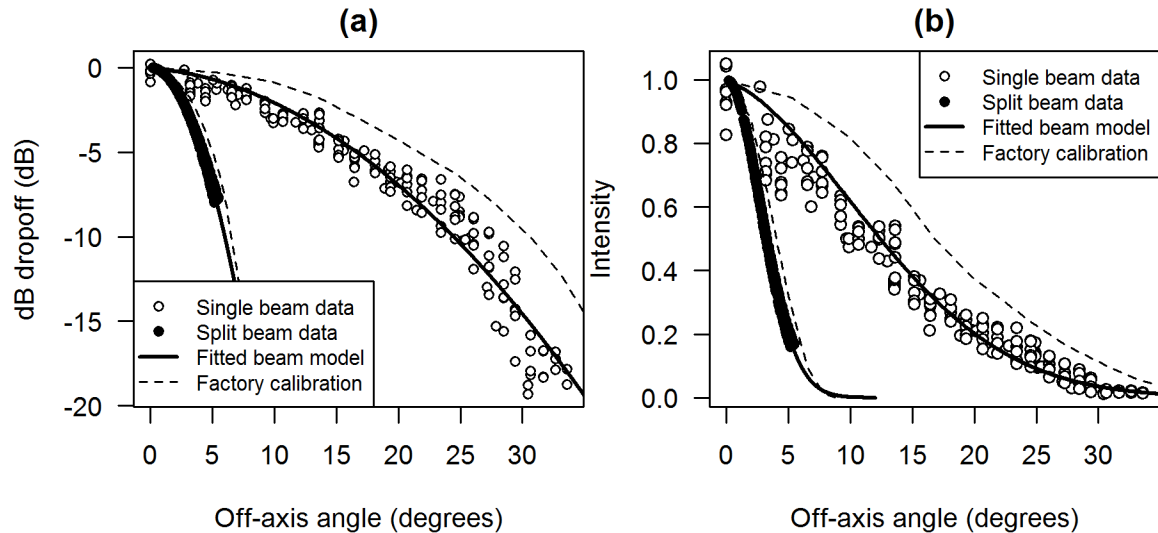

Fig 2.5 Results of echosounder calibrations. Beam pattern shown as (a) dB dropoff and (b) intensity at a range of off-axis angles. Points are calibration data, the thick lines are models fit to each echosounder's calibration data, and the dashed lines are the factory-specified beam patterns of each transducer.

Table 2.3 Single and split beam data calibration parameters. Split beam values were obtained from *in situ* calibrations in August 2012 and March 2013. Single beam values were based on winter calibrations carried out in 2011, 2013, and 2014.

Parameter	Split beam August 2012	Split beam March 2013	Single beam
3 dB (half-power) beam angle	6.6° (major axis) 6.5° (minor axis)	6.5° (major axis) 6.6° (minor axis)	24.8°
Gain	25.7 dB	26.0 dB	8.5 dB
Sa correction	-0.5 dB	-0.6 dB	- 0.3 dB l

2.4.2 Beam pattern PDF

The PDF of the beam for each echosounder (Fig 2.6) matched expectations, indicating the probability of receiving a full-intensity (e.g., on-axis) echo was lower than the probability of receiving weaker-intensity (e.g., off-axis) echoes. Targets within the narrow-angle split beam are more likely to have higher intensities than those within the wide-angle split beam, and less likely to have very low intensities, due to the shape of each beam.
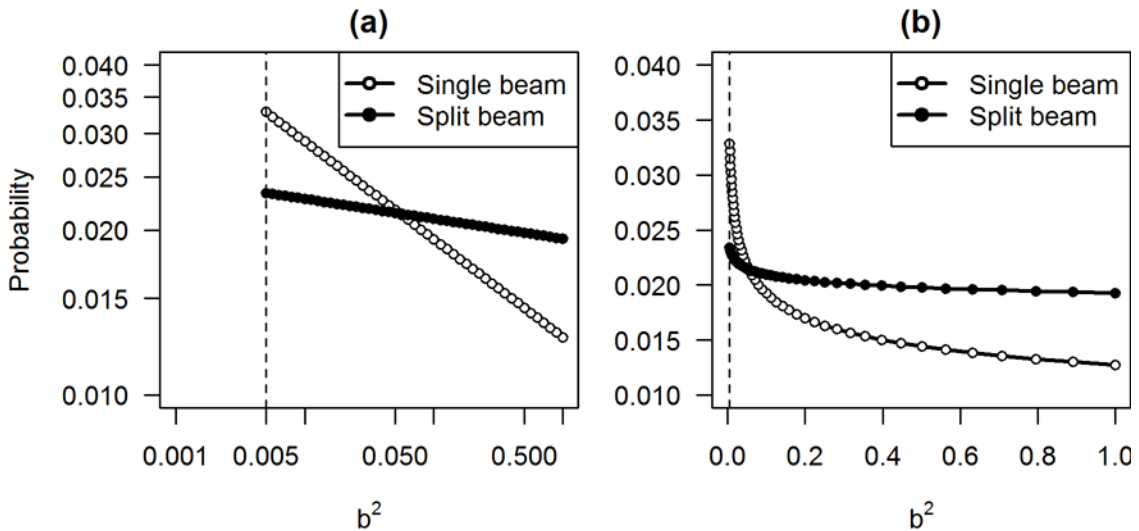

Fig 2.6 Beam pattern probability density function. $w_T(b)$ shown for the 200 kHz single and split beam echosounders, with (a) logarithmic and (b) linear axes. Vertical line indicates minimum intensity included in analyses (0.005). The beam intensity shown is squared, as sound is affected by the beam pattern twice as it travels to and from a reflective object.

51

2.4.3 Fish echo PDF

More fish were detected in August than in March, as expected (Fig 2.7), and more were detected by the wide-angle single beam than the narrow-angle split beam. In August 2012, 501 fish were detected by the single beam, but the split beam detected only 377 fish. In March 2013, only 141 fish were detected by the single beam, and 80 by the split beam. In both months, the distribution of uncompensated single beam backscatter had greater contributions from stronger targets than the uncompensated split beam (Fig 2.7a). In March, the low sample sizes of the split and single beam datasets resulted in highly variable, low-resolution TS distributions (Fig 2.7b).
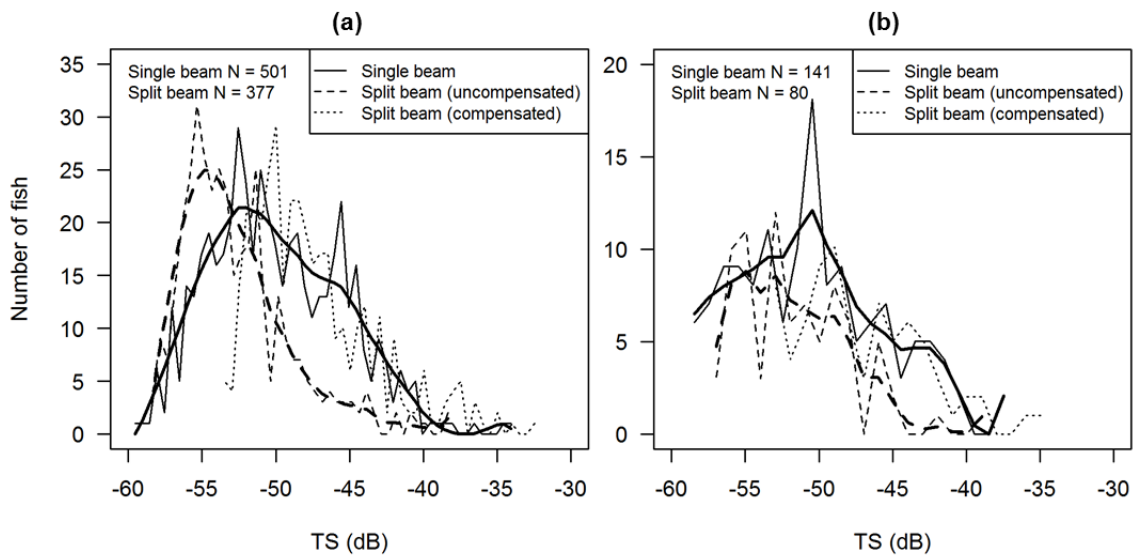
Fig 2.7 Distribution of TS data from single beam and split beam echosounders. (a) August 2012 and (b) March 2013. Data were divided into 20 backscatter bins per decade in August, and 10 per decade in March. The number of fish in each sample (N) shown in upper right. Thick lines indicate smoothed TS distributions (using a window size of 0.5 times the PDF length) which were used in deconvolution.

2.4.4 Deconvolution

For the split beam echosounder data, in August 2012, deconvolved uncompensated backscatter followed a similar distribution as the compensated backscatter, with a main peak near -50 dB and a left skew (Figure 2.8a). However, the

52

deconvolved distribution also had a small secondary main peak near -54 dB which was not present in the compensated data. Also, in its tail, the deconvolved distribution had smaller peaks centered near -43 dB and -40 dB that were not evident in the compensated distribution. All compared distributions were significantly different at the 5% level (Kolmogorov-Smirnov p-value < 0.05).

In March 2013, the deconvolved split beam backscatter did not match the compensated backscatter well (Fig 2.8b). Compensated backscatter indicated a main peak near -49 dB, a secondary peak at -44 dB, and a small peak at -39 dB. The deconvoluted backscatter showed peaks near -52 dB, -47 dB, and -44 dB.

Fig 2.8 Results of deconvolution of uncompensated backscatter from the split beam echosounder. (a) August 2012 and (b) March 2013. Uncompensated (magenta), deconvolved (blue), and compensated (green) TS distributions are shown. The number of fish in each sample (N) shown in upper right. The thick magenta line shows the smoothed TS distribution (using window length of 0.5 times the PDF length) that was used in deconvolution, and the thin magenta line shows the unsmoothed TS distribution. Data were divided into 20 backscatter bins per decade in August, and 10 per decade in March.

For the wide angle, commercial-grade single beam echosounder, in August 2012, the deconvolved distribution was bimodal, with one peak centered below the peak of the compensated split beam backscatter (-50 dB) and the other, larger peak at -44 (Fig 2.9a). In March 2013, the deconvolved single beam backscatter distribution was trimodal, with peaks at -49, -44.5, and -40 dB (Fig 2.9b). These peaks were close to those of the compensated split beam backscatter, but had very different relative sizes, with most echoes in the smallest and largest peaks, and relatively few in the center one.
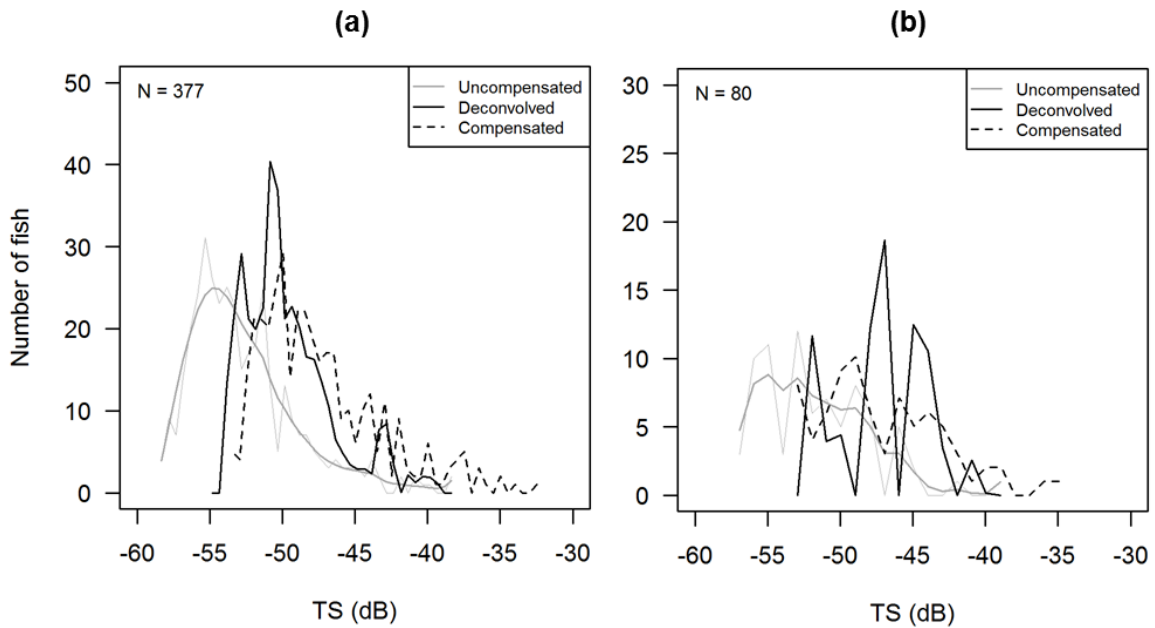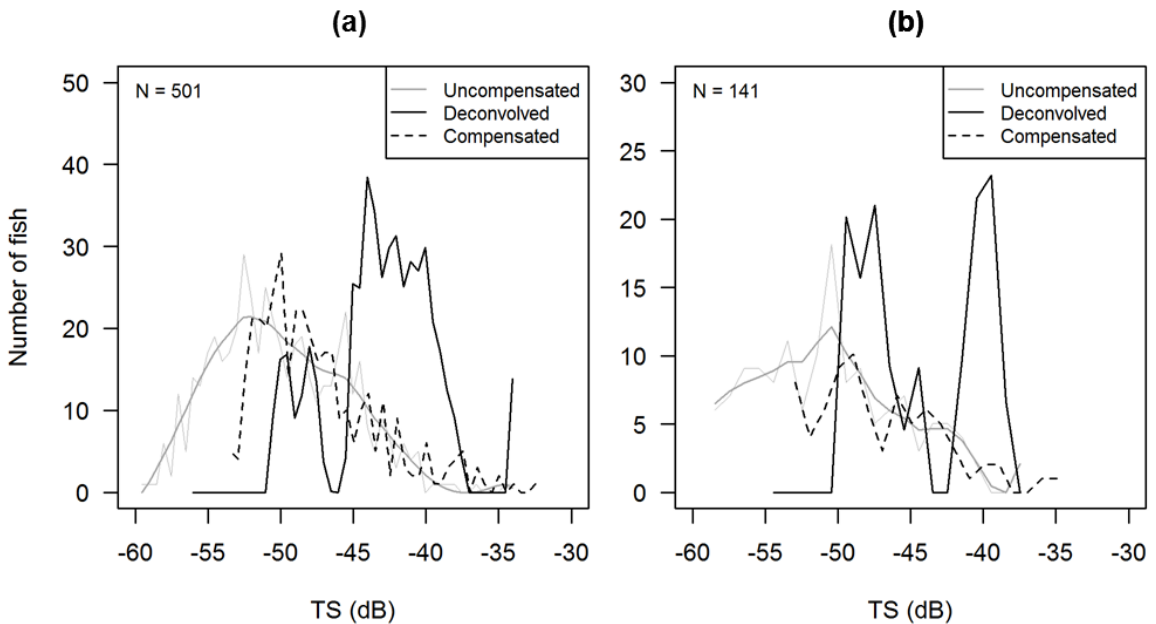

Fig 2.9 Results of deconvolution of uncompensated backscatter from the single beam echosounder. (a) August 2012 and (b) March 2013. Uncompensated (magenta) and deconvolved (blue) single beam TS distributions are shown, as well as the compensated (green) split beam TS distribution. The number of fish in each sample (N) shown in upper right. The thick magenta line shows the smoothed TS distribution (using window length of 0.5 times the PDF length) that was used in deconvolution, and the thin magenta line shows the unsmoothed TS distribution. Data were divided into 20 backscatter bins per decade in August, and 10 per decade in March.

2.5 Discussion

Deconvolution did not adequately correct backscatter data from the wide-angle, commercial-grade single beam echosounder. While the smaller peaks in the deconvolved TS distributions aligned well with reality (the compensated split beam TS distribution), in both surveys, there was a large peak at stronger TS that was not evident in the compensated split beam data. This large peak was likely the result of multiple targets being falsely interpreted as single targets. The single beam's long pulse duration meant that fish passing through the beam at the same time would need to be separated vertically by at least 38 cm to be distinguished from each other. The wide angle increased the likelihood that more than one fish would be present in the beam at similar depths at any given time. Multiple fish interpreted as one target would have stronger TS than the individual fish involved (Simmonds and MacLennan 2005). Deconvolution of data comprised of a mix of single targets and single targets that were actually multiple targets would result in the bimodal TS distribution that we observed, with one peak near the true TS and the other at stronger TS. Without the reference provided by the split beam echosounder, we would not have known that the peak at stronger TS was false, and may have concluded that the fish community sampled had a bimodal length distribution. Given this high uncertainty, it is likely best to limit the use of the wide-angle single beam to relative density measurements (e.g., Viehman et al. 2015, Staines et al. 2015).

Some steps could be taken to improve the suitability of wide-angle single beam data for deconvolution techniques. First, the pulse duration could be reduced, e.g. to 0.064 ms, like the split beam. Using a shorter pulse duration would decrease the volume of each vertical sample, and therefore decrease the likelihood of detecting multiple fish

and classifying them as individuals. Second, single target detection parameters could be stricter. The shape of the echo returned by many targets, as opposed to single targets, is more distorted relative to the sound pulse output by the transducer (Simmonds and MacLennan 2005). Accepting only the least distorted echoes would reduce the multiple targets accepted as single targets. In the present study, further restricting single target acceptance would have eliminated many of the tracked fish. As our sample sizes were already quite low for deconvolution, using stricter single target detection parameters would require collecting data for longer periods of time, particularly at times of the year when fish are scarce. However, sampling for multiple days per survey could more than offset any savings gained by using a single beam transducer, in which case it would be best to use a split beam and acquire accurate TS information for individual fish.

While deconvolution may not be sufficient to correct data from a wide-angle single beam for TS, it may provide useful information for a narrow-angle single beam using a short pulse duration. Deconvolution of the uncompensated split beam backscatter yielded a TS distribution that appeared very similar to that of the compensated data, though shifted slightly toward weaker and statistically different. Unlike the wide-angle single beam, no large peak was observed at stronger TS, indicating multiple-targets were not as much of an issue for the narrow-angle beam. Many of the discrepancies between the deconvolved and compensated TS distributions may therefore have been due to the low sample size increasing variability in the fish echo PDFs. Deconvolution is recommended to be used only with "many" targets by multiple authors (Simmonds and MacLennan 2005, Clay 1983, Stanton and Clay 1986), though no concrete lower limit has been given. Sample size appeared to have a very strong effect on deconvolution

56

results in this study: deconvolution of split beam data performed very poorly in March, when only 80 fish were sampled by the split beam, but resembled the compensated TS distribution well in August, when 377 fish were sampled. It is possible that if more fish were sampled, results would have been more accurate. Other approaches to deconvolution may also perform better with lower sample sizes than the method we followed. For example, the Expectation Maximum and Smoothing approach developed by Hedgepeth et al. (1991) was found to be less sensitive to slight variation in the echo PDFs, which might make it more appropriate for use on fish-scarce datasets.

If split beam echosounders are not an option, it would be best to avoid utilizing TS data from the single beam echosounder unless surveys are long enough to ensure several hundred individual fish tracks are available for deconvolution. An alternative option to using TS data to examine individual fish would be to use echo integration. Volume backscatter (S_V) is a summation of the energy reflected within the acoustic beam, and area backscatter (s_a) is the summation of energy within a certain depth bin (Simmonds and MacLennan 2005). With a calibrated single beam echosounder, S_V and s_a are relative indices of fish density, and these can provide useful information. Viehman et al. (2015) and Staines et al. (2015) both used S_V and s_a to describe relative changes in fish density and their vertical distribution at the tidal power site over time, and these data were sufficient for regulators to issue a pilot project license at the Cobscook Bay site. If absolute fish density is required, these relative values may be converted to absolute estimates of density if the backscattering cross-section of sampled fish is known, but obtaining this value would require the use of a split beam echosounder or high confidence in deconvolved single beam data. In a mixed-species fish community such as Cobscook

Bay (Vieser 2014), accurate absolute fish density estimates would be difficult to obtain via echo integration, even if the backscattering cross-sections of each species were known.

Deconvolution of data from a narrow-angle single beam echosounder operating with a short pulse duration may provide accurate fish TS distributions. In areas or times of year when fish are sparse, this may require sampling for longer periods of time than the 24-hr surveys used in our BACI study of Cobscook Bay. If fish numbers and TS distributions over sufficiently long time scales (e.g., long enough to sample several hundred fish) are all that is necessary in a monitoring plan, the deployment of a single beam echosounder may be sufficient. However, if information on individual fish is needed, or TS distributions with high temporal resolution (e.g., tide by tide), a split beam echosounder would be necessary. The hydroacoustic system used for initial and post-device-deployment monitoring at a tidal power site will therefore depend on the resources available and the questions that are asked.

CHAPTER 3

MULTI-SCALE TEMPORAL PATTERNS IN FISH PASSAGE

IN A HIGH-VELOCITY TIDAL CHANNEL

3.1 Abstract

The natural variation of fish presence in high-velocity tidal channels is not well understood. A better understanding of fish use of these areas would aid in predicting fish interactions with marine hydrokinetic (MHK) devices, the effects of which are uncertain but of high concern. To characterize the patterns in fish presence at a tidal energy site in Cobscook Bay, Maine, we examined two years of hydroacoustic data continuously collected at the proposed depth of an MHK turbine with a bottom-mounted, side-looking echosounder. Fish passage rate maxima ranged from hundreds of fish per hr in the early spring to over 1,000 fish per hr in the fall. Rates varied greatly with tidal and diel cycles in a seasonally changing relationship, likely linked to the seasonally changing fish community of the bay. In the winter and spring, higher passage rates were generally confined to ebb tides and low slack tides near sunrise and sunset. In summer and fall of each year, the highest fish passage rates transitioned to night and occurred during ebb, low slack, and flood tides. Fish passage rate was not linked to current speed, and did not decrease as current speed increased, contrary to observations at other tidal power sites. As fish passage rate may be proportional to the encounter rate of fish with an MHK turbine at the same depth, highly variable passage rates indicate that the risk to fish is similarly variable. The links between fish presence and environmental cycles at this site will likely be present at other locations with similar environmental forcing, making these

observations useful in predicting potential fish interactions at tidal energy sites worldwide.

3.2 Introduction

Relatively little is known about how fish use areas with fast tidal currents. Fish activity levels and movement patterns vary on a wide range of spatial and temporal scales over the course of their lives, often in ways that are species- and life-stage specific (Pittman and McAlpine 2001, Reebs 2002, Gibson 2003). Many fish movements are related to environmental changes; for example, vertical migrations linked to the diel cycle, tidal movements into the intertidal zone, or seasonal movements on- or off-shore (Pittman and McAlpine 2001). In the high-velocity channels targeted for tidal energy extraction, underwater conditions change rapidly and fish presence and distribution likely fluctuates with similar magnitude and frequency. For example, there is already well-established evidence of some fish species changing their location in the water column to take advantage of favorable tidal currents in on- or off-shore migrations, a behavior known as selective tidal stream transport (Forward and Tankersley 2001). However, we lack data with sufficient temporal resolution and duration to fully describe the wide-ranging scales of temporal variation in fish presence in these environments.

The resolution and duration of a study aiming to describe the temporal distribution of marine organisms would ideally be defined relative to the highest- and lowest-frequency cycles present: for sampling to be considered high-resolution, sampling would ideally occur at several times the frequency of the highest-frequency cycle present, and a long-term study would sample for several times the duration of the lowest-frequency cycle (Heath et al. 1991). However, studies must typically be designed

60

to focus either on resolution or duration, rather than both (Urmy et al. 2012), because of cost or gear limitations (such as soak time for nets). Many high-resolution studies occur over the short-term (e.g., Embling et al. 2012, Axenrot et al. 2004, Simard et al. 2002, Zamon 2003, Gibson et al. 1996, Heath et al. 1991). Some have sought to characterize both short- and long-term variability by carrying out multiple short-term, high-resolution surveys over a long period of time (Viehman et al. 2015, Vieser 2014). Prior assumptions about patterns present in the variable of interest influence study design and can greatly restrict the scope of results (Heath et al. 1991).

Long-term, high-resolution sampling has been less common, but is ideal for understanding biological processes at sites where large changes may occur over multiple, wide-ranging time scales. One method of sampling large volumes of water rapidly for long periods of time is stationary hydroacoustics. Long-term stationary echosounder deployments have been used to examine the temporal variability of different biological sound scatterers in the ocean, including phytoplankton and zooplankton (Flagg et al. 1994), zooplankton (Cochrane et al. 1994, Picco et al. 2016), and zooplankton and fish (Urmy et al. 2012). These studies all found their pelagic subjects to be linked to changes in their physical environment on a variety of time scales, including tidal, diel, and/or seasonal cycles, and these patterns were generally not constant over the duration of sampling time.

Transient patterns are a common characteristic of biological processes, and wavelet analysis is an effective tool for detecting and describing such patterns (Cazelles et al. 2008). Wavelet analysis works by simultaneously decomposing time series data across both the frequency and time domains. Blauw et al. (2012) used wavelets to

explore the patterns present in their time series related to phytoplankton, as well as to relate phytoplankton growth with the tidal cycle and suspended particulate matter. Urmy et al. (2012) applied wavelets in part of their assessment of changing patterns in nekton density and vertical distribution. Apart from Urmy et al., the use of wavelets in studies of marine fish has been primarily to assess patterns in fishery catch rates and relate them to climatic oscillations, which occur on long time scales relative to what is pertinent in a tidal channel (Rouyer et al. 2008, Ménard et al. 2007).

In this study, we used wavelet analysis to describe the temporal variation in fish passage rate in Cobscook Bay, Maine. Data collection occurred at a site evaluated for tidal energy development, where an echosounder had been installed on the seafloor to monitor fish encounter with a marine hydrokinetic (MHK) turbine. After the turbine's removal, the echosounder continued to operate, and we detected fish in 2 years of high-resolution hydroacoustic data collected at turbine depth. Our goals were to obtain a better understanding of fish presence in this portion of the water column of this high-speed tidal channel, and to consider the implications of our findings for potential turbine effects.

3.3 Methods

3.3.1 Data Collection

Hydroacoustic data were collected at a tidal energy site in Cobscook Bay, ME, from July 15, 2013, to July 28, 2015 (Fig 3.1). The echosounder was installed by Ocean Renewable Power Company (ORPC) to observe fish behavior near ORPC's TidGen® tidal energy device, which was deployed at the site from August 2012 to July 2013. The use of this location by ORPC was authorized by the Federal Energy Regulatory

Commission (FERC), the Maine Department of Environmental Protection, and the Maine

Department of Conservation. The transducer was oriented to sample the area along the

face of the TidGen® turbine (Fig 3.2), and though the turbine was removed in July 2013,

the echosounder continued to collect data while the turbine was not present. The Simrad

EK60 echosounder used a 200 kHz, 7° split beam transducer, which was mounted 3.4 m

above the sea floor and 44.5 m from the turbine's support frame, and angled 6.2° above

horizontal. The echosounder sampled an approximately conical volume of water 5 times

(pings) per second, using a pulse duration of 0.256 ms and transmit power of 120 W. The

current flowed approximately perpendicular to the sampled volume, and speed in the

channel can range from 0 to approximately 2 m·s^{-1}, depending on the tide and lunar phase

(Viehman et al. 2015, Xu et al. 2006, Brooks 2006). Most fish moved with the current

and were therefore detected by several sequential pings as they passed through the
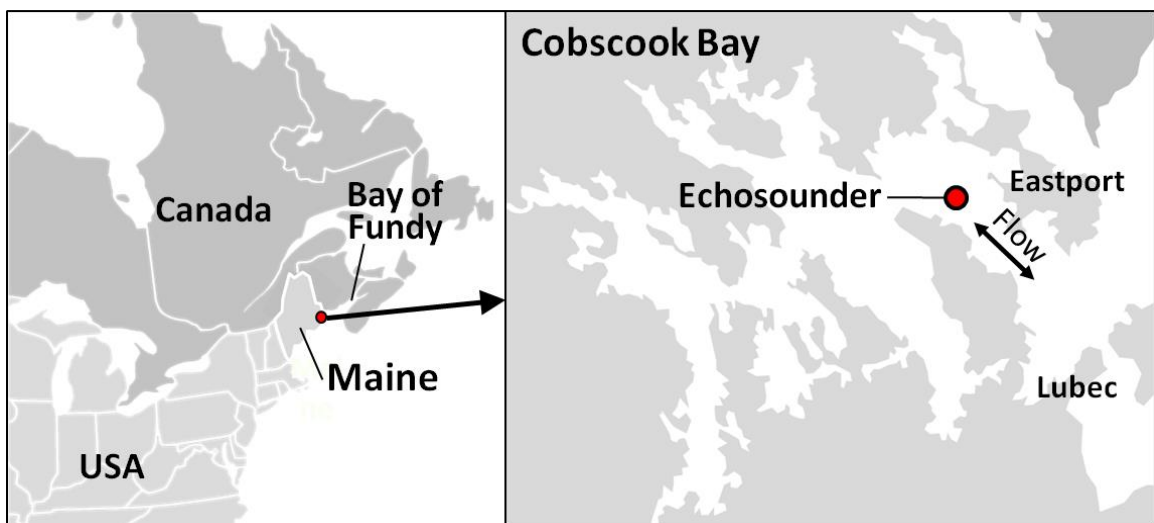
acoustic beam.

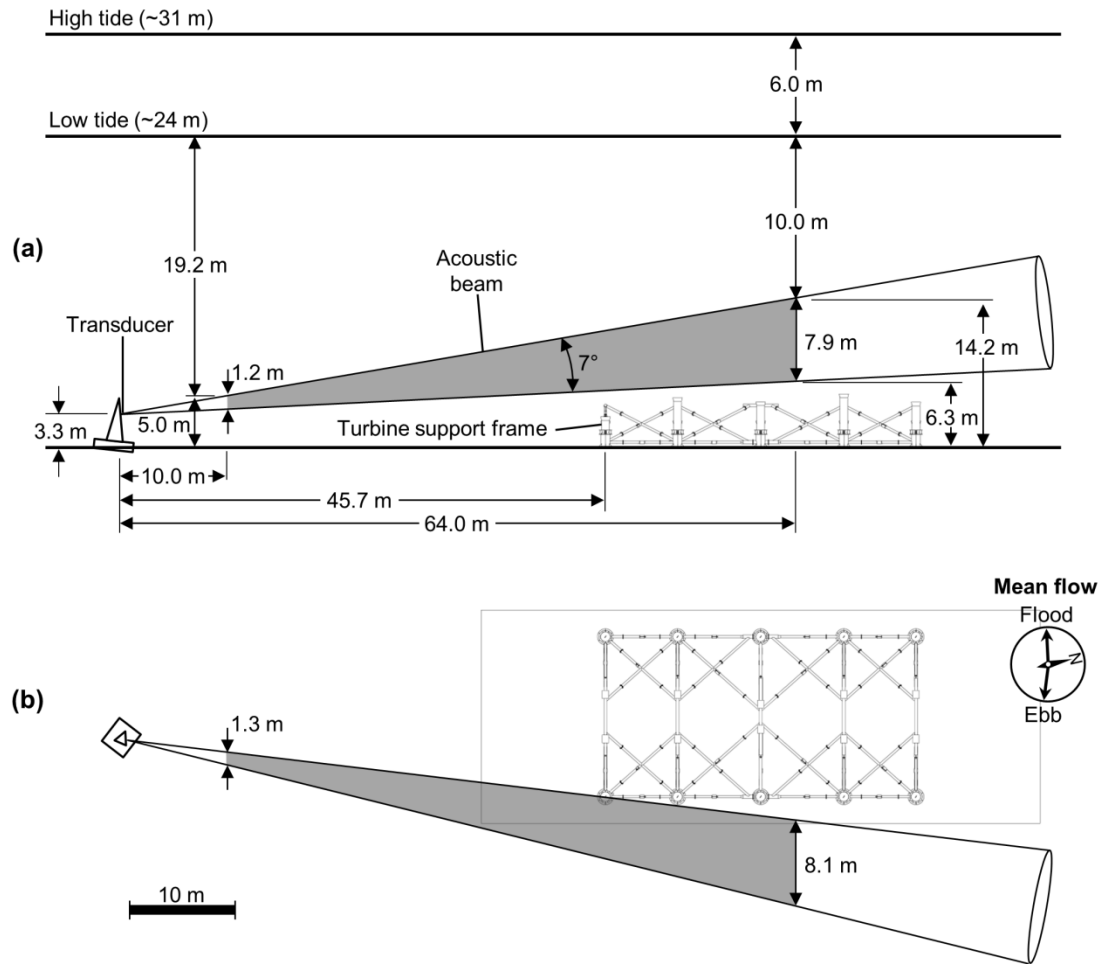**Fig 3.1 Map of study area.** Location of echosounder shown in right panel.

Fig 3.2 Echosounder setup in Cobscook Bay, Maine. The bottom support frame of Ocean Renewable Power Company's TidGen® device was present during data collection. The gray area indicates the sampled volume used in this study. TidGen® schematic provided by Ocean Renewable Power Company

The echosounder operated nearly continuously for the two years it was deployed, but there were several gaps in data collection due to technical issues or necessary shut-down of the echosounder during turbine-related activities, such as diver inspection (Fig 3.3). The final dataset included 582 days of data. However, not all of these data were complete: at times, the angular information associated with detected fish was not returned, which meant 3D positioning of fish within the beam during these times was not possible (Fig 3.3).
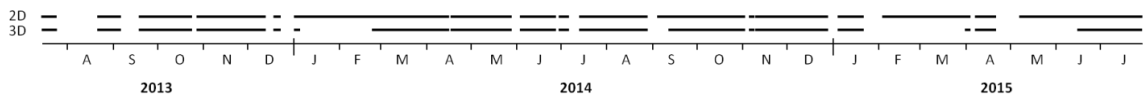
Fig 3.3 Periods of continuous data collection. 2D denotes data which did not always include angular information, which were used for obtaining fish counts; 3D denotes data which did include angular information, which were used for determining times of slack tide.

3.3.2 Data Processing

Acoustic data were processed using Echoview® software (6.1, Myriax, Hobart, Australia). Processing consisted of noise removal, fish tracking, and fish track export. Fish tracking was carried out both in 2D (which uses only time and range of single targets to detect fish) and 4D (which uses time, range, and position in the beam's cross-section). 4D tracking could only be carried out when 3D information was available, which left large gaps in the dataset (Fig 3). 2D tracking was therefore used to generate the time series of fish passage rates, as range and time information were returned whenever the echosounder was running. When angular data were available, fish were tracked in 4D in order to obtain accurate measures of fish target strength (TS), to verify fish counts supplied by 2D tracking, and to accurately model the tidal cycle using the direction traveled by fish (for identifying start and end times of tidal stages).

65

3.3.2.1 Noise removal

The acoustic data included several types of 'noise,' signal that was not from individual fish, which had to be removed before fish could be tracked. This noise included small, non-fish targets (e.g., large zooplankton), interference from the surface and entrained air near the surface, and schools of fish (in which individual fish cannot be accurately tracked). TS is a measure of the proportion of sound energy that is reflected back to the transducer by an object, and it is roughly proportional to the object's size. Applying a TS threshold of -50 dB eliminated most signal from small, non-fish targets, and roughly equates to a fish length of 4 cm (though fish TS varies greatly with anatomy and orientation relative to the beam; Love 1971). Surface interference was removed by limiting the maximum analysis range to 64 m, which is the range at which entrained air from the surface began heavily interfering with the acoustic signal. Background noise tended to increase with range but varied over time with water height and weather conditions. This type of gradually changing noise was removed using the method developed by De Robertis and Higginbottom (2007), modified to apply to TS data. Intermittent noise such as schools and clouds of entrained air was removed using multiple resampling and masking steps with Echoview® virtual operators. All of these methods were worked into a template that was then applied to all data using Echoview®'s scripting module (Fig 3.4).
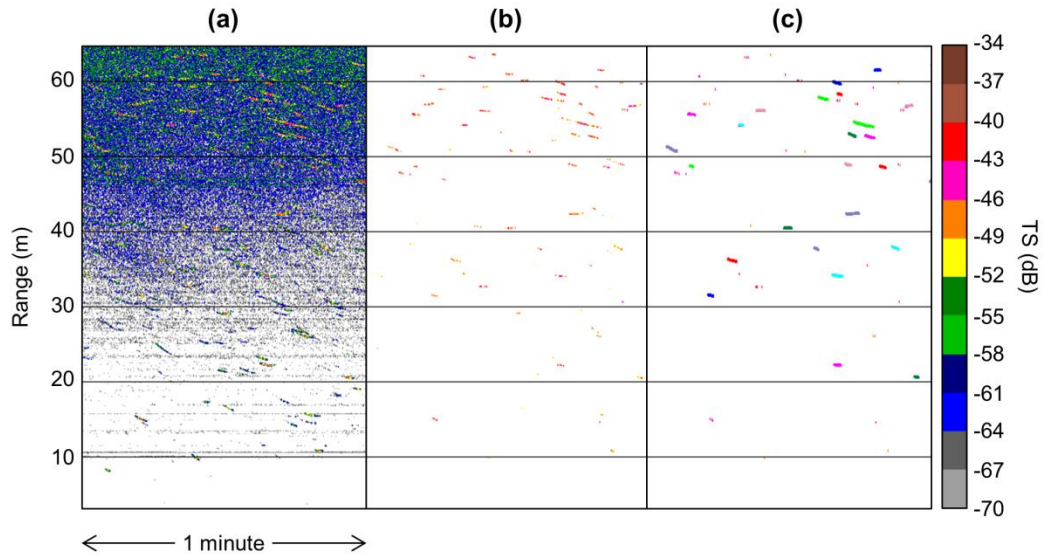
Fig 3.4 Acoustic data processing example. (a) Raw target strength data (scale in dB to right) showing multiple fish tracks and background noise. (b) Target strength data with noise removed and -50 dB TS threshold applied. (c) Single targets detected from cleaned target strength data with fish tracks (colored lines) overlaid.

3.3.2.2 Fish tracking

Once noise was removed from the acoustic data, single targets were detected and fish were tracked using both split beam (4D) and single beam (2D) methods (single target detection and fish tracking parameters shown in Table 1). As mentioned above, both tracking methods were used because of the intermittent angular data. Split beam single target detection and 4D-fish tracking rely on these angular data to determine if each echo was caused by a single object or multiple, and to correct TS values for beam pattern effects. Single beam single target detection and 2D fish tracking methods do not incorporate angular data. While this can result in less accurate fish tracking and TS estimates, in this case it provided a more complete time series of fish passage rates. Fish tracked via single beam, 2D methods were therefore used to construct the time series of passage rate, and split-beam, 4D methods were used to supplement our interpretation of this time series, providing estimates of fish TS and fish swimming direction (as an

67

indicator of tidal stage), and verifying temporal patterns in the time series made from fish

tracked in 2D.   All tracks were exported for further analysis in R (3.1.1, R Core Team,

Vienna, Austria).

Table 3.1 Acoustic data processing parameters. Parameters were used in Echoview® software
to detect and track individual fish.

Process	Parameter	Value
Single target detection: single beam method 2	TS threshold	-50 dB
	Pulse length determination level	6.00 dB
	Min. normalized pulse length	0.50
	Max. normalized pulse length	2.00
Single target detection: split beam method 2	TS threshold	-50 dB
	Pulse length determination level	6.00 dB
	Min. normalized pulse length	0.20
	Max. normalized pulse length	2.00
	Beam compensation model	Simrad LOBE
	Max. beam compensation	12.00 dB
	Max. standard deviation of:	
	Minor-axis angles	0.5°
	Major-axis angles	0.5°
	Minor-axis angle range	-2.5° - 2.5°
	Major-axis angle range	-2.5° - 2.5°
Fish tracking: 2D	Data	2D
	Alpha (range)	0.8
	Beta (range)	0.5
	Exclusion distance (range)	0.5 m
	Missed ping expansion (range)	0 %
	Weights:	
	Range	0
	TS	0
	Ping gap	0
	Min. number of single targets in a track	5
	Min. number of pings in a track	5 pings
	Max. gap between single targets	3 pings
Fish tracking: 4D	Data	4D
	Alpha (major, minor, range)	0.7, 0.7, 0.8
	Beta (major, minor, range)	0.5, 0.5, 0.5
	Exclusion distance(major, minor, range)	1.5, 1.5, 0.5 m
	Missed ping expansion (major, minor, range)	0, 0, 0 %
	Weights:	
	Major axis	0
	Minor axis	0
	Range	0
	TS	0
	Ping gap	0
	Min. number of single targets in a track	5
	Min. number of pings in a track	5 pings
	Max. gap between single targets	3 pings

3.3.3 Data Analysis

Data analysis included time series construction, time series gap-filling, the wavelet transform, and tidal stage modeling. The TS of fish tracked with 4D methods was summarized with median and interquartile range, but closer examination was avoided due to the mixed nature of the fish assemblage in Cobscook Bay and our inability to identify the species of each detected fish.

3.3.3.1 Time series construction

The time associated with each tracked fish was used to acquire counts of fish in 1-hr time increments, equating to a rate of fish passage through the sampled volume with units of fish·hr^{-1}. The distribution of ranges at which fish were detected did not change substantially over time, so individual fish were not weighted to account for beam width.

3.3.3.2 Gap-filling

Before the time series could be used in wavelet analysis, the gaps in the data needed to be filled by new values which would minimally impact subsequent temporal pattern analysis. This was done by mimicking the temporal patterns of the time series to the sides of each gap. For each gap, a Fourier transform was used to identify the most prevalent frequencies in the data within one gap-width before and after the gap (or 48 hours, if the gap was shorter). The upper 50% of the most important frequencies were chosen, which allowed the number of frequencies used to vary with gap size and mimicked the nearby data well. For each set of data from before and after a gap, the selected frequencies were used to construct a model of fish passage rate in the form:

$$y = \sum_{i=1}^{N} A_i \sin(2\pi f_i t) + B_i \cos(2\pi f_i t) + \varepsilon$$

69

where y is modeled fish passage rate, fi is the ith frequency of the N frequencies selected via the Fourier transform method, Ai and Bi are amplitudes, and ε is random error. Coefficients A and B and residual error values were obtained by fitting a linear model of the above form to data before and after the gap. Passage rate was predicted for each time point within the gap using both models, the results of which were weighted and summed: values from the before-gap model were weighted by 1-1/j, where j was the index of the predicted data point; data from the after-gap model were weighted in an opposite fashion. Though residual error was useful in evaluating each model's fit, error was not added to the predicted gap values. Introducing random error based on residuals simply exaggerated high-frequency noise within gaps that was uncharacteristic of the rest of the dataset, and this omission did not significantly alter results.

3.3.3.3 Wavelet transform

Once gaps in the time series were filled, a wavelet transform was used to inspect patterns in passage rate and how they changed over time. Wavelet transforms simultaneously decompose time series data across both the frequency and time domains by convolving the time series with a wave form (the 'wavelet'), which is scaled up or down within a chosen range as it is moved along the time axis. The result is a wavelet spectrum: a 2D representation of the prevalence of periodicities (frequency^{-1}) that compose the original time series, across the time spanned by the dataset (2 years, in this case). We applied a continuous wavelet transform using the Morlet wavelet to our time series of fish passage rate (package WaveletComp in R; Roesch and Schmidbauer 2014). The maximum frequency included was 2 times the sampling frequency (a periodicity of 2 hours), as this would be the highest possible frequency that could theoretically be

70

characterized (i.e., the Nyquist frequency). The maximum periodicity was limited to one-half of the total sampling period (1 year) because larger periodicities are overwhelmed by edge effects. The wavelet spectrum was tested at a 95% confidence level against a theoretical spectrum of white noise fit to the series using 100 iterations.

3.3.3.4 Tidal stage modeling

Fish tracked using split-beam, 4D methods were used to indicate the tidal stage via their direction of movement. At this site, fish move almost exclusively in the direction of the current except at slack tides, when movement was more uniformly distributed for a brief period of time (Viehman and Zydlewski 2015, Viehman et al. submitted). Fish direction could therefore be used as a proxy for tidal current direction, which could indicate tidal stage. This correlation was verified by comparing predicted tidal stages to several instances of ADCP current speed data that were collected from a moored vessel at the same site during the study period (Fig 3.5). Shifts in fish swimming direction (Fig 3.5a) corresponded to slack tides as indicated by the ADCP data (Fig 3.5b). The square-wave pattern of fish movement direction was very similar to the measured and modeled current direction at a nearby location presented by Xu et al. (2006), and flood and ebb tide movement directions (approximately 285° and 120°, respectively) aligned well with the known current direction at our study site (ORPC personal communication).
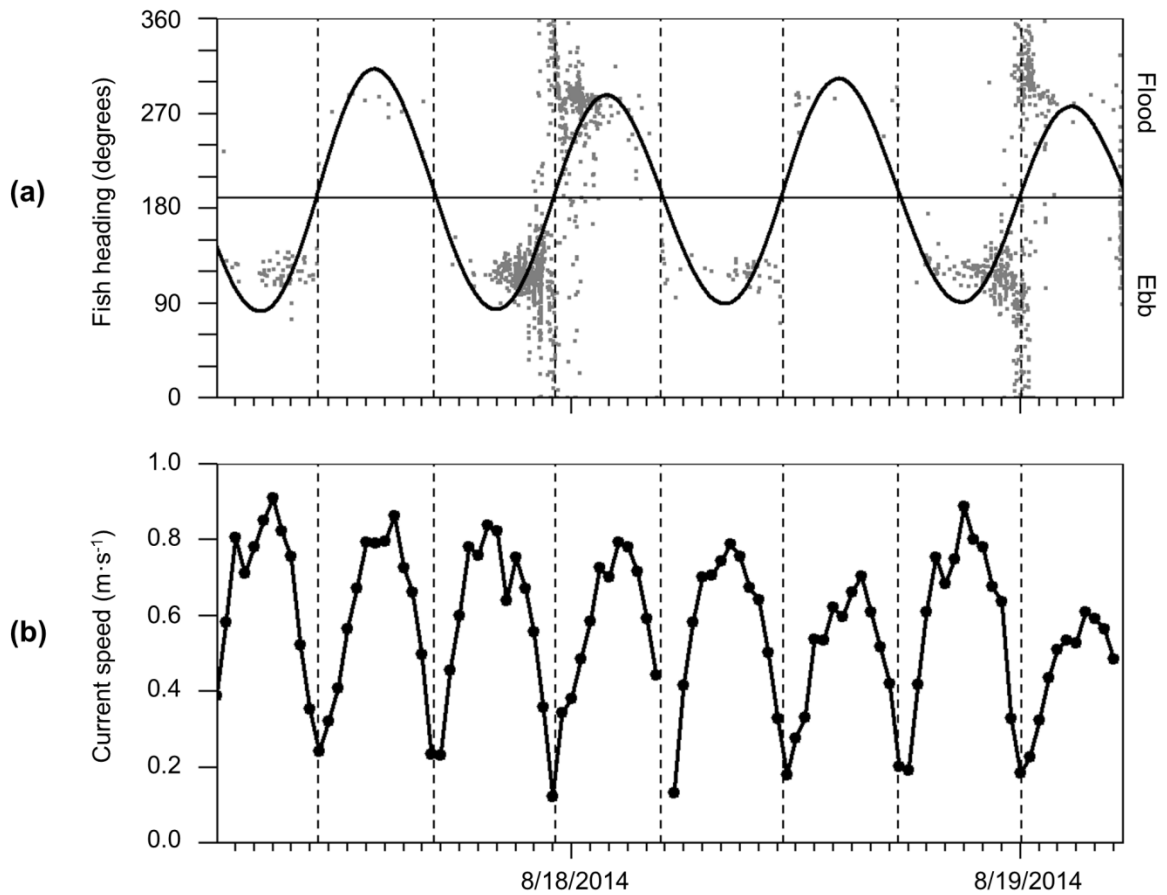
Fig 3.5 Fish heading and current velocity. Data **were** collected at the TidGen® site in March 2013. (a) Individual fish heading (gray points) shown with fitted tidal model (solid line) and its midline (horizontal line), which were used to calculate times of slack tide (vertical dashed lines). (b) Current speed collected concurrently by an ADCP at the same site, with same times of slack tide as shown in (a).

As large gaps existed in the 3D acoustic data, and therefore in the swimming directions available for tidal stage assignment, a tidal model was fit to existing fish direction data which could then be used to accurately predict tidal stage, even when 3D data were missing (thick solid line in Fig 3.5a). This tidal model was a summation of multiple sinusoids with varying periodicities, including the ten tidal components that have been used in shorter-term modeling studies of Cobscook Bay tidal currents (M2, K1, K2, N2, S2, O1, L2, M4, NU2, 2N2; Rao et al. 2015) and five other tidal periodicities that would be relevant to this 2-year span (P1, Q1, MF, MM, SSA). The

72

model was constructed as for the gap-filling step, except in this case fi was the ith tidal frequency of the 15 tidal components listed above (frequency = period^{-1}). Amplitudes A and B were obtained by fitting a linear model of the above form to the available fish direction data from the 3D dataset. The sinusoid peaks were defined as peak flood tides, the troughs were peak ebb tides, and slack tides (high or low) occurred wherever the sinusoid crossed its midline (Fig 3.5a).

3.4 Results

3.4.1 Target strength

The median target strength estimated from fish tracked using the 4D method was -45.1 dB, with an interquartile range of -46.5 to -43.4 dB. Using Love's (1971) general TS-length equation, this corresponds to a median fish length of approximately 6 cm, with an interquartile range of 5 to 7 cm.

3.4.2 Time series

Passage rates determined through 2D and 4D tracking methods agreed well with each other (Fig 3.6). Counts obtained via 2D methods were slightly higher than those obtained using 4D methods due to the less stringent target quality requirements of 2D tracking (Fig 3.6a), but when data were available in both datasets, the patterns were the same (Fig 3.6b).
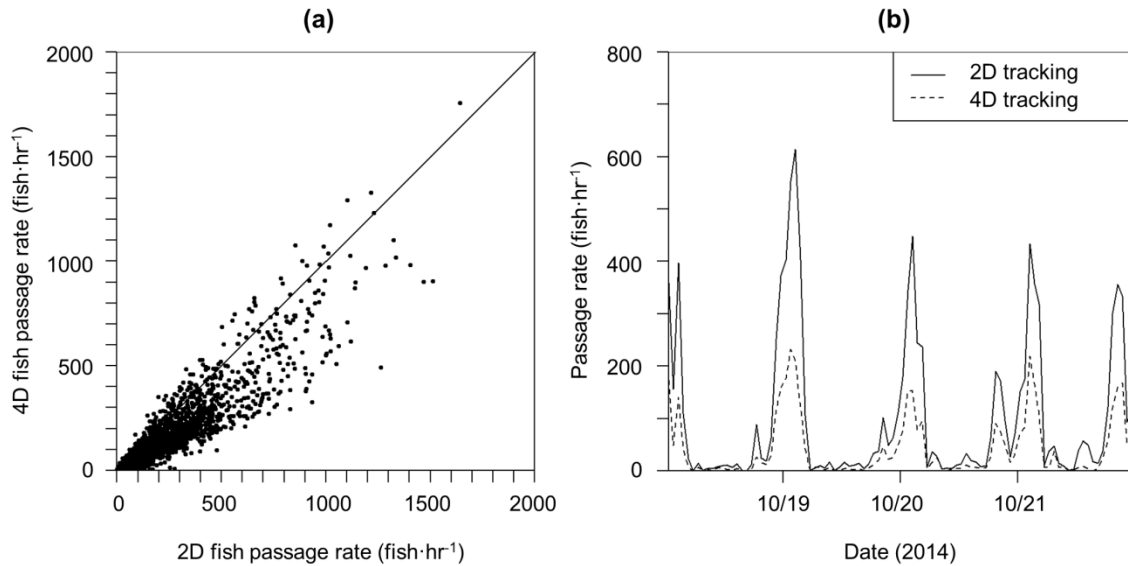
Fig 3.6 Comparison of fish passage rates obtained via 2D and 4D tracking. (a) 4D rates vs. 2D rates, shown with 1:1 line. (b) Subset of 2D (solid line) and 4D (dashed line) passage rates from October 2014.

Fish passage rate varied greatly over the two years spanned by the dataset, on both short and long time scales (Fig 3.7a). Overall, passage rate was highest in late summer and fall of both years, reaching over 1000 fish·hr^{-1}. During winter and spring, rate maxima were in the hundreds of fish·hr^{-1}. Passage rate could increase from 0 to hundreds of fish·hr^{-1} in a matter of hours, and it was evident that this variation was cyclic in nature (Fig 3.6b, Fig 3.7a). Values generated to fill the 20 gaps that existed in the 2D dataset appeared consistent with patterns in the surrounding data (Fig 3.7a) and were unlikely to interfere with interpretation of the wavelet spectrum.

3.4.3 Wavelet transform

The wavelet transform (Fig 3.7b) revealed the presence of a 365-day periodicity, which is indicative of the seasonal cycle that was evident in the raw time series (Fig 3.7a). This seasonal change in passage rate slightly lagged the seasonal change in temperature, with lowest rates in between winter and spring (e.g., March) and highest

74

rates in the fall (August through November). A continuous band in the wavelet transform at the 183-day periodicity and fainter, less continuous bands at around 14 and 28 days were also present, and coincided with tidal periodic components (Rao et al. 2016).

The strongest features of the wavelet transform were bands near 12- and 24-hr periods, which indicated variation in fish passage rate related to the tidal (and/or semi-diel) and diel cycles. These two periodicities were not constant throughout the dataset, but followed similar patterns in every year sampled, though with some variation in timing. The 24-hour periodicity was present only in the summer and fall, emerging in June in 2014 and 2015. The 12-hour periodicity was present throughout the year, but was most evident in the winter and spring (from January through May). For the rest of the year, the 12-hr periodicity was present but intermittent.
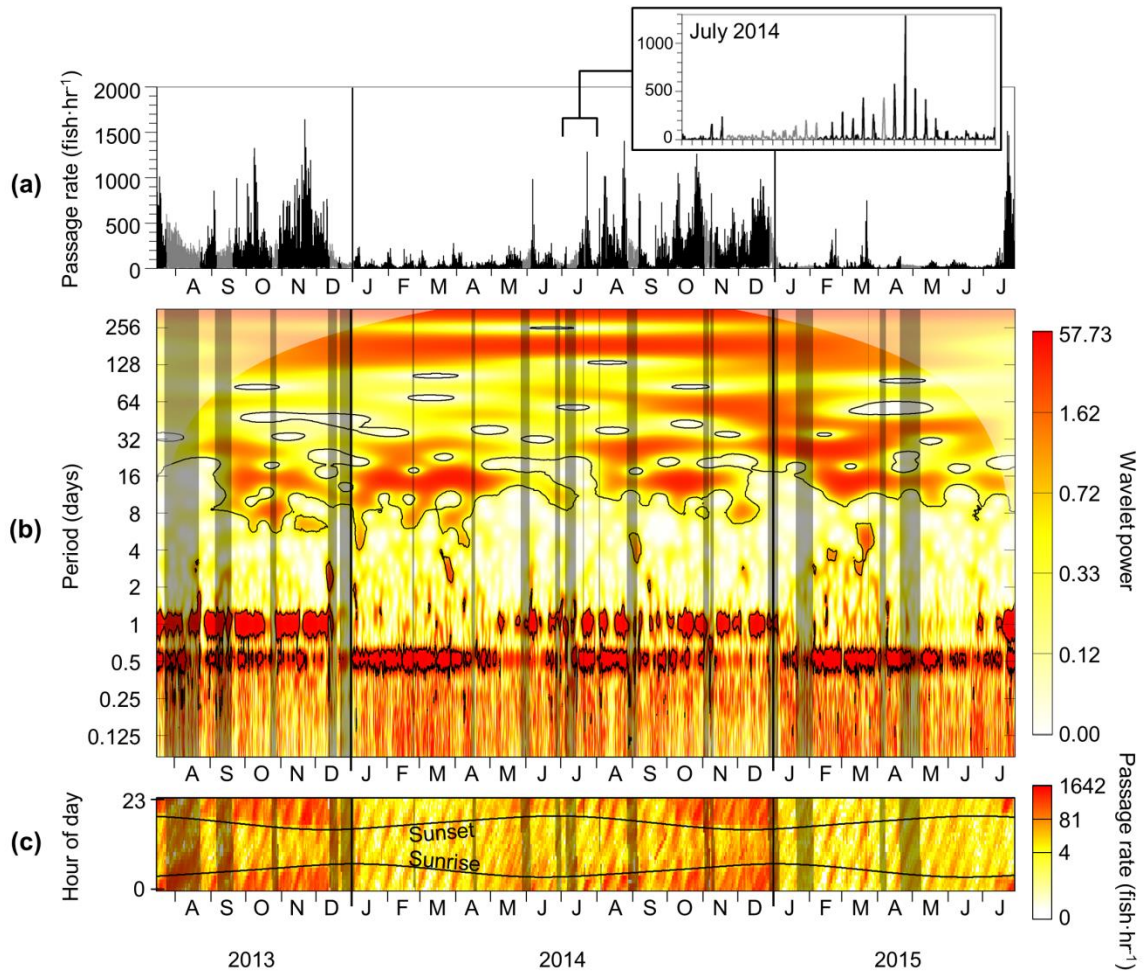
Fig 3.7 Fish passage rate time series and wavelet analysis. (a) Time series of fish passage rate (fish·hour^{-1}). Gaps in data that were filled using the method described in the text are shown in gray. Inset expands time series from July 2014. (b) Wavelet transform of log-transformed time series. Color indicates the magnitude of the wavelet power, with darker, redder colors indicating higher power. Black contours enclose areas of significance at the 5% significance level. The transparent white fill indicates the cone of influence, within which power values may be reduced by edge effects. Darkened rectangles indicate where gaps in the time series were filled. (c) Fish passage rates during each hour of each day of the time series, condensed here for easy comparison to a and b. An expanded version of c is shown in Fig 3.8. Darker, redder colors indicate higher passage rates. Horizontal curved lines indicate times of sunrise and sunset, and shaded rectangles indicate filled gaps in the time series.

76

Visual inspection of passage rate at each hour of the day (Fig 3.7c) revealed obvious changes in passage rate that corresponded with the presence and absence of 12- and 24-hr periodicities in the wavelet transform. When viewed in relation to tidal and diel stage (Fig 3.8), it was clear that fish passage rate varied with tidal and diel cycles in a seasonally shifting relationship. In the winter and spring of each year (from January through May), when the 12-hr periodicity was present but not the 24-hr, the highest rates occurred on the second half of the ebb tide and at low tide, mainly near sunrise and sunset but with no strong difference between day and night. In the summer (June through August), when both the 12-and 24-hr periodicities were evident, the highest passage rates began shifting to night and were still mostly associated with low tide, though sometimes in the second half of ebb or first half of flood. In the fall and early winter (September through December), the 24-hr periodicity became more prominent while the 12-hr periodicity became less consistent. At this time, passage rate was clearly higher at night than during the day, and the association with tidal stage was less clear, though the rate was generally lower at high tide than at ebb, low, and flood tides. Between December and January, this pattern in passage rate quickly returned to peaks at low or ebb tides at sunrise and sunset.
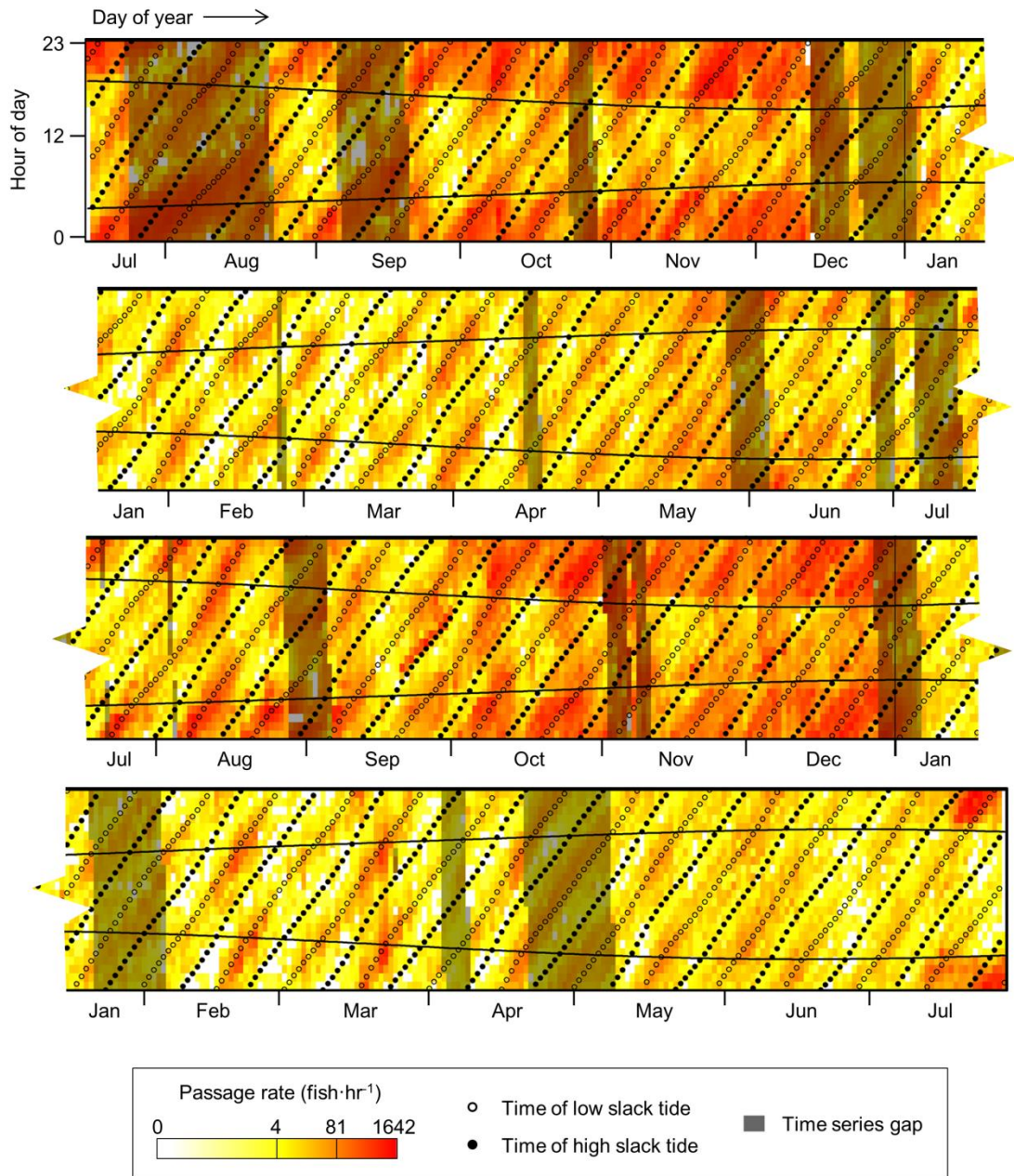
Fig 3.8 Fish passage rate at each hour of the day. Rows correspond to hour of day, columns correspond to day within the time series, which spans July 2013 to July 2015. Darker, redder colors indicate higher passage rates. Gaps in the time series (filled using method described in text) are indicated by darkened rectangles. Horizontal curved lines indicate time of sunrise and sunset. Points indicate times of low (open circles) and high (solid circles) slack tides. A condensed version of this figure is shown in Fig 3.7c.

78

3.5 Discussion

This high-resolution, long-term time series indicated that fish passage rate was highly variable and strongly linked to multiple cyclic changes in the physical environment, including tidal, diel, and seasonal cycles. This is not surprising, given the high-magnitude seasonal shifts and tidal forcing at this site, and that fish movements have been linked to such environmental changes in previous studies (Pittman and McAlpine 2001). The passage rate of fish varied most with tidal and diel cycle, but its relationship with these cycles did not remain constant over a year. Rate was linked strongly to the interaction of these two cycles in a relationship that varied with season. This adds to previous findings linking similarly interacting environmental cycles with fish presence and feeding in intertidal habitats (Krumme et al. 2008, Gibson et al 1996) and spatial distribution of fish and their predators and prey in tidal current systems (Simard et al. 2002, Embling et al. 2012, Zamon 2003).

All interactions of fish passage rate with the tidal cycle were modified by the diel cycle. In the winter through spring, the highest passage rates were confined to low slack and ebb tides, but within crepuscular periods. Higher rates shifted into night during the summer, expanding to flood and ebb tide in addition to low slack tide and remaining this way through the fall. These results are consistent with a previous study we carried out at this site, in which we conducted 24-hr surveys of fish density and vertical distribution using a downward-looking, vessel-mounted echosounder in March, May, June, September, and November 2011 (Viehman et al. 2015). In that study, we did not examine slack tides. However, we found that fish density was generally higher during the ebb tide than the flood tide in the first part of the year, and that this difference was

less evident toward the end of the year. The vertical distribution of fish did not differ consistently between ebb and flood tide, so higher ebb- or flood-tide passage rates may be related to horizontal, rather than vertical, tidal fish movement. For example, fish may move between channel edge habitats and the middle of the channel based on flow direction, or be carried through different parts of the channel during ebb and flood tides on asymmetric flow paths.

The diel differences in passage rate which we observed, on the other hand, could have been related to changes in vertical fish distribution. Unlike tidal stage, our previous study of this site found consistent changes in fish vertical distribution related to diel stage: during the day, fish were more concentrated near the sea floor or surface, depending on time of year, but at night, fish spread out in the water column (Viehman et al. 2015). In that study, this difference was visually apparent in May, June, August, and September surveys, but not in March. In the present study, we sampled only the mid- or lower-water column (depending on water height). So, if the same diel shifts in vertical distribution were occurring during the present study period, from spring through fall most fish would have been outside of our sampled volume during the day but would have moved within view at night, and there would be little day-night difference in passage rate in the winter and early spring. This is consistent with our results, with higher passage rates occurring at night from June through December. However, the influence of diel cycle was not completely lacking in the winter and early spring, as passage rate consistently peaked near dawn and dusk when those times coincided with low or ebbing tides. Our previous work only compared day- and night-averaged vertical distributions, so we had not captured any changes in fish activity related to dawn and dusk. By

80

expecting and searching for 24-hr diel differences in fish distribution at this site, we did

not detect this crepuscular activity pattern that dominated for a large portion of the year.

Prior assumptions such as this have likely constrained results in other studies of fish

biology, as well (Heath et al. 1991), highlighting the utility of long-term, high-resolution

data collection.

It is important to remember that only individual fish were included in this study,

as individuals within schools could not be separated from their neighbors, and fish

schools often could not be distinguished from patches of entrained air. Fish in schools

were therefore omitted, which potentially affected the patterns in passage rate we were

able to measure. For example, we previously observed that many dense schools are

present in Cobscook Bay in the spring (Viehman et al. 2015, unpublished data), likely

larval Atlantic herring (*Clupea harengus*, Vieser 2014). These schools contributed to

high density indices in spring that were comparable to indices from the fall (Viehman et

al. 2015, unpublished data). However, in the present study, passage rates in the spring

were much lower than in the fall, which could have been due to the exclusion of these

schools. Individually, larval herring may not be strong enough acoustic targets to be

tracked with a -50 dB TS threshold, so even if schools were to spread out (e.g., at night;

Heath et al. 1991, Ferreira et al. 2012), they would be unlikely to contribute to fish

passage rate. However, many schooling fish species have been observed to spread out in

lower light levels, including adult Atlantic herring (Blaxter 1985) and Atlantic mackerel

(*Scomber scombrus*, Glass et al. 1986), both of which would be detectable above our TS

threshold. These fish are present in the area in high numbers in the summer and fall

(Vieser 2014, MacDonald et al. 1984), when the diel pattern in passage rate was

strongest. It is possible that the diffusion and formation of schools of fish, such as

herring and mackerel, could have influenced the observed passage rates. Ideally, schools

would be included in this study, but to do so, new processing techniques to separate

schools of fish from entrained air need to be developed.

Hydroacoustics could not reveal the species of fish at this site, but physical

sampling that occurred from 2011 to 2014 (Vieser 2014, Zydlewski et al. 2016) indicated

which species were likely present. These studies sampled the tidal channels of the bay

with pelagic and benthic trawls and the intertidal areas with seine and fyke nets from

spring to fall of each year. They found that Cobscook Bay has a diverse fish assemblage,

with 46 species sampled, many of which have seasonal in- and off-shore movements in

the Gulf of Maine (Bigelow and Schroeder 2002, Tyler 1971). Atlantic herring and

winter flounder (*Pseudopleuronectes americanus*) were by far the most abundant species

caught in the tidal channels, making up 59.6% and 27.1% of the catch (Vieser 2014).

Most fish sampled were juveniles, with lengths agreeing well with the TS of fish detected

in this study. Some larger fish were also likely present and able to avoid the trawls, such

as adult Atlantic mackerel in the summer and fall. Four diadromous species, which have

well-defined annual on- and off-shore movements related to spawning, were also

captured: alewife (*Alosa pseudoharengus*), rainbow smelt (*Osmerus mordax*), blueback

herring (*Alosa aestivalis*), and American eel (*Anguilla rostrata*). The life stages of some

of the fish species sampled were also found to change seasonally: herring sampled in

May and June were typically larval, while those sampled in August and September were

juvenile or adult. Some of the patterns we observed could have been related to fish

growing into the size ranges we sampled by setting a -50 dB TS threshold. For example,

while individual larval herring (not schooling) may be too weak to detect, juvenile herring several cm long would likely be strong enough targets. If larval fish remain in Cobscook Bay and mature over the course of the spring and summer, their growth could contribute to the comparably higher passage rates observed in summer and fall.

The changing patterns in fish passage rate that we observed each year are also likely related to the seasonally changing fish assemblage of Cobscook Bay. Vertical and horizontal movement patterns of fish in response to environmental cues are often specific to species and life stage (Pittman and McAlpine 2001, Neilson and Perry 2001), and can change seasonally even for one species as fish respond to changing day length and temperature (Gibson et al. 1996). Though the vertical diel and tidal movements of most of the species present in Cobscook Bay (Vieser 2014) are not well known, particularly in such fast flows, a seasonally shifting fish assemblage is likely to result in seasonally shifting patterns in passage rates, such as those we observed. The presence of herring and mackerel in the summer and fall, for example, could have substantially contributed to the increase in night-time passage rates, e.g. due to school diffusion (Blaxter 1985, Glass et al. 1986) or diel vertical migrations (Huse and Korneliussen 2000, Nilsson et al. 2003) bringing more individuals into the sampled volume. Without the ability to separate acoustically detected fish by species, the unique movement pattern of any one species at this site is virtually impossible to separate from the combined movement patterns of all the others. In future studies of regions with diverse fish assemblages, it may be helpful to collect data with multiple acoustic frequencies to aid in distinguishing anatomically distinct groups of fish (Korneliussen and Ona 2004).

In the present study, we saw no consistent correlation between fish passage rate and current speed, and this has implications for potential MHK device effects. Previous work by Broadhurst et al. (2014) and Hammar et al. (2015) used video to observe fish interacting with MHK turbines at two other locations, and both studies concluded that fish were less abundant at high current speeds and therefore less likely to come in contact with moving turbine blades. This or any other consistent response to the tidal currents at our study site would have appeared in the wavelet transform as a strong band near the 6-hr periodicity, which was not the case. Instead, we observed that passage rate was frequently high during the flowing tides (not only at slack tides), particularly at night from summer through fall. If passage rate is assumed proportional to rate of encounter with an MHK turbine at the same depth, fish may be more likely to contact moving turbine blades than might be expected based on results of previous studies, particularly if combined with the finding by Viehman and Zydlewski (2015) that fish were less likely to evade an MHK turbine at night than during the day. However, this speculation should be balanced with the results of laboratory studies of fish entrained in MHK turbines, which found survival rates generally exceeded 90% (Amaral et al. 2015, Castro-Santos and Haro 2015). So, even if the rate of fish encountering and entraining in the MHK turbine is high, the magnitude of direct turbine effects such as blade strike may still be minimal. This is particularly true for small fish, such as those detected here: as fish size relative to blade diameter decreases, injury and mortality have also been found to decrease (Amaral et al. 2015).

The high temporal variability in fish passage rate also has implications for monitoring the effects of tidal energy turbines on fish. For example, to monitor near-field

interactions of fish with an MHK device (e.g., direct strike by turbine blades), it would be best to focus sampling efforts on times with high passage rates and a rotating turbine. At this site, the best time to observe turbine interactions in the winter and spring would be near sunrise or sunset during the second half of ebb tide, and in the summer and fall, at night during either flood or ebb tide. Consideration should be given to the fish species and life stages that would be present at different times of the year, as they may all respond differently to an MHK device.

One approach to quantifying less direct MHK device effects is to monitor fish abundance in the area of a device before and during its deployment (Viehman and Zydlewski 2015, Staines et al. 2015). Unless monitoring can be continuous, as in this study, the high temporal variability in fish presence in such dynamic environments could influence results of long-term studies if they are not designed to consider these cycles. This must be kept in mind when interpreting results from tidal energy sites. For example, if our echosounder were duty-cycled to collect data for just a few hours of the month (and therefore reduce processing and analysis time substantially), samples occurring at low tide would be capturing higher passage rates relative to samples occurring at high tide. The timing of observations in relation to underlying cycles in fish presence, which are based on the environment and the behavioral responses of fish, could alias results and produce trends that are not actually there. It is important that results of such monitoring reflect actual trends in fish abundance. Overestimating effects on fish could harm this developing industry but underestimating effects could harm the marine ecosystem. Carrying out 24-hr surveys, which capture the high variation occurring over 12- and 24-hr cycles, spaced over time to characterize the seasonal cycle each year, would be a first

85

step toward achieving accurate long-term monitoring results at tidal energy sites like this one. As more data are collected in the coming years, longer environmental cycles (e.g., climatic oscillations) will need to be taken into account, as they may also influence observed trends. This long-term variation would be difficult to characterize without studies spanning decades, but sampling a control or reference site alongside a tidal energy site would aid in separating this and other sources of natural variation from effects of MHK devices.

Results presented here are specific to one depth at one site, but they may be applicable to other tidal energy sites characterized by similarly high-magnitude environmental cycles. In strongly tidal channels frequented by valuable or endangered fish species (e.g., salmon in the northwest USA or Atlantic sturgeon in the northeast), observing passage rates with high temporal resolution could be very useful in predicting and mitigating MHK device effects. Fish passage rates at turbine depth could be combined with observations of close-range evasion behavior in the field, as well as fish injury and mortality rates obtained in laboratory settings, to estimate the effects of a single turbine on the fishes sharing its depth. When continuous or high-frequency sampling is not an option, known environmental cycles should be used to inform plans for monitoring turbine effects on fish, as well as the interpretation of study results. Better understanding of the effects of a single MHK device on individual fish may help us predict the effects of devices on fish populations as this new renewable energy industry moves toward the deployment of commercial-scale MHK device arrays.

CHAPTER 4

INCORPORATING ENVIRONMENTAL CYCLES INTO STUDY DESIGNS IMPROVES FISH MONITORING AT TIDAL ENERGY SITES

4.1 Abstract

Continuous, long-term (multi-year) monitoring of animal presence at tidal energy sites may be the ideal approach for separating cumulative effects of marine hydrokinetic (MHK) devices on biota in a region from natural variability, which is high in these areas. However, continuous sampling is often unrealistic due to cost or gear limitations, and discrete sampling must be used instead. Fish presence at tidal energy sites is tied to environmental changes, which are often cyclic in nature (e.g., tidal, diel, and seasonal cycles). The timing and duration of discrete samples can therefore greatly affect observed trends. Timing discrete samples to account for the cyclic patterns in fish presence at a tidal energy site may improve the quality of long-term monitoring results and reduce costs of monitoring by avoiding the need for high-frequency or continuous sampling. We explored this idea by subsampling a two-year continuous time series of fish passage rate at a tidal energy site in Cobscook Bay, Maine. We simulated the use of different study designs at the site and compared their ability to capture the seasonal trend in passage rate. Designs used either randomly spaced samples or samples informed by environmental cycles which held the relevant environmental conditions constant (e.g., tidal, diel, and lunar stages). Sample durations simulated were 1, 12, and 24 hours, and frequencies ranged from 3 to 12 per year. The temporal representativeness of each sample duration ranged from 72 hours for 1-hr samples to 44 days for 24-hr samples. Informed designs using 24-hr samples were the most accurate, efficient, and correlated

with the true seasonal trend in fish presence. Sample duration had the largest effect on

design quality, and at least 4 samples per year were required to best reflect the true

seasonal trend. This approach to study design for detecting MHK device effects may be

applicable to tidal energy sites around the world, where similar environmental forcing

exists. As patterns in fish presence will vary with fish assemblage, the species and life

stages of fish present at each tidal power site should be considered when using this

approach to inform study design.

4.2 Introduction

Baseline information on biological systems is important for the prediction,

detection, and understanding of anthropogenic influences (Smith et al. 1993). Even with

baseline information, detecting effects in the natural environment can be difficult due to

natural variation affecting data collected before and after a site is perturbed.   A before-

after-control-impact (BACI) study design can aid in separating natural variation from

effects of an anthropogenic change (Smith et al. 1993, Osenberg et al. 1994). Under this

design, discrete samples are taken at the impact site before and after the perturbation is

made, as well as at a control site that experiences the same natural variation but is not

impacted by the same change. By comparing before to after at each site, effects of

anthropogenic changes may be separated from any natural variation. The ability of a

BACI design to detect impacts relies heavily on the number of samples taken before and

after the change is made, the natural variability of the parameter measured, and the size

of the effect (Osenberg et al. 1994). Without enough baseline information, it can be

difficult to determine the number of samples needed prior to the change being made.

Additionally, BACI comparisons do not necessarily require understanding of the natural

variability to separate it from the effect of interest, but the natural variation may be critical to understanding the mechanisms driving the effects and predicting future effects as anthropogenic perturbations scale up or change in some other way.

Without some understanding of the variation in a biological quantity of interest prior to designing a study, results may be inaccurate or incomplete. For example, the interaction of short-term patterns with longer-term changes, such as diel and tidal movements with the seasonal cycle, can limit the scope of results if not taken into account. Viehman et al. (2015) took discrete 24-hr measurements of fish vertical distribution several times per year for two years, and compared day- and night-averaged distributions. They found that fish were concentrated near the sea floor or surface during the day and were more spread out at night, except in winter, when there was no sign of a diel difference. However, continuous data collection over two years (Chapter 3) revealed high fish passage rates mid-water-column during the crepuscular periods in the winter, a semi-diel pattern that was not seen in the previous study due to prior assumptions about diel fish movements. Both of these studies were carried out to inform predictions of the effects of a marine hydrokinetic (MHK) device on fish and provide a baseline of comparison for data collected post- device installation. As such, it was important that study results accurately represented fish presence at the site, as this largely determines the potential rate of fish encounter with an MHK device.

Fish behavior, and therefore presence at any particular location, vary with species and life stage, the needs of the individual (e.g., feeding, migrating, spawning), and environmental conditions (e.g., light, currents, temperature, and day length; Pittman and McAlpine 2001, Reebs 2002). In dynamic, variable environments such as tidal energy

sites, metrics of fish abundance (e.g., density or passage rate) are similarly highly variable (Viehman et al. 2015, Chapter 3). In such a setting, study design can greatly influence results if the natural variation is not understood well enough to inform the monitoring plan. For instance, the number of samples needed to fully characterize the quantity of interest (e.g., fish passage rate) and to detect any change is dependent on its variability. Under-sampling provides too little information to draw accurate conclusions, but over-sampling can waste limited resources. To optimize sample frequency and duration for specific research goals, the temporal representativeness of a data point, i.e. how much time is represented by the results of a single sample (Jacques and Horne 2014, Anttila 2012) should be defined.

The timing of each individual sample within a study is also important, particularly in areas where the quantity of interest is cyclic in nature. This is because the interaction of sampling frequency with the underlying cycles can generate false patterns in the resulting dataset (e.g., signal aliasing, Vaseghi 2008). Many of the environmental conditions that affect fish activity and movement are cyclic (e.g., diel, lunar, and seasonal cycles), and tidal areas are subjected to the additional influence of the various periodic components of the tidal cycle (Gibson 2003). Fish passage rate at a tidal energy site in Cobscook Bay, Maine was strongly influenced by tidal, diel, and seasonal cycles (Chapter 3), and this is likely to be the case in many areas with environmental forcing of similar magnitude. The best method for characterizing this type of highly variable, cyclic quantity would be to collect high-resolution data (e.g., sample at several times the shortest frequency present) for a long period of time (several times the period of the longest cycle present). One method for sampling large volumes of water at very high

temporal resolution is hydroacoustics. Hydroacoustic equipment can be deployed

remotely and operated for long periods of time, making it suitable for high-resolution,

long-term data collection (Flagg et al. 1994, Cochrane et al. 1994, Picco et al. 2016,

Jacques and Horne 2014, Urmy et al. 2012). However, remote deployments are costly to

build and deploy, and they are limited by battery life if not cabled to shore. Additionally,

acoustic data generally require large amounts of digital storage space and time-

consuming manual processing. For a start-up company monitoring the effects of an

MHK device on fish with limited resources, more realistic options might include discrete

hydroacoustic samples spread out over time (e.g., vessel-based transects at a site), or

duty-cycling a remotely deployed echosounder (to extend battery life, reduce data

storage, and limit processing time).

If continuous sampling is not an option, incorporating the cyclic nature of fish

presence at a tidal energy site into monitoring plans may be advantageous. Several

studies of the temporal variability in the marine realm have suggested such incorporation

of natural patterns to improve the accuracy of study results (Embling et al. 2012, Blauw

et al. 2012). Even without a thorough baseline, if the dominant environmental

periodicities at a tidal energy site are known, the dominant cycles in fish presence may be

inferred. The research question can then determine which cycles are important to

characterize, and which are not necessary to characterize but could influence observed

trends. The cycles to be characterized would set the minimum desired sampling

frequency (several times the frequency of the shortest cycle of interest) and the minimum

total time spanned by the study (several times the length of the longest cycle of interest).

Cycles influencing the results that are not of interest can then inform the duration and

spacing of individual samples. This technique has been used in water quality monitoring to remove the effect of diel and seasonal cycles on long-term chlorophyll-a measurements when seasonal and diel cycles were of less interest than multi-year trends (Anttila 2012). By sampling a station during the same seasonal event each year, the influence of seasonal cycle is avoided, and by sampling for an entire day and obtaining the day's average, the influence of diel cycle is removed (Anttila 2012).

The same method may be applicable to measurements of fish presence at tidal energy sites. A general monitoring goal is to characterize fish presence at a site before and after an MHK device is deployed, in order to detect cumulative device effects. The temporal scale at which these effects occur is not yet known, and is likely to vary based on the stressor (e.g., noise, direct strike) and receptor (e.g., different fish species or life stages) (Boehlert and Gill 2010). To examine the longer-term effects of device operation, a study should be designed to detect changes occurring over months and years, rather than days (which may be more appropriate for monitoring transient effects of device installation activities). This suggests a sampling frequency of several times per year, particularly if a seasonal cycle is present. Next, sample duration and timing must be decided. If sample duration is a multiple of a cycle's period, summary statistics of the sample (e.g., mean or median) can be used to cancel out that cycle's effects. For example, the influence of short-term cyclic variation caused by the tidal or diel cycles (periods of 12 and 24 hr, respectively), could both be removed from the longer-term observations by setting sample duration to 24 hr. Any intermediate cycles, which have periods longer than sample duration and frequencies higher than sample frequency (e.g., the lunar cycle), must be accounted for with sample timing. For example, if 24-hr

samples are carried out at a sampling frequency of 6 per year, the effect of lunar cycle (which has a period of 29.5 days and a frequency of 12 per year) could be limited by timing each of the 6 samples to occur at the same lunar phase.

In this paper, we explored the influence of different study designs on observed temporal trends in fish passage rate at a tidal energy site. We did this by subsampling a two-year time series at an MHK turbine in Cobscook Bay, Maine (Chapter 3). We simulated study designs that used various sample durations (1, 12, and 24 hrs), frequencies (3 to 12 times per year), and timing (random, or informed by temporal cycles). Study designs were judged based on their ability to accurately portray the seasonal trend in fish abundance, which was the longest cycle detected in the 2-year time series. Design quality was assessed using three metrics: accuracy, efficiency, and correlation. Accuracy measured the departure of study results from the true seasonal trend. Efficiency measured the effect that changes in sample timing had on results: ideally, a good study design would not be strongly affected by slight changes in sample timing. Correlation measured the similarity of the trend obtained via the study design and the true trend: whether they showed similar relative changes over time, regardless of absolute differences (accuracy). In addition, we evaluated the temporal representativeness of samples of each duration, to provide a theoretical minimum sample frequency (i.e., number of samples per year) required to fully characterize fish presence at this site, and to better inform interpretation of future sample results.

4.3 Methods

4.3.1 Data

The data used were collected from July 15, 2013 to July 28, 2015 by a side-looking, 7° split beam echosounder mounted on the sea floor at a tidal energy site in Cobscook Bay, Maine (Fig 4.1; Chapter 3). The echosounder used a frequency of 200 kHz, a pulse length of 0.256 ms, and a transmit power of 120 W, and sampled approximately 5 times per second. After noise removal, a target strength threshold of -60 dB was applied to hydroacoustic data to eliminate echoes unlikely to be from fish. Fish were tracked, exported from Echoview®, and compiled into a time series with 1-hr resolution. Further details of the hydroacoustic data processing and time series construction can be found in Chapter 3. The resulting time series was the number of fish detected within the acoustic beam each hour, or fish passage rate in units of fish per hour, for two years.
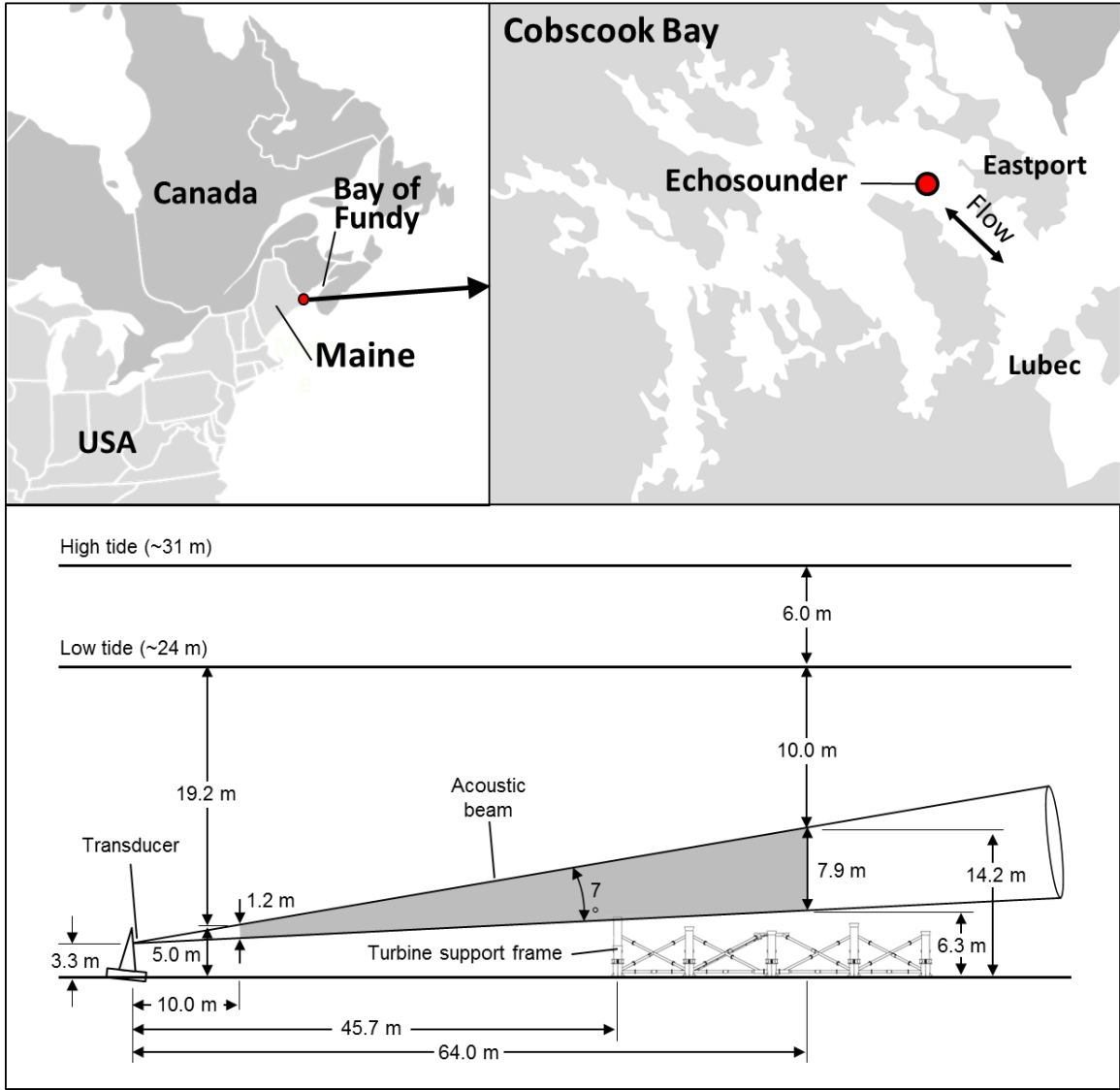
Fig 4.1 Study area and echosounder setup. In lower panel, tidal current moves out of page during the ebb tide and into the page during the flood tide. Figure components from Chapter 3.

4.3.2 Study design simulations

We simulated different study designs by sub-sampling the time series of hourly

fish passage rate. We chose to focus on accurately measuring the seasonal trend in fish

passage rate, which was the longest periodic signal present in the available time series.

The "true" trend in fish passage rate to which we compared simulation results was

obtained by applying a moving median to the time series, using a window length of 61

days (Fig 4.2). The median portrayed the general trends in passage rate more accurately than the mean, which was heavily influenced by the periodic peaks in passage rate.
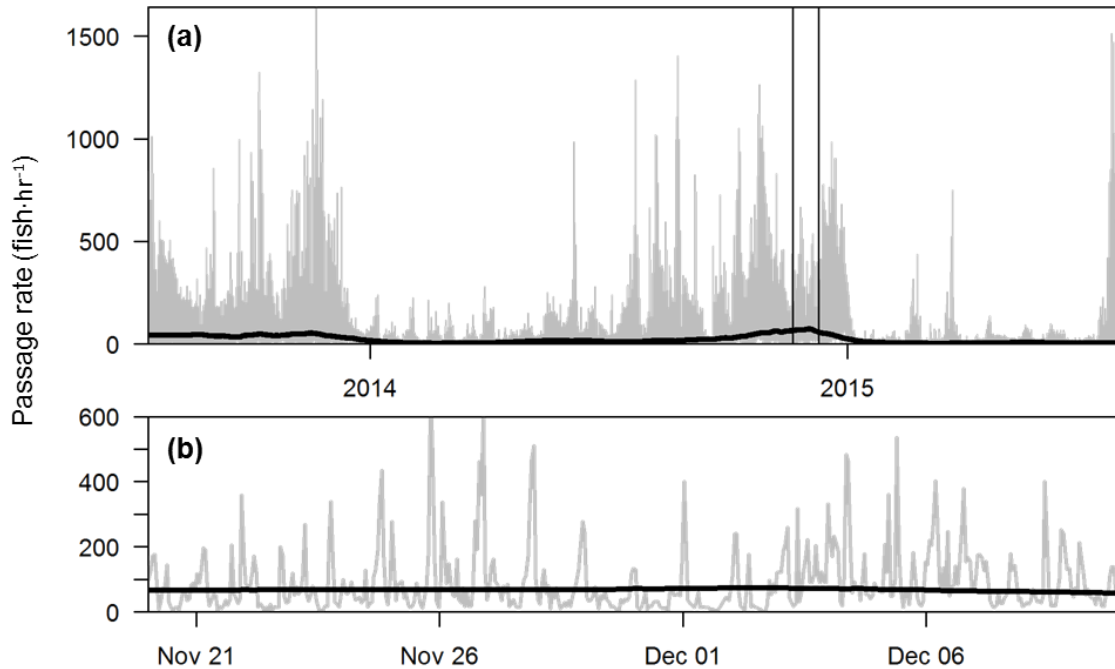

Fig 4.2 Time series of fish passage rate. Time series presented in Chapter 3. Gray line is raw data, thick black line is the moving median showing seasonal variation. (a) Full time series, with vertical black lines indicating 20-day subset shown in (b).

Three sample durations likely to be considered for long-term monitoring at tidal energy sites were tested:1 hr (e.g., a transect or two across a narrow tidal channel), 12 hr (to encompass a complete tidal cycle), and 24 hours (to encompass the tidal and diel cycle; e.g. Viehman et al. 2015 and Staines et al. submitted). All samples were assumed to be either stationary or occurring over a small spatial scale, as the spatial distribution of fish is highly variable and likely difficult to extrapolate beyond a few hundred meters from the point of measurement (Jacques and Horne 2014).

For each sampling duration, two study design types were simulated. These were either "random" or "informed" by the environmental cycles known to be present and influential to fish presence (Table 4.1) Simulating these study designs consisted of

dividing the year into equal time segments based on the number of samples to be carried out, and placing one sample within each of these segments. Random designs placed samples randomly within each segment. Informed designs randomly placed the first sample within the first time segment, then held the relevant environmental conditions constant for each following sample. Environmental cycles known to be influential to fish passage rate at this site were tidal, diel, and lunar cycles (Chapter 3). For the 1-hr sample duration, this meant selecting a data point within each segment at the same tidal stage (ebb or flood), same part of the tide (beginning, middle, or end), same diel stage (day or night), and same lunar phase (29.5 days apart) as the first, randomly-chosen sample. The 12-hr sample duration ensured the same diel stage and lunar phase, and began and ended at the same tidal stage and portion of the tide, as the first sample. The 24-hr sample duration, the length of which encompassed tidal and diel stages, held lunar phase constant and started and ended at the same tide, portion of tide, and diel stage as the first sample. The maximum sampling frequency attainable for informed study designs was 12 samples per year, due to the need to hold lunar phase constant across the entire study. Sample frequency was therefore varied from 3 to 12 for each study design to assess its effect on results.

Table 4.1 Summary of simulated study designs.

Study design type	Sample duration	Sample timing
Random	1 hr	Random within each time segment
	12 hr	Random within each time segment
	24 hr	Random within each time segment
Informed	1 hr	Constant tidal stage, diel stage, lunar stage, and part of tide
	12 hr	Constant diel and lunar stages
	24 hr	Constant lunar stages

Each study design was simulated 500 times, with a different random starting time chosen within the first time segment for each simulation. Using these multiple simulations, we calculated the three metrics of design performance: accuracy, efficiency, and correlation.

Study design accuracy was defined as the average percent error of each simulation's results compared to the true median fish passage rate. For each simulation of a study design, the difference between each sample's median (or single value, in the case of the 1-hr sample duration) and the true median passage rate for the same time frame was calculated. This number was normalized to the true median to represent error as a percentage. The percent errors for all simulations were then averaged to calculate the design's overall accuracy. Larger values indicated greater error, and therefore less accurate results for a given study design.

Study design efficiency indicated how sensitive results were to changes in sample timing. The metric for efficiency was average coefficient of variation, $\overline{CV}$, which was the average of the CV's of all simulated samples within each time segment. A larger value of $\overline{CV}$ indicated greater variation across simulations of a given study design, and therefore lower study design efficiency.

Correlation of sampled passage rate and the true median passage rate (e.g., whether the same relative changes were shown in each dataset) was quantified for each study design using the adjusted correlation coefficient (R_a^2). For each simulation of a study design, sampled passage rate was linearly regressed onto the true median passage rate from the corresponding time bins (with both datasets log-transformed to meet normality assumptions). Once all simulations were complete, R_a^2 values were averaged to

compute $\overline{R_a^2}$, the average adjusted correlation coefficient for the study design. Higher

correlation indicated a stronger linear relationship of the sampled and true values, e.g.

changes in one reflected the changes in the other, which indicated a better study design.

The temporal representativeness, the time span to which a single data point (e.g.,

the median fish passage rate from a sample) may be extrapolated, was then determined

for each sampling duration. This was done by re-sampling the time series at each

sampling duration and calculating the median and interquartile range (IQR) of the data

within each time bin. In the case of the 1-hr sampling duration, only one data point was

selected per sample, so this was used as the median value and the IQR was not calculated.

Autocorrelation functions of the medians and IQRs were generated, and the minimum lag

at which either the median or IQR became independent at the 95% confidence level was

identified. Temporal representativeness was then calculated as twice this lag: an

individual sample could be assumed not independent, and therefore representative, of

samples within this much time either before or after. The minimum sample frequency

(samples per year) needed to fully describe fish passage rate and its variation was

calculated for each sampling duration as 1 year divided by the temporal

representativeness.

4.4 Results

4.4.1 Temporal representativeness

The temporal representativeness of a sample increased with sample duration: 1-hr

samples were representative of the 72 hr (36 hr before and after), 12-hr samples were

representative of 29 days, and 24-hr samples represented 44 days. The minimum sample

frequency needed to fully characterize median fish passage rate and its variability at the

site was therefore 122 per year for 1-hr samples, 13 per year for 12-hr samples, and 8 per year for 24-hr samples.

4.4.2 Study design simulations

Visual inspection of simulation results indicated that variability across simulations and deviation from the true median was greatest for shorter sample durations and smallest for longer sample durations (Fig 4.3). The results of 1-hr samples, for random and informed designs, were highly variable from one simulation to the next and often captured passage rates far from the true median fish passage rate (Fig 4.3a, b). Study designs using 24-hr sample duration (Fig 4.3e, f) showed much better agreement between simulations (higher efficiency), and followed the true trend in passage rate well (higher accuracy). Study designs with 12-hr sample duration were intermediate (Fig 4.3c, d).
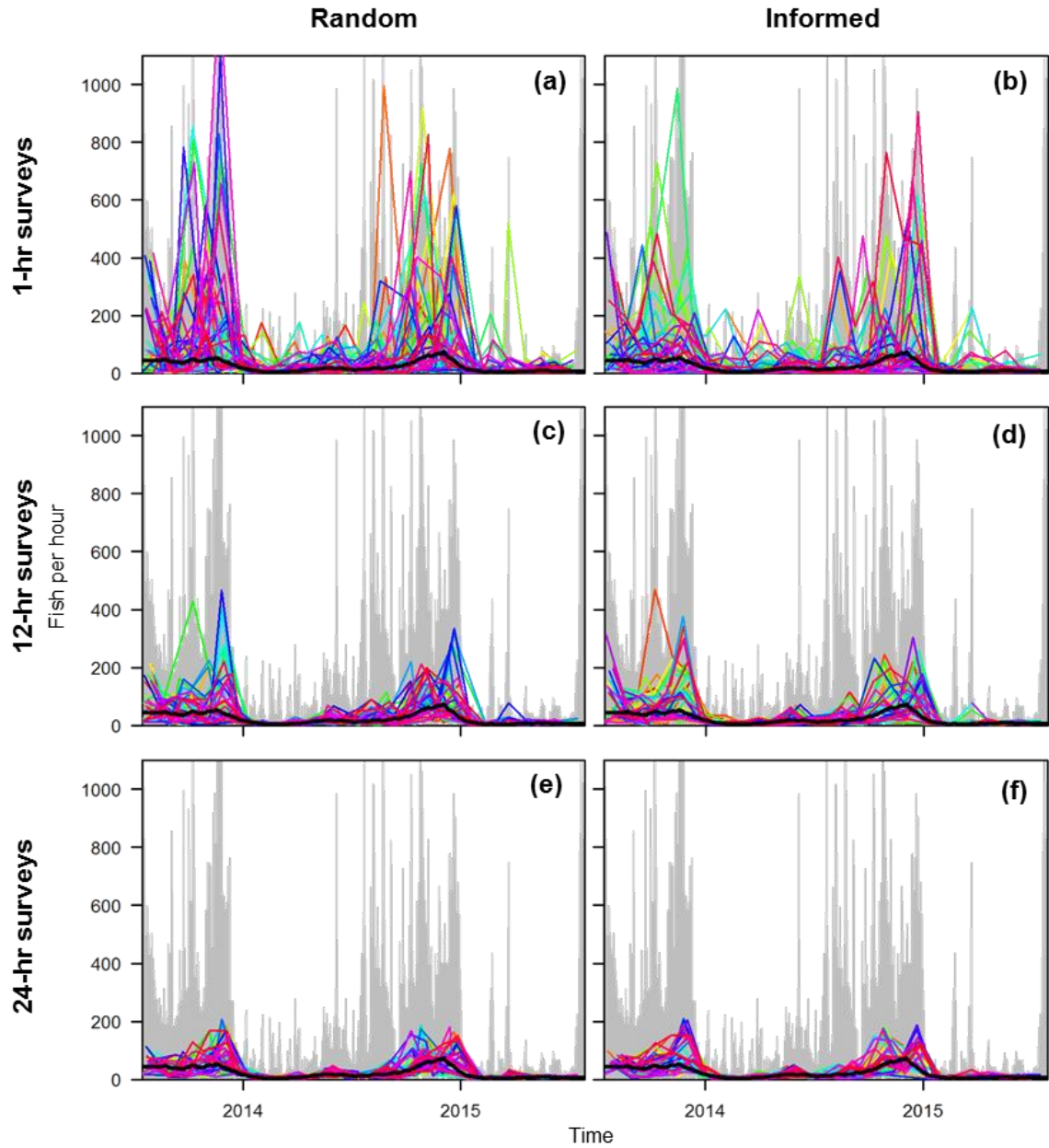
Fig 4.3 Results of study design simulations. 50 (of 500) simulations are shown for clarity. Random (a, c, e) and informed (b, d, f) simulations for each sample duration (1 hr, 12 hr, 24 hr), using sampling frequency of 12 samples per year. The grey line is the raw time series and colored lines show individual simulations (each line is one simulation). The thick black line is the true median trend in fish passage rate.

Accuracy, efficiency, and correlation metrics (Figs 4.4-4.6) supported visual

examination of the results. Sample duration had a greater effect on all metrics than

sampling frequency, with longer samples outperforming shorter ones. The effect of

sample duration was particularly strong for accuracy (Fig 4.4) and correlation (Fig 4.6).

Accuracy improved with longer samples, with error decreasing from about 180% for 1-hr

samples to 65% for 24-hr samples (Fig 4.4). Efficiency increased with longer samples,

with $\overline{CV}$ decreasing from approximately 3.2 for 1-hr samples to 1 for 24-hr samples (Fig

4.5). Correlation ($\overline{R_a^2}$) increased from approximately 0.35 for 1-hr samples to 0.67 for
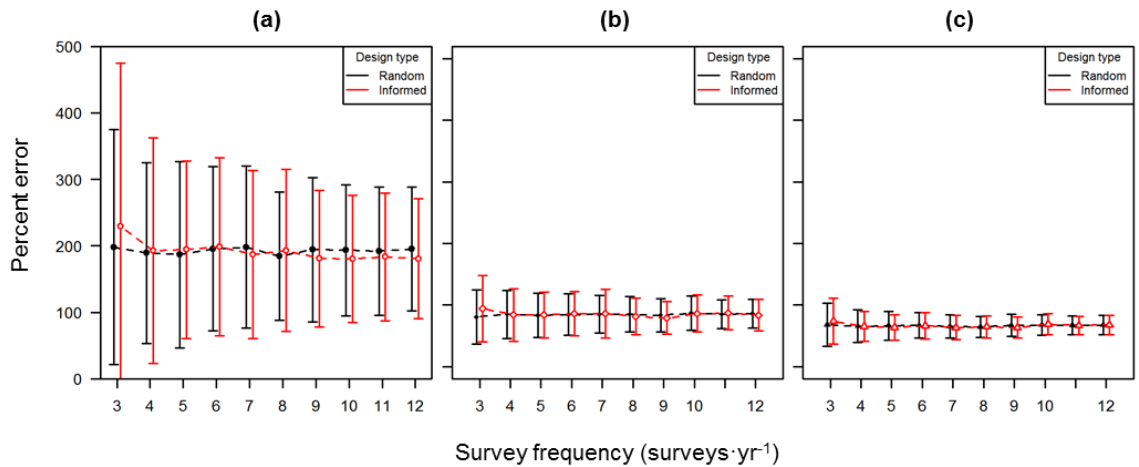
24-hr samples (Fig 4.6).

Fig 4.4 Accuracy of simulated study designs. Accruacy (indicated by percent error) shown for sampling frequencies from 3 to 12 per year, and for sample durations of (a) 1 hr, (b) 12 hr, and (c) 24 hr. Black indicates random design type, red is informed. Error bars indicate standard deviation.
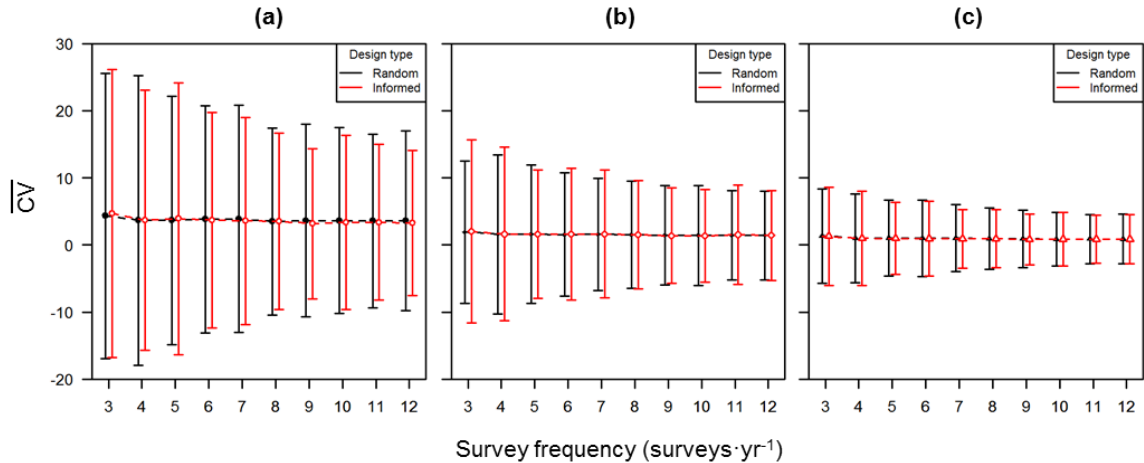
Fig 4.5 Efficiency of simulated study. Efficiency (indicated by average coefficient of variation) shown for sampling frequencies from 3 to 12 per year, and for sample durations of (a) 1 hr, (b) 12 hr, and (c) 24 hr. Black indicates random design type, red is informed. Error bars indicate standard deviation.
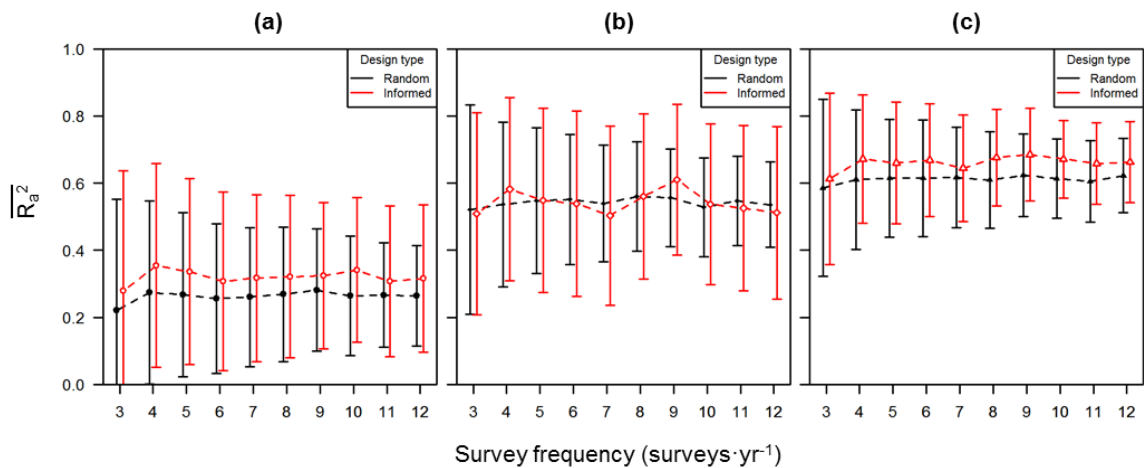

Fig 4.6 Correlation of simulated study designs. Correlation (indicated by the average adjusted correlation coefficient) shown for sampling frequencies from 3 to 12 per year, and for sample durations of (a) 1 hr, (b) 12 hr, and (c) 24 hr. Black indicates random design type, red is informed. Error bars indicate standard deviation.

Sampling frequency affected most study designs in a similar manner, with all designs performing the worst at the lowest frequency, 3 per year, but improving somewhat with increased sampling frequency. However, the three quality metrics improved only slightly from 4 to 12 samples per year. Random and informed study designs performed similarly for accuracy and efficiency, but informed designs showed

103

noticeably higher correlation with the true trend in fish passage rate for designs using 1- and 24-hr sample durations.

4.5 Discussion

At this tidal energy site, study design simulations indicated that informed study designs using 24-hr sample duration provided the best results for a multi-year study which sought to characterize the seasonal trend in fish presence. Simulated study designs with samples duration of 24 hrs were more accurate, less dependent on sample timing, and better reflected the true changes in fish passage rate than designs that used shorter samples. Sample frequency was not as important to design quality as sample duration, though higher frequencies slightly improved results. The design which provided the most accurate results and highest correlation used at least four 24-hr samples per year, with timing informed by the environmental cycles (timed to occur on the same lunar phase). The general lack of improvement at frequencies higher than four samples per year indicate that this frequency may be sufficient to characterize changes occurring on a seasonal scale. Timing 24-hr samples with lunar phase noticeably improved correlation of sample results with the true median fish passage rate, but did not improve the accuracy or efficiency. As relative changes in fish presence are very important to most monitoring goals, the lunar phase should be held constant when planning the dates of 24-hr samples.

Shorter samples showed higher error, greater dependence on sample timing, and poorer correlation with actual trends in fish presence than did the 24-hr samples. Very large peaks in fish abundance occur at this site on 12- and 24-hr periods (Chapter 3), so results from samples shorter than 24 hours are likely to be influenced by extreme values. Holding physical factors such as tidal and diel stage constant did not consistently

improve accuracy or efficiency of results over those of random designs. This could largely be due to the fact that the response of fish presence to the shorter-scale environmental cycles changes over time (Chapter 3; Pittman and McAlpine 2001, Gibson 2003). In Cobscook Bay, Maine, in the spring, passage rates were highest in the sampled volume near dawn and dusk, while in the fall, peak rates occurred at night (Chapter 3). Sampling only at one time of day (e.g., near dawn) for the whole year would not account for this seasonal change in fish presence relative to the diel cycle, resulting in a trend that would not follow the true seasonal trend. Sampling for an entire day encompasses any shifts in abundance relative to the diel cycle, and the resulting trend would not be as influenced by changing diel patterns.

The temporal representativeness of 1-, 12-, and 24- hr samples unsurprisingly indicated that samples with greater duration were representative of larger spans of time. The temporal representativeness is useful in that it can be used to set limits for the applicability of information from individual samples. For example, one day of data should not be assumed to represent more than the nearest 22 days before and after, and one hour of data should not be taken to represent more than the nearest 36 hr before and after. This information should be used to inform study designs, based on study goals, and should be used during the interpretation of study results. The temporal representativeness of 24-hr samples indicated that a minimum of 8 samples per year would be necessary to fully characterize median fish passage rate and the magnitude of its variation. At the other extreme, 121 1-hr samples per year would be needed to acquire the same information. If only seasonal trends are of interest, as in the situation presented here, full characterization of fish passage rate and its variation may not be necessary; this

was indicated by design quality leveling off at sample frequencies higher than 4 per year. However, different study goals may require the minimum sampling frequency or higher. For example, if the goal of a study were to quantify the immediate effects of device deployment on nearby fish abundance, the first few weeks after device deployment may be of the highest interest, and 1-hr samples spaced 72 hrs apart would be sufficient for capturing median fish passage rate and its variability over that time.

The use of 24-hr samples worked well to characterize the seasonal trend in fish passage rate by encompassing much of the influence of the tidal and diel cycle within each sample. However, there remained a good deal of variation that was not removed using this method. For example, the lowest percent error of the informed 24-hr samples was approximately 65%, and was almost entirely due to over-estimating the true median (Fig 4.3f). The highest correlation of the informed 24-hr samples was approximately 0.69, meaning the results reflected the true median relatively well but 31% of the variation was not accounted for by their linear relationship (i.e., there were rises and falls in the simulated study results that were not present in the true median passage rate). This was 7% more variation explained than the best random design with 24-hr samples (correlation of 0.62). Though informed designs improved correlation, the remaining unexplained variation, combined with the tendency to overestimate the true median, indicated that the median rates from 24-hr samples were still influenced by the large peaks in passage rate related to tidal and diel stage, and potentially other sources of variation unrelated to these cycles.

The remaining unexplained variation highlights the importance of using a control site for comparison while monitoring turbine effects, particularly if effects may be small

relative to other potential sources of variation (Osenberg et al. 1994). If both sites are monitored with discrete 24-hr samples informed by environmental cycles, the effects of cyclic variation on the results could be substantially reduced at both sites. Minimizing such variation maximizes the ability to distinguish MHK device effects from other variation, and would additionally ensure data are more comparable and consistent over time. This is encouraging, given the monitoring efforts that have so far taken place in Cobscook Bay. Viehman et al. 2015 began collecting information for a BACI study of the site, which was continued by Staines et al. (submitted) and could be continued when site development recommences. These studies have always collected 24-hr samples at project and control sites, and so have likely substantially reduced the amount of variation that could influence their results. These sampling methods, when continued through future MHK device deployment at this site, will likely improve the chances of detecting device effects through BACI comparisons.

The approach to study design presented here consists of using the known environmental cycles at a tidal energy site to inform studies of fish presence, and it is likely applicable to most tidal energy sites around the world. Many tidal energy sites in the North Atlantic have similar fish assemblages: for example, Cobscook Bay (Vieser 2014) has many species in common with the Bay of Fundy (Mahon and Smith 1989) and coastal waters of the United Kingdom (Henderson and Bird 2010), and MHK devices are being tested in both of these areas (Stokesbury et al. 2016, Broadhurst et al. 2014). For a given study question, the same study design may therefore be applicable at all of these sites. Even if fish assemblages vary across sites, the distribution and behavior of many species is driven by environmental factors (Pittman and McAlpine 2001, Reebs 2002,

Gibson 2003). Areas with similar environmental cycles will likely find related periodicities in fish presence, so basic knowledge of the major environmental cycles at a site can indicate which study designs will gather the most useful information for a given study aim. As initial site evaluations are carried out, study design can be further informed by more detailed information on environmental variability (e.g., current speed, direction, and temporal components; Hardisty 2007, Copping et al. 2016). Any information on the fish assemblage can further refine the final design (e.g., are diel differences in fish activity likely to occur? do species change seasonally?). In addition to reducing the cost of studies by avoiding the need for continuous sampling, the consistent use of this approach for study design at tidal energy sites would improve the detectability of device effects on fish and comparability of results across locations worldwide.

CHAPTER 5

COMBINING SCALES TO UNDERSTAND EFFECTS OF TIDAL ENERGY

DEVELOPMENT ON FISH IN COBSCOOK BAY, MAINE

5.1 Introduction

The environmental effects of marine hydrokinetic (MHK) devices on the

environment are largely unquantified, mainly due to the low number of devices installed

worldwide. Fish are a key component of the marine environment, and effects on fish are

uncertain and of great concern (Copping et al. 2016, Boehlert and Gill 2010). The

possible effects of marine hydrokinetic (MHK) devices span a range of spatial scales,

from "nearfield" effects occurring within a few blade diameters of the device to "farfield"

effects occurring multiple diameters away (Copping et al. 2015). In the case of fish, a

nearfield effect may be blade strike of an individual, or fish aggregating around a

device's structure. A farfield effect may be fish altering migration routes to avoid the

area of an MHK device or array of devices. There is also an intermediate scale between

near- and farfield, for lack of a better term, the 'midfield,' where effects may include

changes to the local fish assemblage, e.g., vertical distribution or abundance, in the

general area of the device.

Potential effects of MHK devices on fish also span a wide range of temporal

scales. The natural horizontal and vertical distribution of fish, and therefore their

likelihood of encountering the MHK device in the first place , are often species- or life-

stage-specific and linked to environmental factors (Seitz et al. 2011, Bradley et al. 2015).

For example, many fish species undertake seasonal migrations that could bring them to a

tidal energy site at certain times of the year (Pittman and McAlpine 2001). On a finer

timescale, a species at a tidal energy site may only be present at turbine depth during

certain tidal stages, when they rise into the water column to take advantage of the current

(Forward and Tankersley 2001). The sensory and swimming abilities of fish, and

therefore their ability to detect and evade an MHK device in their path, also vary with

species and life stage (Beamish 1978, Weihs and Webb 1984, Kim and Wardle 2003).

Effects of turbines on fish will therefore vary with natural temporal changes in the fish

assemblage.

More information on how fish interact with MHK devices at multiple spatial and

temporal scales is necessary to determine at which scales effects actually occur and may

be detectable (Copping et al 2015). As it is impossible to observe all potential spatial and

temporal scales of effects with one study method, studies should occur at multiple scales

to quantify and understand MHK device effects on fish (Copping et al. 2015). Several

studies have been carried out in recent years which are increasing our understanding of

fish interactions with MHK devices and helping identify new methods for observing

effects on fish at different scales.

In the nearfield domain, laboratory studies have been used to characterize fish

behavior and rates of injury and mortality when they are entrained in MHK devices

(Castro-Santos and Haro 2015, Amaral et al. 2015). These studies indicated that survival

is quite high, on the order of 90% or more, and that behavior can change upstream of

devices (e.g., down-stream moving fish may pause before passing through or by the

turbine). In a field setting, Broadhurst et al. (2014) and Hammar et al. (2013) observed

daytime interactions of fish with different MHK devices using video. Broadhurst et al.

(2014) reported that the fish observed at an MHK device in the Orkney Isles (adult

pollack, *Pollachius pollachius*) aggregated near the device at slack tide, but dispersed as the current speed increased. Hammar et al. (2013) examined avoidance of a device in a tropical area, and noted that different species of fish acted differently; for example, predatory species tended to be 'bolder' in approaching the device than herbivorous species. Bevelhimer et al. (2015) used a hydroacoustic camera and observed potential vertical avoidance maneuvers by fish within 0-15 m of an MHK device in the East River, NY, and a decrease in fish numbers when the turbine was present may have indicated fish avoidance of the turbine's general area.

Studies occurring over larger spatial scales (e.g. hundreds of meters from MHK turbines, midfield to farfield) have primarily focused on describing the natural distribution of fish to predict the probability for spatial and temporal overlap of fish and MHK turbines. Jacques and Horne (2014) sought to characterize the natural spatial variability of nekton distribution at a potential tidal energy site to determine the necessary sampling resolution for adequately moniting MHK device effects. Using hydroacoustic transects, they found that a point estimate of nekton density could be considered representative of the nearest 300 m. This spatial representativeness suggested that to fully characterize nekton density at the site, instruments should be deployed at densities of 3.56 per km^2. Using knowledge of natural spatial variation in nekton density was a unique approach to optimizing study design, and it could be applied to monitoring plans at other tidal energy sites. As measurements must often be taken at some distance from a deployed MHK device due to safety precautions, knowledge of the spatial representativeness of a single point estimate can also determine the maximum distance from a device at which a measurement can be taken.

To understand cumulative effects of MHK devices on fish, we need to begin linking near-, mid-, and farfield observations. For example, the natural distribution of fish in space and time at a site relative to a turbine (mid- to far-field; Viehman et al. 2015, Staines et al. 2015, Staines et al. submitted, Shen et al. 2016, Chapter 3) can be combined with nearfield fish behavior when they encounter an MHK device (Viehman and Zydlewski 2015, Hammar et al. 2013, Chapter 1) to predict fish entrainment in the turbine. Survival post-entrainment may then be informed by laboratory studies (Amaral et al. 2015, Castro-Santos and Haro 2015), where events such as fish strike or injury are easier to observe.

Our work in Cobscook Bay over the past several years is an example of multiple scales of study that have been carried out at the same site, around the same device, with the same fish assemblage, over a number of years. In 2010, Viehman and Zydlewski (2015a) observed fish interaction with an MHK turbine (nearfield) for 24 hours. From 2010-2013, we observed the relative density of fish and their vertical distribution at mid- and far-field scales, and tested for effects of turbine deployment (Viehman et al. 2015, Staines et al. 2015, and Staines et al. submitted). At the same time, from 2011 to 2013, Vieser (2014) characterized the finfish community of Cobscook Bay (e.g., mid- to far-field) to inform the hydroacoustic studies and provide a baseline for future comparison. In 2013, we used mobile hydroacoustic transects to connect data from the far- and near-fields to predict the likelihood that fish would encounter the MHK turbine (Shen et al. 2016). In 2013 and 2014, we examined fish behavior in the near/midfield of a deployed, static MHK turbine for several weeks (Chapter 1). Last, from 2013 to 2015, we characterized natural fish presence in the near/midfield, without the turbine present, using

long-term, continuous hydroacoustic data collection (Viehman and Zydlewski 2015b and Chapters 3 and 4).

These results, gathered over multiple spatial and temporal scales, provide the opportunity to build a more comprehensive picture of fish interactions with an MHK device that is not available at most sites around the world. Here, those multiple studies are used to illustrate how various scales of observation can be combined to answer questions about MHK device effects on the local fish assemblage, and to provide recommendations for future research and monitoring approaches at tidal energy sites.

5.2 Cobscook Bay MHK device assessment

In Cobscoook Bay, study goals arose and evolved over time based on conversations with ORPC, regulators, and community members. These goals can be broadly categorized as: (1) describe the near-field interactions of fish with a single device; (2) characterize presence of fish in the area to (3) detect the long-term effects of a single operating device on regional fish presence and abundance and (4) predict the probability of fish encountering the turbine; and (5) use all results to inform future monitoring efforts. Several separate studies were carried out to address these aims, primarily using hydroacoustics, as comprehensive physical sampling could not be carried out with the precision and resolution necessary to address our questions.

5.2.1 Nearfield interactions of fish with the MHK device

The nearfield behavior of fish around the device was quantified in two different studies. The first occurred in 2010 and spanned 24 hrs, using two DIDSON hydroacoustic cameras to observe fish behavior within approximately 3 m up- and down-stream of a test turbine suspended below a barge in Cobscook Bay (Viehman and

Zydlewski 2015a). This study again observed predominantly small fish (10-20 cm in length), which is in line with the physical data later collected. As with the mobile transects over the device, we found that these fish mainly moved with the current. They tended to enter the turbine if they were at its depth, particularly at night, and that larger fish (>10 cm) were more likely to evade the turbine than smaller ones. Schools of fish were also slightly more likely to evade the turbine than individuals. During this nearfield study, the majority of fish were observed at night after the slack tide, which aligns with patterns we observed in the two-year time series at that time of year (Chapter 3). As with our other studies of Cobscook Bay, these results stress the need to consider the species and life stages of fish present and their unique behaviors when predicting device effects.

The second nearfield (bordering on midfield) study spanned several weeks in the spring of 2013 and was used to observed fish movement in the horizontal plane 7-14 m from the static TidGen® turbine using a bottom-mounted, split beam echosounder (Chapter 1). This study revealed that avoidance was likely occurring at those distances, which fills in more information between the observations by Shen et al. (2016) and the DIDSON observations by Viehman and Zydlewski (2015a). The study further indicated that avoidance consisted primarily of small departures from the direction of the current, which may be sufficient for device avoidance at those distances from the device. Assuming these movements could occur in the vertical plane, as well (which we could not observe), this type of movement by small fish could have accounted for the fact that half of the fish within the DIDSON viewing window were already above or below the turbine upon arrival. This avoidance was incorporated into the probability of encounter

model to fill in the 10 m nearest the MHK turbine, decreasing the probability of fish encountering the turbine from 5.8% to 2.9%.

These two nearfield studies also investigated fish behavior directly downstream of the MHK device. The DIDSON cameras revealed that fish were almost constantly milling in the device wake. This behavior was absent in the side-looking split beam data, indicating that the effect was likely confined to the nearest 7 m downstream of the static turbine (this range may be different for an operating turbine). The reason for this behavior could not be determined, but could have been related to fish purposely sheltering in the turbine wake or being disoriented by passage through the turbine. Regardless of the mechanism behind this aggregation, the role of an MHK turbine as a fish aggregating device has potential implications at the ecosystem level. Piscivores like seals, porpoises, and diving seabirds have been found to frequent strong tidal areas where physical forcing can aggregate prey into somewhat predictable patches (Benjamins et al. 2015), and fish aggregating downstream of MHK devices could lead them into close proximity.

5.2.2 Fish presence at the tidal energy site

Characterizing fish presence at the tidal energy site (independent of a turbine) required combining multiple sampling methods, including physical sampling of fish in Cobscook Bay (Vieser 2014, Zydlewski et al. 2016), monitoring fish vertical distribution and relative density over time (Viehman et al. 2015, Staines et al. submitted, Staines et al. 2015), and describing the variability in fish presence over short and long time scales (Chapter 3).

Physical sampling was required for a general understanding of the fish species and life stages that were likely being detected in our hydroacoustic surveys. It also provided a baseline understanding of fish present in the area for comparison to future data collection and detection of farfield, long-term effects on the local fish assemblage. This physical sampling consisted of benthic and pelagic trawls carried out in the inner, central, and outer bays of Cobscook Bay, and seine and fyke nets used in the intertidal areas of each bay, from spring to fall of 2011-2014 (Vieser 2014, Zydlewski 2016). Results showed that Cobscook Bay has a diverse fish assemblage, with 46 species captured (Vieser 2014, Zydlewski et al. 2016). Atlantic herring (*Clupea harengus*) and winter flounder (*Pseudopleuronectes americanus*) were by far the most abundant species caught in the tidal channels (sub-tidal). Most fish sampled were juveniles, with very few over 30 cm in length. Based on local knowledge, it is likely that some larger fish were also present but under-sampled due to their ability to avoid the trawls. These included adult Atlantic mackerel (*Scomber scombrus*), which are present in large numbers in the late summer. Many of the other species detected also have seasonal presence along the coast of Maine (Bigelow and Schroeder 2002, Tyler 1971). The most important results of this sampling with regard to MHK device monitoring were: (1) the baseline dataset it created for future comparisons, and (2) that most fish at this tidal energy were small, mainly juveniles of many different species. The results of our other studies at this site should therefore be interpreted in this context and extrapolated to sites with different fish assemblages with care.

Cumulative effects of an MHK device on fish in the region (i.e., the mid- to far-field) may be reflected by changes in fish presence, e.g. abundance or density. We

therefore began a hydroacoustic study of the vertical distribution and relative density of fish at the tidal energy site years before turbine deployment, to establish a baseline for use in a before-after-control-impact (BACI) study. Down-looking hydroacoustic samples lasting 24 hrs each were carried out at the future site of the MHK device and at a control site 1.6 km seaward, several times per year in 2010 and 2011 (Viehman et al. 2015). This study revealed that fish tended to be in higher densities near the sea floor, though this varied seasonally with the fish assemblage; in the spring, for example, when larval and recently-metamorphosed Atlantic herring were present in large numbers, fish density tended to be highest in the upper water column. At night, fish tended to spread out in the water column. These differences in vertical distribution were the first indication that the likelihood of fish interacting with the MHK device, and therefore its potential effects, were not constant over time. At this site, fish would be more likely to be at turbine depth at night, when fish were spread out in the water column, than during the day, when most fish would be above or below the turbine.

Samples taken during the BACI study provided snapshots of fish density and distribution over the years studied, each with high temporal resolution (24 hours at 1 ping per second) but separated from the others by large time gaps (months). We filled these temporal gaps in our understanding by collecting a two-year, high-resolution (hourly) time series of fish passage rate at turbine depth using a stationary side-looking echosounder mounted on the sea floor at the MHK device site (Chapter 3). Unsurprisingly, we found cyclic variation in fish passage rates linked to environmental cycles, primarily the 12-hr tidal, 24-hr diel, and 365-day seasonal cycles but also various components of the lunar cycle. Surprisingly, fish passage rate did not appear to be linked

to tidal current speed in any consistent manner. This constrasts the results of Broadhurst et al. (2014), who detected fewer fish at higher current speeds. The fish observed by Broadhurst et al. were large adult pollack, and apparently had different responses to changing environmental factors, such as current speeds, than did the smaller fish of the Cobscook Bay assemblage.

The highly variable passage rate at the depth of the MHK turbine indicated that fish encounter rate with the turbine would be similarly variable. The highest times of fish passage rate, and therefore turbine encounter, would generally be at night in the summer and fall, and near sunrise and sunset in the spring and winter, depending on the tidal stage. Whichever species contribute to the high passage rates at these times would likely be the most affected. These patterns were consistent with the snapshots captured by our BACI baseline surveys. However, certain discrepancies between results of the two studies have implications for future work. In the BACI study, data were collected at high temporal resolution but processed to detect diel differences in fish density and vertical distribution. By averaging during the day and night, we did not detect the increased activity occurring during low or ebb tide at dawn and dusk, which was characteristic of the winter and spring in both years of the high-resolution time series. Fine-scale information such as this may be important information for device siting and effect mitigation, e.g. for commercially valuable species like Atlantic salmon (*Salmo salar*), which may also target certain combinations of diel and tidal stage while migrating into or out of rivers (Smith and Smith 1997, Lacroix and McCurdy 1996). Future studies should be careful not to limit results with insufficient temporal resolution due to prior assumptions of fish behavior.

The high-resolution, long-term dataset also informed our interpretation and continued use of the BACI study design at this site. The detailed time series allowed us to determine that summary statistics obtained from our 24-hr surveys were likely to be representative of the nearest 22 days, setting a limit on the time span to which survey results may be extrapolated (Chapter 4). Furthermore, 24-hr surveys (as opposed to shorter ones) were found to substantially reduce the amount of variation in multi-year monitoring results, which should improve the power of BACI comparisons to detect even small turbine effects (Osenberg et al. 1994). As more sites are developed for tidal energy worldwide, implementing measures to reduce variation (e.g., 24 hour surveys, timed with important environmental cycles) should be incorporated into monitoring plans from the outset in order to improve chances of detecting and quantifying effects of MHK devices.

5.2.3 Detect the effects of operating MHK device

Our BACI surveys continued once the turbine was deployed in order to detect turbine effects on regional fish presence (Staines et al. submitted, Staines et al. 2015). However, only three surveys were completed while the device was in place, and these provided mixed results regarding turbine effects on fish density (Staines et al., submitted) and vertical distribution (Staines et al. 2015). The mixed results may have been due to confounding factors during data collection, which included turbine state (for one survey the turbine was rotating, for the others it was static) and construction activities (e.g. boat traffic, divers in the water). The BACI design appeared able to detect anthropogenic effects on fish density at the project site, supporting the design's application in the dynamic environments of tidal energy sites. However, more data need to be collected

while the turbine is present and operational to determine if normal operation has an effect on the local fish assemblage.

5.2.4 Probability of encounter with MHK turbine

Near to midfield data collected for the BACI study also served to estimate the likelihood of fish encountering the MHK device. The vertical distributions of fish from surveys of the project and control sites were used to inform a probability of encounter model (Shen et al. 2016). This model combined the vertical distributions of fish from the 24-hr stationary surveys (Viehman et al. 2015) with vertical distributions from down-looking hydroacoustic transects starting 200 m upstream of the device and ending 10 m upstream of it. By tracking numbers of fish at turbine depth over the 200 m approach to the MHK device, the probability that fish upstream of the device would be at turbine depth upon arrival was found to be approximately 5.8%. These transects provided a much-needed link between the near- and far-field that is difficult to obtain using stationary surveys, and which has not yet been done at other tidal energy device deployments.

The transects also revealed that fish numbers began to decrease as far as 140 m upstream of the MHK device. As no decrease was observed in control transects that took place beside the device, this indicated avoidance behavior beginning as far as 140 m upstream of the turbine. This is some of the first information on the behavioral "footprint" of an MHK device; that is, the distance to which fish behavior may be affected by its presence. At a distance of 140 m, the turbine would not be visible; if fish were avoiding the device that far upstream, it may have been in response to acoustic emissions (Popper and Schilt 2008) or hydrodynamic cues (e.g., low-frequency

vibrations) detected by the fish lateral line system (Bleckman and Zelick 2009). No

hydrodynamic or acoustic measurements were made concurrent to these transects.

However, information gathered previously by ORPC (ORPC 2013) showed that certain

frequencies emitted by the rotating turbine would be above background noise levels up to

277 m away. Whether this noise was within the detection range of the fish species

present remains to be determined.

5.2.5 Informing future monitoring efforts

The 2-year time series of continuous data (Chapter 3) allowed us to examine the

potential for various study designs to capture changes in fish abundance over the seasonal

cycle. Subsampling the time series to simulate these different designs indicated that the

best method for sampling fish presence (e.g., passage rate, or some other metric of

abundance or density) in this highly variable environment was to incorporate

environmental cycles into survey timing and duration. The best design at this site was to

use 24-hr surveys, as in our BACI study, that were timed with the lunar cycle. These

surveys largely removed tidal and diel variation by encompassing those cycles, and

sampling several times per year (4 or more) provided similar levels of accuracy,

efficiency, and correlation with the actual trend in fish passage rate. Our BACI surveys

(Viehman et al. 2015) were mainly carried out near the neap tide, but did not hold lunar

phase constant. Unless surveys could be carried out at higher frequencies that would

allow the effect of the lunar cycle to be characterized (e.g., surveys several times per

month), BACI results could be improved in the future by adjusting survey timing to occur

at the same lunar phase each time.

If shorter surveys (e.g. 1 hr or 12 hr) were used, they would introduce more variation to results that could limit the abilities of BACI comparisons to detect device effects. However, shorter surveys may be more applicable if shorter-scale changes are the goal of a study; e.g., the effect of turbine installation and the corresponding construction activities on fish presence at the site. The temporal representativeness that we calculated for each sample duration could be used to determine the minimum sampling frequency for a given time period to fully characterize fish passage rate (median) and its variation (IQR). For 1-hr surveys, this would be one survey every 36 hrs, one 12-hr survey would be required every 14.5 days, and one 24-hr survey per 22 days. Sampling at the minimum necessary frequency to accurately capture the trend and variation in fish presence can reduce the costs of a study by using resources more efficiently while avoiding the need for continuous data collection.

We also explored the utility of single beam echosounders for providing more accurate information on detected fish using a post-processing method called deconvolution (Chapter 2). This method relies on statistical assumptions to correct the final distribution of fish target strength (TS) for the effect of the beam pattern (Clay 1983). This had not been tested for a wide-angle single beam, such as the one used in our BACI surveys. We also tested the method on a narrow-angle single beam data, which was represented by split-beam that had not been corrected for beam pattern by the software. We found that the method may work reasonably well for a narrow-angle single beam with a short pulse duration (high sampling resolution), but that the method was not sufficient for the wide-angle single beam using a long pulse duration (lower sampling resolution). However, deconvolution requires many fish to be sampled in order to work

well, and it was apparent that in some 24-hr surveys there were simply not enough individual fish present to obtain good results. This method might enable single beam surveys at tidal power sites to provide more useful information, such as fish size and potentially species, but only at times when many (e.g., several hundred) fish can be detected within a survey. Single beam transducers can always provide a relative metric of fish density (volume backscatter, Sv), which we have previously used in our 24-hr BACI surveys (Viehman et al. 2015, Staines et al. 2015, Staines et al. submitted). Relative fish density may be a sufficient metric if the monitoring goal is to detect changes in fish presence at a tidal energy site.

5.3 Summary

The studies of fish in Cobscook Bay, carried out at different spatial and temporal scales relative to the MHK device, allowed us to form a more complete picture of device effects. Fish at the site were small (generally < 20 cm) and represented numerous species. We observed avoidance of the device with a rotating turbine as far as 140 m upstream by using slight movements away from current direction, and even a static turbine appeared to elicit this type of response at least 18 m upstream (Chapter 1). The chance that a fish upstream of the MHK device may encounter its turbine was quite small, on the order of 5.8%, and the chance that fish would enter the turbine was even lower, 2.9% (Shen et al. 2016). Fish directly upstream of the device at close range (e.g. within 3 m) tended to enter the turbine rather than evade it, especially at night (Viehman and Zydlewski 2015a). At these close ranges, larger fish may be more successful in last-minute device evasion than smaller fish, as swimming power is directly related to length (Beamish 1978). To better understand the fate of fish that enter the turbine, these results

may be combined with those from laboratory studies, which are better able to quantify fish strike and injury (Amaral et al. 2015, Castro-Santos and Haro 2015). We also observed that fish may aggregate in the MHK turbine's wake (Viehman and Zydlewski 2015a), and that this effect did not appear to extend beyond 7 m downstream of the turbine (Chapter 1). Marine mammals and diving birds are drawn to areas where prey aggregate (such as eddies and fronts), and such downstream fish aggregations have the potential to attract these predators to operating MHK turbines (Waggitt and Scott 2014, Williamson et al. 2015).

Fish presence at turbine depth, and therefore their potential to interact with the MHK turbine, varied greatly over time and was related to environmental cycles and the species and life stages of the fish present. The most prevalent cycles in fish passage rate were related to the tidal, diel, and seasonal cycles, but rate was not dependent on current speed. Instead, in Cobscook Bay, fish passage rates were often highest at night, and often during the flowing tide, which may place them at greater risk of entering an operational MHK turbine in their path. This result is in contrast with results of Broadhurst et al. (2014), which indicated that the fish observed (pollack) were only present near slack tide. This difference highlights the importance of considering each tidal energy site in the context of the fish present and their behaviors with respect to the prevailing environmental forces, as this determines the potential for spatial overlap between fish and an MHK (Seitz et al. 2011, Bradley et al. 2015).

The links between fish presence and environmental conditions made it possible to use dominant environmental cycles (tidal, diel, lunar, and seasonal) to inform study design and improve the quality of data for detecting device effects. The BACI baseline

dataset we have gathered to date (Viehman et al. 2015, Staines et al. 2015, Staines et al. submitted) used 24-hr surveys, so is nearly the best-case sampling scenario at this site. However, variation could be further reduced by ensuring these surveys are always carried out at the same point in the lunar cycle. The BACI comparisons we have been able to make thus far indicate that we are able to detect effects at the project site (Staines et al. 2015, Staines et al. submitted), but those effects we detected could not be attributed to MHK device operation alone, and more data must be collected while the turbine is present and operational before further conclusions may be drawn.

By comparing concurrently-collected single and split beam data, we also found that narrow-angle single beam echosounders may be able to provide accurate information on fish TS if deconvolution methods are used (Chapter 2). If monitoring questions do not require accurate TS or position measurements of individual fish (perhaps using relative indices of fish density, such as Sv, instead), then assessment costs may be reduced substantially by using narrow-angle single beam echosounders rather than split beam. A study design that incorporates the major environmental cycles into sample timing and duration can also reduce cost by providing better-quality information with fewer samples (Chapter 4). Finer-scale studies of fish interactions with devices would benefit from targeting times of higher fish passage rates (e.g., in Cobscook Bay, at night during the summer and fall; Chapter 3) to maximize the number of interactions captured in a given observation window, and therefore extend the reach of limited project resources.

5.4 Conclusion

In Cobscook Bay, we were able to build a comprehensive picture of fish/turbine interactions by combining studies on multiple scales. These studies were directly

comparable because they all revolved around the same fish assemblage and MHK device design.   The results presented here are applicable to the fish species and life stages that were present in Cobscook Bay during these studies, but some of the general findings may be applicable at other locations. For example, small fish tending to move with the current may be common to most tidal energy sites, as it is likely a result of the strength of the current relative to the swimming power of the fish, which is directly proportional to size across all species (Beamish 1978). The reliance of turbine effects on the spatial overlap of fish and devices, which depends on environmental conditions and the corresponding species- and life-stage-specific behaviors of fish, will also be a common theme at tidal energy sites.

The comprehensive approach to monitoring a device (or array of devices) on multiple spatial and temporal scales that we used in Cobscook Bay should be used at other sites if a more complete, generalizable picture is to be built of the effects these devices have on fish. What we learned here can be useful for informing future studies of other sites and fish assemblages, even if a multi-scale approach is not possible. The most important data to collect at a site will depend on the questions being asked, which may be influenced by the priorities of regulators and other stakeholders. We found that a BACI study design using several 24-hr surveys per year provided information that could be used to answer a number of questions that arose over time. Results from those surveys were useful in detecting anthropogenic effects at the project site, and also provided detailed information on fish use of the water column and therefore their potential for interacting with the MHK device. Data for use in BACI comparisons at tidal energy sites can be improved by adjusting sample timing to account for the effects of dominant

environmental cycles on the behavior of the fish species and life stages present. If fish strike is a higher-priority concern than farfield effect detection, focus should be placed on the device's nearfield and fish behavior should be interpreted in the context of the fish assemblage (which may change over time and between sites) and the cues emitted by the device.

As device installations scale up, monitoring efforts will need to evolve. The methods presented here are tailored for monitoring the near- and mid-field effects of MHK devices on fish, but new methods will need to be developed to address farfield effects.

REFERENCES

Amaral SV, Bevelhimer MS, Čada GF, Giza DJ, Jacobson PT et al. (2015) Evaluation of behavior and survival of fish exposed to an axial-flow hydrokinetic turbine. North American Journal of Fisheries Management 35(1): 97-113.

Anttila S, Ketola M, Vakkilainen K, Kairesalo T (2012) Assessing temporal representativeness of water quality monitoring data. Journal of Environmental Monitoring 14: 589-595.

Axenrot T, Didrikas T, Danielsson C, Hansson S (2004) Diel patterns in pelagic fish behaviour and distribution observed from a stationary, bottom-mounted, and upward-facing transducer. ICES Journal of Marine Science 61: 1100-1104.

Beamish FWH (1978) Swimming capacity. In: Hoar WS, Randal DJ, editors. Fish Physiology, Volume VII: Locomotion. New York: Academic Press. pp.101-187.

Benjamins S, Dale A, Hastie G, Waggitt JJ, Lea M, Scott B, Wilson B (2015) Confusion reigns? A review of marine megafauna interactions with tidal-stream environments. In: Hughes RN, Hughes DJ, Smith IP, Dale AC, editors. Oceanography and Marine Biology: An Annual Review. Vol. 53. Boca Raton: CRC Press. pp. 1-54.

Bevelhimer M, Scherelis C, Colby J, Tomichek C, Adonizio MA (2015) Fish behavioral response during hydrokinetic turbine encounters based on multi-beam hydroacoustics results. Proceedings of the 3rd Marine Energy Technology Symposium. April 27-29, Washington, D.C. Available: http://tethys.pnnl.gov/publications/fish-behavioral-responseduring-hydrokinetic-turbine-encounters-based-multibeam. Accessed: 2016 June.

Bigelow HB, Schroeder WC (2002) Bigelow and Schroeder's Fishes of the Gulf of Maine. 3rd ed. Collette BB, Klein-MacPhee G, editors. Washington, D.C.: Smithsonian Books.

Blauw AN, Benincà E, Laane RWPM, Greenwood N, Huisman J (2012) Dancing with the tides: fluctuations of coastal phytoplankton orchestrated by different oscillatory modes of the tidal cycle. PLoS ONE 7(11): e49319.

Blaxter JHS, Batty RS (1985) Herring behaviour in the dark: responses to stationary and continuously vibrating obstacles. Journal of the Marine Biological Association of the UK 65: 1031-1049.

Bleckman H, Zelick R (2009) Lateral line system of fish. Integrative Zoology 4: 13-25.

Boehlert GW, Gill AB (2010) Environmental and ecological effects of ocean renewable energy development: a current synthesis. Oceanography 23(2): 68-81.

Boswell KM, Roth BM, and Cowan, Jr. JH (2009) Simulating the effects of side-aspect fish orientation on acoustic biomass estimates. ICES Journal of Marine Science 66: 1398-1403.

Bradley PT, Evans MD, Seitz AC (2015) Characterizing the juvenile fish community in turbid Alaskan rivers to assess potential interactions with hydrokinetic devices. Transactions of the American Fisheries Society 144: 1058-1069.

Broadhurst M, Barr S, Orme CDL (2014) In-situ ecological interactions with a deployed tidal energy device: an observational pilot study. Ocean & Coastal Management 99: 31-38.

Broadhurst M, Orme CDL (2014) Spatial and temporal benthic species assemblage responses with a deployed marine tidal energy device: a small scaled study. Marine Environmental Research 99: 76-84.

Brooks DA (2006) The tidal-stream energy resource in Passamaquoddy–Cobscook Bays: A fresh look at an old story. Renewable Energy 31: 2284-2295.

Čada GF, Bevelhimer MS (2011) Attraction to and avoidance of instream hydrokinetic turbines by freshwater aquatic organisms. Oak Ridge, TN: Oak Ridge National Laboratory. Report No.: ORNL/TM-2011/131. Available: http://www.osti.gov/scitech/biblio/1018268-attraction-avoidance-instream-hydrokinetic-turbines-freshwater-aquatic-organisms. Accessed: 2016 May.

Castro-Santos T, Haro A (2015) Survival and behavioral effects of exposure to a hydrokinetic turbine on juvenile Atlantic salmon and adult American shad. Estuaries and Coasts 38(Suppl 1): S203-S214.

Cazelles B, Chavez M, Berteaux D, Ménard F, Vik JO, Jenouvrier S, Stenseth NC (2008) Wavelet analysis of ecological time series. Oeceologia 156: 287-304.

Charlier RH, Finkl CW (2010) Ocean energy: tide and tidal power. Berlin: Springer.

Clay A, Castonguay M (1996) In situ target strengths of Atlantic cod (*Gadus morhua*) and Atlantic mackerel (*Scomber scombrus*) in the Northwest Atlantic. Canadian Journal of Fisheries and Aquatic Sciences 53: 87-98.

Clay CS (1983) Deconvolution of the fish scattering PDF from the echo PDF for a single transducer sonar. Journal of the Acoustical Society of America 73(6): 1989-1994.

Cochrane NA, Sameoto DD, Belliveau DJ (1994) Temporal variability of euphausiid concentrations in a Nova Scotia shelf basin using a bottom-mounted acoustic Doppler current profiler. Marine Ecology Progress Series 107: 55-66.

Copping A, Battey H, Brown-Saracino J, Massaua M, Smith C (2014) An international assessment of the environmental effects of marine energy deployment. Ocean & Coastal Management 99: 3-13.

Copping A, Hanna L, Van Cleve B, Blake K, Anderson R (2015) Environmental risk evaluation system—an approach to ranking risk of ocean energy development on coastal and estuarine environments. Estuaries and Coasts 38(Suppl 1): S287-S302.

Copping A, Sather N, Hanna L, Whiting J, Zydlewski G, Staines G, Gill A, Hutchison I, O'Hagan A, Simas T, Bald J, Sparling C, Wood J, Masden E (2016) Annex IV 2016 State of the Science Report: Environmental Effects of Marine Renewable Energy Development Around the World. Richland, WA: Pacific Northwest National Laboratory. Available: http://tethys.pnnl.gov/publications/state-of-the-science-2016

De Robertis A, Higginbottom I (2007) A post-processing technique to estimate the signal-to-noise ratio and remove echosounder background noise. ICES Journal of Marine Science 64: 1282–1291.

Embling CB, Illian J, Armstrong E, van der Kooij J, Sharples J, Cumphuysen KCJ, Scott BE (2012) Investigating fine-scale spatio-temporal predator-prey patterns in dynamic marine ecosystems: a functional data analysis approach. Journal of Applied Ecology 49: 481-492.

Evans DH, editor (1993) The physiology of fishes. Boca Raton: CRC Press.

FERC (2012) Ocean Renewable Power Company: Order issuing pilot project license Minor Project, Cobscook Bay Tidal Energy Project, Project No. 12711–005 (February 27, 2012).

Flagg CN, Wirick CD, Smith SL (1994) The interaction of phytoplankton, zooplankton, and currents from 15 months of continuous data in the Mid-Atlantic Bight. Deep-Sea Reesearch II 41(2/3): 411-435.

Frid C, Andonegi E, Depestele J, Judd A, Rihan D et al. (2012) The environmental interactions of tidal and wave energy generation devices. Environ Impact Assess Rev 32: 133-139. doi:10.1016/j.eiar.2011.06.002.

Gibson RN (2003) Go with the flow: tidal migration in marine animals. Hydrobiologia 503: 153-161.

Gibson RN, Robb L, Burrows MT, Ansell AD (1996) Tidal, diel and longer term changes in the distribution of fishes on a Scottish sandy beach. Marine Ecology Progress Series 130: 1-17.

Gill, AB (2005) Offshore renewable energy: ecological implications of generating electricity in the coastal zone. Journal of Applied Ecology 42: 605-615.

Hammar L, Andersson S, Eggertsen L, Haglund J, Gullstrom M et al. (2013) Hydrokinetic turbine effects on fish swimming behaviour. PLoS ONE 8(12): e84141.

Hammar L, Eggertsen L, Andersson S, Ehnberg J, Arvidsson R, Gullström M, Molander S (2015) A Probabilistic Model for Hydrokinetic Turbine Collision Risks: Exploring Impacts on Fish. PLoS ONE 10(3f):e0117756. doi:10.1371/journal.pone.0117756

Handegard NO, Michalsen K, Tjøstheim D (2003) Avoidance behaviour in cod (*Gadus morhua*) to a bottom-trawling vessel. Aquatic Living Resources 16: 265-270.

Handegard NO, Tjøstheim D (2005) When fish meet a trawling vessel: examining the behaviour of gadoids using a free-floating buoy and acoustic split-beam tracking. Canadian Journal of Fisheries and Aquatic Sciences 62: 2409-2422.

Hardisty J (2007) Assessment of tidal current resources: case studies of estuarine and coastal sites. Energy & Environment 18(2): 233-249.

Heath M, Brander K, Munk P, Rankine P (1991) Vertical distributions of autumn spawned larval herring (*Clupea harengus* L.) in the North Sea. Continental Shelf Research 11(12): 1425-1452.

Henderson PA, Bird DJ (2010) Fish and macro-crustacean communities and their dynamics in the Severn Estuary. Marine Pollution Bulletin 61: 100-114.

Henkel SK, Conway FDL, Boehlert GW (2013) Environmental and human dimensions of ocean renewable energy development. Proceedings of the IEEE 101(4): 991-998.

Huse I, Korneliussen R (2000) Diel variation in acoustic density measurements of overwintering herring (*Clupea harengus* L.). ICES Journal of Marine Sciences 57: 903-910.

Jacobson MZ (2009) Review of solutions to global warming, air pollution, and energy security. Energy & Environmental Science 2: 148-173.

Jacques DA, Horne JK (2014) Scaling of spatial and temporal biological variability at marine renewable energy sites. Proceedings of the 2nd Marine Energy Technology Symposium. April 15-18, Seattle, WA.

Jansujiwicz J, Johnson T (2015) Understanding and Informing Permitting Decisions for Tidal Energy Development Using an Adaptive Management Framework. Estuaries and Coasts 38(Suppl 1): S253-S265.

Kim Y-H, Wardle CS (2003) Optomotor response and erratic response: quantitative analysis of fish reaction to towed fishing gears. Fisheries Research 60: 455-470.

Korneliussen RJ, Ona E (2004) Verified acoustic identification of Atlantic mackerel. ICES CM2004/R:20, 14pp.

Kramer SH, Hamilton CD, Spencer GC, Ogston HD (2015) Evaluating the potential for marine and hydrokinetic devices to act as artificial reefs or fish aggregating devices, based on analysis of surrogates in tropical, subtropical, and temperate U.S. west coast and Hawaiian coastal waters. Golden, CO: U.S. Department of Energy, Energy Efficiency and Renewable Energy. Available: www.boem.gov/2015-021. Accessed: 2015 May.

Krumme U, Brenner M, Saint-Paul U (2008) Spring-neap cycle as a major driver of temporal variations in feeding of intertidal fishes: evidence from the sea catfish *Sciades herzbergii* (Ariidae) of equitoral west Atlantic mangrove creeks. Journal of Experimental Marine Biology and Ecology 367: 91-99.

Lacroix GL, McCurdy P (1996) Migratory behaviour of post-smolt Atlantic salmon during initial stages of seaward migration. Journal of Fish Biology 49: 1086-1101.

Lima SL, Blackwell BF, DeVault TL, Fernández-Juricic E (2015) Animal reactions to oncoming vehicles: a conceptual review. Biological Reviews 90: 60-76.

Love RH (1971) Measurements of fish target strength: a review. Fishery Bulletin 69(4): 703-715.

Mahon R, Smith RW (1989) Demersal fish assemblages on the Scotian Shelf, Northwest Atlantic: spatial distribution and persistence. Canadian Journal of Fisheries and Aquatic Science 46(Suppl. 1): 134-152.

Martin B, Vallarta J (2012) Acoustic Monitoring in the Bay of Fundy. JASCO Document 00393, Version 1.1. Technical report for the Fundy Ocean Research Centre for Energy. Dartmouth, Nova Scotia: JASCO Applied Sciences. Available: http://fundyforce.ca/wp-content/uploads/2012/05/Appendix-G-Acoustic-Monitoring-in-the-Bay-of-Fundy.pdf. Accessed: 2016 June.

Martin-Short R, Hill J, Kramer SC, Avdis A, Allison PA, Piggott MD (2015) Tidal resource extraction in the Pentland Firth, UK: potential impacts on flow regime and sediment transport in the Inner Sound of Stroma. Renewable Energy 76: 596-607.

McKinstry CA, Simmons MA, Simmons CS, Johnson RL (2005) Statistical assessment of fish behavior from split-beam hydro-acoustic sampling. Fisheries Research 72: 29-44.

Melvin G, Cochrane NA (2015) Multibeam acoustic detection of fish and water column targets at high-flow sites. Estuaries and Coasts 38(Suppl 1): S227-S240.

Ménard F, Marsac F, Bellier E, Cazelles B (2007) Climatic oscillations and tuna catch rates in the Indian Ocean: a wavelet approach to time series analysis. Fisheries Oceanography 16(1): 95-104.

Neilson JD, Perry RI (2001) Fish migration, vertical. In Encyclopedia of Ocean Sciences, Vol 2, 2nd ed, ed. Steel JH, Turekian KK, and Thorpe SA, 411–416. Oxford: Academic Press.

Nilsson LAF, Thygesen UH, Lundgren B, Nielsen BF, Nielsen JR, Beyer JE (2003) Vertical migration and dispersion of sprat (*Sprattus sprattus*) and herring (*Clupea harengus*) schools at dusk in the Baltic Sea. Aquatic Living Resources 16: 317-324.

Ona E, Godø OR, Handegard NO, Hjellvik V, Patel R, Pedersen G (2007) Silent research vessels are not quiet. Journal of the Acoustical Society of America 121(4): EL145-EL150.

ORPC Maine LLC (2014) Cobscook Bay Tidal Energy Project: 2013 Environmental Monitoring Report. Portland, ME: Ocean Renewable Power Company (ORPC). Available: http://www.orpc.co/permitting_doc/P-12711_Report_w_Appendices_FINAL2.pdf. Accessed: 2016 May.

Osenberg CW, Schmitt RJ, Holbrook SJ, Abu-Saba KE, Flegal AR (1994) Detection of environmental impacts: natural variability, effect size, and power analysis. Ecological Applications 4(1): 16-30.

Picco P, Schiano ME, Pensieri S, Bozzano R (2016) Time-frequency analysis of migrating zooplankton in the Terra Nova bay polynya (Ross Sea, Antarctica). Journal of Marine Systems.

Pitcher TJ (2001) Fish schooling. In: Steel JH, Turekian KK, Thorpe SA, editors. Encyclopedia of ocean sciences (2nd edition), vol. 2. Oxford: Academic. pp. 432–444.

Pittman SJ, McAlpine CA (2001) Movements of marine fish and decapods crustaceans: process, theory and application. Advances in Marine Biology 44: 205:294.

Popper AN and Schilt CR (2008) Hearing and acoustic behavior (basic and applied). In: Webb JF, Fay RR, and Popper AN, editors. Fish Bioacoustics. New York: Springer Science+Business Media. pp. 17-48.

Rakowitz G, Tušer M, Říha M, Jůza T, Balk H, Kubečka J (2012) Use of high-frequency imaging sonar (DIDSON) to observe fish behavior towards a surface trawl. Fisheries Research 123–124: 37–48.

Rao S, Xue H, Bau M, Funke S (2016) Determining tidal turbine farm efficiency in the Western Passage using the disc actuator theory. Ocean Dynamics 66(1): 41-57.

Reebs SG (2002) Plasticity of diel and circadian activity rhythms in fishes. Reviews in Fish Biology and Fisheries 12: 349-371.

Roesch, A. and H. Schmidbauer (2014) WaveletComp: Computational Wavelet Analysis. R package version 1.0. http://CRAN.R-project.org/package=WaveletComp.

Rudstam LG, Hansson S, Lindem T, Einhouse DW (1999) Comparison of target strength distributions and fish densities obtained with split and single beam echo sounders. Fisheries Research 42: 207-214.

Sajdlová Z, Draštík V, Jůza T, Říha M, Frouzová J et al. (2015) Fish behaviors in response to a midwater trawl footrope in temperate reservoirs. Fisheries Research172: 105-113.

Seitz AC, Moerlein K, Evans MD, Rosenberger AE (2011) Ecology of fishes in a high-latitude, turbid river with implications for the impacts of hydrokinetic devices. Reviews in Fish Biology and Fisheries 21: 481-496.

Shapiro GI (2011) Effect of tidal stream power generation on the region-wide circulation in a shallow sea. Ocean Science 7: 165-174.

Shen H, Zydlewski GB, Viehman HA, Staines G (2016) Estimating the probability of fish encountering a marine hydrokinetic device. Renewable Energy 97: 746-756.

Simard Y, Lavoie D, Saucier FJ (2002) Channel head dynamics: capeline (*Mallotus villosus*) aggregation in the tidally driven upwelling system of the Saguenay – St. Lawrence Marine park's whale feeding ground. Canadian Journal of Fisheries and Aquatic Science 59: 197-210.

Simmonds J, MacLennan DN (2005) Fisheries acoustics: theory and practice. Oxford: Blackwell.

Smith EP, Orvos DR, Cairns J Jr.(1993) Impact assessment using the before-after-control-impact (BACI) model: concerns and comments. Canadian Journal of Fisheries and Aquatic Sciences 50: 627-637.

Smith IP, Smith GW (1997) Tidal and diel timing of river entry by adult Atlantic salmon returning to the Aberdeenshire Dee, Scotland. Journal of Fish Biology 50: 463-474.

Staines G, Zydlewski GB, Viehman H, Shen H, McCleave J (2015) Changes in vertical fish distributions near a hydrokinetic device in Cobscook Bay, Maine, USA. Proceedings of the 11th European Wave and Tidal Energy Conference. September 6-11 2015. Nantes, France.

Staines G, Zydlewski GB, Viehman HA (submitted) Changes in relative fish density around a deployed tidal turbine in Cobscook Bay, Maine. International Journal of Marine Energy.

Stanton TK and Clay CS (1986) Sonar echo statistics as a remote-sensing tool: volume and seafloor. IEEE Journal of Oceanic Engineering OE-11(1): 79-96.

Stokesbury MJW, Logan-Chesney LM, McLean MF, Buhariwalla CF, Redden AM, Beardsall JW, Broome JE, Dadswell MJ (2016) Atlantic sturgeon and temporal distribution in Minas Passage, Nova Scotia, Canada, a region of future tidal energy extraction. PLoS ONE 11(7): e0158387.

Tyler AV (1971) Periodic and resident components in communities of Atlantic fishes. Journal of the Fisheries Research Board of Canada 28: 935−946.

Urmy SS, Horne JK, Barbee DH (2012) Measuring the vertical distributional variability of pelagic fauna in Monteray Bay. ICES Journal of Marine Science 69(2): 184-196.

Vaseghy SV (2008) Advanced digital signal processing and noise reduction. West Sussex: John Wiley & Sons.

Viehman H, Zydlewski GB (2015a) Fish interaction with a commercial-scale tidal energy device in a field setting. Estuaries and Coasts 38(Suppl 1): S241-S252.

Viehman H, Zydlewski GB (2015b) Using temporal analysis techniques to optimize hydroacoustic surveys of fish at MHK devices. Proceedings of the 11th European Wave and Tidal Energy Conference. September 6-11 2015. Nantes, France.

Viehman H, Zydlewski GB, McCleave J, Staines G (2015) Using acoustics to understand fish presence and vertical distribution in a tidally dynamic region targeted for energy extraction. Estuaries and Coasts 38(Suppl 1): S215-S226.

Vieser JD (2014) Collaborative research on finfish, their distribution, and diversity in Cobscook Bay, Maine. Orono: the University of Maine. 135 pp.

Waggitt JJ, Scott BE (2014) Using a spatial overlap approach to estimate the risk of collisions between deep diving seabirds and tidal stream turbines: A review of potential methods and approaches. Marine Policy 44: 90-97.

Wang T, Yang Z, Copping A (2015) A modeling study of the potential water quality impacts from in-stream tidal energy extraction. Estuaries and Coasts 38(Suppl 1): S173-S186.

Weihs D, Webb PW (1984) Optimal avoidance and evasion tactics in predator-prey interactions. Journal of Theoretical Biology 106: 189-206.

Wilhelmsson D, Langhamer O (2014) The influence of fisheries exclusion and addition of hard substrata on fish and crustaceans. In: Shields MA, Payne AIL, editors. Marine Renewable Energy Technology and Environmental Interactions. New York: Springer. pp. 49-60.

Williamson BJ, Blondel P, Armstrong E, Bell PS, Hall C et al. (2015) A self-contained subsea platform for acoustic monitoring of the environment around marine renewable energy devices–field deployments at wave and tidal energy sites in Orkney, Scotland. IEEE Journal of Oceanic Engineering 99: 1-15.

Xu D, Xue H, Greenberg D (2006) A Numerical Study of the Circulation and Drifter Trajectories in Cobscook Bay. Proceedings of the 9th International Conference on Coastal & Estuarine Modeling 176-195. doi 10.1061/40876(209)11.

Zamon JE (2003) Mixed species aggregations feeding upon herring and sandlance schools in a nearshore archipelago depend on flooding tidal conditions. Marine Ecology Progress Series 261: 243-355.

Zydlewski GB, McCleave J, Altenritter M (2016) 2014 Annual Report to the Department of Marine Resources: Special License Number ME 2014-36-04. Orono, ME: University of Maine.

BIOGRAPHY OF THE AUTHOR

Haley Viehman was born in Allentown, PA in December 1987. Haley has always loved animals, the outdoors, and building things, and her interest in marine biology began at a young age in Maine's tide pools. Haley graduated from Camden Hills Regional High School in 2005, then studied Civil Engineering at Cornell University, spending her junior year abroad at the University of Cantabria in Santander, Spain. During her years at Cornell, Haley became fascinated with work at the intersection of engineering, society, and the environment, particularly related to sustainable development and renewable energy. Haley graduated with a Bachelor of Science in Civil Engineering in May of 2009. Her enthusiasm for invention, the environment, and multidisciplinary work led her to a graduate position at the University of Maine the following fall, researching the effects of novel tidal energy technology on fishes. Haley received her Master of Science degree in Marine Biorsources from the University of Maine in May of 2012, then she continued this work into an interdisciplinary PhD. Haley is a candidate for the Interdisciplinary Doctor of Philosophy degree in Engineering and the Natural Sciences from the University of Maine in December 2016.

Behavioral Responses of Fish to a Current-Based Hydrokinetic Turbine Under Multiple Operational Conditions: Final Report, February 2017

BEHAVIORAL RESPONSES OF FISH TO A CURRENT-BASED HYDROKINETIC TURBINE UNDER MUTLIPLE OPERATIONAL CONDITIONS: FINAL REPORT

Mark Grippo, Argonne National Laboratory

Haixue Shen and Gayle Zydlewski, School of Marine Sciences, University of Maine

Shivanesh Rao, School of Marine Sciences, University of Maine

Andy Goodwin, Environmental Laboratory,

U.S. Army Engineer R&D Center

Page intentionally left blank

CONTENTS

FIGURES

FIGURES (CONT.)

TABLES

v

1 INTRODUCTION AND PROJECT GOALS AND OBJECTIVES

There is significant interest in the interaction of aquatic organisms with current-based marine and hydrokinetic (MHK) technologies. Determining the potential impacts of MHK devices on fish behavior is critical to addressing the environmental concerns that could act as barriers to the permitting and deployment of MHK devices. To address these concerns, we use field monitoring and fish behavior models to characterize the behavioral responses of fish to MHK turbines and infer potential stimuli that may have elicited the observed behavioral changes.

Monitoring fish interactions with hydrokinetic turbines allows one to consider the magnitude and ecological significance of several potential behavioral risks that have been identified for tidal turbines including the disruption of migratory behavior and food acquisition (Boehlert and Gill, 2010; Frid et al. 2011), behavioral attraction to the device (Boehlert and Gill, 2010; Frid et al. 2011), and avoidance of preferred habitat occupied by the device (Boehlert and Gill, 2010; Polagye et al. 2010; Hammar et al. 2013; Broadhurst et al. 2014). These risks can be assumed to be minimal if the observed fish movement patterns suggest the turbine has only small and temporary effects on normal swimming patterns or fish distribution within a channel.

Blade strike has also been identified as a primary concern associated with the operation of tidal turbines (U.S. Department of Energy, 2009). There have been multiple blade strike studies conducted in laboratory settings using fish exposed to turbines in a confined channel. While these studies indicate fish can avoid blade strike if they swim through a turbine, they do not address what proportion of fish will avoid the turbine completely while swimming through a natural channel. This question is critical in assessing the actual risk of blade strike (Hammar et al. 2015). Earlier work in our study area (Viehman and Zydlewski, 2014) partially addressed this data gap using dual-frequency identification sonar (DIDSON) monitoring of fish movement within a few meters of the Ocean Renewable Power Company (ORPC) turbine generating unit (TGU). The work described in this report further expands the spatial scale of analysis by using field surveys, hydrodynamic modeling, and behavioral simulations that cover fish response to the turbine hundreds of meters upstream and downstream.

The overall goal of this project was to monitor fish movements around an ORPC TGU, use the data to characterize the magnitude and ecological significance of behavioral responses, and investigate the potential variables driving the observed behavioral responses. This multi-year

project spanning fiscal years (FYs) 2013–2016 was a collaboration between Principal Investigator Mark Grippo (Argonne National Laboratory), Dr. Andrew Goodwin (U.S. Army Engineer Research and Development Center), Dr. Gayle Zydlewski (University of Maine), and Prof. Huijie Xue (University of Maine). This report describes our activities to (1) collect hydroacoustic fish survey data, (2) produce high-resolution simulated flows for Cobscook Bay for the survey period, and (3) examine whether fish responded to visual and auditory stimuli generated by the turbine as well as natural and turbine-related changes in flows within the channel.

2 METHODS

The study was conducted in Cobscook Bay, Maine (Fig. 1), which is characterized by strong currents and large, daily tidal fluctuations. Over the course of the study, two tidal turbines were deployed. The bottom-mounted ORPC TidGen® power system (TidGen) was the original focus of the study plan developed in 2013. However, following preliminary data collection, in spring 2013, the TidGen foils and generator were removed from Cobscook Bay. The study was delayed until 2014 when the TidGen was replaced with the OCGen® power system (OCGen).

The OCGen was moored to the seafloor with gravity anchors and cables, as illustrated in Figure 2. The entire OCGen system (float and foils) was 5.1 m high and 19.7 m long. The distance of the OCGen to the seafloor varied with the tidal stage, ranging from 5.9 m to 8.4 m during maximum flow. The bottom-mounted, solid steel frame of the TidGen, which was 31.2 m long and 15.2 m wide, remained on the seafloor during the OCGen survey period. The center location of the OCGen was about 100 m seaward from the center location of the TidGen bottom support frame.
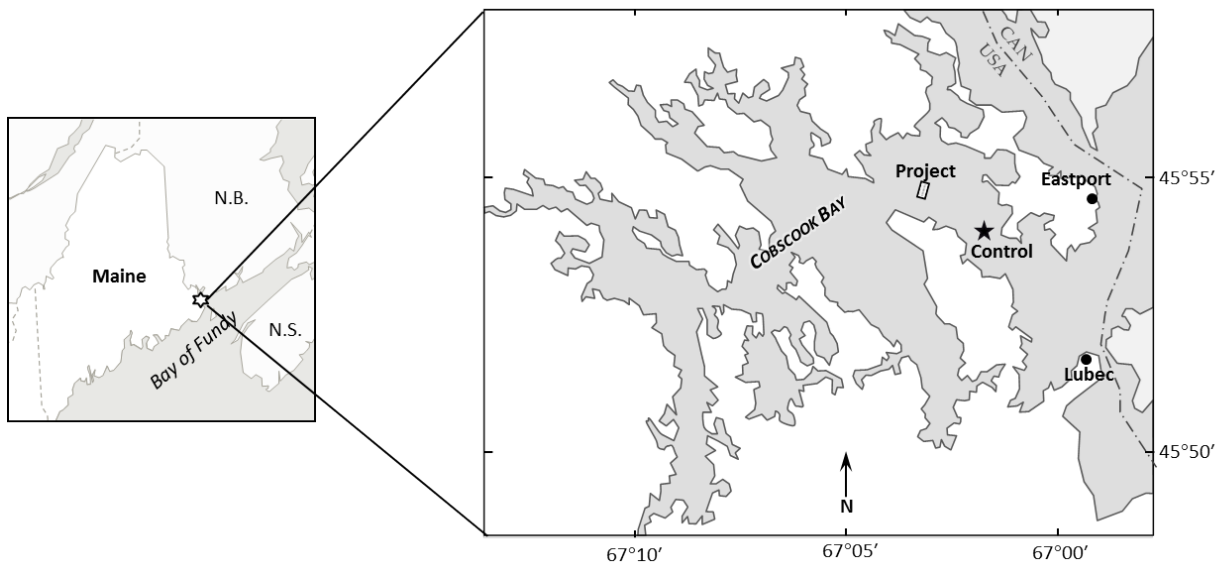

FIGURE 1 Map of Cobscook Bay, Maine, with locations of the project and control sites for fish-MHK interaction research (Source: Shen et al. 2016)

3

TidGen®   OCGen®

FIGURE 2 Schematic representation of the TidGen (9.5×31.2×15.2 m) and OCGen (5.1×19.7×5.3 m) power systems that ORPC installed in outer Cobscook Bay, Maine. Only the bottom mount of the TidGen system was present during the 2014 mobile hydroacoustic fish surveys over the OCGen power system (Source: Shen et al. 2016).

2.1 Mobile Hydroacoustic Fish Surveys

For the field component of this project, we conducted mobile hydroacoustic surveys to determine the position of fish in relation to the OCGen. Mobile, down-looking hydroacoustic fish surveys were initiated in late July 2014 after the OCGen was deployed (Table 1). During each survey period, the mobile hydroacoustic surveys were conducted at typically more than 100 transects covering between 200 m upstream and 200 m downstream of the OCGen, allowing the observation of fish density upstream, over, and downstream of the OCGen. Control transect surveys were also conducted on both sides of the OCGen. Only data collected during flood tides were used in the analysis (Fig. 3) because the TidGen bottom support frame could potentially affect fish behavior as the fish approached the OCGen during ebb tides. Because the seafloor sloped upward when the boat approached the device during the flood tide, fish tracks deeper than the dashed line (Fig. 3) were excluded to ensure equal amounts of water were sampled during the length of a transect.

Following hydroacoustic data collection, the data were processed into fish positions, densities, tracks, or a combination of these. Detected fish tracks were manually inspected for accuracy. A complete description of the hydroacoustic surveys and data processing is provided in Shen's et al. (2016). The survey transect was binned into 10-m segments, and the relationship between the number of fish tracks in the 10-m bin (sum of all surveys) and the distance to the

4

turbine was determined using a simple linear regression which was fitted with the data from 10 m to 140 m upstream of the OCGen. Turbine avoidance was indicated by a decrease in the number of fish tracks with decreasing distance to the OCGen.

TABLE 1 2014 Dates and Conditions for Mobile Hydroacoustic Surveys

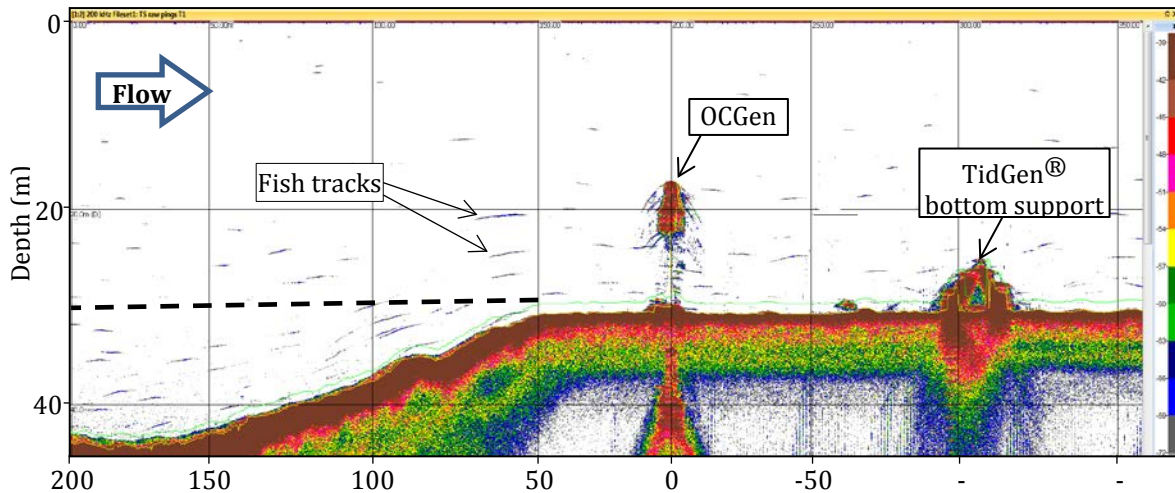| Start time	End time	Tidal pattern	Lunar cycle	Turbine	Number of transects
7/29/2014	7/31/2014	Flood	Neap tide	Free-spinning	100
7/29/2014	7/31/2014	Ebb	Neap tide	Free-spinning	98
7/27/2014	8/3/2014	Flood	Neap tide	Free-spinning	158
8/13/2014	8/16/2014	Flood	Spring tide	Static	128

FIGURE 3 A mobile transect over the OCGen power system and the TidGen bottom support frame during a flood tide (Source: Shen et al. 2016)

After the surveys were completed, we discovered that the OCGen was free-spinning (rotating but not generating power) during the surveys conducted from July 29 to August 3 and that during the August 13 to August 16 survey, the turbine was in a static operational condition and was not spinning (Table 1). As described in Section 2.4, this operational variation allowed us to examine the relationship between fish behavior and the operational status of the turbine.

2.2 Hydrodynamic Modeling of Flows in Cobscook Bay

Using output from two separate hydrodynamic models, flow in the study area was visually simulated to qualitatively assess the magnitude of the hydrodynamic disturbance generated by the OCGen. Using a Finite-Volume Community Ocean Model (FVCOM), high-resolution simulations of flow near the OCGen were generated for the time periods corresponding to the hydroacoustic fish surveys. The objective was to provide simulations of hydrodynamic fields with sufficient detail for the Eulerian-Lagrangian-Agent Method (ELAM) fish behavior analysis; the ELAM depends on accurately capturing not only the flow field (including flow velocities, turbulent kinetic energy), but also the derivative field (including flow velocity gradients, flow acceleration).

A high-resolution FVCOM coastal circulation model (approximately 5 m spatial resolution) was nested in the existing Cobscook-Passamaquoddy model with 20 m resolution of outer Cobscook Bay (Fig. 4a). The location of the OCGen is shown in Figure 4b. The size of the high-resolution area was based on the preliminary estimated area of flow modifications caused by the OCGen, which was estimated to reach hundreds of meters downstream as the flow field leaves the turbine, and tens of meters upstream where the flow field approaches the turbine. The high-resolution area covered the mobile hydroacoustic survey area, with the high-resolution mesh blending into the existing 20-m mesh resolution outside this region. The actual turbine dimensions and the dimensions used in the model are shown in Figure 5. All model runs were conducted on the Argonne Laboratory Computing Resource Center's Blues or Fusion computing clusters.

The FVCOM was designed to follow the operational specification of the OCGen. During the first three fish survey periods (July 29–August 10, 2014), the FVCOM simulated a fully functioning OCGen. Consequently, during slack tide models, drag reduced to 0.3701, which represents a free-spinning, non-power generating OCGen. When the water flow speed exceeded 1 m/s, the OCGen began generating power and the FVCOM drag coefficient became 2.237. The buoyancy floats above the turbine had a continuous drag coefficient of 0.776. The TidGen bottom mount was also accounted for in the model. However, after the model runs were completed, we discovered that the OCGen did not generate any power during the three fish survey periods. Instead, the OCGen was free-spinning from July 29 to August 10, at which point

6

the OCGen blades stopped rotating and remained static. Because the OCGen was free-spinning and never generated power before August 10, the modeled drag of 2.237 was likely never realized; instead, the OCGen had a free-spinning drag coefficient of 0.3701 for all flow conditions. Therefore, the real-world wake was smaller than the FVCOM-modeled wake prior to August 10 when flow speed exceeded 1 m/s. Model runs were not conducted for the non-rotating, static condition that existed after August 10, because there was no drag coefficient available for this condition. This motionless state is not a normal operational condition, and therefore is not relevant to assessing behavioral changes in fish.
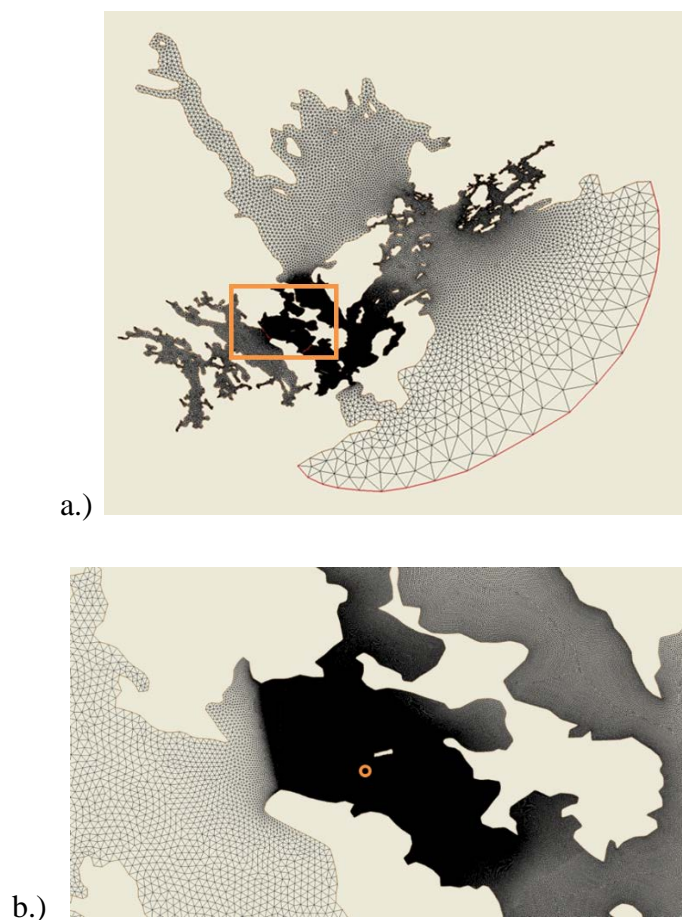

a.)

b.)

FIGURE 4 The Cobscook-Passamaquoddy model regional mesh including Cobscook Bay, Penobscot Bay, and part of the Bay of Fundy on the US-Canada border. (a) The red line on the far right represents the oceanic boundary, and the orange box represents the study area where the OCGen was deployed. (b) A high-resolution, close-up of Cobscook Bay and the location of the turbines, as shown by the orange circle. Figure provided by Shivanesh Rao, University of Maine.
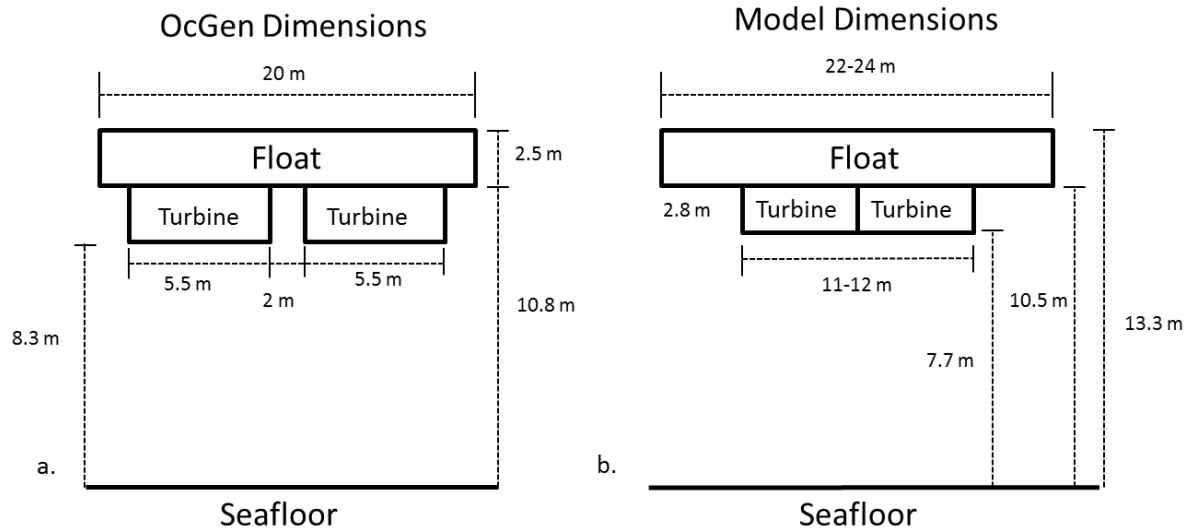
FIGURE 5 **(a) The OCGen power system dimensions and location in the water column and (b) the model equivalent of the OCGen dimensions**

A second hydrodynamic model for Cobscook Bay was developed by Sandia National Laboratory using its Environmental Fluid Dynamics Code (SNL-EFDC). Because different hydrodynamic models have their own strengths and weaknesses, it is advantageous to compare how different modeling methods impact ELAM analysis results. In addition, SNL-EFDC has wide familiarity within the MHK industry and is used by ORPC.

The SNL-EFDC model used a rectangular domain that extended the model's domain 830 m in the streamwise direction (or the direction of net tidal flow) and 320 m in the cross-stream direction. The domain consisted of 10,624 horizontal cells measuring 5×5 m^2 and 11 vertical layers. Turbine dimensions and thrust coefficients used in the SNL-EFDC model were the same as those used in FVCOM.

2.3 ELAM

Individual-based models (IBMs) of behavior are commonly used to assess the impacts of hydraulic modifications on fish populations. However, many existing IBMs are data-intensive and unpractical for meeting the needs of MHK developers. To address this R&D challenge, we applied the comparatively simple ELAM model to simulate fish experience in a flow field

around the OCGen. The ELAM model was developed by the U.S. Army Corps of Engineers (USACE) Engineer Research and Development Center (ERDC) (Goodwin et al. 2014), and was traditionally used in environmental applications for conventional hydropower operations (Goodwin et al. 2007); this was the first application of the model to MHK technology. The ELAM model integrates the hydroacoustic fish position data (Section 2.1) with hydrodynamic modeling simulations (Section 2.2), providing a mechanistic explanation of the observed fish behavioral responses to turbine-related and natural changes in the flow field. Using this information, the ELAM model can simulate fish movement trajectories that characterize fish behavior before, during, and after they encounter a turbine.

There were four overall tasks required to develop the ELAM model: (1) collection of mobile and stationary hydroacoustic data on fish in Cobscook Bay and the processing of this data into fish tracks and/or density information (Section 2.1), (2) development of high-resolution hydrodynamic modeling for Cobscook Bay for periods when fish data are available (Section 2.2), (3) integration of hydrodynamic patterns and fish hydroacoustic data, and (4) simulation of fish movements under various behavior rules.

An ELAM analysis is executed according to the conceptual model in Figure 6. ELAM analysis begins with identifying scenarios and data integration. Scenario identification is an important step, yet is rarely straightforward. Scenarios must have sufficient real-world observations along with hydrodynamic model representations of what the field flow conditions were at the time of an observation. We then synchronized the fish tracks from the hydroacoustic monitoring within the simulated flows corresponding to that survey period. Following the conceptual model in Figure 6, we then evaluated the role of passive behavior and volitional behavior on the densities of simulated fish approaching the turbine, by comparing these simulations to the observed changes in fish track density.
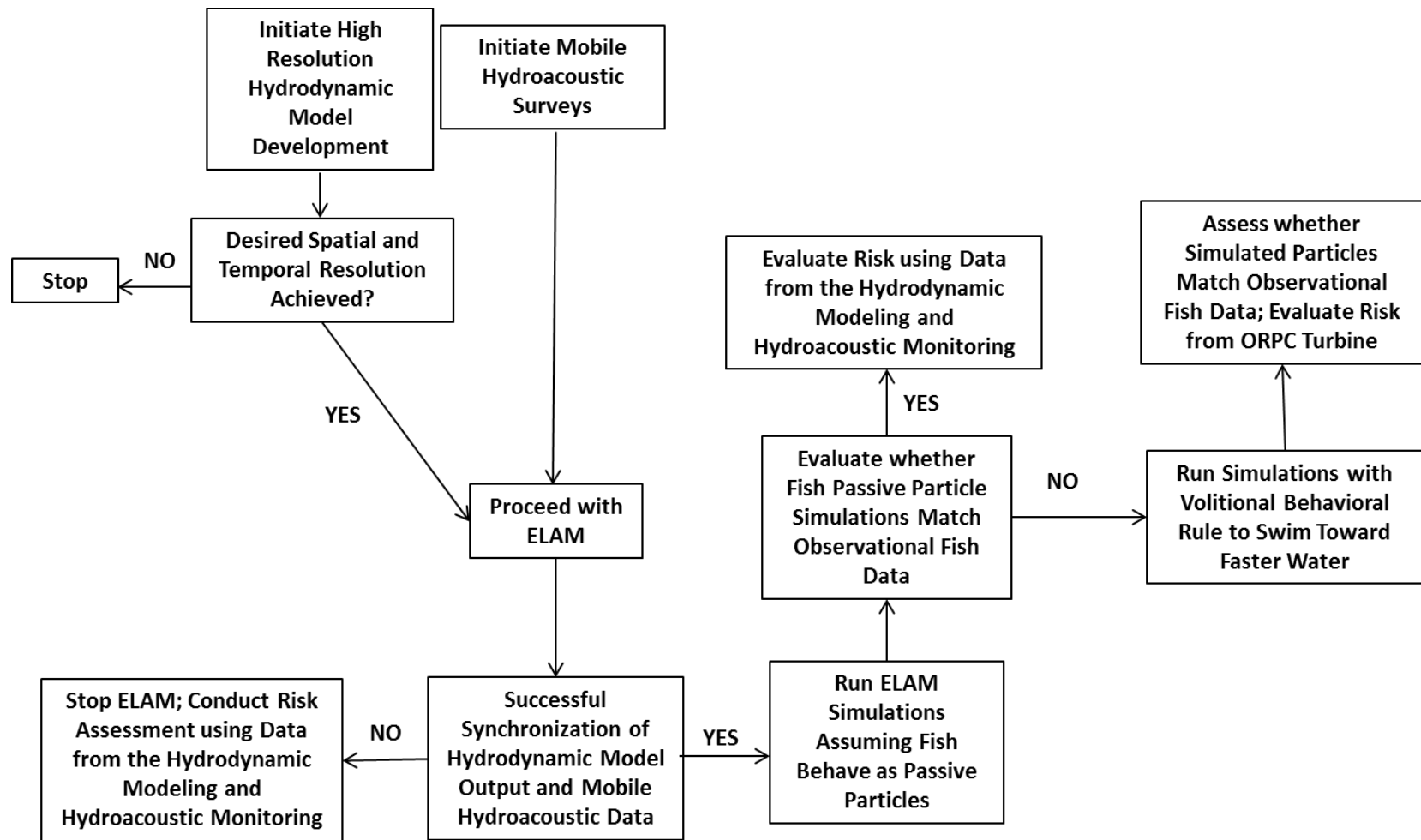
Figure 6 Conceptual model of ELAM analysis. This proposed work effort will evaluate only "direct" response behaviors to hydrodynamics.

2.4 Analysis of Mechanisms for Behavioral Changes

We investigated fish behavior under different environmental and operational conditions in order to test which stimuli were associated with observed behavioral changes. We examined fish behavior in relation to three potential stimuli: (1) natural and turbine-related flow patterns in the channel, (2) noise generated by the turbine, and (3) visual stimuli generated by the turbine. The analyses were not intended to conclusively demonstrate causation, but rather to determine whether the data supports these environmental stimuli as potential explanations for any changes in fish density along the survey transects.

The relationship between the number of fish tracks and the distance to the turbine was used as the metric of behavioral change (Section 2.1). The significance of turbine-associated visual stimuli was investigated by examining differences in fish behavior between fish survey data collected during the day and data collected at nighttime. The turbine would presumably be visible to fish at a greater distance during the daytime compared to night. Therefore, differences in avoidance behavior between the two periods would indicate a visual stimuli effect. Fish response to turbine-generated noise was investigated by examining differences in fish behavior between data collected while the turbine was freespinning (July to early August 2014) versus when it was static (mid-August 2014). Based on prior acoustic monitoring of the TidGen (ORPC, 2014), we assumed that the OCGen would produce significantly less noise when static compared to when it was freespinning. The relationship between track density and distance to the turbine was tested using regression analysis.

Fish respond to hydrodynamic forcings. Hydrodynamic stimuli in Cobscook Bay could result from not only natural flow and channel morphology, but also from disturbance to the flow field generated by the OCGen. To assess the latter, the hydrodynamic model output described in Section 2.2 was used to qualitatively assess the magnitude of the hydrodynamic disturbance generated by the OCGen. The ELAM model was used to assess whether natural flow patterns were the primary influence on fish swimming behavior. Specifically, we tested whether assigning behavioral rules in which the simulated fish followed natural velocity changes within the channel would result in fish density distributions that matched the patterns in the hydroacoustic fish track data. The analysis directly addressed the question of whether natural flows were the cause of the observed avoidance. If the fish did not display the same density

11

patterns as in the field-based data, we would have further confirmation that the turbine itself was the source of the observed behavioral patterns.

Using the ELAM model, we released simulated particles 700 m upstream of the OCGen. Seven-hundred meters was chosen to more realistically simulate the actual experience of fish while at the same time maintaining a manageable model run time. The particles were not released from a central location, but rather randomly across the channel from bank to bank (Figure 7). The released particles were coded to follow one of two decision rules: (1) no volitional behavior (individuals resemble passive particles) and (2) volitional behavior in which fish swim toward faster water. For rule 2, multiple swim speeds ranging from 0.05 to 0.25 were evaluated. A swim speed of 0.1 m/s would best approximate the actual swimming speed of the pelagic fish in Cobscook Bay (Gayle Zydlewski, personal communication). Modeling fish with greater swimming speed allowed the greater expression of volitional behavior, because the fish is better able to resist the prevailing current if it chooses to do so.

To see how fish density distribution changed with distance from the turbine, we then quantified fish density distributions at 25m intervals within a rectangle that extended three hundred meters out from the OCGen (Figure 7). Densities were calculated for multiple rectangle widths (8, 16, 24, and 32 m) which covered the approximate width of all of the hydroacoustic field survey tracks (Figure 7). The comparison of ELAM-generated fish densities and observed fish densities was conducted qualitatively because methods are still lacking for rigorous quantitative comparisons that account for underlying idiosyncrasies between field-monitored and modeled-trajectory data.
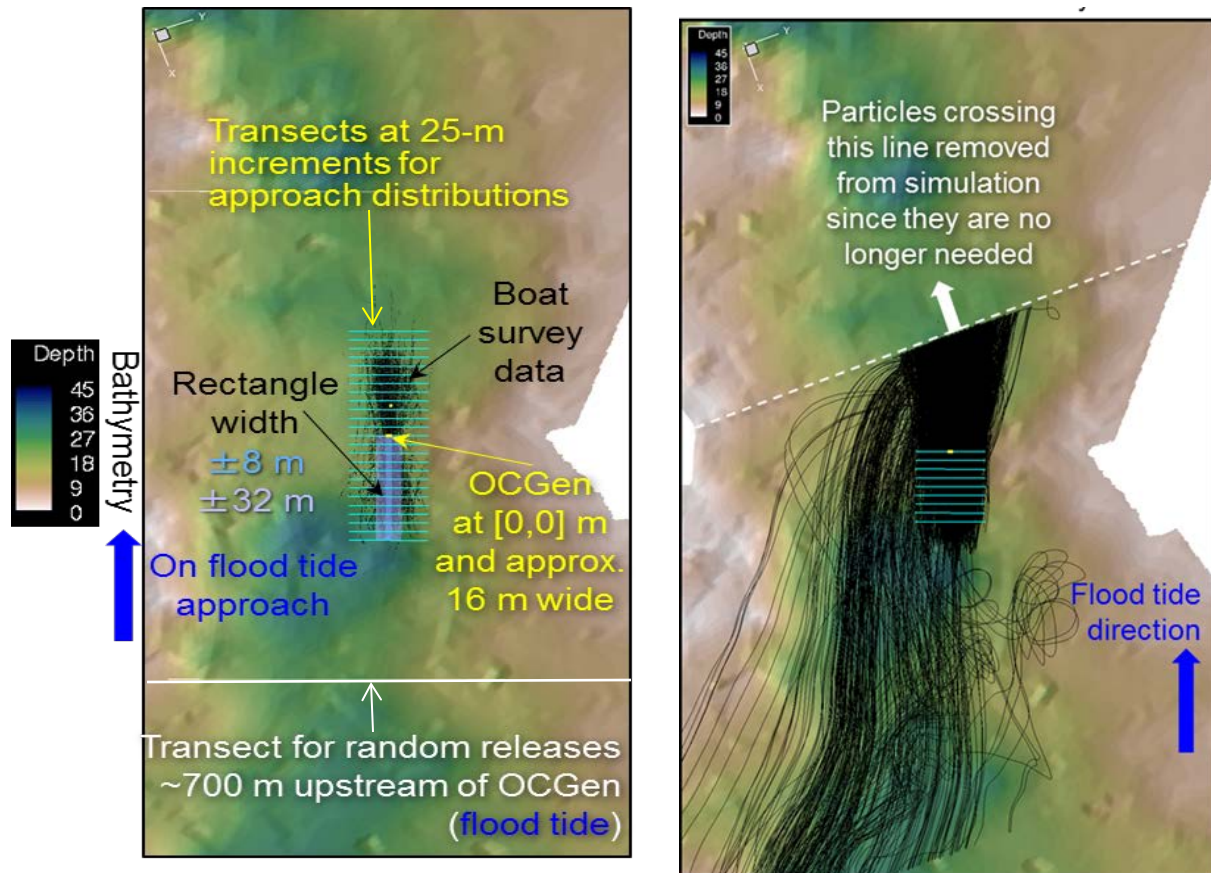
Figure 7. Location of ORPC turbines and survey transects, random fish particle releases, and the transects at which fish density distributions were calculated.
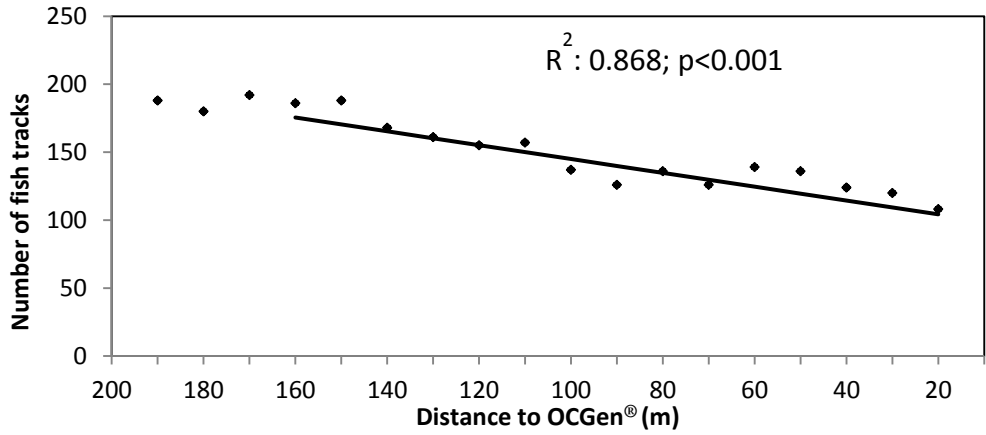
3 RESULTS
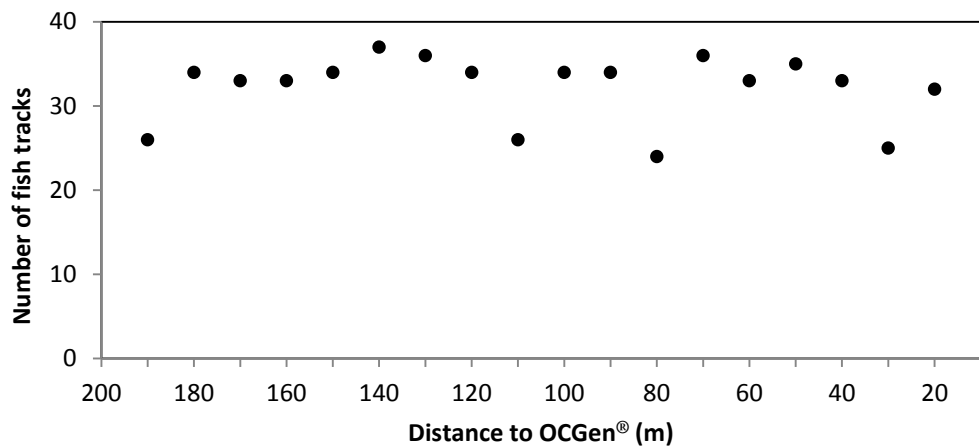
3.1 Hydroacoustic Fish Surveys

When flood tide surveys conducted under the freespinning condition were combined, there was a significant negative relationship between the number of fish tracks within the 10-m distance bins and the distance to the OCGen ($y = -0.5093x + 103.78$; $R^2 = 0.86$). The number of fish tracks began decreasing approximately 140 m upstream of the OCGen (Fig. 8a), and there was a 37.2% (95% CIs: [21.8%, 49.4%]) decrease in the number of fish between 140 m and 10 m upstream of the OCGen. The significant decrease in fish tracks approaching the spinning turbine was found for both daytime ($R^2 = 0.7402$; $p<0.001$) and nighttime ($R^2 = 0.7648$; $p<0.001$) surveys, and the decline in fish tracks began at approximately 140 m from the turbine during both day and night (Figs. 9a and 9b). No relationship between the number of fish tracks and the distance to the OCGen was found for control transects (Fig. 8b) or control transects parsed by day (Fig. 9c) or night (Fig. 9d). However, it should be noted that the number of control transect surveys was less than the number turbine surveys.

To examine whether fish avoided the turbine using vertical or horizontal movements, we examined the proportion of total fish in the water column that were located between 0 and 10 m (the approximate depth of the OCGen) (Fig. 8c). The proportion of fish near the bottom showed little variation across the survey transect indicating the decrease in the number of fish tracks between 140 and 10 m is the result of a change in horizontal rather than vertical position as they approach the device.
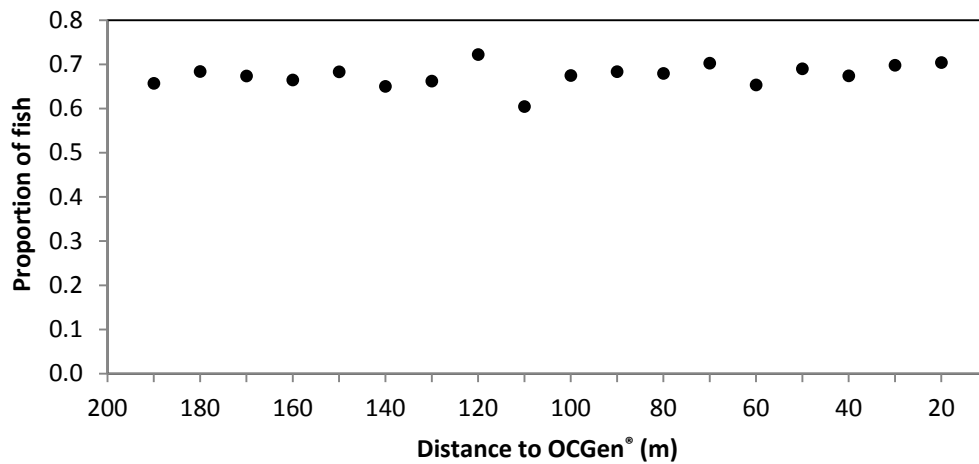
For surveys conducted in mid-August, when the turbine was static, there was a weak relationship ($p=0.0357$) between the number of fish tracks and the distance to the OCGen for all turbine transects combined (Fig. 10a). This weak relationship was present in daytime survey data ($p=0.0154$), but not for nighttime survey data (Fig. 10a). A similarly weak relationship was observed at control transect surveys conducted during the static turbine period for nighttime surveys (p=0.02557), but not daytime surveys ($p=0.3031$) (Figs. 10b and 10c).
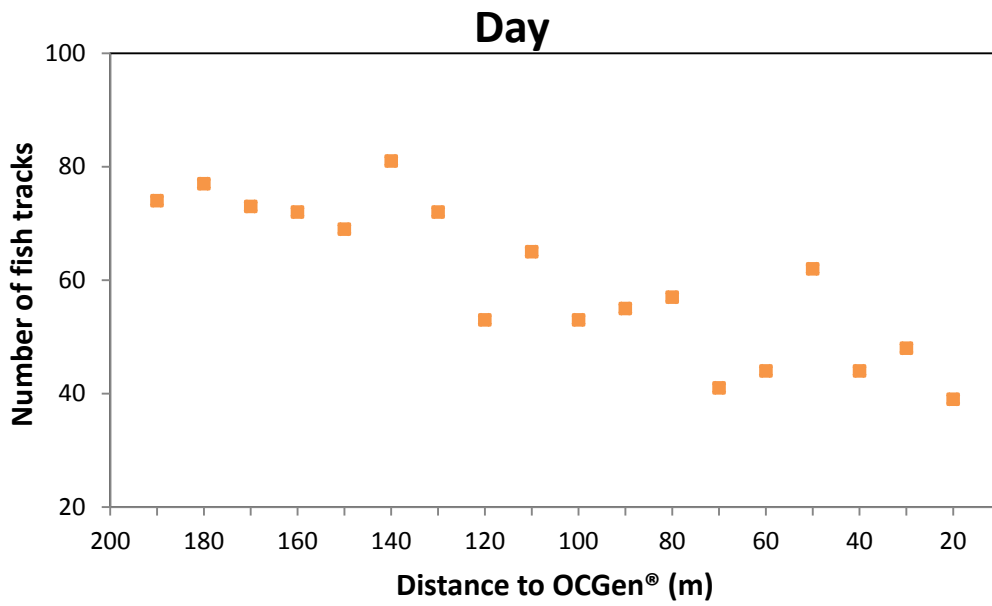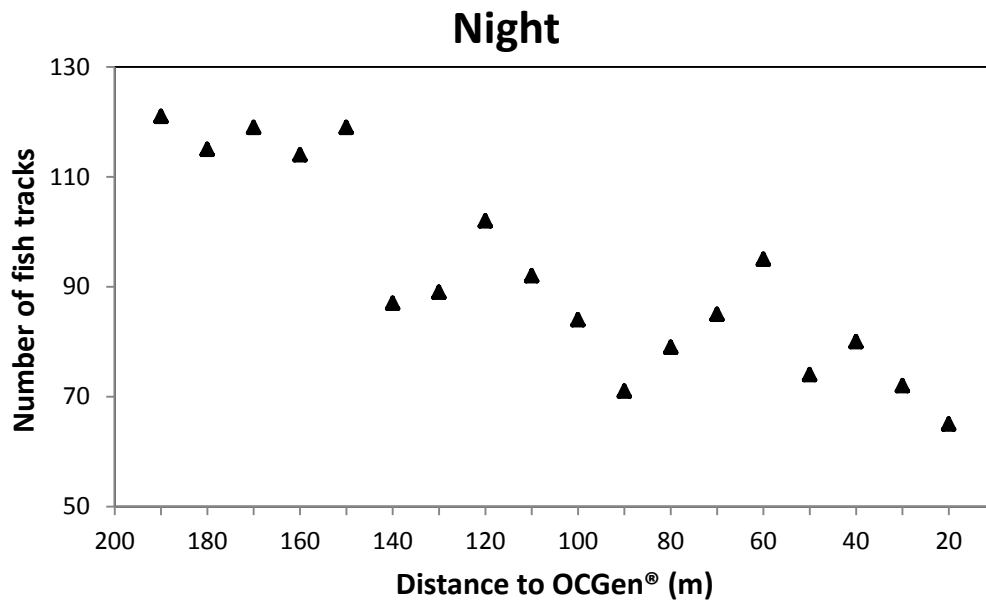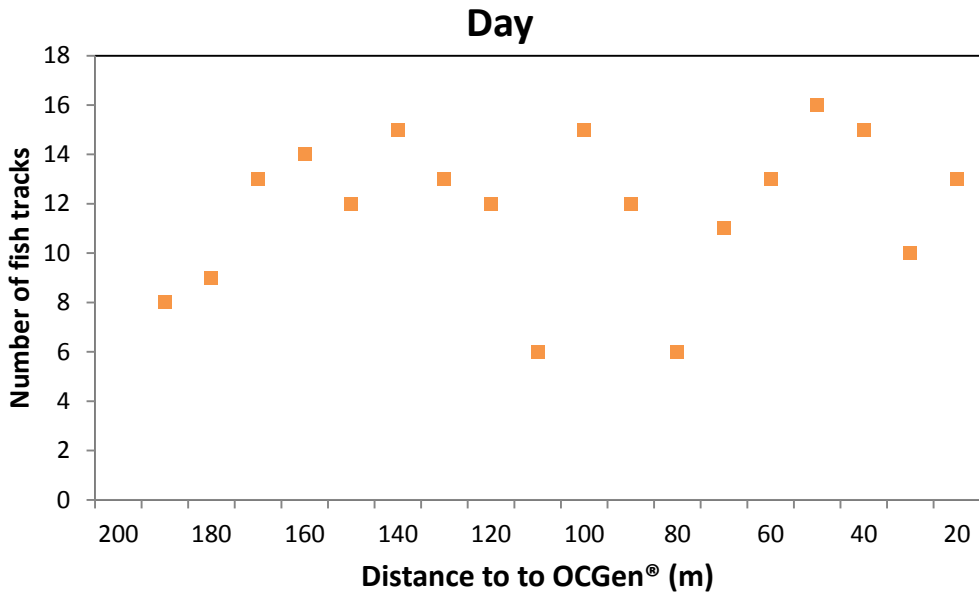
FIGURE 8 **(a) The relationship between the number of fish tracks and the distance of the track to the OCGen and (b) the number of fish tracks versus the distance to the theoretical location of the OCGen at control transects. The data points represent the total number of fish tracks (sum of all surveys) in each of the 10 m distance intervals between 200 and 20 m from the OCGen. Figure 8c shows the proportion of fish at the depth of entire OCGen (0-10 m above the seafloor) relative to fish in the entire water column (Source: Shen et al. 2016).**

Day

a)

Night

b)

16

Day

c)

Night
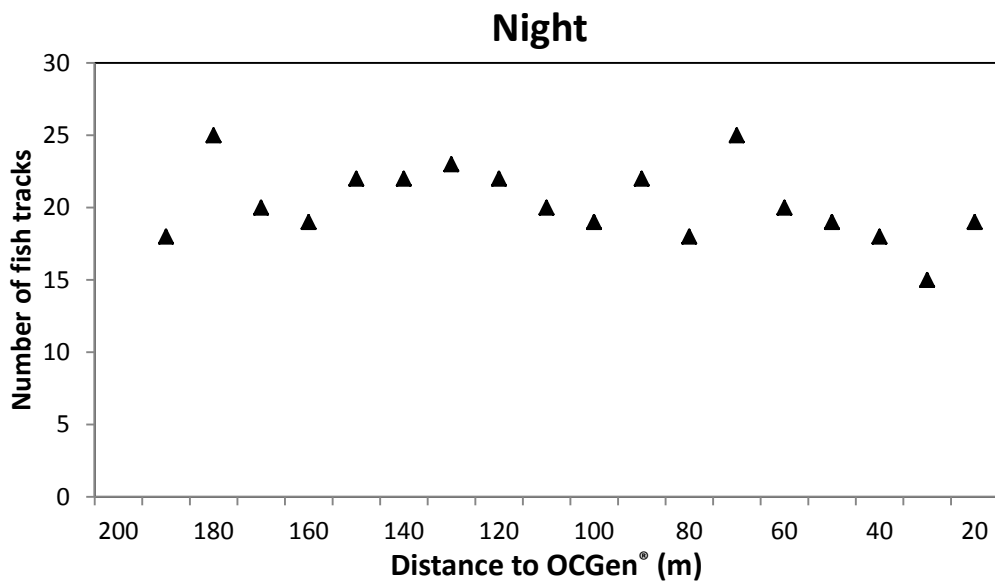
d)

FIGURE 9 **The relationship between the number of fish tracks and the distance of the track to the OCGen when the turbine was spinning during (a) daytime and (b) nighttime surveys and (c and d) at control transects. The data points represent the total number of fish tracks (sum of all surveys) in each of the 10 m distance intervals between 200 and 20 m from the OCGen.**

FIGURE 10 The relationship between the number of fish tracks and the distance of the track to the OCGen when the turbine was static (a) during daytime and nighttime at turbine transects and (b and c) at control transects. The data points represent the total number of fish tracks (sum of all surveys) in each of the 10 m distance intervals between 200 and 20 m from the OCGen.
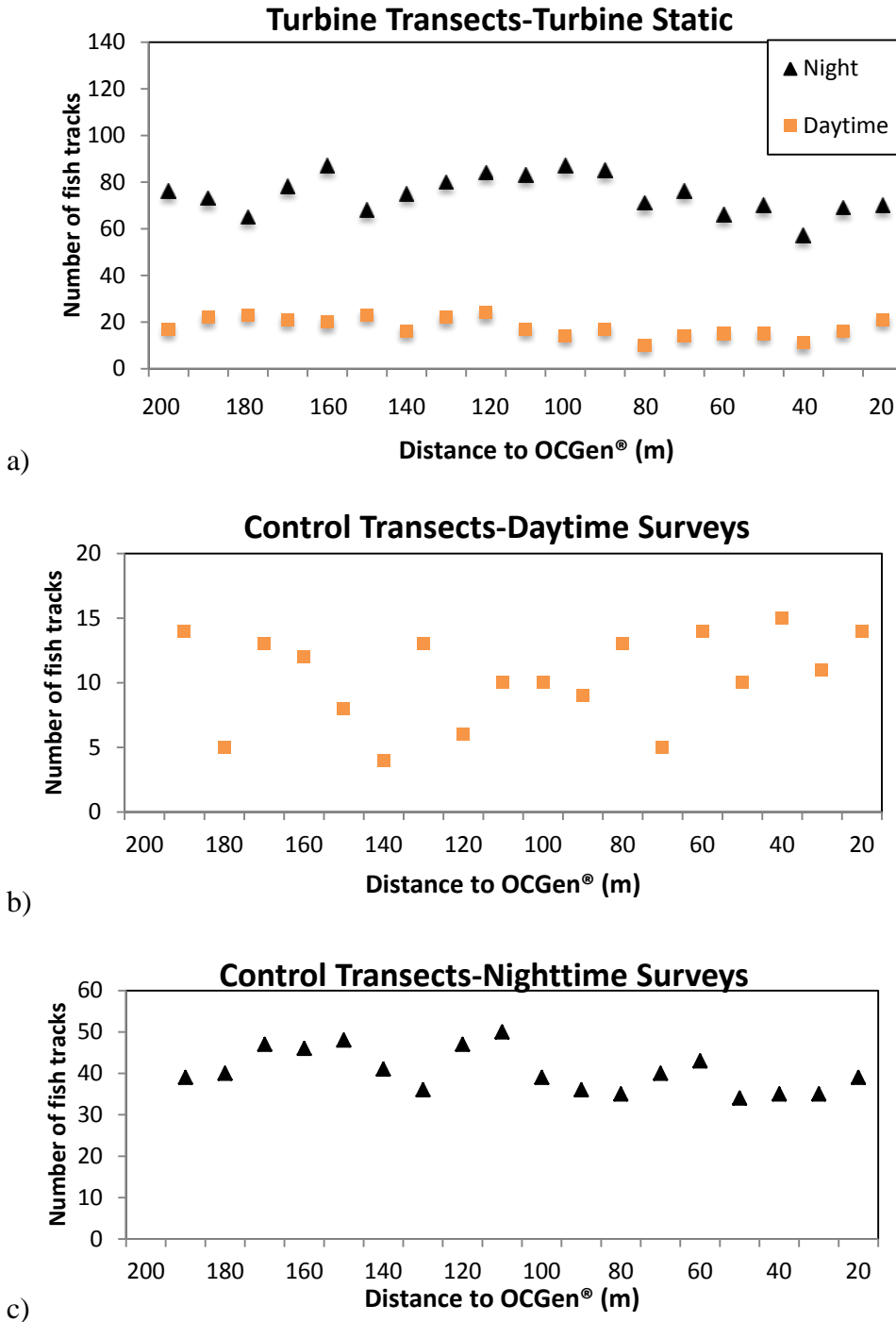
18

3.2 Hydrodynamic Modeling

3.2.1 FVCOM Model

To assess the accuracy of the FVCOM output, model results were compared to the surface elevations from two Acoustic Doppler Current Profiler (ADCP) devices latterly positioned approximately 74 m from the OCGen. The ADCP devices recorded the elevation and velocity of the flow, and surface elevations were extracted from the model cell corresponding to the ADCP locations, referred to as "Lubec" and "Goose" (Fig. 11). We also compared the model surface elevations with those recorded by the National Oceanic Atmospheric Administration (NOAA) tidal gauge at Eastport, which was located farther away from the turbine location. The modeled surface elevation and the elevation measured by the ADCPs aligned closely (Fig. 11). The modeled and NOAA tidal gauge surface elevations at Eastport also matched closely, with only a slight phase difference between the two. This comparison shows that the model reasonably approximated the volume flux entering and exiting the location of the turbine in Cobscook Bay.
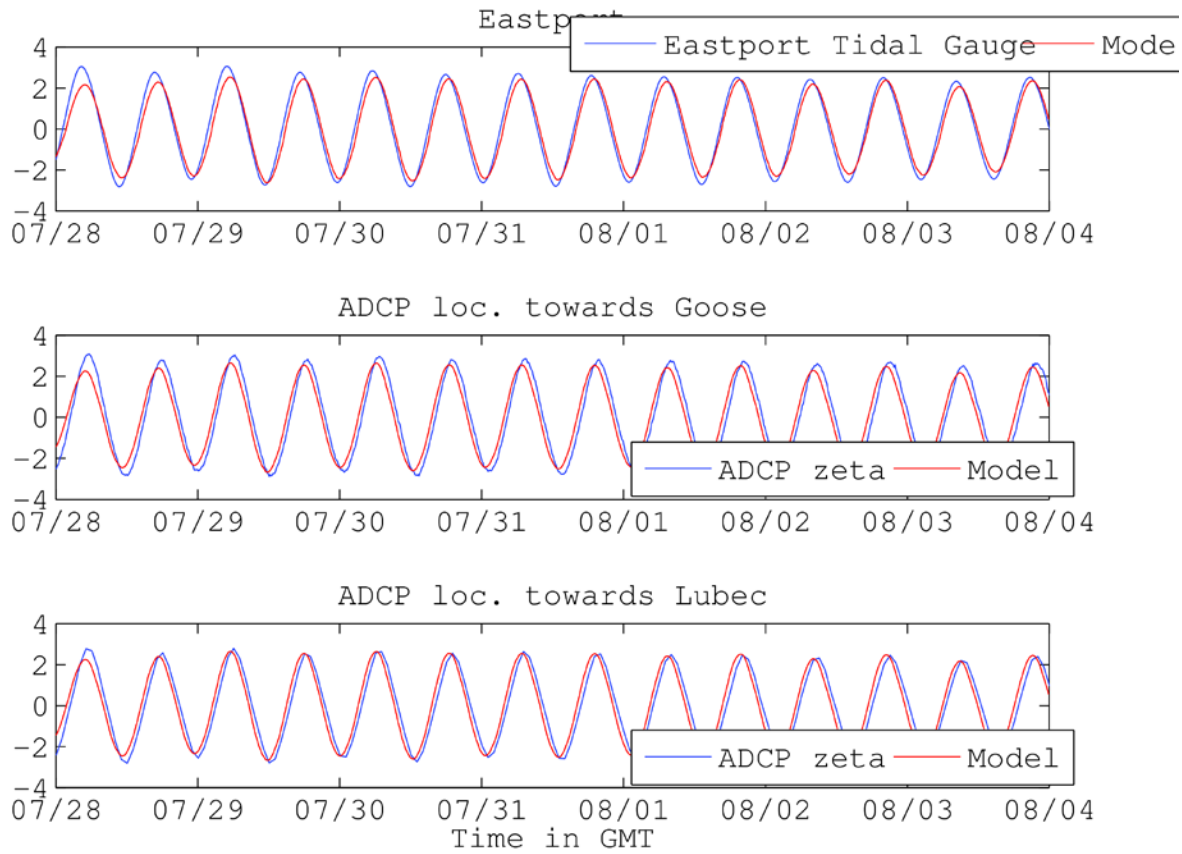
FIGURE 11 Comparison of FVCOM output and tidal elevation measured by the study's ADCP devices and a NOAA tidal gauge. The tidal elevations at the three locations closely match the measurements from the ADCP and tidal gauge.

3.2.2 SNL-EFDC Model

Water levels and depth-averaged velocity magnitudes from the calibrated model closely matched ADCP measurements (Figs. 12 and 13). Modeled depth-averaged velocity magnitudes were on average within 0.07 m/s of measured values, which is within the typical measurement errors for an ADCP.

FIGURE 12 Comparison of the SNL-EFDC modeled water levels to measured water levels at the ADCP location for all sampling events

FIGURE 13 Comparison of SNL-EFDC modeled depth-averaged velocity to measured depth-averaged velocities at the ADCP location for all sampling events
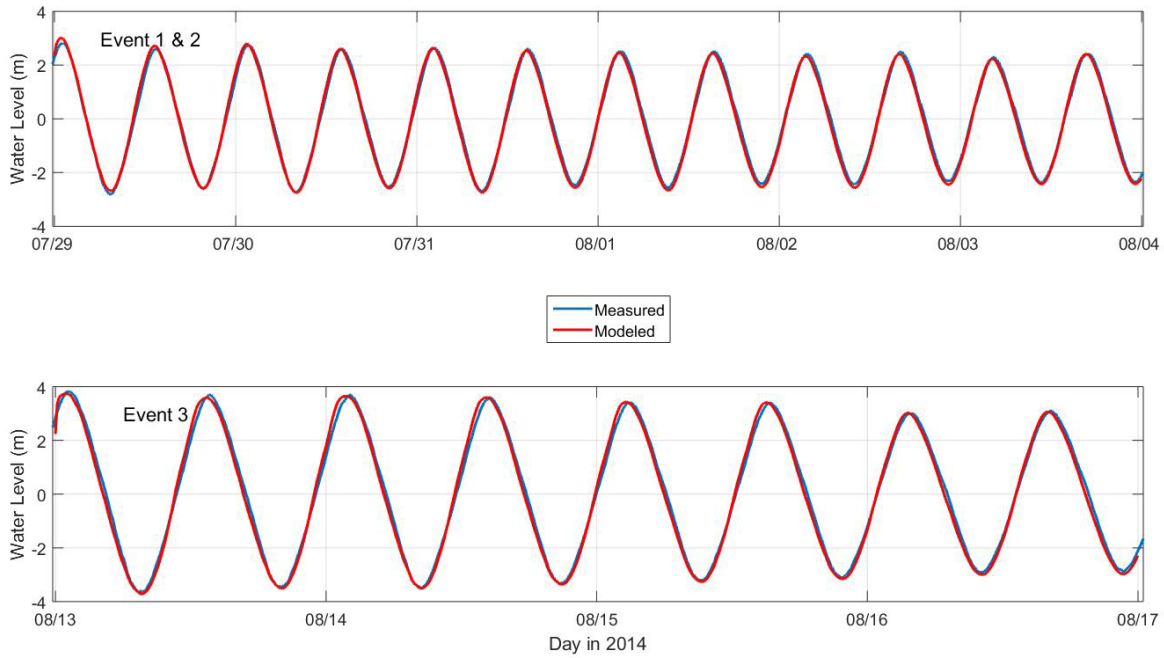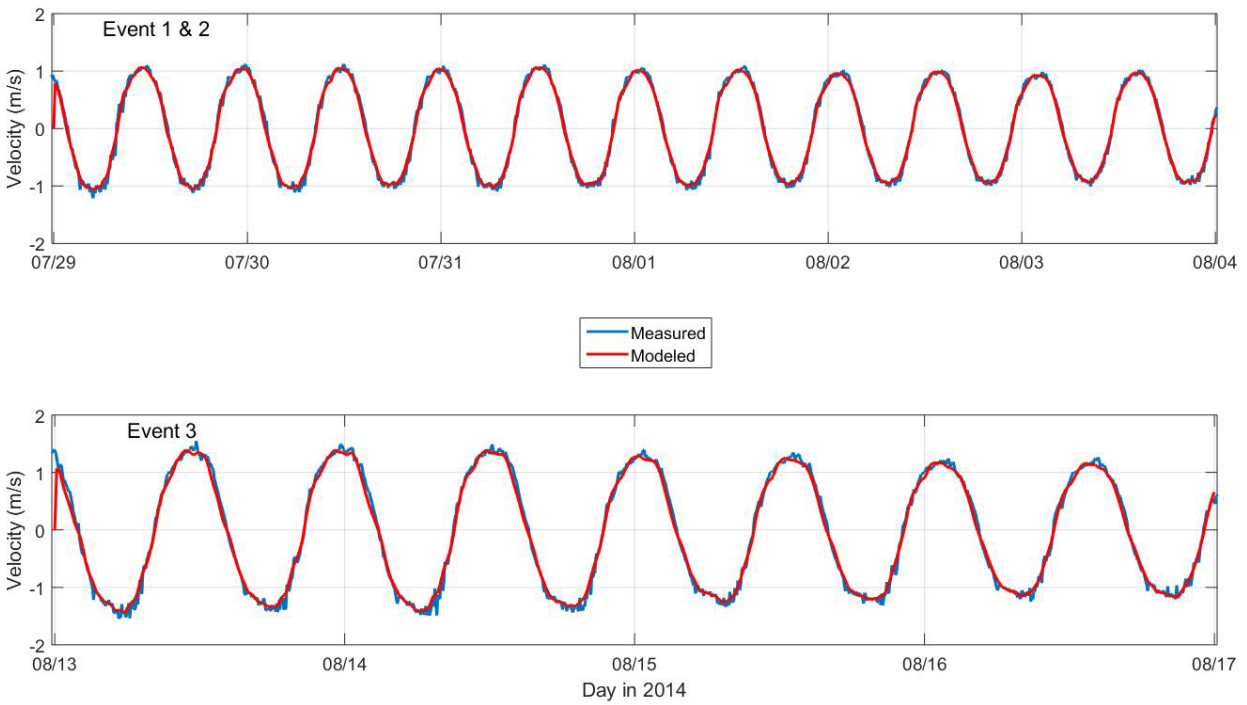
21

Both the FVCOM and SNL-EFDC simulations suggested that the project site has very high natural turbulence as is typical of a strong tidal system. Even with the overestimated drag coefficient in the period before August 10 (due to the fact that the turbine was freespinning, not generating), the model output simulations indicate the flow field disturbance associated with the OCGen was not clearly discernable from background flow. Earlier hydrodynamic modeling of the TidGen in Western Passage showed only a 10% drop in water velocity (S. Rao, personal communication). The TidGen turbine is 3–4 m high and 25 m long, which is larger than the OCGen. Therefore, the velocity reduction due to the OCGen is likely to be smaller—10–15 cm/s at most—and difficult to identify against the high natural background turbulence. Thus the small reduction in velocity associated with the larger TidGen in Western Passage is consistent with our assessment that the hydrodynamic impact of the OCGen was minimal.

3.3 ELAM Analysis

Overall, the number of simulated fish detections decreased with decreasing distance to the OCGen, although the decline was not continuous (Figure 14). Between 175 m and 150 m, the number of fish detections increased briefly, but then generally declined again until 40 m from the OCGen, at which point the number of fish increased. Although the general trend in simulated fish detections matched the trends in the hydroacoustic fish data (i.e. a decline in fish density nearer the turbine; Figure 14), there were differences at different segments of the survey transect. The sharpest decline in simulated fish detections was between 200 and 300 m. However, no field data was collected at these distances so a comparison is not possible. Between approximately 200m and 150 m, simulated fish detection either increased or remained constant, while the number of observed fish tracks was relatively constant (Figure 14, Segment 4). The number of fish appeared to decrease between 150 and 90 m for both simulated and observed datasets (Figure 14, segment 3). However, between 20 and 60m, the simulated and observed data diverged with the former showing an increase in fish and the latter showing a decrease (Figure 14, Segment 1). These patterns were similar in simulations using fish speeds of 0.1 m/s and 0.25 m/s, and among the four rectangle widths. While the patterns were similar, the simulated fish density fluctuations along the transects increased with rectangle width and were more pronounced at 0.25 m/s and (Figure 14 a and b).

a)

23
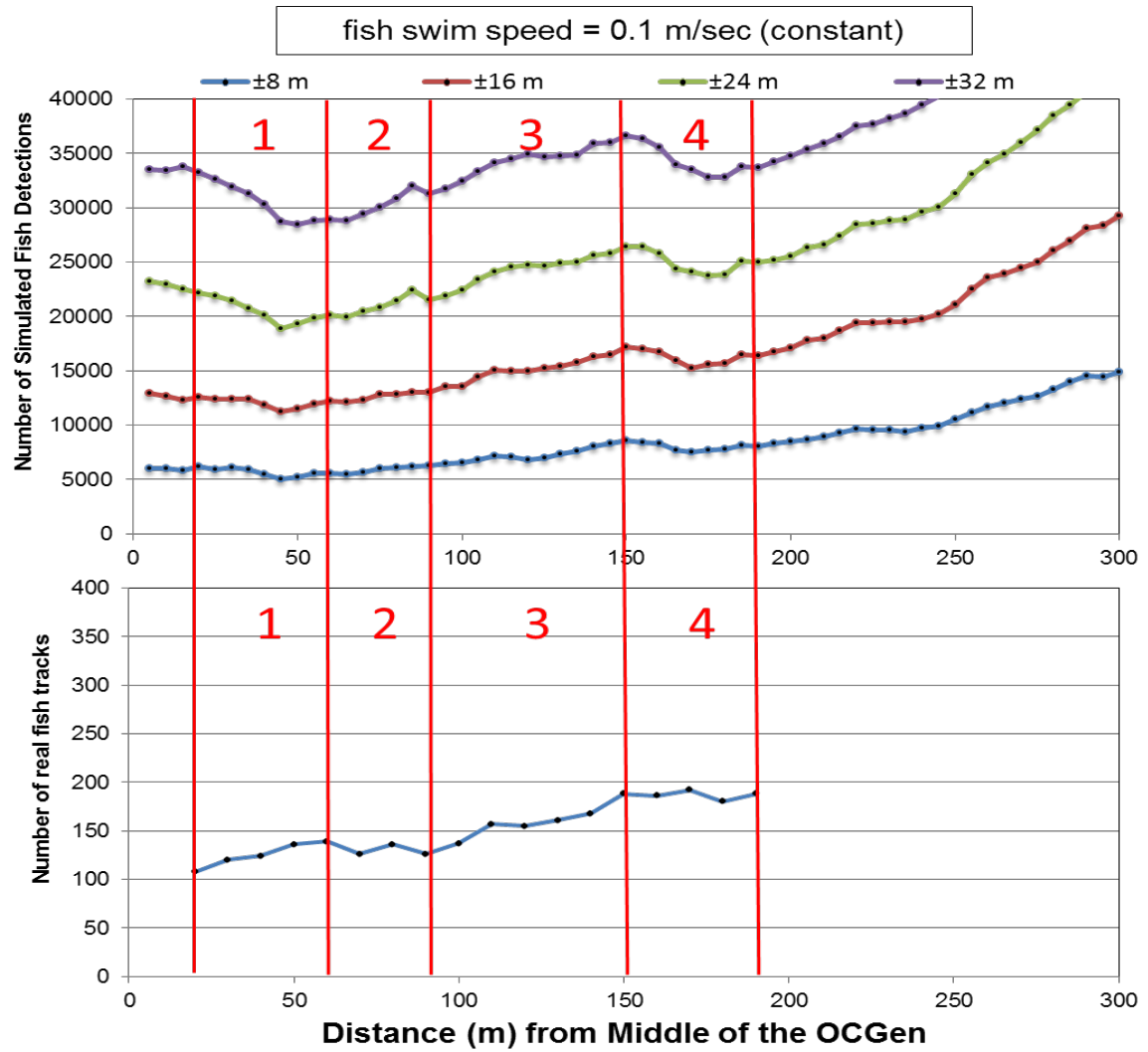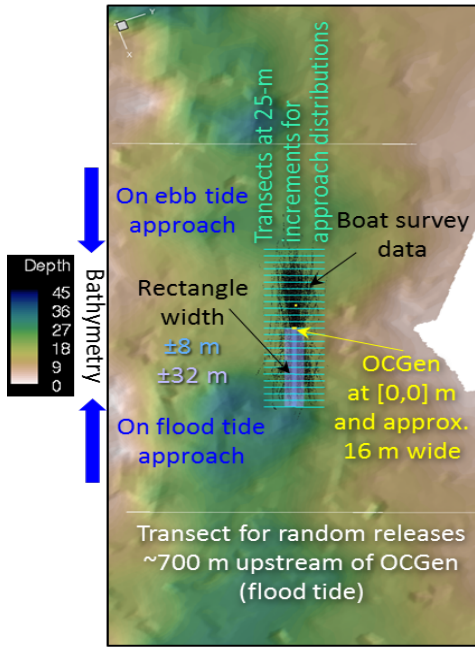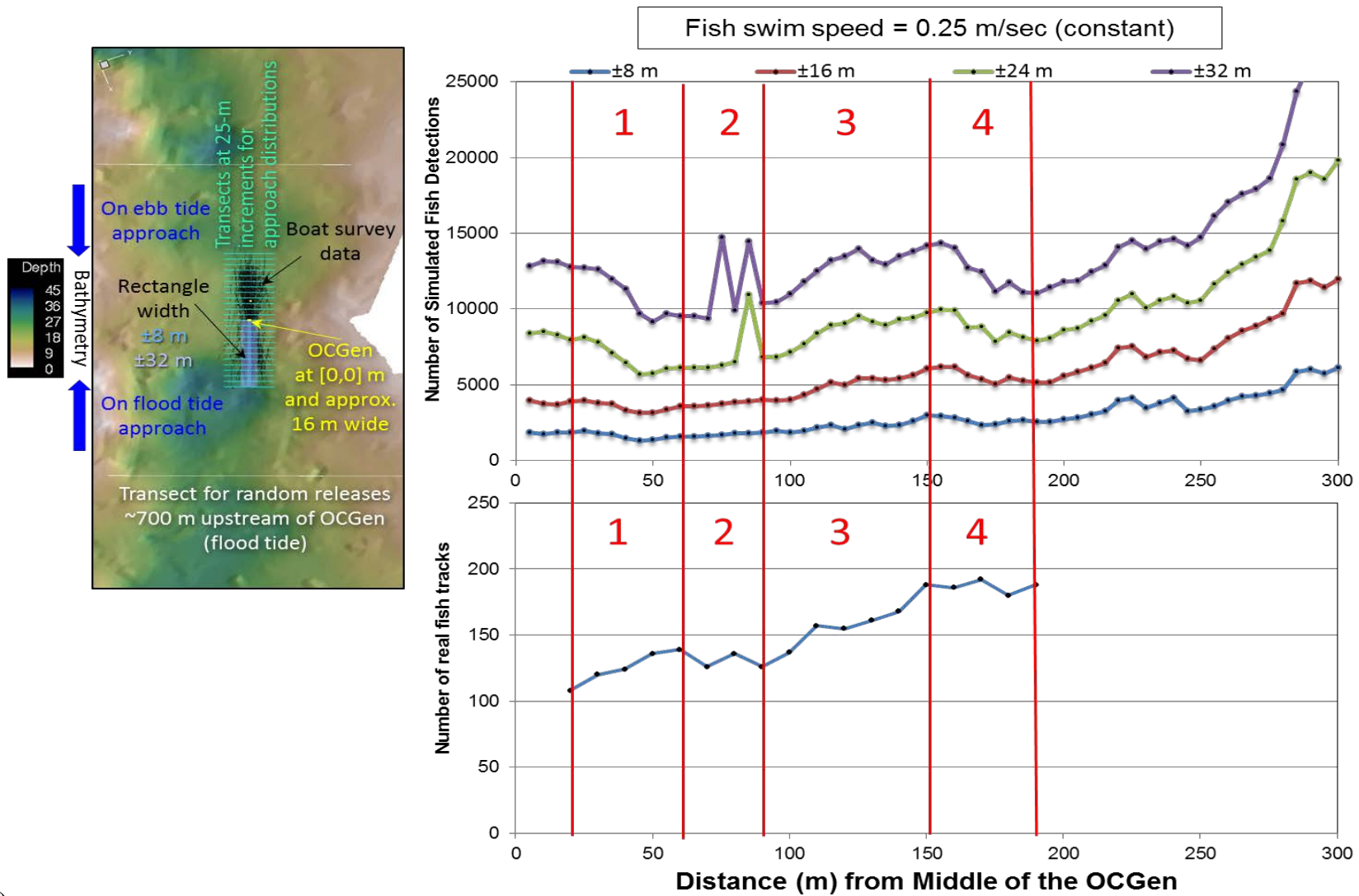
b)

Figure 14. Comparison of trends between the numbers of ELAM simulated fish and the number of hydroacoustic fish tracks with distance from the OCGen. Simulations using a fish swim speed of 0.1 m/s are shown in Figure 14a and 0.25 m/s are shown in Figure 14b.

4 DISCUSSION

The key finding of the hydroacoustic surveys was that there was a significant decline in fish density with decreasing distance to the OCGen. The decline appeared to be the result of horizontal, not vertical, movements to avoid the turbine. Because of the uneven bathymetry, fish track counts excluded the bottom third of the water column between 200 and 50 m from the OCGen in order to equalize the amount of water column surveyed across the transect (Figure 3). This meant that bottom fish were not counted except in the final 50 m of the transect nearest the turbine. If bottom fish were relatively abundant compared to fish higher in the water column, this could have led to an underestimate of fish densities between 200 and 50 m. However, if this were true there would have been an increase in fish densities from 50 m to the turbine, when bottom fish were included in the fish track counts. In fact, however, the decrease in fish density continued all the way to the turbine, suggesting that excluding bottom fish did not significantly affect the results.

In contrast to surveys conducted while the turbine was freespinning, there was a weak or non-existent relationship between the number of fish tracks and the distance from the OCGen for transects surveys conducted during the static turbine condition. These results support the hypothesis that stimuli produced by the spinning turbine (e.g. noise, visual cues) could potentially explain the decrease in fish density along the survey transect when the turbine was spinning. We investigated three potential OCGen related explanations for the observed avoidance behavior: (1) noise generated by the turbine, (2) visual stimuli generated by the turbine, and (3) turbine-generated flow patterns in the channel. As an alternative explanation, natural flow patterns within the channel were also investigated using ELAM simulations. Each explanation is reviewed below.

4.1 Explanations for Avoidance Behavior

4.1.1 Noise

Noise is one possible turbine-generated stimuli. Fish density began to decline approximately 140 m from the OCGen when it was free-spinning. Therefore, if noise is the source of the avoidance behavior, the noise from the OCGen would have to be of sufficient levels to elicit avoidance at a distance of 140 m. The ability of fish to detect turbine noise is related to the hearing sensitivity of the fish, the sound produced by the MHK technology, and the ambient noise generated by existing natural processes or human activity within the area. No noise studies are available for the OCGen that could be used to determine noise levels at incremental distances from the turbine. However, ORPC has previously measured noise generated by a small, test turbine and the commercial scale TidGen system (ORPC 2011; ORPC 2014). For the test turbine, there was an increase of up to 35 dB re 1 μPa^2/Hz above the ambient background noise level 68 m from the turbine, although the turbine-generated noise level was typically only around 10 dB re 1 μPa^2/Hz above background (Table 2). Sound pressure levels from the turbine were below 100 dB re 1 μPa^2/Hz, even at the maximum rotational speed (ORPC 2011). Considering these results were for the smaller test unit, the noise levels and distance the sound travelled are likely greater for the commercial-scale OCGen.

Table 2. Comparison of ambient noise and noise measured at 68 m from the ORPC test unit under varying environmental conditions (Source: ORPC 2011).

| | dB re μPa^2/Hz | | | | | | TGU |
| | Ambient | | | | | | |
Current (Knots)	1.1	1.5	2.2	2.9	3.0	3.3	2.9
80	65.3	54.8	58.3	64.6	66.7	76.9	65.3
100	67.7	59.5	64.7	69.7	72	81.5	67.7
125	76.7	64.7	69.2	77.4	75.4	82.9	76.7
160	86	70.4	81.2	80.6	78.3	85.2	86
200	89.6	70	76.8	80.4	80.7	87.8	89.6
250	94.3	72.2	81.5	80.9	85.7	87.1	94.3
315	94.3	70.8	85.4	90.1	85.9	96.2	94.3
400	98.7	70.1	85.6	91	87.2	91.8	98.7
500	101.8	71.4	83.2	90.9	91.5	91.6	101.8
630	95.4	72.7	84.8	98.6	88.5	97.8	95.4
800	95.9	77.1	83.8	89.1	88.7	95.3	95.9
1000	98.9	76.1	85	91.3	80.6	96.5	98.9
1250	104.9	76.8	87.6	89.2	81.6	92.4	104.9

(Third Octave Band (Hz))

In April 2013, noise measurements of the TidGen (ORPC 2014) were conducted during ambient, freewheeling, and turbine generating periods. The noise signals recorded were different for the spinning and non-spinning states. Increased sound levels were detected at certain frequencies (i.e. 105 and 210 Hz) anytime the turbine was rotating, but the peaks were higher when the turbine was freespinning (Fig. 15) suggesting greater noise was generated when the turbine was not generating power. However, at certain distances there were low frequency sound peaks while the turbine was generating that were not present when free spinning (Figure 15). Low frequency sound peaks were also detected in the non-spinning state, but these were attributed to boat noise (ORPC, 2014). Overall, the in-water sound peaks associated with the TidGen was less than 120 dB re 1 μPa^2/Hz at all measured frequencies (Fig. 15). This was true when the turbine generated power and when freespinning (ORPC 2014). Measurements taken at 154 m from the TidGen indicate that at frequencies around 100 Hz, the turbine generated the highest noise levels, or slightly over 100 dB re 1 μPa^2/Hz (Fig. 15). Although these noise levels would not be injurious to fish, multi-species studies suggest that fish would be able to detect sounds within this frequency and noise level (Popper and Hastings 2009), and 154 m is similar to the 140 m at which the avoidance behavior was observed in this study. However, the TidGen turbine is much larger than the OCGen, so the noise levels may be higher than those generated in our study by the OCGen. Also, the detection of turbine noise by fish does not mean the noise level would induce the observed turbine avoidance behaviors.
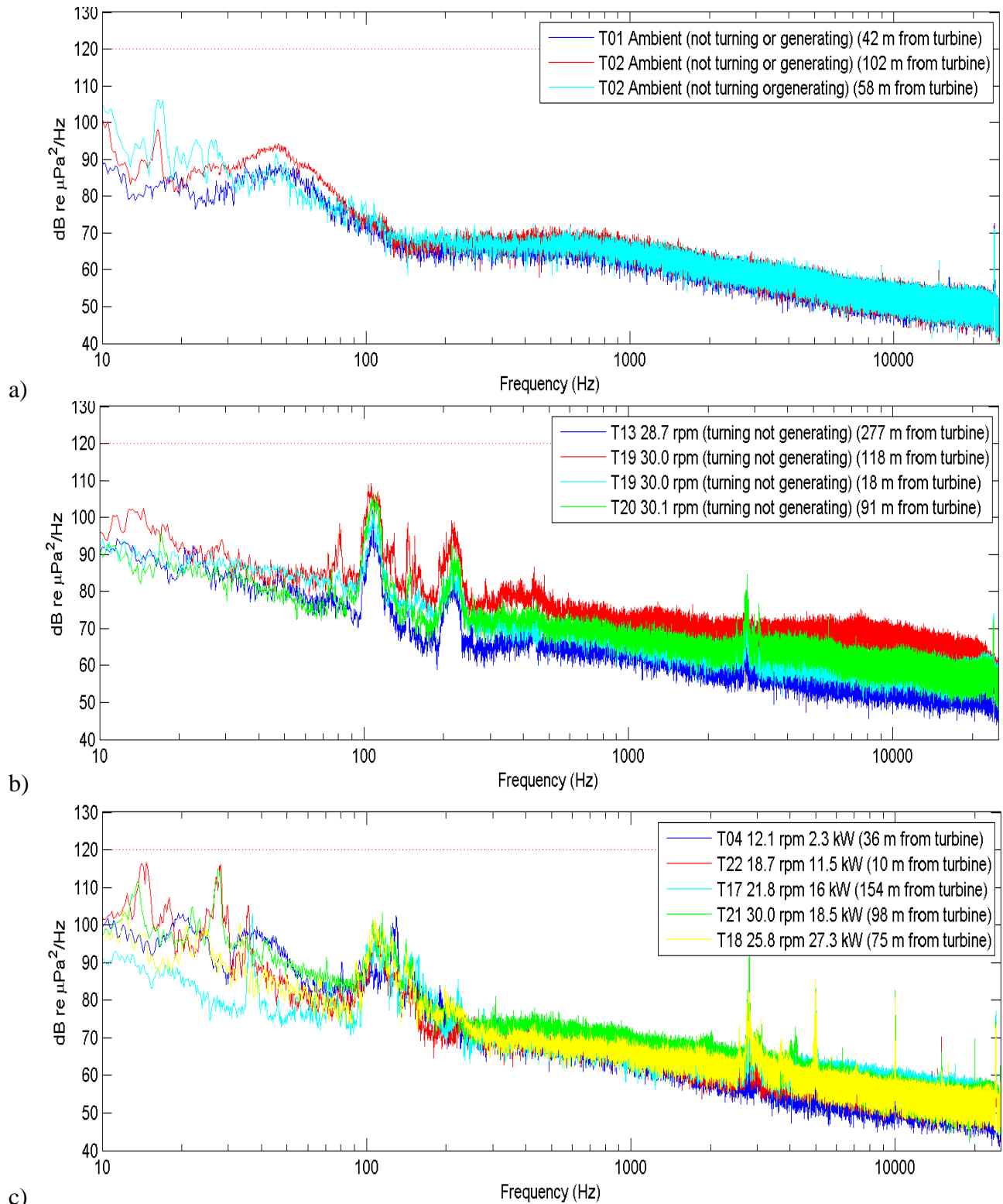
FIGURE 15 Power spectral density for the TidGen turbine during (a) ambient (not rotating), (b) free spinning, and (c) generating conditions at various frequencies and distances from the turbine on April 2-3, 2013 (Source: ORPC 2014).

Species-specific sensitivity to noise is another important consideration. Pelagic and benthic trawl samples collected during the OCGen hydroacoustic surveys indicated that Atlantic mackerel (*Scomber scombrus*) and Atlantic herring (*Clupea harengus*) were the pelagic species most likely to be interacting with the OCGen (Shen et al. 2016). Clupeids, such as the Atlantic herring, are known to be sensitive to noise (Popper and Hastings 2009), while mackerel are likely less sensitive to noise because they lack a swim bladder (Hawkins and Popper 2014). Given the economic importance of these species, more testing is needed to determine the relative sensitivity of mackerel to noise (Normandeau Associates 2012; Hawkins 2014).

By necessity, MHK devices are placed in areas like Cobscook Bay that have high flow and turbulence. This placement may reduce the ability of fish to detect noise from the turbine, because ambient noise increases with tidal flow (Willis et al. 2013). Therefore, it is difficult to evaluate with confidence the potential effects of noise generated by MHK devices on specific fish species. Other studies of MHK technology suggest that noise from vessel traffic, seismic surveys, and other existing anthropogenic noise will be more significant than noise generated by MHK devices, although the studies also suggest that turbines can increase noise levels above background levels within some distance to the devices (Verdant Power 2010; ORPC 2011; Polagye et al. 2012). For example, Verdant Power made underwater noise measurements surrounding the four operating turbines in the East River and found that turbine-generated noise was 145 dB re 1μPa at 1 m from the turbines, which would be audible to most fish species. The noise level appeared to return to background levels (~125 dB re 1μPa) less than 200 m from the turbine, meaning this turbine-generated increase in noise above background appeared to be small (Verdant Power 2010).

4.1.2 Visual Cues

Another explanation for the avoidance behavior observed near the OCGen in Cobscook Bay is that fish were able to see the turbine as they approached, and therefore changed their direction. Near-field (<5 m from the turbine) DIDSON studies of fish interaction with an ORPC TidGen found that fish that passed through the turbine generally did so at night rather than during the day (Viehman et al. 2014). These results indicate that fish behavior changed because

they could see the turbine. Other field studies also suggested that near-field turbine visibility reduced fish interactions with turbines (Hammar et al. 2013).

However, while sight may have played a role in near-field studies, it is unlikely fish would be able to see the turbine from a distance of 140 m where avoidance behavior was observed. To confirm, we investigated whether there were differences in avoidance behavior between transects conducted at night versus the day, with diurnal differences indicating a visual response to the turbine. We found the decline in the number of fish tracks with decreasing distance to the turbine was significant for both day and night surveys, and, most importantly, the decline in fish tracks began at approximately 140 m from the turbine during both day and night. These results suggest that visual stimuli were not the source of the avoidance behavior at the distances examined.

4.1.3 Turbine-Related Hydrodynamic Changes

The SNL-EFDC and the FVCOM hydrodynamic simulations do not suggest that the turbines created a significant flow disturbance above background flow conditions and that the hydrodynamic disturbance would not have extended 140 m upstream of the turbine during the incoming tide. Therefore, turbine related hydrodynamic stimuli were not likely to be responsible for the observed avoidance behavior. The study area is a high-velocity system with naturally turbulent flows which may have overwhelmed the more localized disturbance to the flow field generated by the OCGen. Turbines are purposely placed in areas of high flow in order to optimize power generation. Therefore, our results may not be atypical of tidal MHK projects. If so, behavioral impacts in fish resulting from hydrodynamic alterations may be minor and localized for single MHK device deployments. However, economically viable MHK deployments will ultimately require the deployment of additional devices in an array, which would likely increase the magnitude of hydrodynamic change. If plans by ORPC to deploy a turbine array are implemented, further study would be needed to assess the nature of the hydrodynamic changes and any subsequent behavioral alterations. As described in Section 5, following additional data collection around the array, the ELAM can be used for this purpose.

4.1.4 Natural Hydrodynamic Stimuli

Channel bathymetry and morphology create flow field conditions, particularly water velocity and acceleration fields, that significantly influence fish movement decisions (Goodwin et al. 2014). The natural flow patterns visible in the Cobscook Bay flow simulations, specifically high-velocity flow in the southern portion of the channel, could have caused fish to move away from the northern bank where the OCGen is located. The high-velocity corridor was likely generated by a bathymetric change which began approximately 150 m from the OCGen (Fig. 3). Consequently, the observed avoidance response may have been related to natural flow conditions rather than the OCGen.

To test the significance of natural flow patterns on behavior, we ran ELAM simulations of fish particles that behave passively and fish particles that follow natural flow velocity changes, to see if they match the patterns found in the hydroacoustic fish track data. From approximately 50 to 200 m from the turbine, the ELAM simulations reproduced the general spatial trends in fish density observed in the hydroacoustic fish surveys. Both data sets showed a general decrease in fish density with decreasing distance to the turbine. However, from 0 to 50m from the turbine, the ELAM simulated an increase in fish densities, which was the opposite of the continued decrease in fish densities found in the hydroacoustic surveys. This suggests that additional hydrodynamic behavioral response parameters may be needed in the ELAM model to more accurately reproduce the avoidance behavior. Alternatively, it suggests that turbine related stimuli, such as noise, began to influence fish behavior closer to the turbine.

Overall, the ELAM analysis provides some support for the alternative hypothesis that fish are following the natural water flow away from the device at distances between 50-200 m from the OCGen, rather than responding to stimuli generated by the OCGen. These results correspond to the behavioral rules identified by a prior ELAM analyses of how fish navigate water currents by following accelerating water (Goodwin et al. 2014). However, while the ELAM simulations can partially reproduce the patterns in the hydroacoustic detections, the fact that the avoidance behavior was not found at control transects or when the turbine was not spinning, suggests that it was the rotating turbine that was responsible for the avoidance behavior.

4.2 Ecological Implications of Findings

As demonstrated by this study, MHK devices have the potential to alter the behavior of individual fish that move within the vicinity of the device while it is in operation. Of further interest is whether these behavioral changes could result in ecologically meaningful impacts such as the disruption of spawning and migratory runs or the avoidance by fish of their normal habitats due to the presence of the turbine. For species that do interact with an MHK device, blade strike is among the factors of concern to regulators. As described below, the results of this study suggest that the risk of significant ecological impacts is low for a single MHK device.

4.2.1 Displacement from Preferred Habitats

Fish were found to actively avoid the OCGen, which could result in displacement or avoidance of preferred habitat. To assess the potential of this impact in Cobscook Bay, one must know the relative spatial distribution of fish populations within Cobscook Bay and the vertical distribution of fish in the water column. Down-looking hydroacoustic surveys conducted during 2010–2013 in the area of the proposed TidGen deployment indicated fish density was generally highest near the sea floor and the probability of fish being present in the same location as the TidGen was between 0.5 and 0.8 for all seasons and tidal conditions (Viehman et al. 2014; Shen et al. 2016). However, these data refer to the vertical distribution of fish that are actually present at the site and not the relative abundance of fish at the TidGen site compared to other locations in Cobscook Bay. For example, if most fish prefer inshore habitat, only a small percentage of the total population may be present at the location of the TidGen, which was located more centrally in the channel.

No studies of the habitat-wide distribution of fish within Cobscook Bay were available specific to ORPC turbine deployments. However, there are studies of fish interactions with tidal MHK devices in other systems from which to glean information on the distribution of fish within high-flow channels. For example, fixed hydroacoustic studies of Verdant Power axial turbines in New York's East River indicated that, even when the turbines were not operating, there were fewer fish in the mid-channel habitat where the turbines were located compared to the slower velocity zones inshore, Although these findings may be an artifact of the weaknesses of fixed

hydroacoustic devices to detect fish in high velocity conditions, they do suggest that fish are less abundant in open channels during periods of high flow. In a European Marine Energy Centre study conducted in Scotland, video recordings around an OpenHydro turbine (Broadhurst et al. 2014) showed that pollack (*Pollachius pollachius*) generally were not present around the turbine, although aggregations of fish were occasionally observed (Broadhurst et al. 2014). Tidal stage and water velocity appeared to be the primary determinant of fish presence or absence around the turbine with greater a number of fish present during slack tide.

In summary, while tidal turbine studies in Cobscook Bay and other locations indicate that turbines do elicit species-specific behavioral changes in fish, the installation of turbines in the strong current zones (consistent with energy production needs), may minimize the potential for displacing fish from areas where they are most abundant.

4.2.2 Disruption of Fish Movement

The primary goal of this study was to assess the magnitude of change in fish movement patterns upstream, over, and downstream of the OCGen. The empirical data derived from the hydroacoustic surveys suggest the fish move horizontally away from the path of the OCGen (Shen et al. 2016). Unfortunately, the presence of the TidGen bottom mount confounded the interpretation of movement patterns downstream of the OCGen. However, the lack of flow field disturbance evident in the FVCOM flow simulations suggests that it is highly unlikely that a single turbine deployment in Cobscook Bay would pose a significant fitness cost to individual fish or disrupt ecologically significant life-history activities such as migration and spawning.

Our findings are similar to those in other systems. Hammar et al. (2013) used underwater video to record fish movement through a narrow tidal channel. They found that passage through the channel was significantly lower for 6 of the 16 genera recorded when the turbine was present, compared to when it was absent from the channel. The passage rate was negatively related to water velocity, but only when the turbine was present, indicating that the decrease in passage was due to the higher rotational speeds of the turbine, not the water velocity itself (Hammar et al.

2013). However, fish that passed through the channel avoided the turbine by only 0.3 to 1.7 m, indicating minimal disruption of movement and energetic cost to the fish.

Most MHK project development plans include the deployment of an array of turbines, which increases the potential for hydrodynamic disturbance and subsequent behavioral changes over a large portion of the deployment site (Hammar et al. 2013). These impacts can be mitigated to some degree by turbine placement in areas where fish are less likely to be present. As described in Section 5, following additional data collection around the array, the ELAM can be used identify array configuration that minimize impacts to fish.

4.2.3 Blade Strike

As summarized in Table 3, existing blade strike studies do not suggest a significant risk for fish from direct blades strike. Near-field studies of fish interactions with the TidGen using a DIDSON acoustic camera indicated that few fish entered the device while it was static, and the number of fish entering the turbine decreased by 35% when the turbine was rotating (Viehman and Zydlewski 2014). For fish that do approach the device, recent studies in laboratory and natural settings suggest a low potential for injury and mortality from blade strike, except in the case of very young, larval stages of fish (Table 3). For example, in studies in a narrow tidal channel, Hammar et al. (2013) recorded only two individuals entering the turbine rotor and no individuals were observed being hit by the blade. They also found that fish passage through a tidal channel was negatively related to the rotational velocity of the turbine, which would likely reduce the probability a turbine blade actually striking a fish.

For mid-field and far-field interactions, whether the MHK device is located in the habitat preferred by the species is a significant factor in the probability of a fish-turbine encounter. Most studies suggest that a significant number of interactions is unlikely because the locations or time periods in which the turbines typical operate are generally not suitable for aquatic organisms (Section 4.2.1). As reported in Viehman et al. (2014) and Shen et al. (2016), the probability of fish being present in the same location as the proposed TidGen deployment was generally between 0.5 and 0.8 in all seasons and tidal conditions. However, the probability of the fish being at the same depth as the turbine blades was much lower, ranging from 0.079 to 0.093 (Shen et al. 2016).

TABLE 3 Summary Fish and Blade Strike Studies

Reference	Variables Measured	Results
Amaral et al. 2015	Entrainment avoidance, injury, and survival of hybrid striped bass, rainbow trout, white sturgeon	• Entrainment varied by species. • Survival rate of entrained fish exceeded 95%. • Overall survival probability was 0.95 for striped bass and >0.99 for rainbow trout and white sturgeon.
Castro-Santos and Haro 2015	Mechanical injury, avoidance behaviors, and migratory delay in Atlantic salmon smolts and adult American shad interacting with a vertical-axis turbine	• Salmon smolts did not show avoidance behavior toward the turbine and no injuries were recorded from passing through the turbine. • Survival was 98.3% for treatment smolts and 96.4% for controls. • Shad appeared to actively avoid the turbine and no injuries were observed. • Adult shad mortality was not statistically different between control and treatment groups.
Hammar et al. 2013	Field study of multi-species fish movement patterns through a narrow strait with and without a turbine	• Only one species on two occasions was detected passing through the turbine. • Reduced passage when turbine was operating, especially at higher speeds.
Jacobson et al. 2011	Injury, survival rates, and behavior of two size classes of rainbow trout and largemouth bass	• Survival was greater than 98%. • Fish that were struck were typically hit in the caudal fin, and fish were not stunned or severely injured. • Both species seem to avoid the turbine.
Normandeau Associates, Inc. 2009	Injury and mortality of five species ejected through a Hydro Green turbine	• Survival was 98% or greater for all fish, which was similar to controls. • No fish that passed through the turbine had evidence of injury or descaling, and no post-passage predation was observed.
Schweizer et al. 2012	The risk of blade strikes on four species of larval and juvenile freshwater fish	• Mean survival of one to 14 days post-hatch striped bass for fish that had passed through the blade were typically not significantly lower than control fish. • The post-blade passage survival appeared to increase with age, as older fish were able to avoid the blade. • Significant differences between blade-exposed and control groups were not observed for walleye/sauger, fathead minnows, or crappie, all of which were more than 20 days post-hatch.

TABLE 3 (Cont.)

Reference	Variables Measured	Results
Verdant Power 2010	DIDSON imagery of fish interactions with Verdant turbines	• No blade strikes of fish were observed during turbine operation.

This study significantly expands the range of earlier near-field blade strike and DIDSON studies by observing fish behavioral changes as they approached the device over hundreds of meters. The results of this study indicate that fish in Cobscook Bay begin to avoid the OCGen at 140 m from the device, further reducing the probability fish will physically interact with the device. Overall, the probability of fish encountering the turbine blade appears to be low, due to behavioral preferences related to natural water flow and active avoidance of the turbine. This finding combined with near-field blade-strike studies indicating low risk for juvenile and adult fish suggests that a single OCGen poses a minimal risk to pelagic fish.

5 FUTURE STUDIES

While existing data suggest small, localized ecological risk to fish from a single MHK device, the risk may increase with additional devices. This will become more relevant as commercial-scale MHK arrays come under consideration by regulators. Therefore, the ecological risks associated with commercial scale operations will ultimately have to be evaluated to fully understand the ecological impacts of MHK devices.

In the future, the ELAM could be used to generally forecast fish behavior under alternative array configurations at commercial scales to evaluate alternatives that may minimize impacts to fish movement. Because fish response to an array could be different from their response to a single turbine, extending the ELAM to an ORPC commercial array and different array designs would require 1) the deployment of additional TGUs in Cobscook Bay, to study the unique hydrodynamic patterns generated by the hydraulic interactions between the turbines, 2) collecting fish monitoring data around the TGU array, and ,3) benchmarking the ELAM generated simulations against available monitoring data and refining the encoded behavior hypothesis as needed. Beyond assessing and improving the encoded behavior hypothesis, the ELAM requires no other refinement to be applied to a commercial array. Thus, the ELAM could help commercial developers to identify configurations that minimize impacts to the extent practicable, as required by the National Environmental Policy Act.

6 CONCLUSIONS

The key finding of the hydroacoustic surveys was that there was a significant decline in fish density beginning approximately 140 m from the free-spinning OCGen. Similar avoidance behavior was not observed at control transects or when the turbine was not spinning. Visual cues and turbine-related hydrodynamic stimuli did not appear to be detectable to fish at 140 m. Of the other potential explanations we investigated, noise and natural flow patterns appeared to be the most plausible explanations for the observed patterns in fish behavior. However, several uncertainties remain. First, we don't have sufficient data to evaluate with confidence the distance at which noise generated by MHK devices are detected by specific fish species, nor what behavioral changes they would elicit at different noise levels. Second, while the ELAM results provide some support for the alternative hypothesis that natural hydrodynamics were responsible for the observed patterns of fish behavior, the ELAM model parameters cannot account for the decrease in fish density closer to the turbine. Therefore, it is possible that turbine related stimuli, such as noise, influenced fish behavior closer to the turbine.

Overall, this study provides additional confirmation for the idea that a single turbine is unlikely to result in more than negligible impacts to fish communities. Assuming that the observed fish avoidance behavior was related to the OCGen, the installation of turbines in the strong current zones that fish may tend to avoid, may minimize the potential for displacing fish from areas where they were most abundant. I addition, if the turbine elicited the avoidance behavior, it would minimize the already low probability of blade strike revealed in near-field laboratory studies. Alternatively, if the avoidance behavior was the result of the fish following natural flow patterns in the channel, it would confirm that turbine related disturbances are only one of a number of stimuli in the fish's environment and that they are relatively insignificant compared to the overwhelming influence of the natural channel bathymetry and hydrodynamics.

7 REFERENCES

Amaral, S., M. Bevelhimer, G. Cada, D. Giza, P. Jacobson, B. McMahon, B. Pracheil, 2015, "Evaluation of Behavior and Survival of Fish Exposed to an Axial-Flow Hydrokinetic Turbine," *North American Journal of Fisheries Management* 35:97–113.

Boehlert, G.W., and A.B. Gill. 2010. "Environmental and Ecological Effects of Ocean Renewable Energy Development: A Current Synthesis." Oceanography 23: 68–81.

Castro-Santos, T., and A. Haro, 2015, "Survival and Behavioral Effects of Exposure to a Hydrokinetic Turbine on Juvenile Atlantic Salmon and Adult American Shad," *Estuaries and Coasts* 38:203–214.

Frid, C., E. Andonegi, J. Depestele, A. Judd, D. Rihan, S.I. Rogers, and E. Kenchington, 2011, "The Environmental Interactions of Tidal and Wave Energy Generation Devices," *Environmental Impact Assessment Review* 32:133–139.

Goodwin, R.A., J.M. Nestler, J.J. Anderson, and L.J. Weber, 2007, "A New Tool to Forecast Fish Movement and Passage," *Hydro Review* 26:2–8.

Goodwin. R.A., M. Politano, J.W. Garvin, J.M. Nestler, D. Hay, J.J. Anderson, L.J. Weber, E. Dimperio, D.L. Smith, and M. Timko, 2014, "Fish Navigation of Large Dams Emerges from Their Modulation of Flow Field Experience," *Proceedings of the National Academy of Sciences* 111:5277–5282.

Hammar, L., S. Andersson, L. Eggertsen, J. Haglund, M. Gullström, J. Ehnberg, and S. Molander, 2013, "Hydrokinetic Turbine Effects on Fish Swimming Behaviour," *Plos One* 8:1–12.

Hammar L., L. Eggertsen, S. Andersson, J. Ehnberg, R. Arvidsson, M, Gullström, et al., 2015, "A Probabilistic Model for Hydrokinetic Turbine Collision Risks: Exploring Impacts on Fish," *PLoS ONE* 10(3): e0117756. doi:10.1371/journal.pone.0117756

Hawkins, A.D., 2014, "Responses of Free-Living Coastal Pelagic Fish to Impulsive Sounds." Paper presented at the 2nd International Conference on Environmental Interactions of Marine Renewable Energy Technologies, Isle of Lewis, Scotland, April 28–May 2.

Hawkins, A.D., and A.N. Popper, 2014, "Assessing the impacts of underwater sounds on fishes and other forms of marine life," *Acoustics Today* 10:30–41.

Jacobson, P.T., 2011, "Assessment of the Environmental Effects of Hydrokinetic Turbines on Fish: Desktop and Laboratory Flume Studies." Webinar presentation sponsored by the U.S. Department of Energy, Aug. 29.

Normandeau Associates, Inc., 2009, *An Estimation of Survival and Injury of Fish Passed through the Hydro Green Energy Hydrokinetic System, and a Characterization of Fish Entrainment Potential at the Mississippi River Lock and Dam No. 2 Hydroelectric Project (P-4306)*, Final Report, Hastings Minnesota, Hydro Green Energy, LLC.

Normandeau Associates, Inc., 2012, *Effects of Noise on Fish, Fisheries, and Invertebrates in the U.S. Atlantic and Arctic from Energy Industry Sound-Generating Activities*. Workshop report prepared for the U.S. Department of Interior Bureau of Ocean Energy Management, Dec.

ORPC (Ocean Renewable Power Company), 2011, *Underwater Noise Measurements of a Proposed Tidal Generator Site in Cobscook Bay Using a Drifting Noise Measurement Buoy, Including Ambient Noise and Estimates of Tidal Generator Noise*, Cook Inlet (Fire Island) Tidal Energy Project, P-12679-003, Progress Report No. 2.

ORPC, 2014, *Cobscook Bay Tidal Energy Project* (P-12711-005), 2013 Environmental Monitoring Report. Available at: https://tethys.pnnl.gov/publications/cobscook-bay-tidal-energy-project-2013-environmental-monitoring-report

Polagye, B., B. Van Cleve, A. Copping, and K. Kirkendall, ed., 2010, *Environmental Effects of Tidal Energy Development*. Proceedings of U.S. Department of Commerce National Oceanic and Atmospheric Association scientific workshop, March 22–25.

Polagye, B., J. Thomson, C. Bassett, J. Wood, D. Tollit, R. Cavagnaro, and A. Copping, 2012, *Study of the Acoustic Effects of Hydrokinetic Tidal Turbines in Admiralty Inlet, Puget Sound*, DE2012-1039434, U.S. Department of Energy Final Report.

Popper, A.N., and M.C. Hastings, 2009, "The Effects of Anthropogenic Sources of Sound on Fishes," *Journal of Fish Biology* 75:455–489.

Schweizer, P.E., G.F. Cada, and M.S. Bevelhimer, 2012, *Laboratory Experiments on the Effects of Blade Strike from Hydrokinetic Energy Technologies on Larval and Juvenile Freshwater Fishes,* Oak Ridge National Laboratory, ORNL/TM-2010/108.

Shen, H., G.B. Zydlewski, H.A. Viehman, and G. Staines, 2016, "Estimating the Probability of Fish Encountering a Marine Hydrokinetic Device." Renewable Energy 97:746–756.

U.S. Department of Energy, 2009, *Report to Congress on the Potential Environmental Effects of Marine and Hydrokinetic Energy Technologies*, Wind and Hydropower Technologies Program. Available at: http://energy.gov/sites/prod/files/2013/12/f5/doe_eisa_633b.pdf.

Verdant Power, 2010, *Roosevelt Island Tidal Energy Project: FERC No. 12611*. 4 vols. Available at: http://www.theriteproject.com/Documents.html.

Viehman, H.A., and G.B. Zydlewski, 2014, "Fish Interactions with a Commercial-Scale Tidal Energy Device in the Natural Environment," *Estuaries and Coasts* 38:S241–S252.

Viehman, H.A., G.B. Zydlewski, J.D. McCleave, and G.J. Staines, 2014, "Using Hydroacoustics to Understand Fish Presence and Vertical Distribution in a Tidally Dynamic Region Targeted for Energy Extraction," *Estuaries and Coasts* 38:S215–S226.

Willis, M.R., M. Broudic, C. Haywood, I. Masters, S. Thomas. 2013. Measuring underwater background noise in high tidal flow environments. Renewable Energy 49: 255–258.

Pacific Northwest
NATIONAL LABORATORY

Proudly Operated by **Battelle** *Since 1965*

Triton: Igiugig Video Analysis

FY16 Progress Report

September 2016

A Avila
R Hull
S Matzner
G Staines
C Trostle
G E L Harker-Klimeš

TRITON

DISCLAIMER

This report was prepared as an account of work sponsored by an agency of the United States Government. Neither the United States Government nor any agency thereof, nor Battelle Memorial Institute, nor any of their employees, makes **any warranty, express or implied, or assumes any legal liability or responsibility for the accuracy, completeness, or usefulness of any information, apparatus, product, or process disclosed, or represents that its use would not infringe privately owned rights**. Reference herein to any specific commercial product, process, or service by trade name, trademark, manufacturer, or otherwise does not necessarily constitute or imply its endorsement, recommendation, or favoring by the United States Government or any agency thereof, or Battelle Memorial Institute. The views and opinions of authors expressed herein do not necessarily state or reflect those of the United States Government or any agency thereof.

<div align="center">

PACIFIC NORTHWEST NATIONAL LABORATORY
operated by
BATTELLE
for the
UNITED STATES DEPARTMENT OF ENERGY
under Contract DE-AC05-76RL01830

Printed in the United States of America

Available to DOE and DOE contractors from the
Office of Scientific and Technical Information,
P.O. Box 62, Oak Ridge, TN 37831-0062;
ph: (865) 576-8401
fax: (865) 576-5728
email: reports@adonis.osti.gov

Available to the public from the National Technical Information Service
5301 Shawnee Rd., Alexandria, VA 22312
ph: (800) 553-NTIS (6847)
email: orders@ntis.gov <http://www.ntis.gov/about/form.aspx>
Online ordering: http://www.ntis.gov

</div>

Triton: Igiugig Video Analysis

FY16 Progress Report

A Avila
R Hull
S Matzner
G Staines
C Trostle
GEL Harker-Klimeš

September 2016

Summary

This document summarizes the processes developed for the manual and automatic analysis of the Igiugig fish video data. The manual analysis is described, giving key points where decisions were made for the analysis methods. The report then summarizes the approach to the automated algorithm development and how this is using the manual analysis to date.

Acronyms and Abbreviations

DOE	Department of Energy
DM	Dedicated Micros
LGL	LGL Alaska
ORPC	Ocean Renewable Power Company
PNNL	Pacific Northwest National Laboratory
RPCA	Robust Principle Components Analysis
ViBE	Video Background Extraction

Contents

Figures

Tables

1.0   Introduction

This document gives a brief summary of the Igiugig fish video data analysis progress made from February to September 2016. It follows the data quality analysis report[1] that was issued in February 2016, and therefore only summarizes activities since that point.

The manual (visual) analysis is described initially, with key aspects highlighted that determine how the analysis has been undertaken. A description of the approach to the automated algorithm is then given.

A chronology of main events is provided at the end.

2.0   Key Points in Manual Analysis

2.1   Data and Quality Check

In late January 2016, the Pacific Northwest National Laboratory (PNNL) received LGL Alaska's (LGL's) full fish event dataset, detailing the interactions with Ocean Renewable Power Company's (ORPC's) RivGen® Power System (hereafter referred to as RivGen®) during July 19-25 and August 19-28, 2015. This was initially used for the quality check[1], which considered whether the data were suitable for more detailed analysis. The event log, based on analyzing 10 minutes per hour, provides an ideal comparison for the manual analysis that is being undertaken. In addition, these events have been useful in determining appropriate 5 minute clips for a subset specifically aimed at algorithm development, as described in Section 3.1.

In February 2016, PNNL reviewed the quality of the data, as summarized in the "Igiugig Fish Video Study – Quality Check" report. This analysis confirmed that the data could be visually analyzed to determine numbers, size and behavior of fish, but species could not be determined.

2.2   Advisory Committee Meeting

In March 2016, representatives from ORPC, PNNL, University of Washington and University of Maine discussed the Igiugig fish video in an initial effort to define roles and delegate tasks, discuss the most appropriate approach for algorithm development and visual analysis, and determine 2016 fiscal year (FY16) objectives and long-term goals.

2.3   Manual Analysis of the Full Dataset

The outcomes from the advisory committee meeting were that all the data should be manually analyzed, prioritizing night time segments during July due to the large number of fish interactions that were documented by LGL. This full analysis can then be used for both the automated algorithm verification and for a comparison with the 10-minute analysis, to see how representative the subsampling is for future projects.

To document the observations, the University of Maine sent a copy of their Dual Frequency Identification Sonar (DIDSON) processing spreadsheet along with an extensive explanation of fish behavior that they observed and qualified. In addition, the University of Washington sent a copy of their image logging

---

[1] Trostle, 2016 *Igiugig Fish Video Study – Quality Check, Summary Report*

spreadsheet, which included an example of the numerical annotation metadata; using numbers instead of words to describe the parameters enables more efficient, statistical analysis of the information. These were combined with LGL's event spreadsheet, and PNNL's previous quality check documentation to produce a final format for the observations.

In late March 2016, review efforts began by looking at footage between the hours of 23:00:00 and 06:00:00 (night time), starting from July 19th, 2015.

2.3.1   Camera prioritization

Due to the large amount of data, the decision was made to prioritize video from camera 2 that looked directly at the upstream side of the turbine, as this could reveal potential strike or near misses, and was likely to capture more diverse fish behavior. The "Igiugig Fish Video Study – Quality Check" had identified that most of the behavior-based interactions were seen in camera 2.

2.3.2   Added behavior and size classes

Through reviewing the data it was apparent that additional descriptors for behavior were required to those in previous analyses:

- Cannot determine/single frame - if the fish was only in one frame, the viewer could not determine the direction, behavior or note any negative impact. While it was later decided to remove these single frame instances from the full dataset analysis, it was important to note them for the fish algorithm development and comparison.
- Avoid around - when a fish is observed going around the turbine, either towards the camera or away from the camera.
- Into static structures - when an object is seen moving toward the static structure of the RivGen® device, rather than the dynamic turbine blades.
- Anterior first (face first) - when a fish is seen swimming with its anterior pointed towards the viewer's right. Usually, fish are seen facing upstream as they have more control over their motion, but sometimes they are seen swimming anterior first.
- Unidentifiable size - when an object is only partially in the frame, it is not possible for the viewer to determine the size of the object.

2.3.3   Added video quality parameter

Video quality was added as a parameter because of the large variability among the visual value of the video. Depending on the environmental contrast, whether the lights are on/off, debris, time of day, and potential buildup of algae on the camera lenses, the video quality ranges from zero (worst) to five (best). This quality parameter refers to how easily a fish can be distinguished from the background.

2.3.4   Additional personnel

Initially, the manual analysis was undertaken by a single PNNL staff member to ensure consistency of analysis. However, the large amount of data meant this was not sustainable, and in August a second PNNL staff member, with extensive experience in acoustic instrumentation and fish analysis around other ORPC deployments, was brought on to the team. These two individuals worked closely together on subsamples of data to ensure consistency in the annotation results before continuing the broader analysis.

2.4   Troubleshooting

2.4.1   Dedicated Micros NetVu Observer

Initially, the proprietary software associated with the video system (Dedicated Micros (DM) NetVu Observer) was used for the manual analysis. This software regularly froze during playback, and was found to skip frames when in fast-forward mode.

Multiple instances of skipping frames were observed which led to the omission of various events. This was illustrated by comparing PNNL analysis at 1x speed to LGL identified events for a short time span and observing no common events. From July 19th to 21st PNNL reviewed only night footage (defined as 23:00 to 06:00), identifying 358 fish events, while LGL only documented 1 fish event during this period, which occurred outside of PNNL review timings (at 13:06:06 on July 19th). While a large number of these fish events were single frame occurrences (which LGL did not record), some of them were more extensive, lasting up to 18 seconds or multiple fish. A test replay of fish events confirmed that in fast-forward playback mode DM NetVu Observer skipped frames.

Due to the skipping incidents, it was decided that NetVu Observer was unreliable, and new software should be used. The original data were in .PAR file format, which is mainly used for surveillance, and despite contacting various companies, more reliable software that could directly read these files was not found.

To remedy this, PNNL personnel wrote software to convert the .PAR files into a different video format, (.AVI) while maintaining the time information (a feature that was excluded from the NetVu conversion). This enabled other commercial software to be used to review the data, such as Media Player Classic, which has subsequently been used. This software is described more in Section 3.4.

2.5   Test Dataset

As described in Section 3.1, a test dataset was identified that provided sixteen (16) different observations of fish within frames, based on the original LGL analysis. These included a mix of night and day observations, with and without the turbine spinning. These 5-minute clips were analyzed by the manual review team to provide annotations consistent with the rest of the manual review effort, and to provide millisecond precision time information that was needed for algorithm development.

3.0   Algorithm Development

3.1   Dataset for Development

As mentioned previously, sixteen 5-minute clips were identified to represent different conditions within the video. These are described in Table 1.

Table 1   Test video clips

Date	Start	Camera	Turbine On	LGL Events	PNNL Multiple Frame Events	PNNL Single Frame Events
7/19/15	17:58:30	1	Y	3	7	1
7/20/15	11::00:30	1	Y	3	5	4
7/22/15	03:02:00	1	N	1	30	0
		2	N	1	40	33
		3	N	1	7	0
7/23/15	00:03:30	1	Y	1	2	0
		2	Y	1	33	35
		3	Y	1	7	0
		4	Y	1	7	1
7/24/15	00:00:00	1	N	1	5	0
		2	N	1	38	17
		3	N	1	9	1
		4	N	1	8	1
8/25/15	04:03:30	1	Y	1	3	0
		2	Y	1	29	9
		4	Y	1	3	0

3.2   Algorithm Testbed

A testbed was developed for evaluating different video pre-processing methods and detection algorithms. The code from the Fish4Knowledge project (https://sourceforge.net/projects/fish4knowledgesourcecode/files/) was used as a base. The Fish4Knowledge researchers provided support and recommendations for algorithms to apply. The PNNL team customized the code to work with the development dataset and to compare algorithm output with the manual annotations. The testbed allows the user to select a preprocessing method and a detection algorithm and then runs the selected algorithm on the development dataset and quantifies the results in terms of detections and false positives. A summary of the results is generated in a scatter plot that shows the performance by video and by preprocessing method.

Fish4Knowledge

Fish4Knowledge was a European funded research project (2010-2013) to develop automated video analysis techniques to extract marine animal information from underwater video and produce a database of observations, which could then be intelligently queried.

3.3   Preliminary Baseline Results for ViBE Detector

The Video Background Extraction (ViBE) detector was evaluated based on the recommendations made by the Fish4Knowledge researchers. The detector was initially applied to the development video dataset using default parameter values and no pre-processing. Each frame of each video was labeled "fish" or

"no fish" to indicate whether any fish were present or not. The labels were compared to the true labels generated from the visual analysis of the video. The results are presented in a confusion matrix: the top left to bottom right diagonal terms of the matrix are the number of correctly labeled frames (true positive and true negative) and the bottom left to top right diagonal terms are the incorrectly labeled frames. These results were not expected to be very accurate because there was no pre-processing and default parameter values were used. However, the results serve as a baseline to quantify the improvements gained by pre-processing the frame images to improve overall quality and signal-to-noise ratios, and by tuning the algorithm parameters for this dataset.

The performance varied across the videos. The best performance in terms of false positives was on the video from camera 1 with no turbine in view, at night with lights on (Figure 1). There were no false positives but about a third of the fish were not detected. The fish in this case were small juvenile fish. The best performance in terms of missed detections was on the video with the turbine in view, at night with lights on. However, there was an extremely high number of false positives due to the debris in the water. The frames correctly labeled "fish" may have been labeled that way coincidentally due to debris.

ViBE

	fish	no fish
fish	65	32
no fish	0	7403

True

Figure 1   Example of frame with juvenile fish at night with lights on (top) and confusion matrix (bottom)

ViBE

	fish	no fish
fish	837	80
no fish	5865	717

(True)

Figure 2   Example of frame with turbine and debris at night with lights on (top) and confusion matrix (bottom)

Two different pre-processing methods, histogram equalization and contrast stretching, were included with the Fish4Knowledge code. These were applied to evaluate their effect on the performance of the ViBE detector, to see if performance was improved relative to the baseline results using no pre-processing.   In general, the pre-processing increased the number of false positives (Figure 3).

Moving forward, the next steps are to develop new pre-processing algorithms that are specific to underwater video and to evaluate other detectors such as robust principle components analysis (RPCA) and dynamic mode decomposition (DMD), which have shown promise based on work done by UW.
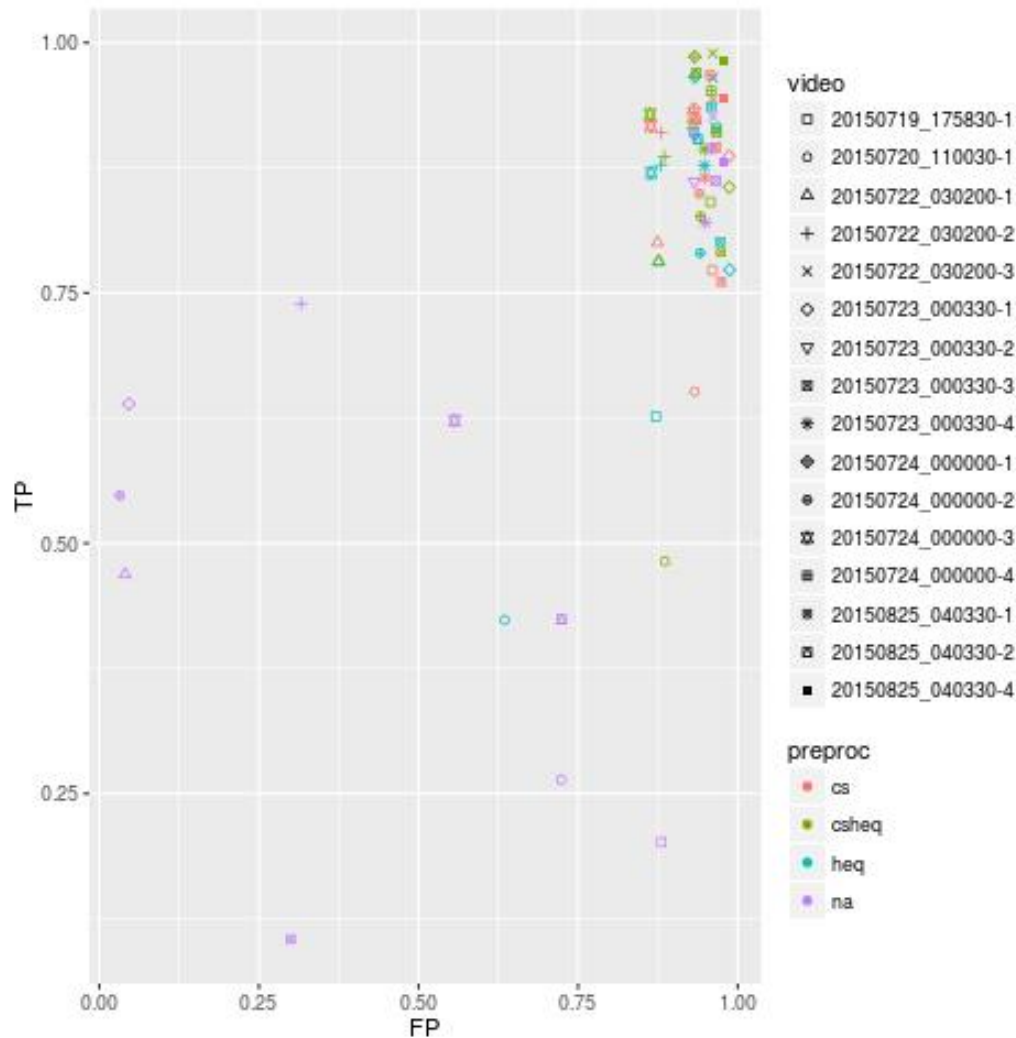
Figure 3   **Results of ViBE detector on the development video dataset using different pre-processing methods. The pre-processing methods were contrast stretching (cs), contrast stretching + histogram equalization (csheq), histogram equalization (heq), and none (na)**

3.4 EyeSea Development

In parallel with testing different algorithm codes, a web-based application for viewing the video and annotations was developed. The initial version allows a user to generate a video clip from the Igiugig video collection for a selected time period. EyeSea converts the video from the .PAR format to a more standard format (.AVI) that can be viewed on a Mac or PC using standard software like VLC or MediaViewer. This capability was used to generate the development video dataset and was used to support the manual analysis. EyeSea incorporates a database based on the manual analysis spreadsheet form, and a script was developed to ingest the manual analysis annotations into the database. The ability to select an event from the database and "fast forward" to the video containing the event is currently under development. In the future, when the detection algorithms are mature they will be integrated into EyeSea so that EyeSea can be used to interactively explore the videos and detected events.

4.0 Summary

Table 2 provides a summary of the key events and activities associated with the project.

Table 2   Chronology of events for manual and automated processing

Date	Manual Events	Algorithm Events
2016/03/07	Decision made to move forward with analysis, summarized by "Igiugig Fish Video Study - Quality Check"	
2016/03/17	Igiugig fish video data advisory committee meeting	
2016/03/18	Received visual analysis spreadsheet formats from the University of Maine and the University of Washington	
2016/03/28	Decided to prioritize camera 2 because this had the best view for potential fish interactions with the RivGen®	Initial draft of Fish Identification Technology Roadmap[2]
2016/03/29	Completed layout for visual analysis spreadsheet	
2016/03/29	Began manual analysis of the full dataset	
2016/03/31	Received RivGen® operating status (rotating or braked) for 2015 deployment	
2016/04/06	Added single frame/partial field of view (FOV) options to visual analysis spreadsheet	
2016/04/08	Added behavior classes to better describe fish movements near the device	
2016/04/20		Received Robust Principle Component Analysis (RPCA)-based fish detection code from the University of Washington
2016/04/28		Technology Roadmap finalized with input from University of Washington[2]
2016/05/06		Completed initial testing of University of Washington code after modifications to work with Igiugig data
2016/05/11	Added video quality column to visual analysis spreadsheet	
2016/05/14	Discovered that Dedicated Micros (DM) NetVu Observer software skipped frames	
2016/05/22	Decided that DM NetVu Observer software was unreliable	

---

[2] Complementary work that informed this study undertaken as part of a different project.

Date	Manual Events	Algorithm Events
2016/05/23		Developed schema for database of fish events, and the structure of EyeSea website for accessing video and events.
2016/06/07		Investigated conversion of PAR files (original format of Igiugig video data) to standard formats that are easier to work with.
2016/06/14		Stood up server for EyeSea and created initial database as per the analysis spreadsheet.
2016/06/21		Populated database with video information using developed script
2016/06/24		Decided on H264 format, constant frame rate video for analysis work; prepared a sample dataset of converted video for algorithm developers. Shared converted videos with UW.
2016/07/06	Began manual analysis of sample dataset for algorithm development	Started development of EyeSea website functionality.
2016/07/14		Established relationship with Fish4Knowledge researchers.
2016/07/30		Created a converted video dataset for development based on LGL reported events.
2016/08/17	Decision to omit single frame events for full data analysis	Video transcoding (conversion) enabled based on user-selected time interval.
2016/08/28		Developed code to check original video for gaps in recording.
2016/08/29		Development dataset annotated – more fish events were found than LGL reported.
		Identified methods for pre-processing and detection to investigate using development dataset and testbed. Three pre-processing methods (none, histogram equalization, color compensation) and three detection methods (RPCA, ViBE, and dynamic mode decomposition), for a total of 9 experiments.
	Algorithm development data subset processing complete	
2016/09/01		Completed testbed for investigating fish detection methods. Combined custom code with Fish4Knowledge code.
2016/09/08		Started investigating deep learning for fish event detection and classification. This is a parallel effort with the testbed experiments.
2016/09/12		Preliminary results for Video Background Extraction (ViBE) method for fish event detection.